TOWARD THE SYNTHESIS OF AN AROMATIC BELT

RUDOLF J. VERMEU

TOWARD THE SYNTHESIS OF AN AROMATIC BELT

by

doctorandus Rudolf J. Vermeij

A thesis submitted to the

School of Graduate Studies

in partial fulfillment of the

requirements for the degree of

Doctor of Philosophy.

Department of Chemistry

Memorial University of Newfoundland

St. John's, Newfoundland, Canada

August, 2001

Abstract

The work described in this thesis deals mainly with the application of the valence isomerization-dehydrogenation (VID) approach, previously developed by our group, to the synthesis of pyrenophanes with extended aromatic surfaces. As ultimate goal a fully aromatic "Vögtle" belt is proposed.

Key intermediates for the synthesis of pyrenophanes *via* the VID approach are *syn*-2,11-dithia[3.3]metacyclophanes. In Chapter 2 the results of a study of the bridge conformational behavior of these compounds is discussed. This behavior is correlated with Hammett's constant (σ_m) of the substituents in the 6- and 15-positions. The effect of the solvent is discussed and the study is completed with a DNMR study on several of the 6,15-disubstituted *syn*-2,11-dithia[3.3]metacyclophanes.

In Chapter 3, a synthetic effort toward the synthesis of a pyrenophane with two *para*-phenylene units in the tether is described. In this case the VID methodology fails to give the desired pyrenophane.

A straightforward synthetic plan for the synthesis of a Vögtle belt is described in Chapter 4. The synthesis stalled due to unavoidable side reactions during ring contraction of an advanced intermediate.

The synthesis of pyrenophanes with one phenylene unit in the tether is described in Chapter 5. For two such pyrenophanes, [2]paracyclo[2](2,7)pyrenophane and [2]meta-cyclo[2](2,7)pyrenophane, a successful synthesis is reported, as well as their X-ray crystal structures. In both compounds the tether forces the pyrene unit to adopt a non-planar geometry and a spoons-like orientation of the aromatic decks is observed.

Acknowledgements

I would first like to thank my supervisor Dr. Graham J. Bodwell for his support and encouragement over the past years. His constant enthusiasm has made this period an exciting and instructive experience. All members of the Bodwell group 1997 - 2001 should be acknowledged for creating a great atmosphere in and around the lab. Special thanks are due to Mike Mannion, Tom Houghton and Shu-Lin Chen, whose work formed the basis of the projects described in this thesis. Jon Langille, Jiang Li and Ian Pottie should also be thanked for providing samples for the work described in Chapter 2. Special thanks also to Paul Hurley for his help in the synthesis of precursors for the project described in Chapter 4.

Dr. Paris Georghiou and Dr. Ray Poirier, members of my supervisory committee, are acknowledged for their helpful discussions and for proofreading this thesis. Special thanks also to Dr. Graham Bodwell, Dr. Paris Georghiou and Dr. Jean Burnell for the excellent teaching I have received. I would like to thank all faculty and staff of the chemistry department, as well as all fellow graduate students in the department, for making it a great place to work.

I am grateful to Mr. David Miller for assistance with collecting NMR spectra, which form a great part of this thesis, especially Chapter 2. Dr. John Bridson and Mr. David Miller are also acknowledged for their X-ray crystallographic work. For mass spectral analyses Dr. Brian Gregory and Ms. Marion Baggs are acknowledged.

Finally I would like to thank my friends and family who have supported me throughout the period of my graduate studies. Special thanks to my fiancée, Janine Post, for always being there to talk to and for her patience over the past years.

Financial support from the School of Graduate Studies and the Chemistry Department is gratefully acknowledged.

Table of contents

List of Figures

List of Schemes

List of Tables

List of Abbreviations and Symbols Used

α	bend angle (in cyclophanes)
Á	Ángstrom
Abs.	Absolute (with ethanol)
Ac	acetyl
Anal.	Analysis (combustion)
AM	Austin Model
β	bend angle (in cyclophanes)
Borch reagent	dimethoxycarbonium tetrafluoroborate
b.p.	boiling point
br	broad (in NMR)
Bu	butyl
ca.	*circa*
calc'd	calculated
cat.	catalytic
χ	mole fraction
COSY	correlation spectroscopy
δ	chemical shift in ppm downfield from tetramethylsilane
Δ	heat
Δδ	difference in chemical shift values (in ppm)

$\Delta\nu$	difference in chemical shift values (in Hz)
d	deuterium (in structural formulae)
d	doublet (in NMR)
D	Debye
dd	doublet of doublets (in NMR)
ddd	doublet of doublet of doublets (in NMR)
DBU	1,8-diazabicyclo[5.4.0]undec-7-ene
DDQ	2,3-dichloro-5,6-dicyano-1,4-benzoquinone
dec.	decomposition (with melting point)
Dess-Martin periodinane	1,1,1-triacetoxy-1,1-dihydro-1,2-benziodoxol-3(1*H*)-one
DIBAL-H	diisobutylaluminum hydride
DMAc	*N*,*N*-dimethylacetamide
DME	ethylene glycol dimethyl ether (1,2-dimethoxyethane)
DMF	*N*,*N*-dimethylformamide
DMSO	dimethyl sulfoxide
DNMR	dynamic nuclear magnetic resonance (spectroscopy)
dt	doublet of triplets (in NMR)
ε	dielectric constant
EI-MS	electron impact – mass spectrum
Et	ethyl
$\mathcal{F}$	Swain-Lupton constant for induction effect of a substituent

FVP	flash vacuum pyrolysis
FVT	flash vacuum thermolysis
HRMS	high-resolution mass spectrum
h	hour(s)
HMQC	heteronuclear multiple quantum correlation (spectroscopy)
hν	light
Hz	hertz
IR	infrared (spectroscopy)
J	coupling constant (Hz)
K	kelvin
kcal	kilocalorie(s)
kJ	kilojoule(s)
LDA	lithium diisopropylamide
LHMDS	lithium hexamethyldisilazide
lit	literature
m	multiplet (in NMR)
m	medium (IR)
$M^{\cdot}$	molecular ion
Me	methyl
MHz	megahertz
min	minute(s)
mM	millimolar

mp	melting point
NBS	*N*-bromosuccinimide
NMR	nuclear magnetic resonance (spectroscopy)
NOESY	nuclear Overhauser effect spectroscopy
obs	observed
[Ox]	oxidation
Pearlman's catalyst	Pd(OH)/C (20% on dry basis)
Ph	phenyl
ppm	parts per million
pyr	pyridine
q	quartet (in NMR)
$\mathcal{R}$	Swain-Lupton constant for resonance effect of a substituent
rt	room temperature
σ_I	Taft's constant for inductive effect of a substituent
σ_m	Hammett's constant for *meta*-substituents in aromatics
σ^0_R	Taft's constant for resonance effect of a substituent
s	singlet (in NMR)
s	strong (in IR)
θ	bend angle (in pyrenophanes)
t	triplet (in NMR)
t-BuLi	*tert*-butyllithium

T_c	coalescence temperature
TCNE	tetracyanoethylene
Tf	trifluoromethylsulfonyl, CF_3SO_2-
TFA	trifluoroacetic acid
THF	tetrahydrofuran
TMS	tetramethylsilane (in NMR), trimethylsilane (in structures)
TPE	tetraphenylethylene
triflic anhydride	trifluoromethanesulfonic anhydride
Ts	*p*-toluenesulfonyl
UV	ultraviolet (spectroscopy)
VID	valence isomerization – dehydrogenation
vs.	*versus*
w	weak (in IR)

Chapter 1

Introduction

1.1 Fullerenes and fullerene fragments

The isolation and characterization of the first fullerene (Figure 1.01) in 1985 by Kroto *et al.* at Rice University[1] caused a surge of interest in several research areas. The now well-established cage-like structure of C_{60} had previously been predicted by other scientists to be a stable, soccer-ball-shaped molecule,[2-7] but only after the 1985 communication by the group at Rice University could their predictions be confirmed by experimental results. The C_{60} molecule was given the name "buckminsterfullerene" in honor of Buckminster Fuller, the American architect renowned for his geodesic domes, since the shape of the molecule (a truncated icosahedron) resembles such domes.

1

Figure 1.01: Structure of buckminsterfullerene **1**.

Buckminsterfullerene consists only of carbon atoms and can be seen as the third carbon allotrope. The other two allotropes, graphite and diamond, are available in macroscopic quantities, and the technological importance of these compounds is enormous.[8] Graphite is used as a solid lubricant, in pencils and as a reinforcement material in carbon fiber

composites.[8-12] Diamond is used in the jewelry industry and in drilling heads for the extraction of crude oil. This importance of graphite and diamond has been the cause for a great interest in the fullerenes from the field of material sciences. Also, all-carbon molecules are believed to be present in some stars and interstellar dust, which has caused interest from astronomers and astrophysicists,[8,13] and the first preparation of macroscopic quantities of C_{60} was reported by a group of astronomers.[14]

In the field of synthetic organic chemistry, several groups became interested in designing synthetic approaches toward molecular carbon allotropes. One approach is based on the collapse of polyethynylated cyclic π-systems such as **2** (Scheme 1.01).[15] In Fourier transform laser desorption mass spectrometric experiments on **2** the [60]fullerene cation ($\mathbf{1}^+$) has been observed.[16-19] The precursors in this approach have not become available on a macroscopic scale yet, and isolation of fullerenes from this route has not (yet) been published. However, this approach seems promising for the synthesis of fullerenes and simple (hydrogenated) derivatives[20] but is outside the scope of this thesis and will not be discussed in detail here.

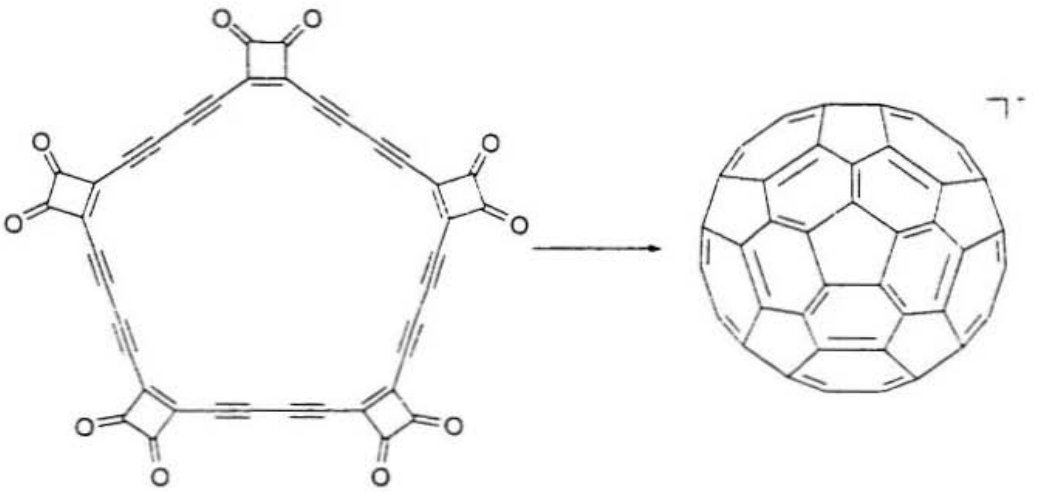

2 **1⁺**

Scheme 1.01: Formation of 1^+ from **2**.

Another approach is initially directed toward the synthesis of fullerene subunits with the view to the synthesis of fullerenes *via* elaboration of these units. This approach is based on the observation that the fullerenes can be viewed as curved aromatic surfaces. The fullerene subunits then are polycyclic hydrocarbons. One property that these polycyclic compounds must possess in order to be considered a subunit of a fullerene is an inherently curved aromatic surface (i.e., the lowest energy conformer should possess a nonplanar geometry). The smallest example of such a fullerene fragment is corannulene **3** (Figure 1.02), which maps onto the surface of most fullerenes, as illustrated with C_{60} and D_{5h}-C_{70} (**4**; Figure 1.02).

3 1 4

Figure 1.02: Structure of corannulene **3**, the smallest fullerene fragment mapped onto the surfaces of C_{60} (**1**) and D_{5d}-C_{70} (**4**).

Corannulene **3** (or [5]circulene)[21] was first synthesized in 1966 (almost two decades before the first report on buckminsterfullerene!) by Barth and Lawton in a formidable 16-step synthesis.[22,23] Corannulene consists of a central 5-membered ring, annellated by five 6-membered rings. The molecule is bowl-shaped and, at room temperature, undergoes rapid bowl-to-bowl inversion (Scheme 1.02). Scott *et al.* estimated the energy barrier for this process to be 10 kcal mol based on a DNMR study of methylcorannulene (**5**, Scheme 1.02).[24,25]

Scheme 1.02: Bowl-to-bowl inversion of **5**.

After the discovery of the fullerenes in 1985, an efficient synthetic strategy toward **3** became the focus of the work of several groups, as the initial synthetic route was lengthy

and low yielding. In 1992 the Scott group published a short synthesis of **3**.[24,25] In their approach they took advantage of the thermal isomerization of terminal bis(acetylene) **6** to give a vinylidene carbene (**7**) under flash vacuum pyrolysis conditions at 1000 °C.[26] The highly reactive intermediate **7** underwent insertion of the carbene into the proximate C-H bond to form corannulene **3** in approximately 10% yield.

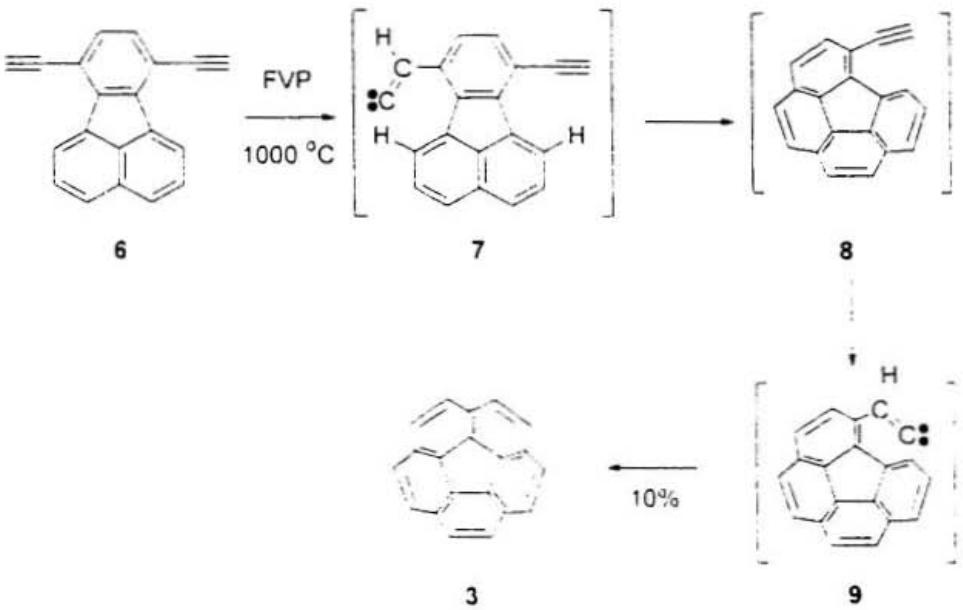

Scheme 1.03: Scott's synthesis of **3**.

For the successful formation of corannulene **3** from diethynylfluoranthene **6** the pyrolysis conditions were assumed to be crucial for both steps in the mechanism. The first step (1,2-H-shift to form vinylidene carbenes) only occurs at temperatures above 700 °C, and temperatures up to 1200 °C are frequently used for this process.[26] In the second step (stepwise insertions of the vinylidene carbene into the C-H bond), the bowl shape of the

product is introduced. In their lowest energy conformations the intermediates **7** and **9** are less planar than **8** and **3**, respectively, and the distance between the reacting centers would be too great for reaction to occur. At high temperatures, intermediates **7** and **9** will fluctuate from this planar geometry and allow the reacting centers to approach.

The pyrolytic ring closures of readily available compounds stood as the basis of several routes to corannulene **3** that were published in the years following Scott's initial report.[27-30] Most routes employed simultaneous formation of two 6-membered rings in the final (pyrolytic) step and yields varied from 7% to 40%.

The first nonpyrolytic synthesis of corannulene was published in 1992 by Siegel *et al.* (Scheme 1.04).[27] In this synthesis they used traditional cyclophane chemistry to convert tetrabromide **10b** to a dithiacyclophane that could be ring contracted and dehydrogenated to give corannulene **3** in 7% yield. For the ring contraction, a thermolytic step was still needed (400 °C), which is similar to a pyrolysis. This route was still quite inconvenient for large scale synthesis and did not allow for many functional groups to be introduced. In 1996 the same group reported the first truly nonpyrolytic, solution phase synthetic route to a corannulene derivative.[31] In this route tetrabromide **10b** was subjected to reductive coupling conditions ($TiCl_3/LiAlH_4$ or $VCl_3/LiAlH_4$) to give **11**, which was treated with DDQ to yield dimethylcorannulene **12**. This synthesis is a more general one, can be employed on gram scale and tolerates more functionality in the system than the pyrolytic syntheses. Although the yield of 18% was somewhat low, this work

demonstrated that nonpyrolytic routes might be reasonable alternatives for the synthesis of fullerene fragments (*vide infra*).

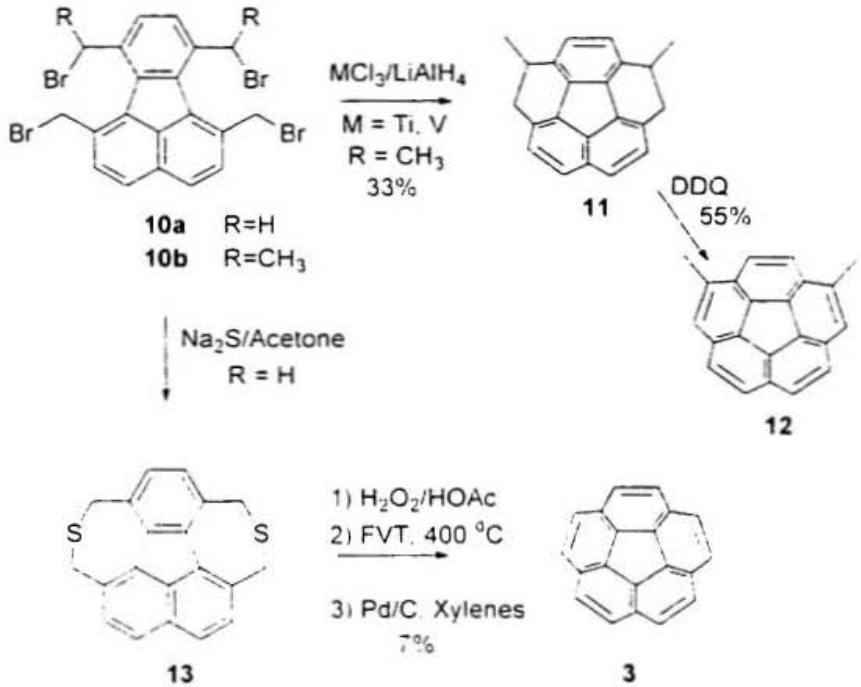

Scheme 1.04: Nonpyrolytic synthesis of **3** and **13**.

Over the past decade a large number of syntheses of fullerene fragments has appeared in the literature.[30,32,33] Most syntheses employ some sort of pyrolytic ring formation as the key step. In this step, ring closures based on vinylidene carbenes have been used to form 6-membered rings, but other pyrolytic processes that involve radical or carbene intermediates have been described for the formation of 5- and 6-membered rings.

The formation of highly strained systems by ring closure of 5-membered rings, such as those in fullerene fragments, has been accomplished by Mehta *et al.*, who employed a pyrolytic dehydrobromination of **14** to form **15**.[34] Unfortunately, the last ring closure to form the highly curved sumanene **16** did not proceed. Sumanene has been proposed as a highly curved polycyclic aromatic compound that maps onto the surface of C_{60}.[35] Its synthesis has still not been achieved.

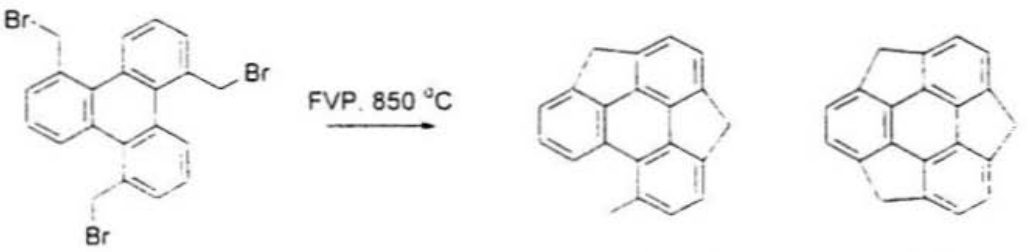

14 **15** 17% **16** 0%

Scheme 1.05: Dehydrobromination of **14** to give **15**.

A variation of the dehydrobromination to close 5-membered rings is based on a 1,2-H shift in aryl radicals. This hydrogen shift has been applied to the synthesis of **18** from **17**.[36] Initial homolytic cleavage of the C-Br bonds, followed by a 1,2-H shift, ring closure and loss of hydrogen radical is believed to be the reaction pathway. Pyrolysis product **18** is a 30-carbon fragment of the [60]fullerene C_{60}.

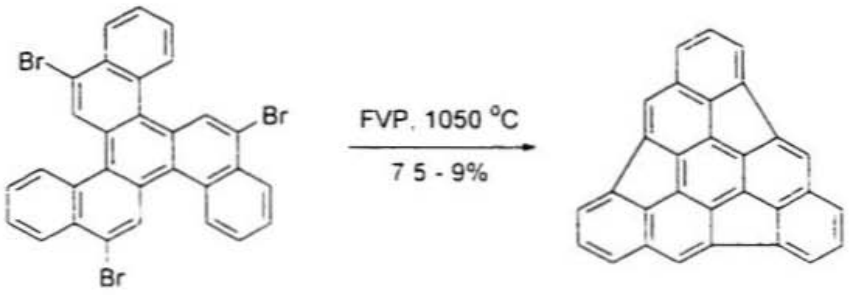

17 **18**

Scheme 1.06: Pyrolysis of **17** to give **18**.

In principle, the same type of dehydrobromination pyrolysis that was used to form the 5-membered rings in **18** could be used to form 6-membered rings. Scott *et al.* have shown however, that, for the formation of 6-membered rings dehydrogenative pyrolysis can also be employed.[37] This method is much more convenient, as unfunctionalized starting materials can be used, but often suffers from low yields. The dehydrogenative approach was used in the synthesis of circumtrindene **20** from commercially available **19a**. This "brute force"[38] triple dehydrogenation of **19a** only yielded 0.2 – 0.6% of the desired product. A higher yielding pyrolysis step to circumtrindene **20** was later reported using a dehydrochlorination approach of precursor **19b** in 25 - 27% yield.[38] The overall yield of **20** from commercially available 2-chloronaphthalene (including the 5-step synthesis of **19b**) was 4%, which demonstrates the "striking superiority"[38] of the dehydrohalogenation route. Circumtrindene is a 36-carbon fragment of C_{60} and is the largest fullerene fragment that has been synthesized to date.

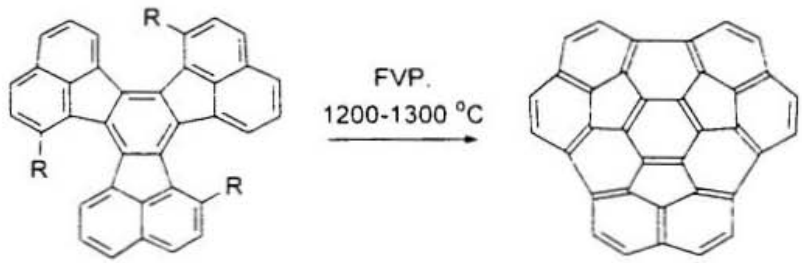

19a R=H 0.2 - 0.6% **20**
19b R=Cl 25 - 27%

Scheme 1.07: Synthesis of circumtrindene **20**.

Several more fullerene fragments have been synthesized using the pyrolytic approaches just described. Unfortunately, these pyrolytic approaches also are quite low yielding, and the synthesis of larger fullerene fragments becomes increasingly difficult as the volatility of starting materials decreases with increasing molecular size. Therefore the trend in this area of research seems to have been toward the development of nonpyrolytic methods for the synthesis of curved polycyclic aromatic hydrocarbons.

The first nonpyrolytic synthesis of a fullerene fragment was Siegel's 1996 synthesis of dimethylcorannulene **13** (*vide supra*). This was followed in 1998 by the synthesis of semibuckminsterfullerene **22** by Rabideau *et al.* in 20% yield from **21**.[39,40] In Rabideau's synthesis the same type of low-valent titanium reductive coupling was used as described by the Siegel group. Application of this coupling also led to the successful synthesis of cyclopentacorannulene **24** (20-30%) and an improved synthesis of corannulene **3** (70-75%).[41,42]

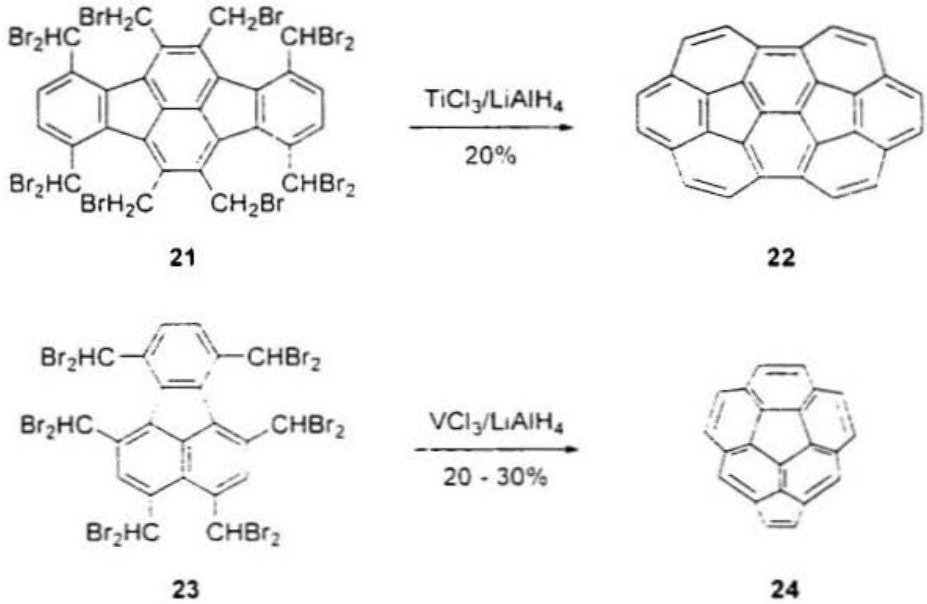

Scheme 1.08: Low-valent titanium coupling to give **22** and **24**.

More recently, palladium-catalyzed routes have become available for the construction of 5- and 6-membered rings to form curved polycyclic aromatic hydrocarbons. Scott *et al.* published an intramolecular arylation to yield **26** in 50 – 60% from **25**, compared to 38% for the same conversion when it was attempted using a pyrolytic dehydrobromination.[43] A similar approach led to the synthesis of **25** *via* palladium-catalyzed ring closure of the 5-membered rings in excellent yield (79 - 94%).[44] The functional group compatibility of these solution-phase syntheses, together with the ease of performing these conversions on a relatively large scale, demonstrates the synthetic power of these methods for future applications in the synthesis of curved polycyclic aromatic hydrocarbons.

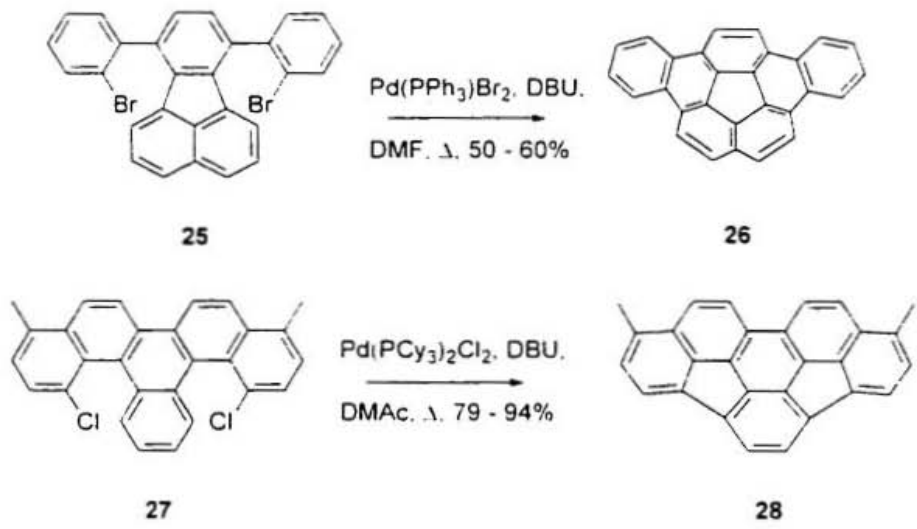

Scheme 1.09: Palladium-catalyzed synthesis of **26** and **28**.

The synthetic approaches discussed so far have all been aimed at the synthesis of fragments of the most abundant C_{60} fullerene. Not many syntheses of fragments specific to the larger fullerenes have been reported. Mehta has published a retrosynthetic analysis of the second-most abundant fullerene D_{5h}-C_{70}, leading back to a fragment **29**, which he called pinakene.[45] However, to date this group has published no experimental work in this area. The key feature of pinakene that renders it specific to D_{5h}-C_{70} and other higher fullerenes is the presence of a pyrene moiety, which is not present in C_{60}.

29

Figure 1.03: Pinakene (**29**).

In 1994 Plater *et al.* reported that pyrolysis of **30** led to formation of cyclopenta[*cd*]pyrene **31** *via* Stone-Wales rearrangement.[46] Compound **31** does not map onto the surface of C_{60}, but is a fragment of the larger fullerenes. Jenneskens published a synthesis of **31** in the same year, in which the final step was a pyrolytic dehydrochlorination of **32** to afford **31**.[47] Syntheses of three isomeric dicyclopentapyrenes **33**, **34** and **35** were published by Scott in 1996.[48] For the synthesis of these compounds, pyrolytic dehydrochlorination (similar to that reported by Jenneskens) was the key step in the simultaneous formation of the 5-membered rings.

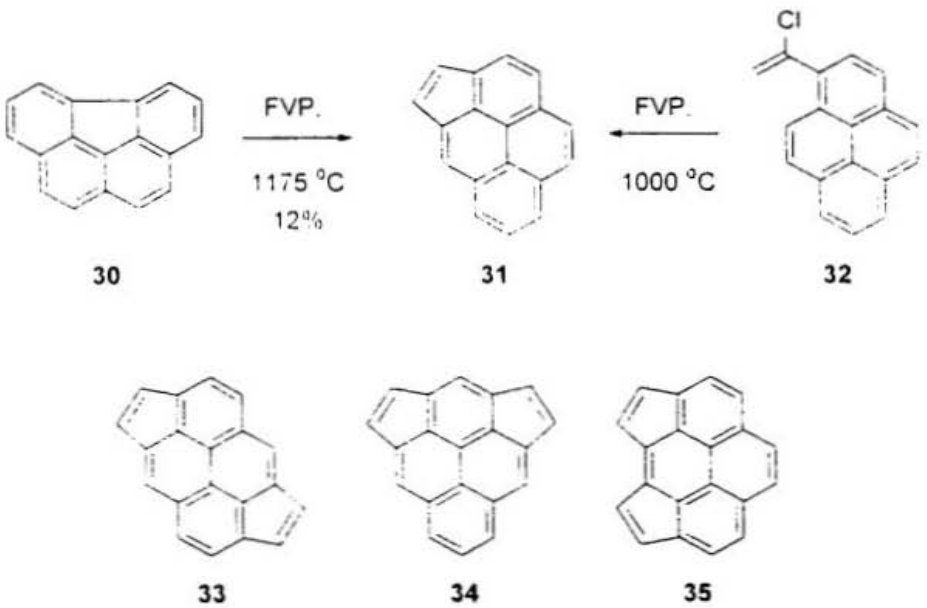

Scheme 1.10: Synthesis and structures of some C_{70} fullerene fragments.

In 1999, a computational study by Siegel and Baldridge proposed the "canastanes" **36** – **39** (Figure 1.04) as a new curved hydrocarbon motif.[49] The same paper mentioned that

"the canastane motif should provide a significant challenge to synthetic.... methods" and no experimental work in this area has been reported to date. The canastanes are fragments of the C_{70} fullerene and other higher fullerenes. These compounds also include the pyrene cores.

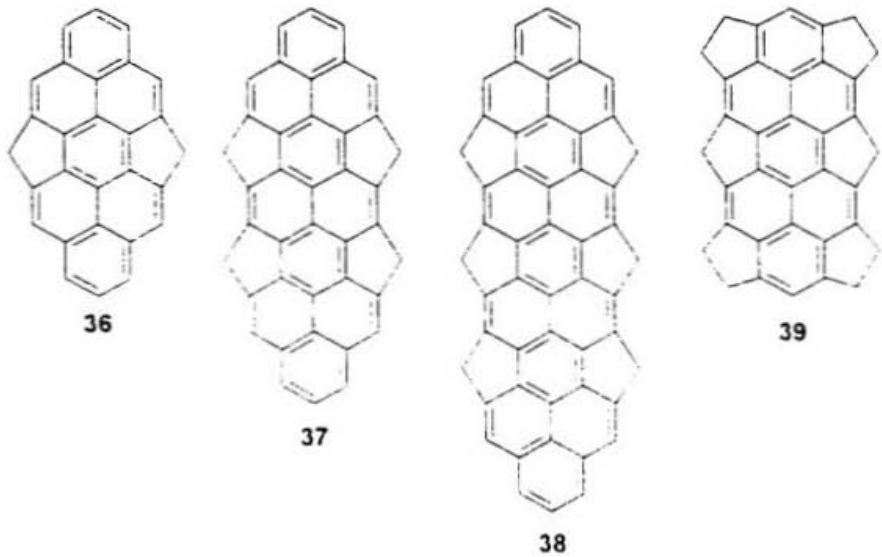

Figure 1.04: Structure of canastanes **36** – **39**

1.2 Curvature in aromatic systems

The key synthetic feature of C_{60} and C_{70} fullerene fragments is the presence of 5-membered rings. Without these 5-membered rings, these polycyclic compounds would not exhibit the curvature that distinguishes them as fullerene fragments. The curvature of

the fullerene fragments can then be attributed to their architecture: i.e., the presence of rings other than 6-membered rings causes certain polycyclic aromatic systems to deviate from planarity. The principle of curvature originating from architecture was described by Hopf.[21] According to his discussion, other ways to cause aromatic rings to adopt nonplanar geometry (Figure 1.05) are based on non-bonded interactions (such as in [6]helicene **40**) or the tethering of non-adjacent positions of the aromatic system (e.g. [5]metacyclophane **41**).

40 **41**

Figure 1.05: Curvature of aromatic rings due to sterics (**40**) and tethering (**41**).

In **40** the two termini of the molecule would, if it were to adopt a planar geometry, have to occupy the same region of space. This steric interaction between the termini causes the molecule to adopt a helical shape. The nonplanarity that is linked inherently to this helical shape can be increased or decreased by increasing or decreasing the steric bulk on the repelling ends of the molecule. The aromatic ring in [5]metacyclophane **41** is bridged by a pentamethylene tether. This tether is too short to permit the aromatic ring to adopt a planar geometry and causes the aromatic ring to adopt a boat-like geometry. Changing the length of the tether can vary the degree of distortion from planarity in the aromatic ring.

The most successful synthetic approaches that have been used to synthesize highly curved examples of helicenes and cyclophanes are based on the formation of a curved aromatic nucleus late in the synthesis. The origin of the curvature (i.e., the steric repulsions in the helicenes and the tether in the cyclophanes) is usually already in place when the strained aromatic system is formed. The exothermicity from formation of the aromatic system (*ca.* 37 kcal mol resonance energy) compensates for the introduced strain energy, permitting such reactions to be done under relatively mild conditions. This approach to introduce curvature in aromatic systems is conceptually different from the approach that has been used in the synthesis of fullerene fragments.

In the synthesis of fullerene fragments (Section 1.1) curvature is usually introduced by subjecting a starting material with a planar aromatic system to high-energy conditions. Once the system absorbs enough energy, the aromatic system will fluctuate from its planar geometry, so that the strained rings can be formed in this step. In this approach the stability of the aromatic system is not exploited, but works *against* formation of the desired product by its resistance to deviations from planarity.

The question then arises whether the helicene- or cyclophane-approach to introduce curvature to aromatic systems can be applied to the synthesis of fullerene fragments. Based on energetic and geometric considerations, it should be possible to incorporate the curved aromatic rings of suitably functionalized helicene or cyclophane precursors into

fullerene fragments under relatively mild conditions. Some of the fullerene fragments of the higher fullerenes (C_{70} and larger) contain pyrene units (*vide supra*) and at the outset of the work described in this thesis the Bodwell group had successfully developed methodology for the synthesis of cyclophanes containing curved pyrene units. The curvature in these systems was comparable to the bend in the pyrene units in the D_{5h}-C_{70} fullerene. This led to the proposal to apply this cyclophane methodology to the synthesis of fullerene fragments. This approach will be discussed in more detail in Section 1.5, after a brief overview of cyclophane chemistry in the literature (Section 1.3).

1.3 Cyclophanes

1.3.1 Nomenclature of cyclophanes

The first occurrence of a cyclophane in the literature was in to 1899, when Pellegrin reported the synthesis of what he called "di-*m*-xylylene" ([2.2]metacyclophane **72**). Cyclophane chemistry expanded rapidly after 1949, when Brown described the synthesis and X-ray crystal structure of [2.2]paracyclophane **42a**, which he called "di-*p*-xylylene".[50,51] The name "cyclophane" was first introduced by Cram in 1951 when he described the synthesis of a series of paracyclophanes **42a** - **c** (Figure 1.06).[52] This name was suggested as a contraction of three terms: *cyclo*, *ph*enyl and alk*ane*. After some comments on the nomenclature issue by Schubert *et al.*[53] and Cram *et al.*,[54] Vögtle

introduced a systematic nomenclature for the cyclophanes, which is now generally accepted.[55,56] The only papers on nomenclature are in German, so a quite extensive description will be given in this Section. For convenience, reference to Vögtle's numbering (P-1 to P-6) and IUPAC (A-..) numbering will be given for each set of rules.

42a $m = n = 2$
42b $m = 3$, $n = 2$
42c $m = 4$, $n = 2$

Figure 1.06: Structure of a paracyclophanes **42a - c**.

Rule P-1.1[57] In order to develop effectively a nomenclature system, Vögtle defined several concepts. First, "phanes" were defined as all compounds that contain at least one aromatic nucleus and at least one aliphatic bridge, which could contain any number of atoms ($n \geq 0$). For the nomenclature of the aromatic nuclei, IUPAC nomenclature is used (A-21.1 to A-22.5). A bridge is defined by the IUPAC rules (A-31.1(1)) as "a valence compound or atom or unbranched chain of atoms that connect two parts of a molecule". The atoms that are connected directly to the bridge are bridgehead atoms and the number of atoms in the bridge is the number of "bridge members." The number of "ring members" is given by the sum of the number of bridge members (10 + 1 for **43** in Figure 1.07), number of bridgehead atoms (4 in **43**) and the smallest number of atoms between

the bridgehead atoms of the aromatic nucleus (in **43** that is 1 for each nucleus for a total of 17 ring members).

43

Figure 1.07: [1.1.0]metacyclophane.

Rule P-1.2 The cyclophane class of compounds is first divided into two groups: the "heterophanes" and the "carbophanes" (Figure 1.08). The heterophanes are cyclophanes in which at least one of the aromatic nuclei is a heteroaromatic ring (e.g. **46** or **47**) and the carbophanes only contain all-carbon aromatic nuclei (e.g. **44** or **45**). The names heterophane and carbophane do not indicate the presence of heteroatoms in the bridge. Heteroatoms in the bridge are indicated with prefixes as aza-, oxa-, thia, etc. according to IUPAC nomenclature. Based on the presence of heteroatoms in the bridge, cyclophanes can then be classified as a carba-phanes (only carbon atoms in the bridge, e.g. **44** or **46**) or hetera-phanes (at least one heteroatom in the bridge, e.g. **45** or **47**).

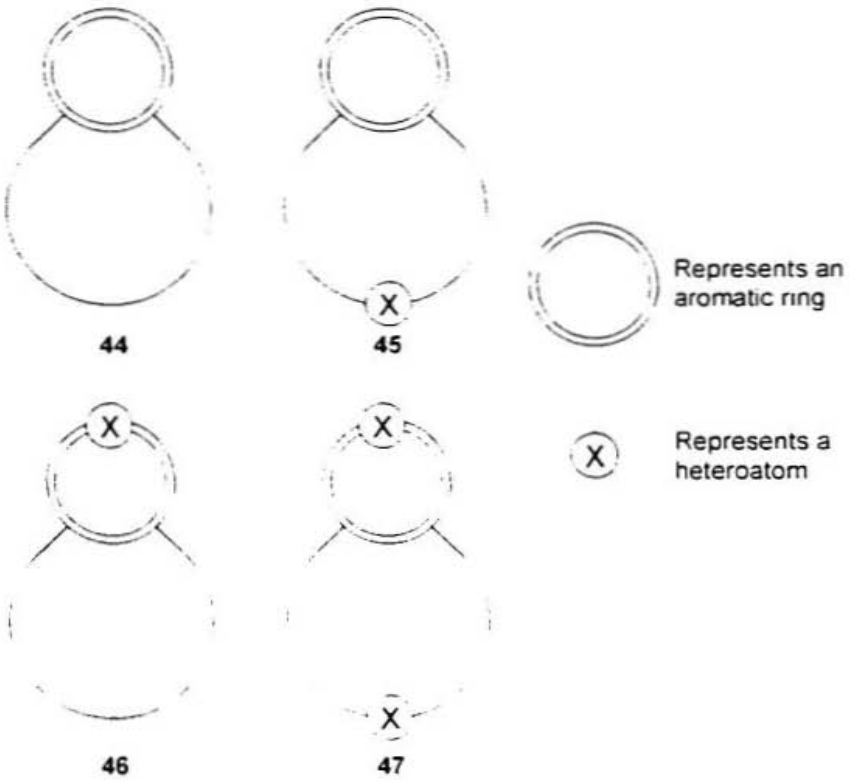

Figure 1.08: Carbophanes, heterophanes, carba-phanes and hetera-phanes.

Rule P-1.3 If a phane contains carbocyclic as well as heterocyclic aromatic nuclei, the heterocycles have priority over the carbocycles.

Rule P-2.11 – P-2.14 When naming a cyclophane, the root of the name is formed by adding the ending "-o" to the name of the aromatic nucleus, followed by the suffix "phane" (P-2.11). Examples are "thiophenophane" for a thiophene-containing cyclophane and "indolophane" for a cyclophane with indole as the aromatic nucleus. If benzene is the aromatic nucleus, the root of the name is, by definition, "cyclophane" (P-2.12). If the

cyclophane structure contains two or more aromatic nuclei (single rings or fused ring-systems) that are bonded to one another, the root will be derived from the IUPAC name of the system (P-2.13). In doubtful cases the shorter or simpler name should be chosen. If the aromatic nucleus carries a charge, the ending "-o" remains and the suffix "phane" should be replaced by "phanium" (for aromatics with a positive charge) or "phanate" (for aromatics with a negative charge) (P-2.14).

Rule P-2.21 - P-2.24 In front of the name of the aromatic nucleus, the number of aliphatic bridge members is indicated in square brackets. This number is indicated separately for each bridge, separated by a period. If two aromatic rings are bonded directly, this number is indicated as "0" (zero) (P-2.21). Heteroatoms in the bridge are indicated as usual by the prefix aza-, oxa, thia, etc. (P-2.22). When three or more bridges of equal length are present, this can be indicated by adding the number of the bridges as a subscript to the length of the bridges (P-2.23). The position of the bridges on the aromatic nuclei is indicated by a set of numbers between round brackets, separated by a comma. The numbers are based on the conventional numbering of each aromatic nucleus. For cyclophanes (carbophanes) this numbering is replaced by the prefixes *ortho*, *meta*, and *para* (P-2.24).

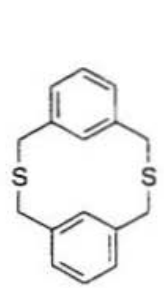

2,11-dithia[3.3]metacyclophane

48

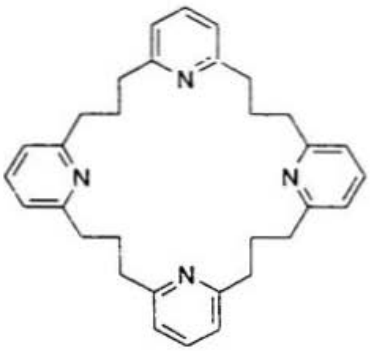

[3_4](2,6)pyridinophane

49

Figure 1.09: Structures and names for phanes **48** and **49**.

Rule P-2.25 – P-2.27 If several bridges between *different* aromatic nuclei are present (e.g. compound **50**), the longest bridge is named first, followed by the shorter bridge(s) (P-2.25). If more than two aromatic nuclei are present, naming (and numbering, *vide infra*) still commences with the longest bridge, followed by the next longest remaining bridge. Further naming continues in the same direction (clockwise or counterclockwise), even if this means that the shorter of the remaining bridges is named before the others (P-2.26). In the round brackets the bridgehead atom with the lowest number (in cyclophane numbering) is assigned first (P-2.27). This last, somewhat confusing rule can be illustrated with compound **50**. The pyridine nucleus is assigned as ...(4,6)pyridino... and *not* as ...(4,2)pyridino... or ...(2,4)pyridino... (Figure 1.10). When a phane contains several aromatic nuclei that only differ in the positions in the bridges, the numbers in square brackets can be combined (P-2.28; e.g. [2.2](2,6)(3,5)pyridinophane **51** in Figure 1.10).

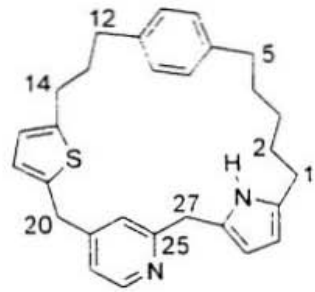

[5]Paracyclo[3](2,5)thiopheno[1](4,6)pyridino[1](2,5)pyrrolophane

50

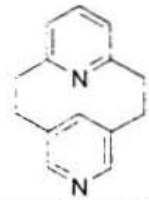

[2,2](2,6)(3,5)Pyridinophane

51

Figure 1.10: Compounds **50** and **51**

Rule P-2.29 – P2.31 When one aromatic nucleus is bridged by more than one bridge, the numbers indicating each bridge length are listed separately in square brackets. The positions of the aromatic nucleus that are bridged are listed immediately after this (P-2.29; compound **52** in Figure 1.11). If several bridges link *two* aromatic nuclei, the number of bridge members for all bridges is listed between a single pair of brackets, separated by a period and starting with the longest bridge. The connection positions to the aromatic rings are listed (in the same order) directly after that (P-2.30; compound **53** in Figure 1.11). In cyclophanes with more than two aromatic nuclei and several (more than three) bridges, the aromatic ring containing the bridgehead atom of which the number

appeared last in the round brackets is the starting point for the next bridge system (P-2.31; compound **54** in Figure 1.12). This aromatic ring is also numbered first when the system is numbered (*vide infra*).

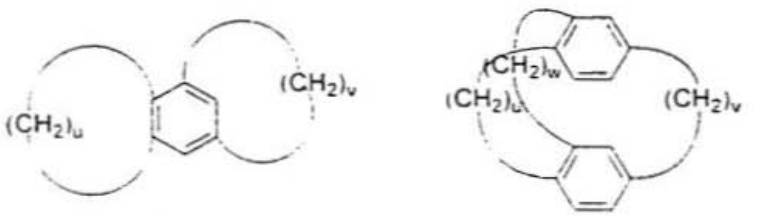

u > v
[*u*](1,2)[*v*](3,5)Cyclophane
52

u > v > w
[*u v w*](1,4,2)Cyclophane
53

Figure 1.11: Cyclophanes **52** and **53**.

Rule P-2.31 is somewhat ambiguous when it was presented in the original papers by Vögtle.[55,56] Later a different nomenclature for phanes with more than two aromatic nuclei and more than three bridges was proposed.[58] This system describes the phane with a "layer number", which is the number of core arene building blocks. The layer number is depicted in angular brackets ‹ › and names compound **54** (Figure 1.12) as a [k.l](1,3)‹1,3›[m.n](4,6)‹1,4›benzeno-3-phane. Although the new system with angular brackets is inconsistent in the use of "benzenophane", where "cyclophane" was suggested in the initial system, it is preferable when cyclophane systems become larger and more complex. Expansion of the new system to belt shaped molecules, by introducing the prefix "belta" (Figure 1.12), has been suggested as well (e.g. phane **55**).[59]

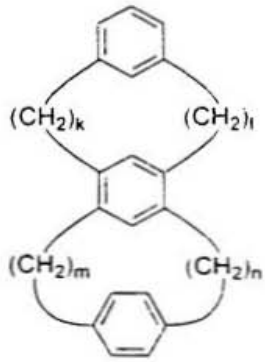

k > l > m > n
[*k l*](1,3)(1,3)[*m n*](4,6)(1,4)Cyclophane
or
[*k l*](1,3)(1,3)[*m n*](4,6)(1,4)Benzeno<3>phane

54

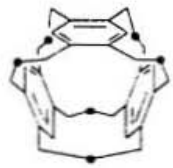

• =NH

Belta-2,11,20,29,32,35-hexaaza[3.3](1,3)(1,3)-[3.3](4,6)(1,3)[3.3](4,6)(4,6)benzeno<3>phane

55

Figure 1.12: Structures and names for cyclophane **54** and phane **55**.

Rule P-3.1 – P-3.3 Numbering of phanes starts at the longest bridge, closest to an aromatic nucleus and continues until a bridgehead atom is reached (P3.1). The bridgehead atom to which the longest bridge is connected receives the lowest number of the atoms in the aromatic nucleus (P-3.1). Numbering of the aromatic nucleus continues toward the next bridgehead atom along the longest route, except when heteroatoms are present. When both routes are equal in length, the most substituted receives the lower numbers. The periphery of an aromatic nucleus is numbered in its completion before continuing on along the next bridge (P-3.3). Examples of numbering can be found in Figure 1.13 and in Figure 1.10 (compound **50**).

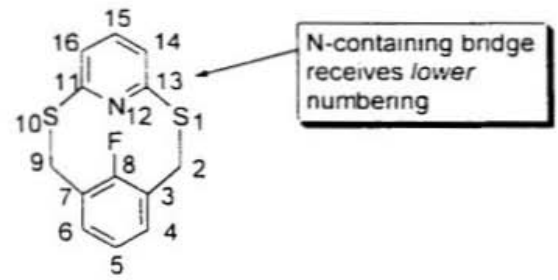

8-Fluoro-1,10-dithia[2]metacyclo[2]pyridinophane

56

Figure 1.13: Numbering of phane **56**.

Rule P-4.1 - P-4.2 Phanes that possess aromatic as well as aliphatic bridgehead atoms are named as the [*n*]phane that contains the longest bridge. This phane is then numbered according to the phane nomenclature. In front of the number of bridge members (in square brackets), each bridge is indicated by the number of bridge atoms between the aliphatic bridgeheads, again separated by a period and between square brackets. The bridges are given in order of the number of bridge members, starting with the longest bridge. The position of the aliphatic bridgehead atoms is given in superscript, separated by a comma, for each bridge (P-4.1; compound **57** in Figure 1.14). In numbering, the longest bridge is numbered first, followed by the aromatic nucleus. Numbering of the bridges is then continued based on the number of bridge members (starting with the longest bridge) (P-4.2).

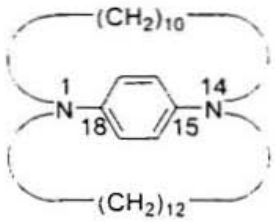

1.14-Diaza[10^{1,14}][14]paracyclophane

57

Figure 1.14: Compound **57**.

Rule P-5.1 – P-5.6 The last remaining issue in the nomenclature of phanes is the assignment of priorities, most of which have already been established above. Longer bridges in phanes have priority over short bridges, i.e. [3.2]metacyclophane and not [2.3]metacyclophane (P-5.1). When the bridges are of equal length, the aromatic nuclei are given in alphabetic order ("C" for cyclophane; in the cyclophane series *ortho* comes before *meta* and *para*) (P-5.2). If there is a heteroatom present in an aromatic nucleus, the side containing this atom will receive the lowest numbering. In the absence of heteroatoms, the longest route between bridgehead atoms in an aromatic nucleus receives lowest numbering (P-5.3). When both sides of the aromatic nucleus contain the same number of atoms, the side that carries substituents is numbered first (P-5.4). If numbering cannot be based on one of the above, the sum of the number of substituents is decisive, followed by alphabetic order (P-5.5). Once numbering has started along the longest bridge, numbering is continued in this direction (P-5.6).

In Vögtle's nomenclature system, rules P-6 describe the naming of metallocenophanes. As this area is outside the scope of this thesis it is omitted here and the reader is referred to the original literature for a discussion of the nomenclature of this type of phane.[56]

1.3.2 Small phanes: structure and synthesis

A naïve retrosynthetic analysis of a [*n*]cyclophane **58** might lead back to compound **59** or **60** by cleaving the bridge of the cyclophane.[91] This approach will usually only be successful in orthocyclophanes or if the tether is sufficiently long for the atoms, between which the ring-closing bond is formed, to approach each other. For phanes with smaller tethers ([*n*]paracyclophanes $n \leq 8$ and for [*n*]metacyclophanes $n \leq 7$) this ring closure process is not applicable because the reacting ends "will not meet"[91] and, as a result, intermolecular reaction (dimerization or oligomerization) rather than intramolecular reaction (cyclophane formation) is often predominant.

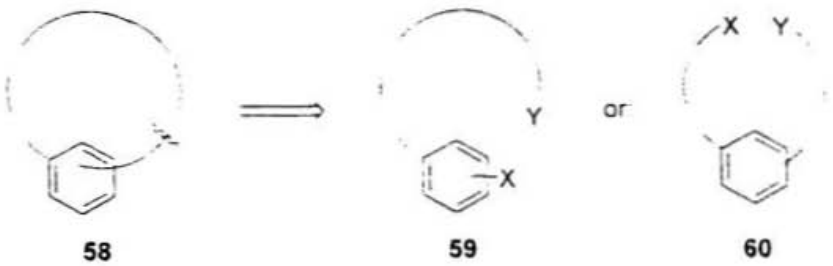

58 **59** **60**

Scheme 1.11: A retrosynthetic analysis of [*n*]cyclophanes.

The reluctance of conventional ring closure methodology to form small metacyclophanes and paracyclophanes is a result of the strain that is introduced in that step. When the bridge is smaller than 9 atoms in the paracyclophanes, or smaller than 8 atoms in the metacyclophanes, the bridges become too short to span the aromatic ring in its planar geometry. The benzene ring is then forced to adopt a boat-shaped geometry to accommodate the short bridge.

The degree to which the benzene ring of a cyclophane is distorted is a function of the length of the bridge and has traditionally been described with the parameters α and β (Figure 1.15). The angle α describes the degree to which the aromatic ring is distorted from planarity and β describes the degree to which the aromatic bridgehead carbon is distorted from planarity. The angles can be measured from calculated or crystallographically determined structures as follows.[21,61,63] A plane "c" is defined as the mean plane formed by four aromatic carbons C^A, C^B, C^D and C^E (the atoms C^C and C^F that form the "tips" or "bows" of the boat are excluded; Figure 1.15). Plane "a" is then defined by the plane of an "adjoining flap" (atoms C^B, C^C and C^D or atoms C^E, C^F and C^A) and a line "b" is defined as the line that is formed by connecting the benzylic carbon atom with a neighboring aromatic bridgehead carbon. The smallest angle that plane "a" makes with plane "c" is defined as α. Angle β is then defined by the smallest angle between plane "a" and line "b" (in paracyclophanes) or by the smallest angle between line "b" and plane "c" (in metacyclophanes), whichever is smaller.

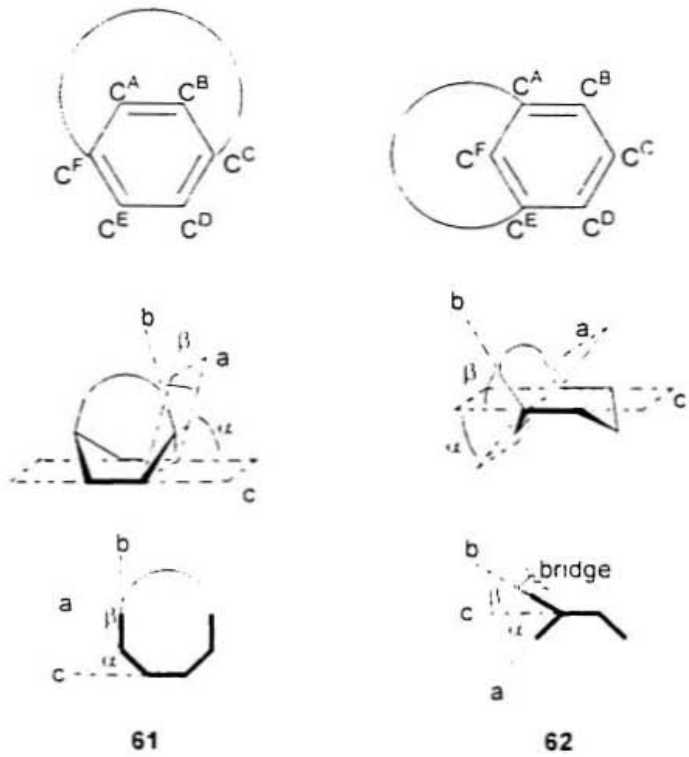

61 62

Figure 1.15: Definition of α and β angles in cyclophanes.

Scheme 1.12 gives examples of two approaches to the synthesis of cyclophanes *via* formation of the aromatic nucleus. In the first example the precursor for cyclophane formation, compound **63**, possesses a strained cyclopropane ring.[64,65] The strain energy in the cyclopropane ring, combined with the energetic advantage of aromatization in the last step, has made this approach a successful one for several [5]metacyclophanes. The reactive intermediate for formation of the aromatic ring can also be generated *in situ*, as illustrated by the synthesis of **69** from **66**.[66] In this example, carbene **68** is the highly reactive species that will lead to the desired product in the aromatization step. The disadvantage of this approach is, that in order to form the reactive intermediate, harsh

conditions are often needed. In the first approach the strain in the synthetic precursor allows for mild reaction conditions to be used in the last step. This has the advantage that a wide range of functional groups is tolerated, and labile reaction products can still be isolated.

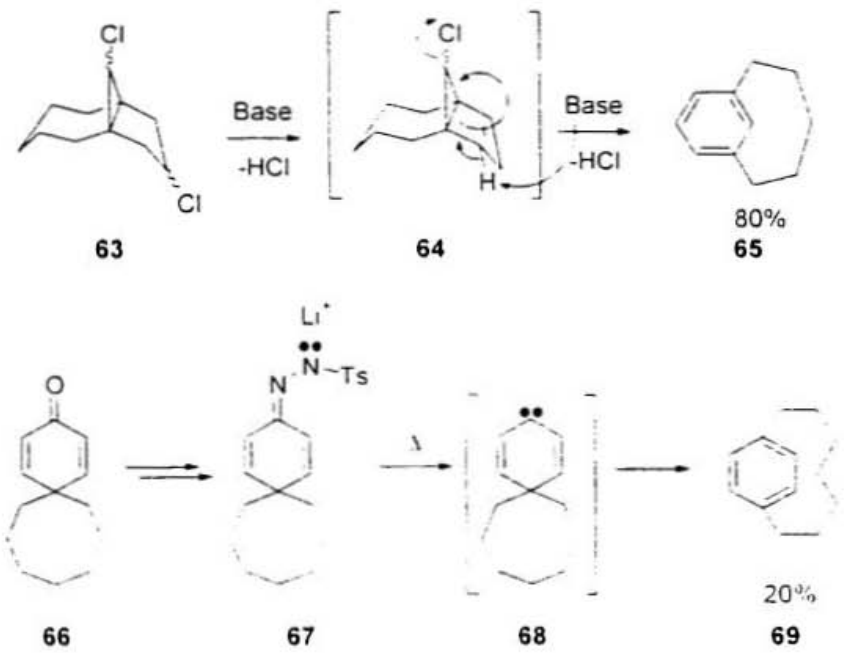

Scheme 1.12: Syntheses of [5]metacyclophane **65**[61,64] and [7]paracyclophane **69**.[70]

A different synthetic approach to the synthesis of cyclophanes has been based on ring contraction reactions (Scheme 1.13). The systems that have been synthesized using this type of methodology are not as strained as the systems that can be formed using the approach just described. Ring contraction (Wolff rearrangement) has been used in the synthesis of [7]paracyclophane system **71** from **70**.[67,68] The ring contraction is highly

exothermic due to the loss of N_2, which supplies the required energy to the system to form the strained cyclophane system. Wolff rearrangement was not successful for the synthesis of the lower homologue (6-carbon bridge),[28] which illustrates a limitation of this approach.

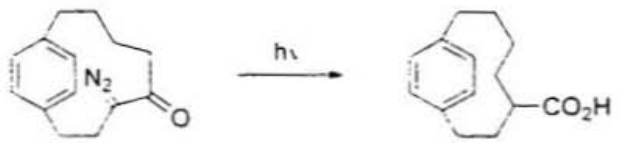

70 **71**

Scheme 1.13: Synthesis of [7]paracyclophane derivative **71**.

Some more commonly used ring contraction methodologies are illustrated in Scheme 1.14. The 2,11-dithia[3.3]metacyclophane system **48** is used as an example because of its direct relation to work described later in this thesis. Photolysis of **48** in a trialkyl phosphite as the solvent leads to ring contraction and loss of the sulfur atoms to provide [2.2]metacyclophane **72** and $(RO)_3P{=}S$.[69-71] This contraction likely occurs by a stepwise radical mechanism, in which the newly formed C-C bond is formed by the combination of two radicals. [2.2]Metacyclophane **72** can also be formed *via* oxidation of the thioether bridges in **48** to give disulfone **73**, which can be ring contracted using thermal SO_2 extrusion.[74] Again, a stepwise process that involves radicals is presumably in operation. Ring contraction of dithiacyclophane **48** can also be achieved using Wittig[75-77] or Stevens[75,78-80] rearrangement to give ring contracted products **74**. Compound **74** can be reduced using Raney nickel/H_2 to give **72**. Elimination of a suitably modified derivative

of **74** can lead to [2.2]metacyclophanediene **75**.[78,81] which can be hydrogenated to yield **72**.[78] Cyclophanediene **75** undergoes valence isomerization to form 10*b*,10*c*-dihydropyrene **76**.[82] which can easily undergo dehydrogenation to give pyrene **77**.[75] This valence isomerization – dehydrogenation (VID) sequence can therefore be used for the synthesis of polycyclic aromatic hydrocarbons[75] and is the basis for the majority of the work described in this thesis (see also Section 1.4 and Chapters 3 - 5).

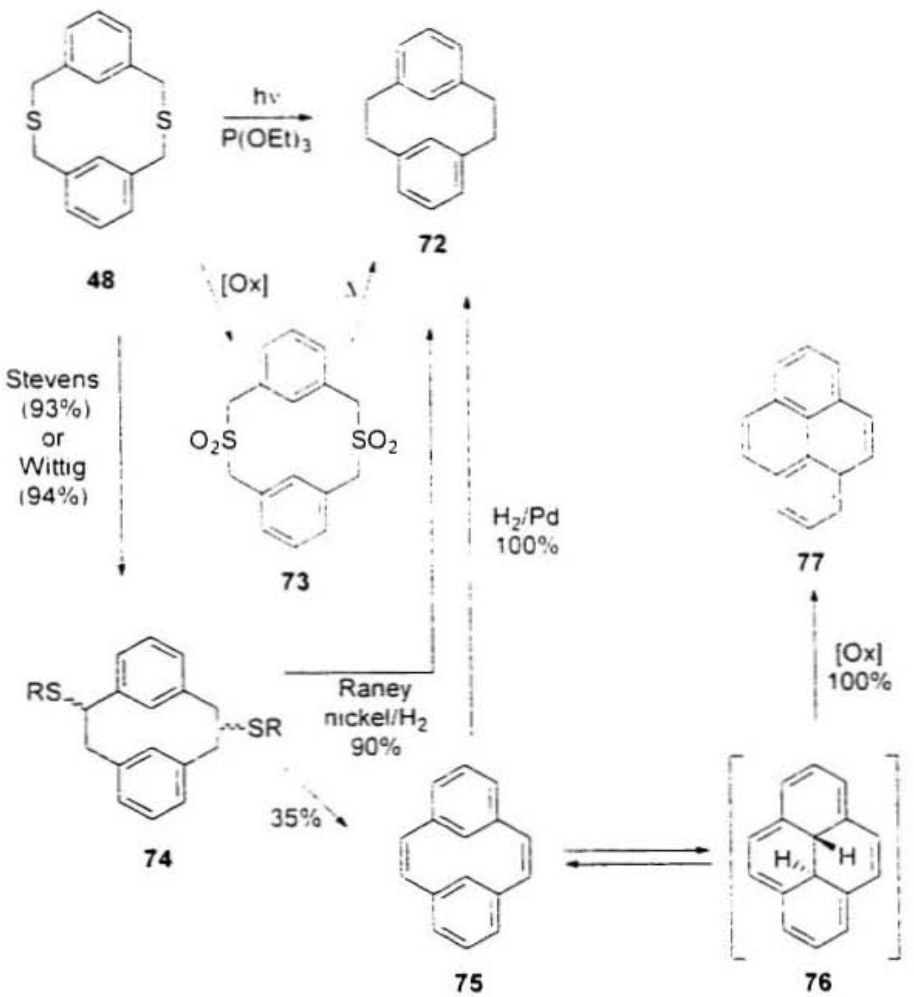

Scheme 1.14: Ring contractions of **48**.

Over the past decades, chemists have attempted to synthesize cyclophanes with the shortest possible bridges. For the paracyclophane system, this has led to the synthesis and isolation of [6]paracyclophane derivatives[83-86] and synthesis and isolation of [5]paracyclophane derivatives,[87-91] but no X-ray crystal structures could be obtained due to the low stability of these phanes. Attempted syntheses of [4]paracyclophanes have suffered from decomposition of the desired products at low temperatures[92-96] and only one successful isolation of a [4]paracyclophane has been reported.[97] The X-ray crystal structure of an unusually stable [1.1]paracyclophane **79** (Scheme 1.15) has been reported by Tsuji.[98,99] Cyclophane **79** was generated *via* photoisomerization of a Dewar benzene **78**. The [1.1]paracyclophane moiety in **79** readily underwent a unique transannular addition to form **80**, which illustrates the effect of the strain in **79** on its reactivity. Cyclophane **79** has α angles of 24.3° and 25.6° and β values of 22.9° and 26.8°.

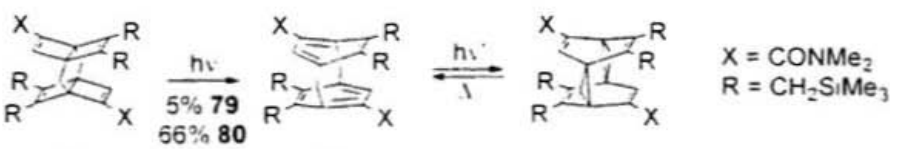

78 **79** **80**

Scheme 1.15: [1.1]Paracyclophane **79**.

Small metacyclophanes are much less abundant in the literature than are the paracyclophanes. Bickelhaupt *et al.* have reported the synthesis and reactivity of several [5]metacyclophanes **81**.[64,65,100-106] They also reported the observation of [4]metacyclophane **82** at –60 °C[107] and claimed the existence of a [1.1]metacyclophane

83 as "a highly strained aromatic intermediate".[108] X-ray crystal data for 8,11-dichloro[5]metacyclophane (**81**: X = CH_2, Y = Cl) showed an α angle of 22.2° and a β angle of 40.9°.

81 **82** **83**

Figure 1.16: Structures of selected metacyclophanes.

1.3.3 [2.2]Phanes

A group of phanes that forms a large portion of the total number of known cyclophanes, is the [2.2]phanes.[21,51,63,109] The classical method for the synthesis of [2.2]paracyclophane **88** is based on a dimerization of a *p*-xylylene derivative **87**. This (formal) [6+6] dimerization is not allowed according to the Woodward-Hoffmann rules and presumably proceeds by a stepwise mechanism.[110,111] *In situ* generation of *p*-xylylene compounds can be performed on large scale *via* Hofmann elimination of an ammonium salt **84**[112,113] or Diels-Alder reaction of a 1,2,4,5-hexatetraene (e.g. **85**) and an alkyne (e.g. **86**).[114]

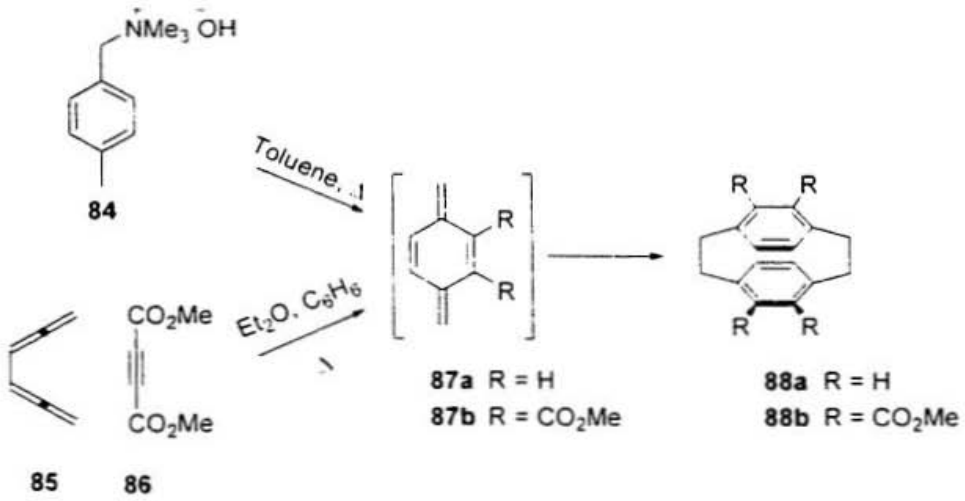

Scheme 1.16: Dimerization of *p*-xylylenes to give [2.2]paracyclophanes.

This dimerization approach has been applied in the synthesis of several interesting [2.2]phanes (Figure 1.17). [2.2](1,4)Naphthalenophane **89** was synthesized using this approach.[115,116] as were [2.2](9,10)anthracenophane **90**[117,118] and [2.2](1,4)anthracenophane **91**.[119] Cyclophanes **89** and **90** were among the first reported phanes that were based on polycyclic aromatic hydrocarbons.[120]

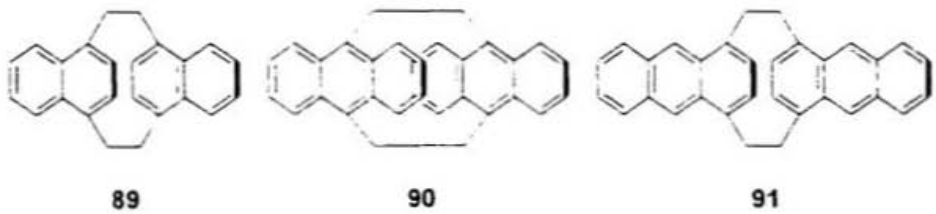

Figure 1.17: Structures of some [2.2]phanes.

The *p*-xylylene dimerization approach is specific for the synthesis of phanes with 1,4-positioning of the bridges and cannot be applied to the synthesis of [2.2]metacyclophanes **72**. [2.2]Metacyclophanes are synthesized most conveniently *via* the ring contraction methodology that was discussed in Section 1.3.2. A useful alternative synthesis is the reductive (Wurtz) coupling of benzylic dibromide **92** (Scheme 1.17).[121-125]

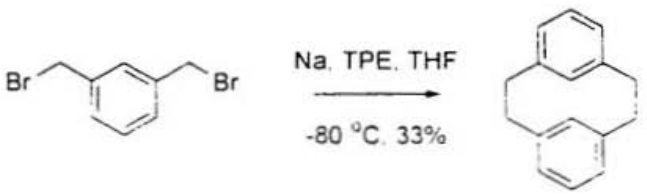

92 **72**

Scheme 1.17: Wurtz coupling to give [2.2]metacyclophane **72**.

A unique method for the synthesis of [*n*.2]phanes ($n \geq 2$) has been developed by Nishimura.[126-128] This methodology has not only led to the synthesis of some interesting [*n*.2]phanes but also to the synthesis of calixarenes and crown-ethers.[128] The key step in this approach is a [2+2]photocyclization of vinylarenes, and yields are usually reasonable if the reaction is performed in an intramolecular fashion (Scheme 1.18). Yields of the intermolecular variation are low when benzene is the aromatic nucleus of the reacting system (0 – 11%), but increased yields are observed with polycyclic aromatic systems (naphthalene 15 – 47%; phenanthrene 33 – 46%).[126]

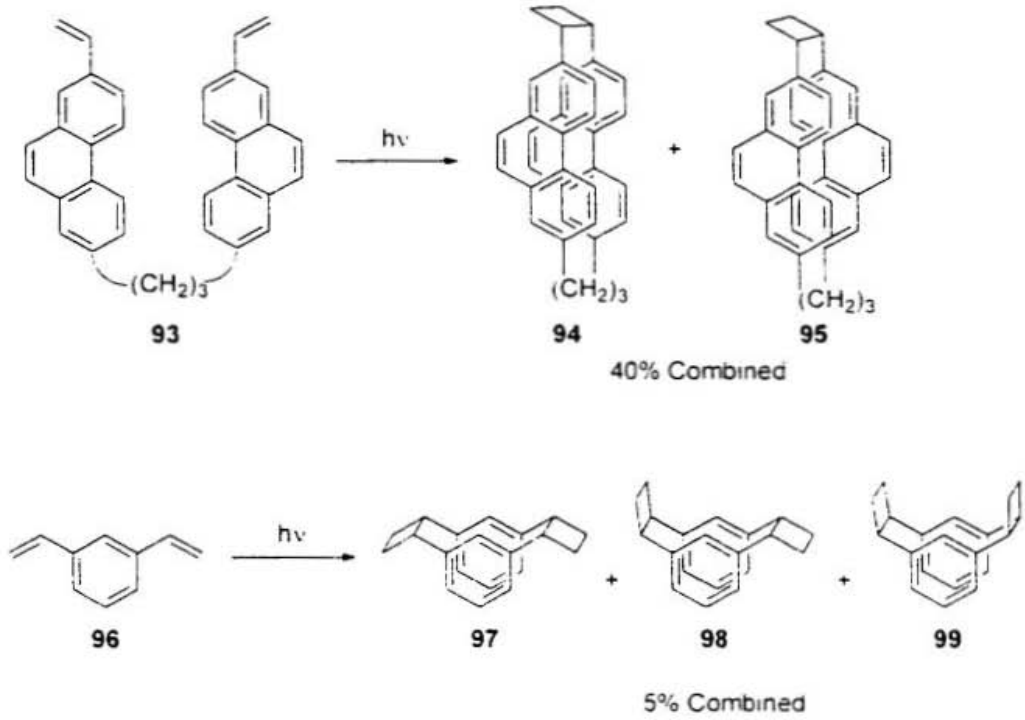

Scheme 1.18: [2+2]Photocyclization to give [*n*.2]phanes

The sulfur extrusion ring contraction methodology that has been used for the synthesis of [2.2]metacyclophane **72** has also led to the synthesis of [2.2]pyrenophanes **100** - **105**.[129-132]

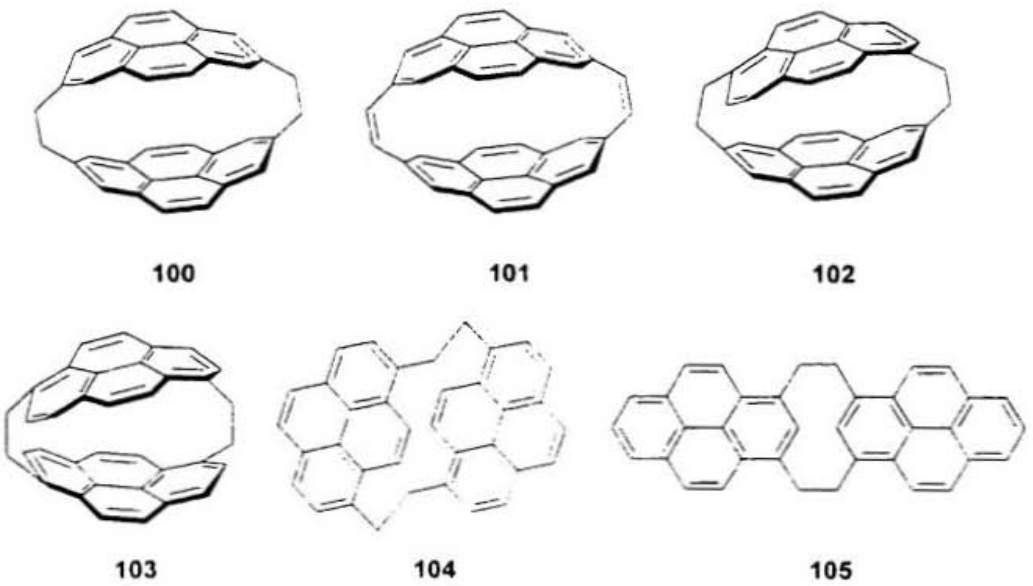

Figure 1.18: Structures of some pyrenophanes.

1.4 Nonplanar aromatic compounds: (2,7)pyrenophanes

Upon examination of the cyclophane literature in 1995, no *systematic* study of cyclophanes in which the curvature was spread over the full surface of a polycyclic aromatic system could be found. However, some interesting cyclophanes that contained nonplanar polycyclic aromatic hydrocarbons had been described (*vide supra*). In order to take advantage of traditional cyclophane methodology to enter the area of synthesis of fullerene fragments, a more thorough and systematic study of curved polycyclic aromatic compounds was initiated. The pyrene unit was selected as the aromatic nucleus for this project, as it maps onto the surface of some of the higher fullerenes (Figure 1.19). Based

on known cyclophane methodology (VID: Scheme 1.14), a potentially new entry into the synthesis of curved pyrenes was identified.

106 107 108

Figure 1.19: Structures of D_{2h}-C_{70} (**106**),[133,134] D_{5h}-C_{60} (**107**)[135] and D_{5h}-C_{41} (**108**).[136-138] Double bonds have been omitted for clarity.

In Section 1.3.2, two general approaches to the synthesis of cyclophanes with curved aromatic surfaces were described. The first approach used highly reactive intermediates (generated *in situ* or as precursors) for the formation of the aromatic moiety. The second approach used ring contraction to introduce or increase nonplanarity in the aromatic nucleus. At the outset of our work in this area it was anticipated that the first approach could be applied by using the valence isomerization-dehydrogenation (VID) sequence to form a (curved) pyrene unit from a cyclophanediene precursor (Scheme 1.14). A more detailed discussion of this approach is given in Section 1.4.1.

1.4.1 Retrosynthetic analysis of [*n*](2,7)pyrenophanes

Using curved pyrene units as the aromatic nucleus in cyclophanes, the synthetic target for the study of curved polycyclic aromatic compounds became the family of [*n*](2,7)pyrenophanes **109** (Scheme 1.19; *Z* represents a bridge/tether). The first step in the retrosynthetic direction of a cyclophane (based on the outlined approach) should remove (part of) the aromatic character that is present in **109**, so that in the synthetic direction the molecule is given the energetic incentive of aromatization to facilitate the final step. The retrosynthetic step can be achieved by breaking the central bond in the pyrene unit of **109** to give, *via* dihydropyrene **110**, a cyclophanediene **111**, which still contains the tether that was present in **109**. In pyrenophane **109** this tether was expected to cause the curvature of the pyrene unit, while in **111** this tether would force the metacyclophanediene unit to adopt a *syn* geometry.

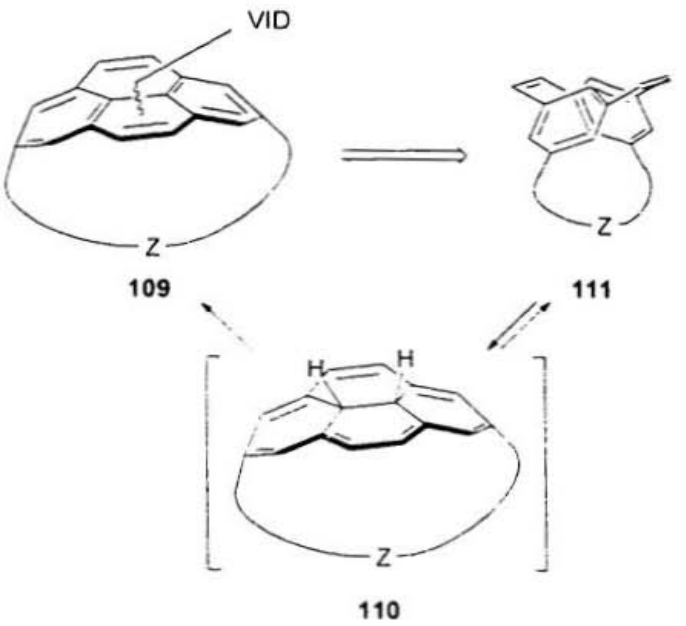

Scheme 1.19: Retrosynthetic analysis of a [2,7]pyrenophane **109** – Part I

The carbon atoms in **111** between which the central bond is formed in the synthetic direction are often referred to as the "internal" carbons and, similarly, the attached hydrogens are referred to as "internal" hydrogens. In the *syn* conformation of **111**, the internal carbon atoms are expected to be in close proximity, which should facilitate the desired valence isomerization to give a tethered *cis*-dihydropyrene **110**. This process is, at least in principle, reversible but **110** is expected to lose H_2 in an irreversible step. The dehydrogenation of **110** is expected to be much more facile than for the untethered *trans*-dihydropyrene system **76**, due to the *cis* orientation of the hydrogen atoms in **110**. Dehydrogenation of **76** had been reported to occur readily in the presence of oxygen. An X-ray crystal structure of a system very similar to **110** has been published[139]

(dioxadecamethylene tether) with methyl groups as substituents at the internal positions to prevent the irreversible dehydrogenation.

Based on the ring contraction methodology that was described in Section 1.3.2 (Scheme 1.14) a tethered cyclophanediene **111** can, retrosynthetically, lead to a tethered dithiacyclophane **112** by replacing the C-C double bonds with thioether linkages. The methodology in this area had been well developed by Boekelheide *et al.*,[78-82] and it was anticipated that the presence of the tether in **112** would not interfere with these transformations, provided certain functional groups were absent.

111 **112**

Scheme 1.20: Retrosynthetic analysis of a (2,7)pyrenophane **109** Part II.

The key functions of the tether in the system under consideration were the introduction of curvature to the pyrene nucleus in **109** and assurance of a *syn*-geometry in **111** to facilitate the VID sequence. For the *syn* geometry of dithiacyclophane **112**, the presence of the tether was not expected to be crucial, as Mitchell had shown the preference for the *syn* conformation of several untethered 2,11-dithia[3.3]metacyclophane systems.[140,141] This conformational preference of a 2,11-dithia[3.3]metacyclophane for a *syn*-

conformation is the basis for the next retrosynthetic cuts (route "a" in Scheme 1.21), in which the tether in **112** is cleaved to give a difunctionalized dithiacyclophane **113** and an acyclic building block **114**. Some initial synthetic investigations of this approach showed that synthesis of certain suitably difunctionalized dithiacyclophanes **113** was a nontrivial task and the route was eventually abandoned. As a result of these initial investigations, however, our group became interested in the conformational behavior of the 2,11-dithia[3.3]metacyclophane system. This interest has formed the basis of the work that will be presented in Chapter 2.

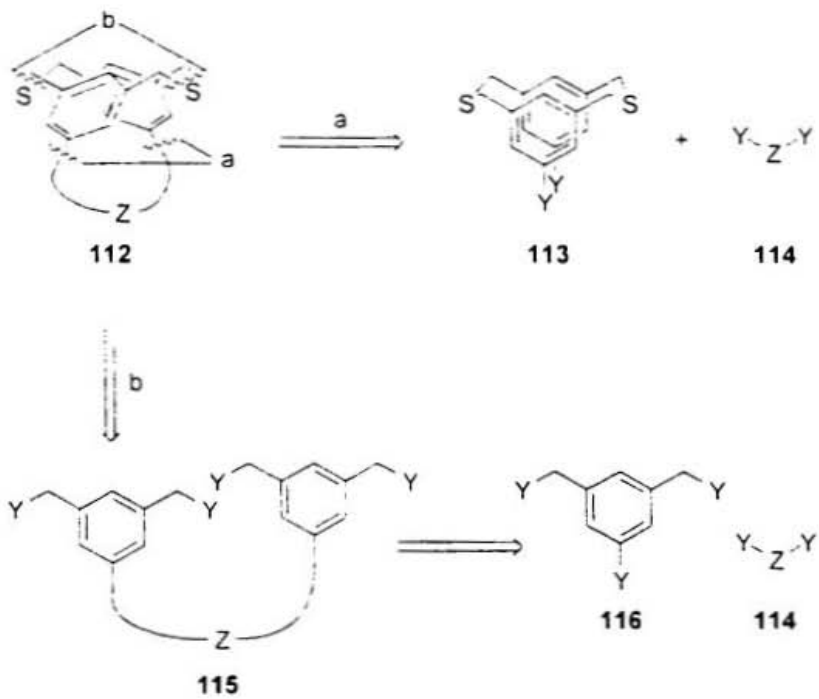

Scheme 1.21: Retrosynthetic analysis of a [2.7]pyrenophane **109** - Part III.

A complementary retrosynthetic approach to route "a" (Scheme 1.21) is first to cleave the thioether bridges that are present in dithiacyclophane **112**. This leads to an acyclic precursor **115**. Retrosynthetic analysis of **115** leads to cleavage of the tether to give two small building blocks **116** and **114**. In the synthetic direction the conditions for this transformation will depend on the nature of the tether. Preference for this route in the synthesis of **112** is based on the availability of Na_2S/Al_2O_3[142] as an efficient reagent for the cyclization of **115** to give **112**.

1.4.2 Synthesis of [*n*](2,7)pyrenophanes

The synthesis of several 1,n-dioxa[*n*](2,7)pyrenophanes **117** and [*n*](2,7)pyrenophanes **118** by our group has been reported in several publications.[143-148] Due to the great similarities of the syntheses, a general discussion will be given here. For a more detailed discussion the reader is referred to the individual papers.

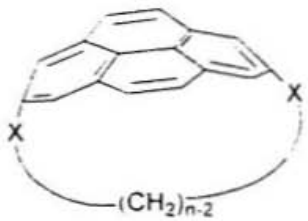

117 X = O
118 X = CH_2

Figure 1.20: Structure of pyrenophanes **117** and **118**.

Synthesis of **117** started with the coupling of dimethyl 5-hydroxyisophthalate **119** and α,ω-dibromoalkanes **121** to give tetraesters **123**. For the synthesis of the carba-phanes **118**, triflate **120** (available from triflation of **119**) was coupled with diynes **122** to give **124** after catalytic hydrogenation of the products. Hydride reduction of the esters was followed by treatment of the resulting alcohols with HBr and gave tetrabromides **125** and **126**. Treatment of the tetrabromides with Na_2S/Al_2O_3 gave dithiacyclophanes **127** and **128**.

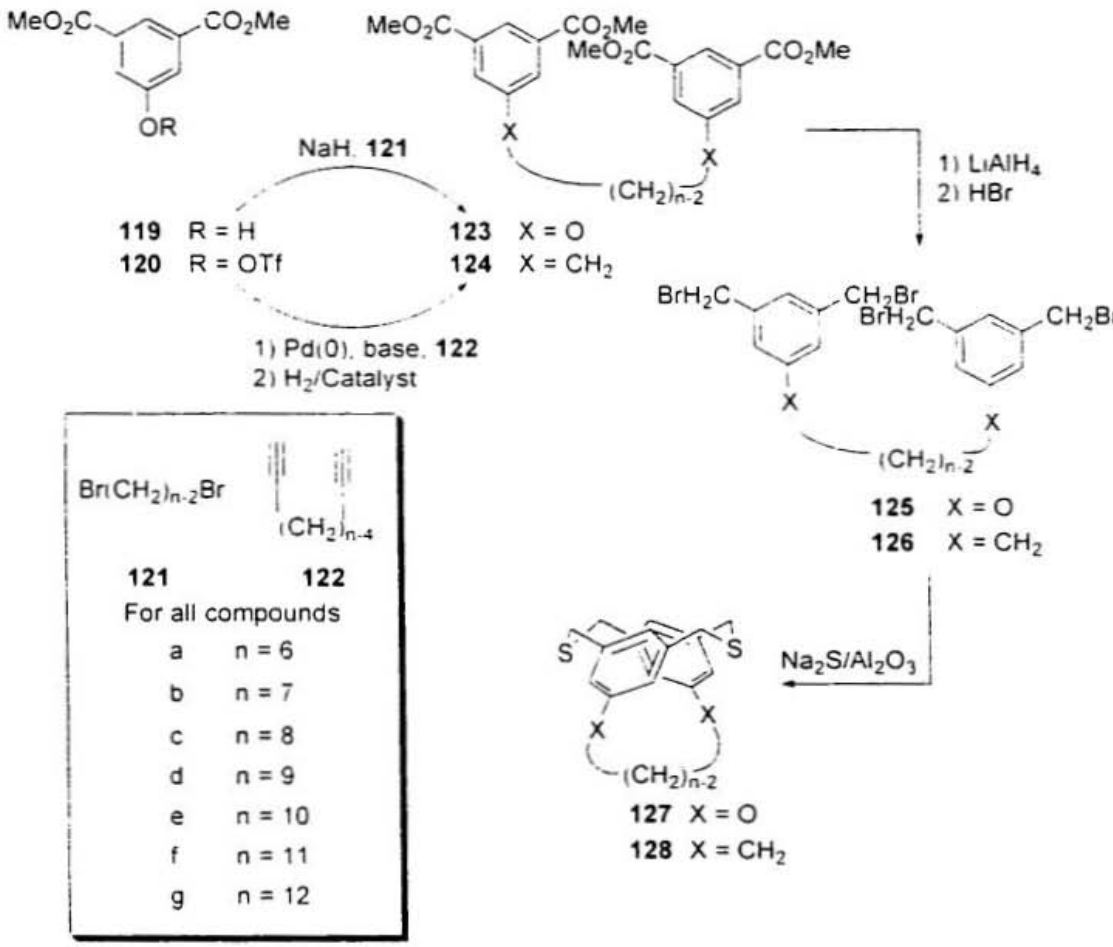

Scheme 1.22: Synthesis of dithiacyclophanes **127** and **128**.

Ring contraction of dithiacyclophanes **127** and **128** was performed to give bis(methylthio) ethers **129** and **130** (Scheme 1.23). Depending on the length of the tether, Hofmann elimination of **129** and **130** gave either cyclophanedienes **131** and **132** (**131a-c** and **132a-c**: 6 – 8 atom tethers) or a mixture of compounds, which could be converted to pyrenophanes **117** and **118** (**117d-g** and **118d**: 9 atoms or more in the tether). Treatment of dioxacyclophanedienes **131b** and **131c** and carba-cyclophanedienes **132b** and **132c** with DDQ led to the formation of the corresponding pyrenophanes **117b**, **117c**, **118b** and **118c**. Cyclophanedienes **131a** and **132a** did not form the corresponding pyrenophanes when treated with DDQ, although formation of **118a** as a fleeting intermediate has been claimed.[145]

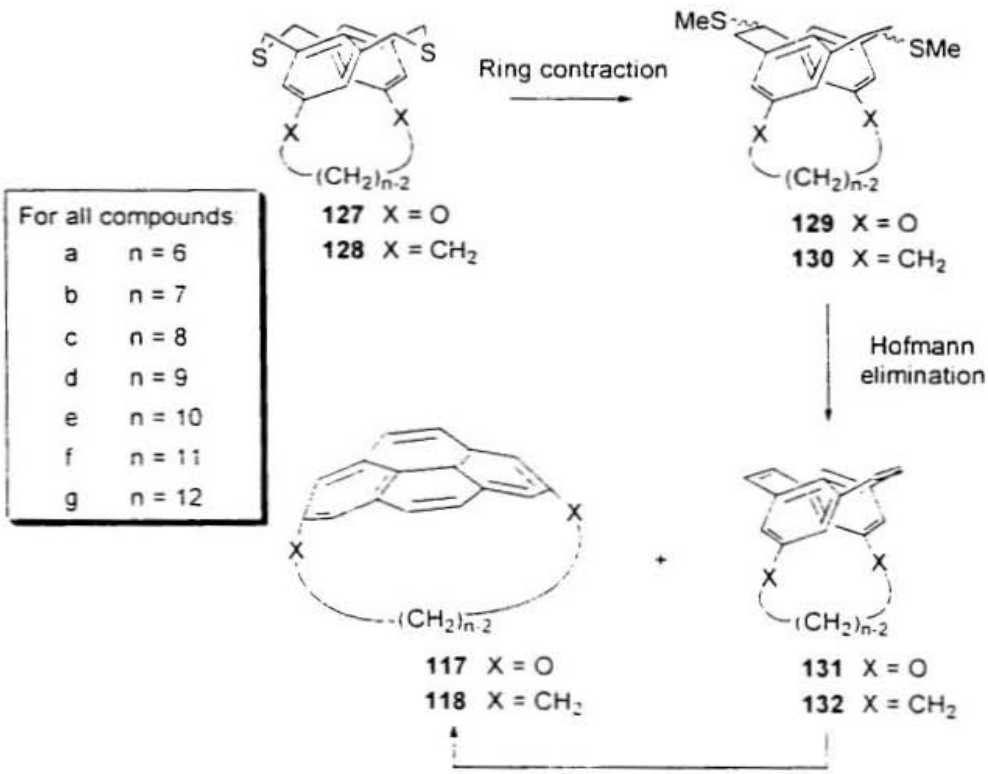

Scheme 1.23: Synthesis of pyrenophanes **117** and **118**.

1.4.3 Structure and properties of [*n*](2,7)pyrenophanes[143-145,148]

In the formation of pyrenophanes **117** and **118**, it was observed that relatively mild reaction conditions (DDQ in refluxing benzene) often sufficed to drive the reaction, although the process was slow for the lower homologues of the series. The reactivity of the pyrenophanes increased with decreasing tether length: some of the lower homologues readily underwent apparent Diels-Alder reaction with tetracyanoethylene (TCNE), while the higher homologues were unreactive under the same conditions (Scheme 1.24). When

dioxapyrenophane **117b** or **117c** was reacted with *t*-BuLi in an attempt to perform *ortho*-metallation, tether cleavage occurred. The next higher homologue **117d** was unreactive under the same conditions. Attempted bromination of carba-pyrenophane **118b** and treatment of **118b** with a strong Lewis acid ($AlCl_3$) led to the formation of complex mixtures.

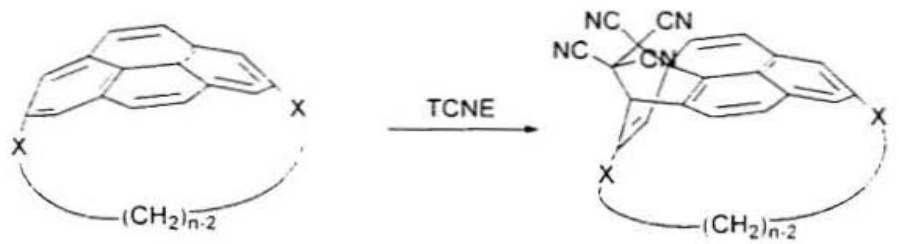

117b X = O
118b X = CH_2

133b X = O; *n* = 7
134b X = CH_2, *n* = 7

Scheme 1.24: Diels-Alder reaction of **117b** and **118b**

In the ^1H NMR data of the pyrenophanes, a clear trend could be seen for the chemical shift of the protons on the aromatic nucleus. On shortening of the tether, an upfield shift of these protons occurred in both series of pyrenophanes. Some of the protons in the tethers of **117** and **118** were shifted significantly upfield, which was attributed to the positioning of these protons in the shielding cone of the aromatic nucleus.

X-Ray crystal structures of **117b-g** and **118c** were determined, and they revealed the extended bend over the full length of the pyrene moiety. No suitable crystals of the other carba-pyrenophanes could be obtained, partly due to their high solubility. In order to be able to compare the degree of curvature, a bend angle (θ) was defined (Figure 1.21). The angle α that is used to describe distortions from planarity in cyclophanes with monocyclic aromatic nuclei is not appropriate for the description of distortions in the pyrene unit. However, the angle β that is used for the [*n*]paracyclophanes is still meaningful in case of the pyrenophanes. Table 1.01 gives AM1 calculated and experimental bend angles for selected pyrenophanes.

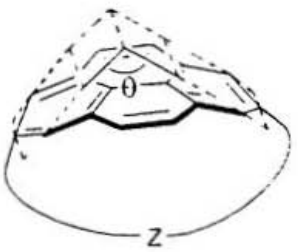

Figure 1.21: Definition of bend angle (θ) in a pyrenophane.

Tether length	**117**		**118**	
(series member)	$\theta_{X\text{-ray}}$	θ_{calcd}	$\theta_{X\text{-ray}}$	θ_{calcd}
6 (a)		132.1°		122.9°
7 (b)	109.2°	113.3°		104.5°
8 (c)	87.8°	94.9°	80.8°	87.0°
9 (d)	72.9°	77.8°		70.3°
10 (e)	57.7°	61.2°		
11 (f)	39.9°	46.6°		
12 (g)*	34.6°	33.1°		

Table 1.01: Calculated (AM1) and experimental bend angles for pyrenophanes **117** and **118**.

From the 1,*n*-dioxa[*n*](2,7)pyrenophane series, it can be seen from the X-ray data that the bend angle of the pyrene unit increased with decreasing tether length. The same trend was expected for the carba-pyrenophanes, although the true value could only be obtained for **118c**. AM1 calculations gave bend angles for both series that indicated the same trend

* In the X-ray crystal structure of **117g** showed disorder in one end of the tether suggesting large error in the experimental value.

as was observed from the available X-ray data. An important result from the calculated and measured bend angles is that the calculations consistently overestimated the bend angle by 4-7°, so they seemed to be useful as a predictive tool.

The most bent pyrenophane that was stable enough to be isolated (**117b**; $\theta_{X\text{-}ray}$ = 109.2°) had a calculated bend angle of 113.3°, while attempts to isolate pyrenophane **118a** with a calculated bend angle of 122.9° were unsuccessful. These results provided a useful tool to design future synthetic targets, as compounds with calculated bend angles larger than *ca.* 115 - 120° were not likely to be accessible *via* the VID protocol. An attempt to narrow this gray area of 115 - 120° led to the attempted synthesis of **135** (θ_{calcd} = 117.2°), but only a trace amount could be isolated.[14b] Synthesis of **136**, as predicted correctly by the calculations (θ_{calcd} = 108.3°), was more successful and from the X-ray data a bend angle of 102.9° was determined.

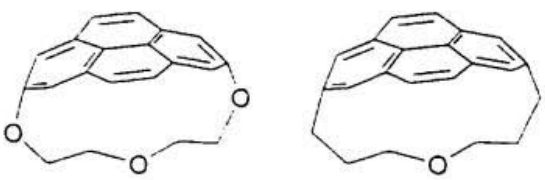

135 **136**

Figure 1.22: Structure of pyrenophanes **135** and **136**.

1.5 Outline of this thesis

In the strategy for the synthesis of fullerene fragments using our cyclophane methodology, functionalization of pyrenophanes **117b** and **118b** was shown to be inefficient as no selectivity for the formation of desired ring-functionalized products was observed. It was therefore decided to attempt syntheses of pyrenophanes with additional functionality in the tether. As the ultimate goal of this approach was to synthesize large fragments of fullerenes, attention was focused on the incorporation of aromatic rings in the tether. Target pyrenophanes were identified with aromatic rings incorporated in such a manner that the total aromatic component of the hypothetical pyrenophane would map onto the surface of (some of) the fullerenes. Table 1.02 gives the structure and calculated bend angles of the compounds that will be described in this thesis.

Structure of compound	Compound number	θ_{calcd}[149]
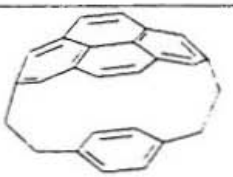	**137**	100.4°
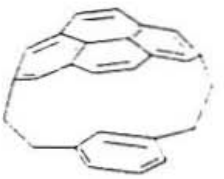	**138**	106.6°
	**139**	114.4°
	**140a** (n = 0)	108.8° per pyrene unit
	140b (n = 1)	90.3° per pyrene unit

Table 1.02: Structure and calculated bend angle of selected pyrenophanes.

Compounds **137** and **138** can be viewed as [*n*](2,7)pyrenophanes in which part of the aliphatic tether has been replaced by a single aromatic ring. These pyrenophanes do not directly map onto the surface of the fullerenes, but are still related to the ultimate goal. The calculated bend angles of 100.4° and 106.6° for **137** and **138**, respectively, are well

within the limits of the VID approach (pyrenophanes with θ_{calcd} = 104.5°,[143] 108.3°[146] and 113.3°[144] have been synthesized: *vide supra*). Efforts in the syntheses of these systems will be described in Chapter 5.

In compound **139** two *p*-phenylene units have been incorporated in the tether. This pyrenophane is substantially closer to a fully aromatic belt (**140a**) than compound **137**. Pyrenophane **139** has a calculated bend angle of 114.4° and the aromatic portion of **139** maps onto the surface of the fullerenes D_{5h}-C_{70}, D_{5d}-C_{80} and D_{6h}-C_{84}. The θ_{calcd} value is slightly higher than θ_{calcd} for the most curved pyrenophane that had been isolated at that point in time (**117b**: θ_{calcd} = 133.3°) and thus constitutes, in principle, a useful system for further development of a calculation-based prediction method for curvature in pyrenophanes. Efforts toward the synthesis of **139** will be described in Chapter 3.

Chapter 4 of this thesis will describe a synthetic approach to the assembly of a fully aromatic belt **140b**. In this compound the tether of a [*n*](2,7)pyrenophane has been replaced by an aromatic system and, as such, the tether becomes indistinguishable from the pyrene nucleus. Values of θ_{calcd} for the individual pyrene units in **140b** are approximately 90.3°, which suggests these pyrene nuclei might be formed using the VID protocol.

1.6 References

(1) Kroto, H. W.; Heath, J. R.; O'Brien, S. C.; Curl, R. F.; Smalley, R. E. *Nature* **1985**, *318*, 162-163.

(2) Stankevich, I. V.; Nikerov, M. V.; Bochvar, D. A. *Russ. Chem. Rev. (Engl. Transl.)* **1984**, *53*, 640-655.

(3) Jones, D. E. H. *New Sci.* **1966**, *32*, 245.

(4) Osawa, E. *Kagaku (Kyoto)* **1970**, *25*, 854-863.

(5) Yoshida, Z.; Osawa, E. *Aromaticity*; Kyoto, 1971; p 174.

(6) Bochvar, D. A.; Gal'pern, E. G. *Dokl. Akad. Nauk SSSR* **1973**, *209*, 610-612.

(7) Davidson, R. A. *Theor. Chim. Acta* **1981**, *58*, 193-231.

(8) Diederich, F.; Rubin, Y. *Angew. Chem., Int. Ed. Engl.* **1992**, *31*, 1101-1264 and references therein.

(9) Fitzer, E. *Carbon Fibers and Their Composites*; Springer: Berlin, 1985.

(10) Reisch, M. C. *Chem. Eng. News* **1987**, *65*, 621.

(11) Thayer, A. M. *Chem. Eng. News* **1990**, *68*, 37.

(12) Fitzer, E. *Carbon* **1989**, *27*, 621.

(13) Kroto, H. W.; Allaf, A. W.; Balm, S. P. *Chem. Rev.* **1991**, *91*, 1213.

(14) Krätschmer, W.; Lamb, L. D.; Fostiropoulos, K.; Huffman, D. R. *Nature* **1990**, *347*, 354-358.

(15) Faust, R. *Angew. Chem., Int. Ed. Engl.* **1998**, *37*, 2825-2828 and references therein.

(16) McElvany, S. W.; Ross, M. M.; Goroff, N. S.; Diederich, F. *Science* **1993**, *259*, 1594-1596.

(17) Rubin, Y.; Kahr, M.; Knobler, C. B.; Diederich, F.; Wilkins, C. L. *J. Am. Chem. Soc.* **1991**, *113*, 495-500.

(18) Goroff, N. S. *Acc. Chem. Res.* **1996**, *29*, 77-83.

(19) Bunz, U. H. F.; Rubin, Y.; Tobe, Y. *Chem. Soc. Rev.* **1999**, *28*, 107-119.

(20) Tobe, Y.; Nakagawa, N.; Kishi, J.-Y.; Sonoda, M.; Naemura, K.; Wakabayashi, T.; Shida, T.; Achiba, Y. *Tetrahedron* **2001**, *57*, 3629-3636.

(21) Hopf, H. *Classics in Hydrocarbon Chemistry*; Wiley-VCH: Weinheim, 2000.

(22) Barth, W. E.; Lawton, R. G. *J. Am. Chem. Soc.* **1966**, *88*, 380-381.

(23) Barth, W. E.; Lawton, R. G. *J. Am. Chem. Soc.* **1971**, *93*, 1730-1745.

(24) Scott, L. T.; Hashemi, M. M.; Meyer, D. T.; Warren, H. B. *J. Am. Chem. Soc.* **1991**, *113*, 7082-7084.

(25) Scott, L. T.; Hashemi, M. M.; Bratcher, M. S. *J. Am. Chem. Soc.* **1992**, *114*, 1920-1921.

(26) Brown, R. F. C. *Eur. J. Org. Chem.* **1999**, 3211-3222.

(27) Borchardt, A.; Fuchicello, A.; Kilway, K. V.; Baldridge, K. K.; Siegel, J. S. *J. Am. Chem. Soc.* **1992**, *114*, 1921-1923.

(28) Zimmermann, G.; Nuechter, U.; Hagen, S.; Nuechter, M. *Tetrahedron Lett.* **1994**, *35*, 4747-4750.

(29) Liu, C. Z.; Rabideau, P. W. *Tetrahedron Lett.* **1996**, *37*, 3437-3440.

(30) Mehta, G.; Panda, G. *Tetrahedron Lett.* **1997**, *38*, 2145-2148.

(31) Seiders, T. J.; Baldridge, K. K.; Siegel, J. S. *J. Am. Chem. Soc.* **1996**, *118*, 2754-2755.

(32) Mannion, M. R. Ph.D. Dissertation, Memorial University of Newfoundland, **1999**. 83-114 and references therein.

(33) Necula, A.; Scott, L. T. *J. Anal. Appl. Pyrolysis* **2000**, *54*, 65-87.

(34) Mehta, G.; Shah, S. R.; Ravikumar, K. *J. Chem. Soc., Chem. Commun.* **1993**, 1006-1008.

(35) Sastry, G. N.; Jemmis, E. D.; Mehta, G.; Shah, S. R. *J. Chem. Soc., Perkin Trans. 2* **1993**, 1867-1871.

(36) Hagen, S.; Bratcher, M. S.; Erickson, M. S.; Zimmermann, G.; Scott, L. T. *Angew. Chem., Int. Ed. Engl.* **1997**, *36*, 406-408.

(37) Scott, L. T.; Bratcher, M. S.; Hagen, S. *J. Am. Chem. Soc.* **1996**, *118*, 8743-8744.

(38) Ansems, R. B. M.; Scott, L. T. *J. Am. Chem. Soc.* **2000**, *122*, 2719-2724.

(39) Sygula, A.; Rabideau, P. W. *J. Am. Chem. Soc.* **1998**, *120*, 12666-12667.

(40) Sygula, A.; Marcinow, Z.; Fronczek, F. R.; Guzei, I.; Rabideau, P. W. *J. Chem. Soc., Chem. Commun.* **2000**, *48*, 2439-2440.

(41) Sygula, A.; Rabideau, P. W. *J. Am. Chem. Soc.* **1999**, *121*, 7800-7803.

(42) Sygula, A.; Xu, G. P.; Marcinow, Z.; Rabideau, P. W. *Tetrahedron* **2001**, *57*, 3637-3644.

(43) Reisch, H. A.; Bratcher, M. S.; Scott, L. T. *Org. Lett.* **2000**, *2*, 1427-1430.

(44) Wang, L.; Shevlin, P. B. *Org. Lett.* **2000**, *2*, 3703-3705.

(45) Jemmis, E. D.; Sastry, G. N.; Mehta, G. *J. Chem. Soc., Perkin Trans. 2* **1994**, 437-441.

(46) Plater, M. J. *Tetrahedron Lett.* **1994**, *35*, 6147-6150.

(47) Sarobe, M.; Zwikker, J. W.; Snoeijer, J. D.; Wiersum, U. E.; Jenneskens, L. W. *J. Chem. Soc., Chem. Commun.* **1994**, 89-90.

(48) Scott, L. T.; Necula, A. *J. Org. Chem.* **1996**, *61*, 386-388.

(49) Baldridge, K. K.; Battersby, T. R.; Vernonclark, R.; Siegel, J. S. *J. Am. Chem. Soc.* **1997**, *119*, 7048-7054.

(50) Brown, C. J.; Farthing, A. C. *Nature* **1949**, *164*, 915-916.

(51) Brown, C. J. *J. Chem. Soc.* **1953**, 3265-3270.

(52) Cram, D. J.; Steinberg, H. *J. Am. Chem. Soc.* **1951**, *73*, 5691-5704.

(53) Schubert, W. M.; Sweeney, W. A.; Latourette, H. K. *J. Am. Chem. Soc.* **1954**, *76*, 5462-5466.

(54) Cram, D. J.; Abell, J. *J. Am. Chem. Soc.* **1955**, *77*, 1179-1186.

(55) Vögtle, F.; Neumann, P. *Tetrahedron Lett.* **1969**, *60*, 5329-5334.

(56) Vögtle, F.; Neumann, P. *Tetrahedron* **1970**, *26*, 5847-5863.

(57) The rules in phane-nomenclature were numbered by Vögtle as follows: P-1 describes the phanes as a class of compounds. P-2 describes cyclophanes with only aromatic bridgehead atoms. P-3 describes numbering of the phanes. P-4 describes cyclophanes that contain aromatic as well as aliphatic bridgehead atoms. P-5 gives the priority rules for nomenclature and numbering of phanes and P-6 describes the naming of metallocenophanes. This thesis will apply the same numbering.

(58) Hohner, G.; Vögtle, F. *Chem. Ber.* **1977**, *110*, 3052-3077.

(59) Josten, W.; Neumann, S.; Vögtle, F.; Hägele, K.; Przybylski, M.; Beer, F.; Müllen, K. *Chem. Ber.* **1994**, *127*, 2089-2096.

(60) Bickelhaupt, F.; Dewolf, W. H. *J. Phys. Org. Chem.* **1998**, *11*, 362-376.

(61) *Cyclophanes, Vols. 1 and 2*; Keehn, P. M., Rosenfeld, S. M., eds.; Academic Press: New York, 1983.

(62) Vögtle, F. *Cyclophan-Chemie*; B. G. Teubner: Stuttgart, 1990.

(63) Diederich, F. *Cyclophanes*; Royal Society of Chemistry: London, 1991.

(64) van Eis, M. J.; Wijsman, G. W.; de Wolf, W. H.; Bickelhaupt, F.; Rogers, D. W.; Kooijman, H.; Spek, A. L. *Chem. Eur. J.* **2000**, *6*, 1537-1546.

(65) Van Straten, J. W.; de Wolf, W. H.; Bickelhaupt, F. *Tetrahedron Lett.* **1977**, 4667-4670.

(66) Wolf, A. D.; Kane, V. V.; Levin, R. H.; Jones Jr., M. *J. Am. Chem. Soc.* **1973**, *95*, 1680.

(67) Allinger, N. L.; Walter, T. J. *J. Am. Chem. Soc.* **1972**, *94*, 9267-9268.

(68) Newton, M. G.; Walter, T. J.; Allinger, N. L. *J. Am. Chem. Soc.* **1973**, *95*, 5652-5658.

(69) Boekelheide, V.; Reingold, I. D.; Tuttle, M. *J. Chem. Soc., Chem. Commun.* **1973**, 406-407.

(70) Bruhin, J.; Jenny, W. *Tetrahedron Lett.* **1973**, 1215-1218.

(71) Umemoto, T.; Otsubo, T.; Misumi, S. *Tetrahedron Lett.* **1974**, 1573-1576.

(72) Fukazawa, Y.; Aoyagi, M.; Ito, S. *Tetrahedron Lett.* **1978**, 1067-1070.

(73) Corey, E. J.; Block, E. *J. Org. Chem.* **1969**, *34*, 1233-1240.

(74) Vögtle, F.; Schunder, L. *Chem. Ber.* **1969**, *102*, 2677-2683.

(75) Mitchell, R. H. *Heterocycles* **1978**, *11*, 563-586.

(76) Mitchell, R. H.; Otsubo, T.; Boekelheide, V. *Tetrahedron Lett.* **1975**, 219-222.

(77) Boekelheide, V.; Tsai, C.-H. *Tetrahedron* **1976**, *32*, 423-425.

(78) Mitchell, R. H.; Boekelheide, V. *J. Am. Chem. Soc.* **1974**, *96*, 1547-1557.

(79) Otsubo, T.; Boekelheide, V. *Tetrahedron Lett.* **1975**, *45*, 3881-3884.

(80) Otsubo, T.; Boekelheide, V. *J. Org. Chem.* **1977**, *42*, 1085-1087.

(81) Mitchell, R. H.; Boekelheide, V. *Tetrahedron Lett.* **1970**, 1197-1202.

(82) Mitchell, R. H.; Boekelheide, V. *J. Am. Chem. Soc.* **1970**, *92*, 3510-3512.

(83) Kammula, S. L.; Iroff, L. D.; Jones Jr., M.; Van Straten, J. W.; de Wolf, W. H.; Bickelhaupt, F. *J. Am. Chem. Soc.* **1977**, *99*, 5815.

(84) Van Straten, J. W.; Turkenburg, L. A. M.; de Wolf, W. H.; Bickelhaupt, F. *Recl. Trav. Chim. Pays-Bas* **1985**, *104*, 89-97.

(85) Tobe, Y.; Kakiuchi, K.; Odaira, Y.; Hosaki, T.; Kai, Y.; Kasai, N. *J. Am. Chem. Soc.* **1983**, *105*, 1376-1377.

(86) Tobe, Y.; Nakayama, A.; Kakiuchi, K.; Odaira, Y.; Kai, Y.; Kasai, N. *J. Org. Chem.* **1987**, *52*, 2639-2644.

(87) Jenneskens, L. W.; de Kanter, F. J. J.; Kraakman, P. A.; Turkenburg, L. A. M.; Koolhaas, W. E.; de Wolf, W. H.; Bickelhaupt, F.; Tobe, Y.; Kakiuchi, K.; Odaira, Y. *J. Am. Chem. Soc.* **1985**, *107*, 3716-3717.

(88) Tobe, Y.; Kaneda, T.; Kakiuchi, K.; Odaira, Y. *Chem. Lett.* **1985**, 1301-1304.

(89) Van Straten, J. W.; de Wolf, W. H.; Bickelhaupt, F. *Recl. Trav. Chim. Pays-Bas* **1977**, *96*, 88.

(90) Kostermans, G. B. M.; de Wolf, W. H.; Bickelhaupt, F. *Tetrahedron Lett.* **1986**, *27*, 1095-1098.

(91) Kostermans, G. B. M.; de Wolf, W. H.; Bickelhaupt, F. *Tetrahedron* **1987**, *43*, 2955-2966.

(92) Tsuji, T.; Nishida, S. *J. Chem. Soc., Chem. Commun.* **1987**, 1189-1190.

(93) Kostermans, G. B. M.; Bobeldijk, M.; de Wolf, W. H.; Bickelhaupt, F. *J. Am. Chem. Soc.* **1987**, *109*, 2471-2475.

(94) Tsuji, T.; Nishida, S. *J. Am. Chem. Soc.* **1988**, *110*, 2157-2164.

(95) Tsuji, T.; Nishida, S. *J. Am. Chem. Soc.* **1989**, *111*, 368-369.

(96) Tsuji, T.; Nishida, S.; Okuyama, M.; Osawa, E. *J. Am. Chem. Soc.* **1995**, *117*, 9804-9813.

(97) Okuyama, M.; Tsuji, T. *Angew. Chem., Int. Ed. Engl.* **1997**, *36*, 1085-1086.

(98) Kawai, H.; Suzuki, T.; Ohkita, M.; Tsuji, T. *Chem. Eur. J.* **2000**, *6*, 4177-4187.

(99) Kawai, H.; Suzuki, T.; Ohkita, M.; Tsuji, T. *Angew. Chem., Int. Ed. Engl.* **1998**, *37*, 817-819.

(100) van Eis, M. J.; de Kanter, F. J. J.; de Wolf, W. H.; Bickelhaupt, F. *J. Am. Chem. Soc.* **1998**, *120*, 3371-3375.

(101) van Eis, M. J.; Komen, C. M. D.; de Kanter, F. J. J.; de Wolf, W. H.; Lammertsma, K.; Bickelhaupt, F.; Lutz, M.; Spek, A. L. *Angew. Chem., Int. Ed. Engl.* **1998**, *37*, 1547-1550.

(102) van Eis, M. J.; van der Linde, B. S. E.; de Kanter, F. J. J.; de Wolf, W. H.; Bickelhaupt, F. *J. Org. Chem.* **2000**, *65*, 4348-4354.

(103) van Eis, M. J.; de Wolf, W. H.; Bickelhaupt, F.; Boese, R. *J. Chem. Soc., Perkin Trans. 2* **2000**, *47*, 793-801.

(104) van Eis, M. J.; de Kanter, F. J. J.; de Wolf, W. H.; Lammertsma, K.; Bickelhaupt, F.; Lutz, M.; Spek, A. L. *Tetrahedron* **2000**, *56*, 129-136.

(105) van Es, D. S.; Egberts, A.; Nkrumah, S.; de Nijs, H.; de Wolf, W. H.; Bickelhaupt, F.; Veldman, N.; Spek, A. L. *J. Am. Chem. Soc.* **1997**, *119*, 615-616.

(106) van Es, D. S.; Gret, N.; de Rijke, M.; van Eis, M. J.; de Kanter, F. J. J.; de Wolf, W. H.; Bickelhaupt, F.; Menzer, S.; Spek, A. L. *Tetrahedron* **2001**, *57*, 3557-3565.

(107) Kostermans, G. B. M.; Van Dansik, P.; de Wolf, W. H.; Bickelhaupt, F. *J. Am. Chem. Soc.* **1987**, *109*, 7887-7888.

(108) van Eis, M. J.; de Kanter, F. J. J.; de Wolf, W. H.; Bickelhaupt, F. *J. Org. Chem.* **1997**, *62*, 7090-7091.

(109) Vögtle, F.; Neumann, P. *Synthesis* **1972**, 85-103.

(110) Hoffmann, R.; Woodward, R. B. *J. Am. Chem. Soc.* **1965**, *87*, 2046-2048.

(111) Longone, D. T.; Reetz, M. T. *J. Chem. Soc., Chem. Commun.* **1967**, 46-47.

(112) Wynberg, H. E.; Fawcett, F. S.; Mochel, W. E.; Theobald, C. W. *J. Am. Chem. Soc.* **1960**, *83*, 1428-1435.

(113) Wynberg, H. E.; Fawcett, F. S. In *Organic Syntheses, Coll. Vol. V*; Wiley: New York, 1973; pp 883-886.

(114) Hopf, H.; Bohm, I.; Kleinschroth, J. In *Organic Syntheses, Coll. Vol. VII*; Wiley: New York, 1990; pp 485-490.

(115) Wassermann, H. H.; Keehn, P. M. *J. Am. Chem. Soc.* **1969**, *91*, 2374-2375.

(116) Brown, G. W.; Sondheimer, F. *J. Am. Chem. Soc.* **1967**, *89*, 7116-7117.

(117) Staab, H. A.; Haenel, M. *Tetrahedron Lett.* **1970**, 3585-3588.

(118) Haenel, M. *Tetrahedron Lett.* **1977**, 4191-4194.

(119) Toyoda, T.; Otsubo, I.; Otsubo, T.; Sakata, Y.; Misumi, S. *Tetrahedron Lett.* **1975**, 3159-3162.

(120) Reiss, J. A. In *Cyclophanes, Vol. II*; Keehn, P. M., Rosenfeld, S., eds.; Academic Press: New York, 1983; pp 443-484.

(121) Baker, W.; McOmie, J. F. W.; Norman, J. M. *J. Chem. Soc.* **1951**, 1114-1118.

(122) Burri, K.; Jenny, W. *Helv. Chim. Acta* **1967**, *50*, 1978-1993.

(123) Flammang, R.; Figeys, H. P.; Martin, R. H. *Tetrahedron* **1968**, *24*, 1171-1185.

(124) Pellegrin, M. *Recl. Trav. Chim. Pays-Bas* **1899**, *18*, 457.

(125) Müller, E.; Röscheisen, G. *Chem. Ber.* **1957**, *90*, 543-553.

(126) Nishimura, J.; Nakamura, Y.; Hayashida, Y.; Kudo, T. *Acc. Chem. Res.* **2000**, *33*, 679-686.

(127) Nishimura, J.; Doi, H.; Ueda, E.; Ohbayashi, A.; Oku, A. *J. Am. Chem. Soc.* **1987**, *109*, 5293-5295.

(128) Nishimura, J.; Okada, Y.; Inokuma, Y.; Gao, S. R. *Synlett* **1994**, 884-894.

(129) Kawashima, T.; Otsubo, T.; Sakata, Y.; Misumi, S. *Tetrahedron Lett.* **1978**, 5115-5118.

(130) Umemoto, T.; Satani, S.; Sakata, K.; Misumi, S. *Tetrahedron Lett.* **1975**, 3159-3162.

(131) Irngartinger, H.; Kirrstetter, R. G. H.; Krieger, C.; Rodewald, H.; Staab, H. A. *Tetrahedron Lett.* **1977**, 1425-1428.

(132) Mitchell, R. H.; Carruthers, R. J.; Zwinkels, J. C. M. *Tetrahedron Lett.* **1976**, 2585-2588.

(133) Bürgi, H. B.; Venugopalan, P.; Schwarzenbach, D.; Diederich, F.; Thilgen, C. *Helv. Chim. Acta* **1993**, *76*, 2155-2159.

(134) Balch, A. L.; Catalano, V. J.; Lee, J. W.; Olmstead, M. M.; Parkin, S. R. *J. Am. Chem. Soc.* **1991**, *113*, 8953-8955.

(135) Wang, C.-R.; Sugai, T.; Kai, T.; Tomiyama, T.; Shinohara, H. *J. Chem. Soc., Chem. Commun.* **2000**, 557-558.

(136) Avent, A. G.; Dubois, D.; Penicaud, A.; Taylor, R. *J. Chem. Soc., Perkin Trans. 2* **1997**, 1907-1910.

(137) Manolopoulos, D. E.; Fowler, P. W. *J. Chem. Phys.* **1992**, *96*, 7603-7614.

(138) Tagmatarchis, N.; Avent, A. G.; Prassides, K.; Dennis, T. J. S.; Shinohara, H. *J. Chem. Soc., Chem. Commun.* **1999**, 1023-1024.

(139) Bodwell, G. J.; Bridson, J. N.; Chen, S.-L.; Poirier, R. A. *J. Am. Chem. Soc.* **2001**, *123*, 4704-4708.

(140) Anker, W.; Bushnell, G. W.; Mitchell, R. H. *Can. J. Chem.* **1979**, *57*, 3080-3087.

(141) Mitchell, R. H. Nuclear Magnetic Resonance Properties and Conformational Behavior of Cyclophanes: In *Cyclophanes, Vol. I*; Keehn, P. M., Rosenfeld, S., eds.; Academic Press: New York, 1983; pp 239-310.

(142) Bodwell, G. J.; Houghton, T. J.; Koury, H. E.; Yarlagadda, B. *Synlett* **1995**, 751-752.

(143) Bodwell, G. J.; Bridson, J. N.; Houghton, T. J.; Kennedy, J. W. J.; Mannion, M. R. *Angew. Chem., Int. Ed. Engl.* **1996**, *35*, 1320-1321.

(144) Bodwell, G. J.; Bridson, J. N.; Houghton, T. J.; Kennedy, J. W. J.; Mannion, M. R. *Chem. Eur. J.* **1999**, *5*, 1823-1827.

(145) Bodwell, G. J.; Fleming, J. J.; Mannion, M. R.; Miller, D. O. *J. Org. Chem.* **2000**, *65*, 5360-5370.

(146) Bodwell, G. J.; Fleming, J. J.; Miller, D. O. *Tetrahedron* **2001**, *57*, 3577-3585.

(147) Houghton, T. J. Ph.D. Dissertation, Memorial University of Newfoundland, **1999**.

(148) Mannion, M. R. Ph.D. Dissertation, Memorial University of Newfoundland, **1999**.

(149) Bend angles of pyrene units in pyrenophanes were calculated using the Chem3D package of software (MOPAC, AM1, closed shell).

Chapter 2

NMR Investigations of the Bridge Conformational Behavior of 6,15-Disubstituted *syn*-2,11-Dithia[3.3]metacyclophanes.

2.1 Introduction

When our group first became interested in [*n*](2.7)pyrenophanes **1** as synthetic targets, two synthetic routes were investigated. The route that is currently used is described in Chapter 1 and several examples of its application can be found in Chapters 3-5. The first route received some initial attention, but is not currently used. The retrosynthetic analysis of this route is given in Scheme 2.01.

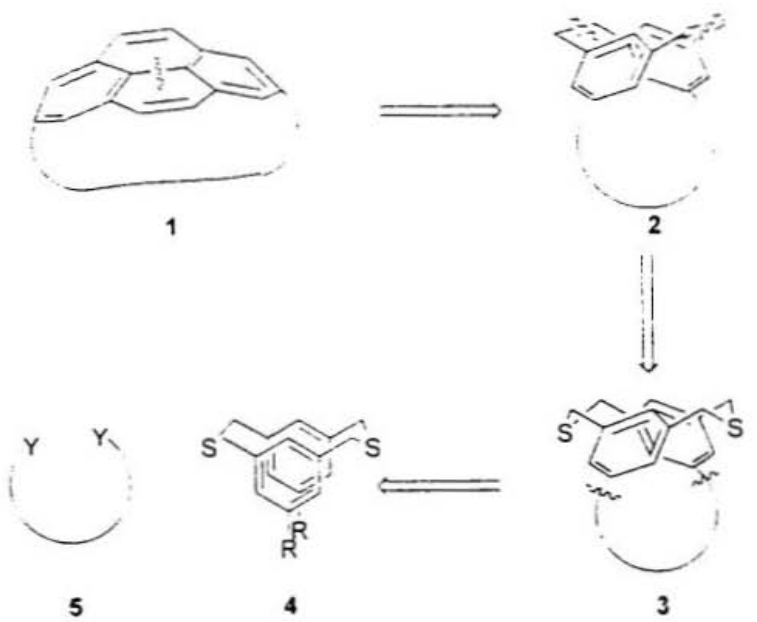

Scheme 2.01: Alternative retrosynthetic analysis of a pyrenophane.

The initial retrosynthetic cut is the central bond of the pyrene unit in **1**, which can be formed in the synthetic direction using a valence isomerization-dehydrogenation (VID)

sequence.[1] Cyclophanediene **2** can be derived from a dithiacyclophane **3** using standard cyclophane methodology.[1,2] These retrosynthetic steps are identical with those used in the currently used synthetic approach, so, for a more detailed discussion of this sequence, the reader is referred to Chapter 1. The next retrosynthetic cuts remove the tether from dithiacyclophane **3** to give **5** and a 6,15-disubstituted *syn*-2,11-dithia[3.3]metacyclophane **4**.[3] Introduction of a tether at this stage was anticipated to be feasible based on Mitchell's observation[4] that 2,11-dithia[3.3]metacyclophanes with H atoms as substituents on the internal (9- and 18-) positions prefer to adopt the *syn* conformation. The advantage of this route is that it gives access to derivatives of **3** with different tether lengths from one common precursor **4**.

Initial investigations of this synthetic route led to the synthesis of *syn*-6,15-dicyano-2,11-dithia[3.3]metacyclophane **4a**[5] by our group.[5] This particular cyclophane shows some very unusual features in its X-ray crystal structure. Perhaps the most surprising feature is that both bridges are in the so-called *pseudo-boat* conformation (sulfur "up", *b,b*-**4a**, Figure 2.01). Neither AM1 calculations nor *ab initio* calculations (3-21G(*)) predict this to be the lowest energy conformer for **4a** in the gas phase. AM1 calculations found the heat of formation of the *pseudo-boat,pseudo-chair* (*b,c*) and the *pseudo-boat,pseudo-boat* (*b,b*) conformer to be 0.57 kcal/mol and 1.77 kcal/mol higher than the heat of formation of the *pseudo-chair,pseudo-chair* (*c,c*) conformer, respectively. This difference in the gas phase can easily be outweighed by crystal packing forces.

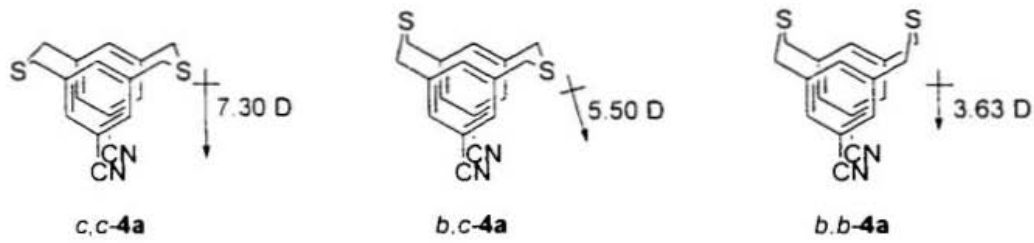

Figure 2.01: Bridge conformations and AM1 calculated dipole moments of ***syn*-4a**.

When published X-ray crystal structures of other *syn*-[3.3]metacyclophanes are examined, by far the majority of structures are of parent (all-carbon) *syn*-[3.3]metacyclophanes,[6,7] and *syn*-2,11-dithia[3.3]metacyclophanes[4-8] (some *syn*-2,11-diaza[3.3]metacyclophanes are known.) Most structures have the bridges in the *c,c* conformation. This is in agreement with the calculated gas phase structures, for which this conformation is consistently calculated to be the most stable.[9,10] The only other *syn*-[3.3]metacyclophane derivatives reported to crystallize in the *b,b* conformation are *syn*-1,3,10,12-tetrathia[3.3](2,6)pyridinophane **6**[11] and *syn*-[3.3](2,6)pyridinophane **7** (Figure 2.02).[7] The crystal structure of **4a** is the first (and only) one in which a *syn*-2,11-dithia[3.3]metacyclophane has both bridges in the *pseudo-boat* conformation.

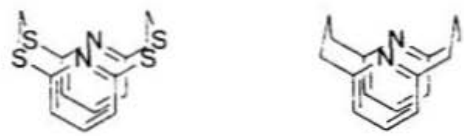

Figure 2.02: *Pseudo-boat,pseudo-boat* conformations of *syn*-[3.3]pyridinophanes **6** and **7**.

In the case of **6**, "N-S repulsions" were invoked as the cause of the unusual conformations,[11] but no explanation was offered as to the origin of those interactions or why they would favor the *b,b* conformation. Upon examination of the system, it would appear as though the "N-S-repulsions" refer to an unfavorable alignment of lone pairs on the nitrogen and sulfur atoms in **6** when a bridge adopts a *pseudo-chair* conformation. For **7**, weak hydrogen bonding between the internal nitrogen atom and the inner hydrogens of the central methylene group in the bridges was deemed to be the primary cause for the unusual bridge conformations. The hydrogen bonding argument does not seem applicable to *syn*-6,15-dicyano-2,11-dithia[3.3]metacyclophane **4a**, since the heteroatom in this case is a considerably weaker donor atom (S vs. N). Furthermore this weak hydrogen bonding could presumably occur for a *pseudo-chair* bridge as well as for a *pseudo-boat* bridge.

The origin of the unusual bridge conformational behavior of **4a** in its crystal structure was ascribed to a dipolar effect,[5] i.e., the molecule adopts the conformation with the smallest dipole moment. The calculated (AM1) dipole moments for the *c,c*, *b,c* and the *b,b* conformers of **4a** are given in Figure 2.01. In the *b,b* conformer, the vector sum of the dipole moment of the two cyano groups directly opposes that of the four C-S bonds in the bridges. As a result, the calculated dipole moment of the *b,b* conformer (3.63 D) is considerably smaller than that of the *c,c* conformer (7.30 D), in which the vector sums point in the same direction.

If this dipolar effect is indeed responsible for the bridge conformational behavior of **4a** in the solid state it might be expected that 6,15-disubstituted *syn*-2,11-dithia[3.3]metacyclophanes will show a dependence of the bridge conformations on the electronic properties of the substituents in the 6- and 15- positions. Studying this effect in the solid state would not be very meaningful due to different crystal packing effects of different cyclophanes. It was therefore decided to study this effect in solution using NMR techniques, for which the conditions can be kept constant for a series of compounds.

In the following paragraphs, a short overview will be given of published studies of conformational behavior of cyclophanes. This will be followed by a detailed discussion of the bridge conformational behavior of a series of 6,15-disubstituted *syn*-2,11-dithia[3.3]metacyclophanes.

2.2 Overview of the literature

syn-2,11-Dithia[3.3]metacyclophane **4b** was first synthesized by two independent groups in 1968.[12,13] Based on observations of [2.2]metacyclophane[9,14,15] and various internally substituted 2,11-dithia[3.3]metacyclophanes,[1] in which the *anti* conformer was the sole conformer in X-ray and NMR studies, the parent 2,11-dithia[3.3]metacyclophane **4b** was initially thought to exist in the *anti* conformation only (Scheme 2.02).[13] The ^{1}H NMR spectrum of **4b** shows a singlet at δ 6.6 ppm for the internal aryl protons (H_i), which was

assumed to be an average chemical shift of all contributing conformers.[12] DNMR* studies showed that the ^{1}H NMR spectrum of **4b** did not change upon cooling to –90°C, indicating a low energy barrier (estimated at <9.3 kcal/mol in toluene)[16] between the conformers.

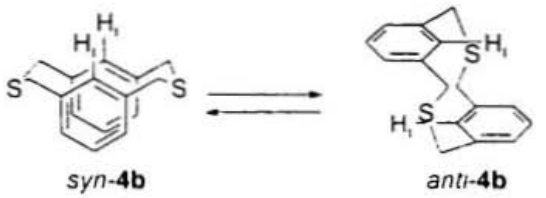

syn-**4b** *anti*-**4b**

Scheme 2.02: Proposed *syn* to *anti* interconversion of **4b**.[12]

In a paper published in 1979,[4] Mitchell and co-workers described the X-ray crystal structure of **4b** and showed not only that the *syn* conformer was the sole conformer present in the solid state but that the bridge conformation of **4b** was the *c,c* conformation. From a ^{1}H NMR study Mitchell also concluded that, in solution at room temperature, **4b** exists, as in the crystalline state, only in the *syn* conformation. Although no freezing of the bridges was observed in this study, wobbling of the bridges (Scheme 2.03)[16,17] was not ruled out as one of the conformational processes of **4b**. Although *syn* to *anti* (benzene ring) inversion was not considered a contributor to conformational processes, *syn* to *syn'* benzene ring inversion could not be eliminated. The *syn* to *syn'* inversion involves a flip of both aromatic rings so that effectively a *pseudo-chair* to *pseudo-boat* (or *vice versa*)

* DNMR: Dynamic NMR. The term VTNMR has also been used to describe the same technique.

inversion of both bridges takes place at the same time (Scheme 2.03). This *syn* to *syn'* inversion could also actually be a *syn* to *anti* to *syn'* process in which the *anti* conformer is a high energy and short-lived intermediate.

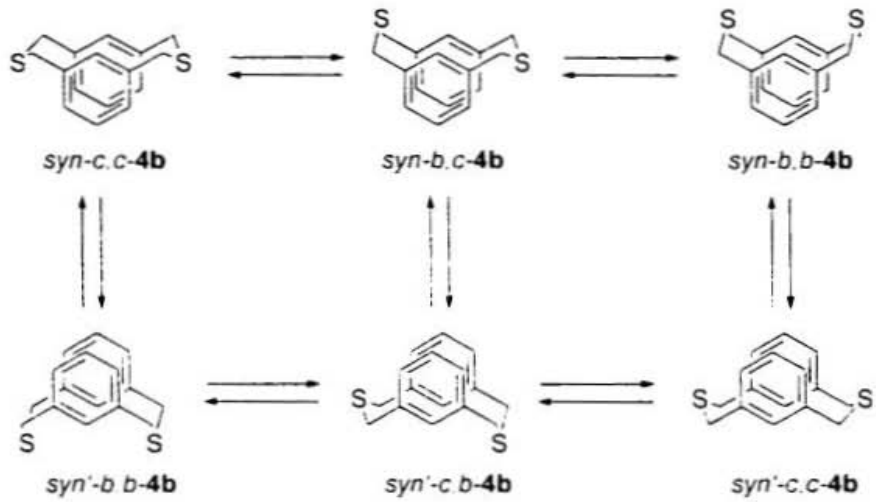

Scheme 2.03: Bridge wobbling and *syn* to *syn'* benzene ring inversion of **4b**.

Since the appearance of Mitchell's paper, only a few bridge conformational studies of *syn*-2,11-dithia[3.3]metacyclophanes have appeared in the literature. Most of these describe syntheses and structures of *syn*-[3.3]metacyclophanes with large substituents at the internal (9- and 18-) position(s),[18-20] which limits the conformational motion of the bridges and the aromatic rings. Other papers describe cyclophanes with atoms other than sulfur at the 2- and 11-positions,[21,22] or cyclophanes with (hetero)aromatic units other than benzene.[11,23] Since our work in this area is concerned with bridge conformational behavior of *syn*-2,11-dithia[3.3]metacyclophanes with substituents in the 6- and 15-

positions only, the reader is referred to an excellent review by Ernst[24] for a comprehensive discussion of the literature since 1983 on NMR studies of other cyclophanes.

The parent [3.3]metacyclophane **8** was first synthesized in 1976.[11,23,25] Later, several other syntheses were published,[26-29] and in 1985 Semmelhack published a leading paper on the conformational behavior of this compound.[10] Semmelhack showed that **8** is present only in the *syn* conformation in the solid state, with both bridges in the *pseudo-chair* conformation. In solution, two conformers could be observed by ^{1}H-NMR (270 MHz) below 223 K. Both conformers were assigned the *syn* conformation based on the chemical shift of the internal protons. Based on the results of calculations,[10] the major conformer was assigned the *c,c* conformation and the minor isomer was assigned the *b,c* conformation.

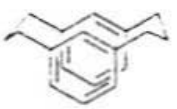

8

Figure 2.03: *syn*-[3.3]Metacyclophane **8**.

A conformational study of a bridged derivative of a *syn*-[3.3]metacyclophane was published in 1988 by Shinmyozu *et al.*[30] Cleverly, they designed and synthesized a deuterated cyclophane **9** (Figure 2.04) with an extra bridge linking the 6- and 15 positions

of the *syn*-[3.3]metacyclophane unit. The presence of the third bridge ensures that the [3.3]metacyclophane moiety can exist only in the *syn* conformation. The aromatic region of its ^{1}H NMR spectrum is less complex than that of **7**. The *syn* to *syn'* benzene ring inversion process is also eliminated due to the presence of this tether, simplifying the system for dynamic studies. Deuteration of the 2- and 11- positions of the bridges was performed to simplify the aliphatic region of the ^{1}H NMR spectrum.

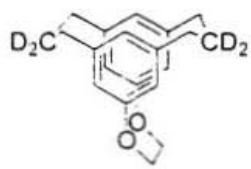

9

Figure 2.04: Structure of **9**.

Conformational analysis of **9** using DNMR methods showed that (at least) three conformers of **9** are present at lower temperatures in an approximate ratio of 47 : 44 : 9 (203 K; 270 MHz ^{1}H NMR in CD_2Cl_2). Based on work by Semmelhack, which suggested a stability order of *c,c* > *h,c* > *h,h*,[19] Shinmyozu assigned the three conformers of **9** as *c,c*-**9**, *h,c*-**9** and *h,h*-**9**, respectively (Figure 2.05). Assignment of these conformations was consistent with the observed trend of the chemical shifts of the internal protons. The proximity of two bridges to the internal proton in *h,h*-**9** leads to greater steric deshielding of that internal proton than for the corresponding proton in the other two conformers. The strongly deshielded internal proton (two proximate bridges) in *h,h*-**9** appears in the ^{1}H NMR spectrum at δ 6.83, while the slightly less sterically deshielded internal proton (one

proximate bridge) in *h,c*-**9** appears at δ 6.71 and the least sterically deshielded internal proton (no proximate bridges) in *c,c*-**9** appears at δ 6.61. For the external proton the same effect can be observed. Steric deshielding of the external protons by a proximate bridge (in the *c,c* conformation) causes a downfield shift of the corresponding signal (δ 6.32) relative to the chemical shift of the same proton in the *h,h* conformation (δ 6.16) in which no steric deshielding occurs. In the *h,c* conformer, the external protons are nonequivalent. The signal for the external proton close to the *pseudo-chair* bridge (H_e': δ 6.29) was observed at approximately the same chemical shift as the signal for the external proton of the *c,c* conformer (δ 6.32). The signal for the external proton in *h,c*-**9** closest to the *pseudo-boat* bridge was observed at almost the same chemical shift (H_e: δ 6.20) as the signal for the external proton of the *h,h* conformation (δ 6.16). Activation energy barriers for the inversion of the trimethylene bridges in **9** were estimated to be 12.1-12.3 kcal mol.

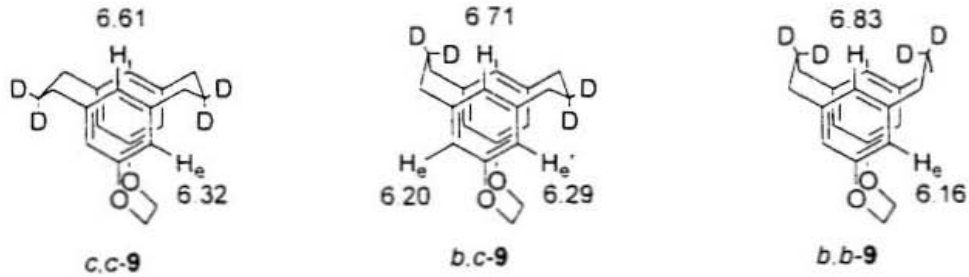

Figure 2.05: Bridge conformations and ^{1}H NMR data of cyclophane **9** at 203 K.

The chemical shift difference between the equatorial and axial protons in the *pseudo-chair* bridges was shown to be 0.48-0.49 ppm, with a coupling constant between equatorial and axial protons of 13.7-13.8 Hz. The corresponding values for the protons in the *pseudo-boat* bridges are 0.67-0.71 ppm and 14.4-14.7 Hz. This information was used to assign conformations in a later paper by the same group,[31] in which compound **8b-d_4**, as well as its 6,15-dimethoxy derivative **8c-d_4**, was studied.

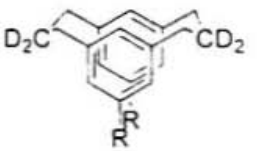

8b-d_4 R = H

8c-d_4 R = OMe

Figure 2.06: Deuterated cyclophanes **8b-d_4** and **8c-d_4**.

The results Shinmyozu obtained in his study of deuterated *syn*-[3.3]metacyclophanes **8b-d_4** and **8c-d_4** were similar to that of the tethered system **9**, but freezing out of only one (major) conformer was observed for each cyclophane. In all cases this major conformer was assigned the *c,c* conformation. Assignment of the minor signals to a single conformer could not be made because of broadening of the signals of the benzylic protons. Shinmyozu suggested that "the presence of another dynamic process, i.e., interconversion of the minor conformers *via* an *anti* conformer (benzene ring inversion)" was still a possibility. No evidence was presented to support this inversion or any other process at low temperature (203 K), but in the same paper it was shown that benzene ring inversion occurs at room temperature. Decomplexation of enantiomerically pure **10**

yielded racemic **11**, independent of which enantiomer of **10** was used (Scheme 2.04). If benzene ring inversion was prohibited, this decomplexation should have yielded a single enantiomer of **11**.

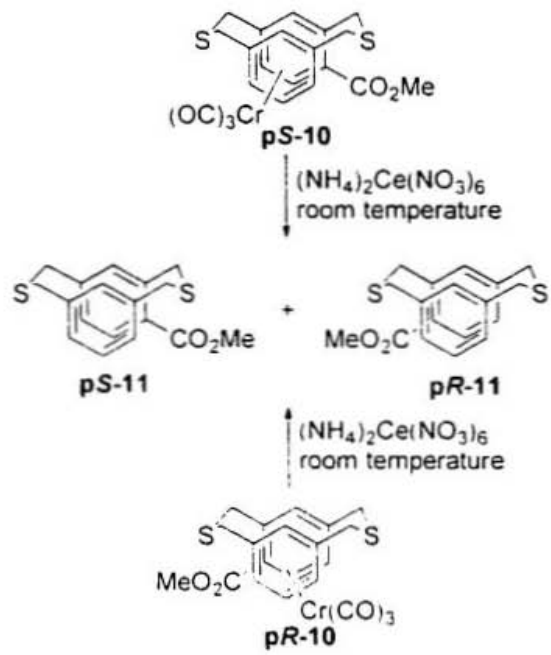

Scheme 2.04: Decomplexation of cyclophanechromium tricarbonyl complex **10**.

Analysis of the spectral data of Shinmyozu's "tethered" *syn*-[3.3]metacyclophane **9** shows that the steric shielding of an aromatic proton by a nearby dideuteriomethylene group amounts to *ca.* 0.1 ppm per dideuteriomethylene group. If this is indeed the case, then the chemical shifts of the internal and external protons in *syn*-2,11-dithia[3.3]metacyclophanes might be subject to a similar (additive) steric influence of, in

this case, the sulfur atoms in the bridges. Implications of this hypothesis are delineated in the next Section.

2.3 Elaboration of a hypothesis

Low temperature ^{1}H NMR studies might provide information about the bridge conformational behavior of *syn*-2,11-dithia[3.3]metacyclophanes. At the outset of this project, it was realized that studying a broad range of cyclophanes using DNMR would be impractical for several reasons: (1) solubility of *syn*-2,11-dithia[3.3]metacyclophanes is often poor at lower temperatures; and (2) Mitchell's[4,32] and Sato's[12,16] studies suggested that the activation barriers for conformational processes are quite small (<9.3 kcal/mol in toluene), requiring high-field spectrometers and low temperatures to observe freezing of the processes. (We were limited to −100 °C at 500 MHz; estimated 8-9 kcal/mol (33-38 kJ/mol) minimum energy barrier is required to observe freezing.)

At room temperature, interconversion of the various bridge conformers will be expected to be rapid, so the expectation is a ^{1}H NMR spectrum that is a weighted average of all conformers present.[33] Unfortunately there is no easy technique by which the chemical shifts of those different conformers at room temperature can be measured. This problem brought us to use the method described below. 6,15-Disubstituted *syn*-2,11-dithia[3.3]metacyclophanes were used in this study primarily since they were of interest

to us from a synthetic point of view. A coincidental advantage of studying this class of cyclophanes is their relatively uncomplicated ^{1}H NMR spectra.[34]

In our study of 6,15-disubstituted *syn*-2,11-dithia[3.3]metacyclophanes the following assumptions have been made: (a) the only conformers that contribute to the observed ^{1}H NMR spectrum at room temperature are the *c,c*, the *b,c* and the *b,b* conformers (see Figure 2.01), (b) the steric deshielding effect of a sulfur atom in a bridge is equal for each interaction and (c) this steric deshielding effect is additive for each interaction. Validity of these assumptions will be discussed in Section 2.4.3.1. The observed chemical shift of the internal proton (δH_i^{obs}) at room temperature can then be described as follows.

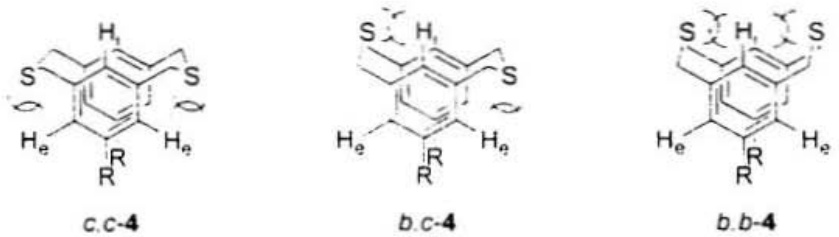

Figure 2.07: Bridge conformers of *syn*-2,11-dithia[3.3]metacyclophane **4**.

If the chemical shift of the internal proton of the *c,c* conformer (*c,c*-**4**) at room temperature is given by $\delta H_i^{c,c}$, and each proximate thioether bridge deshields a nearby aryl proton by an amount x, then the chemical shift of the internal proton of the *b,c* ($\delta H_i^{b,c}$) and the *b,b* conformers ($\delta H_i^{b,b}$) can be given by:

$$\delta H_i^{b,c} = \delta H_i^{c,c} + x \qquad \text{(eq. 1)}$$

$$\delta H_i^{b,b} = \delta H_i^{c,c} + 2x \qquad \text{(eq. 2)}$$

The conformers are present in a ratio that can be represented by their relative mole fractions ($\chi^{c,c}$, $\chi^{b,c}$ and $\chi^{b,b}$) so the observed chemical shift of the internal proton at room temperature can be given by an average that is weighted according to the mole fractions (equation 3). Substitution of equation 1 for $\delta H_i^{b,c}$ and equation 2 for $\delta H_i^{b,b}$ in equation 3 gives equation 4, which can be rewritten to give equation 5.

$$\delta H_i^{obs} = \chi^{c,c}\ \delta H_i^{c,c} + \chi^{b,c}\ \delta H_i^{b,c} + \chi^{b,b}\ \delta H_i^{b,b} \qquad \text{(eq. 3)}$$

$$= \chi^{c,c}\ \delta H_i^{c,c} + \chi^{b,c}\ (\delta H_i^{c,c} + x) + \chi^{b,b}\ (\delta H_i^{c,c} + 2x) \qquad \text{(eq. 4)}$$

$$= \delta H_i^{c,c} + x\ (\chi^{b,c} + 2\,\chi^{b,b}) \qquad \text{(eq. 5)}$$

For the external proton (H_e), the chemical shifts of the three conformers can be formulated similarly. Again the chemical shift of the *c,c* conformer is taken as a reference shift at $\delta H_e^{c,c}$. The *b,c* conformer should have a chemical shift that can be represented by the average of the signals of two different external protons ($H_e^{b,c}$ and $H_e^{b,c}$). $H_e^{b,c}$ is the external proton close to a *pseudo-chair* bridge and thus has a chemical shift $\delta H_e^{c,c}$, which already includes a steric deshielding factor (equation 6), and $H_e^{b,c}$ is the proton close to a *pseudo-boat* bridge. It is not deshielded by a proximate bridge, so x is substracted (equation 7).

$$\delta H_e^{b,c} = \delta H_e^{c,c} \qquad \text{(eq. 6)}$$

$$\delta H_e^{b,c} = \delta H_e^{c,c} - x \qquad \text{(eq. 7)}$$

The average chemical shift for the external protons in the *b,c* conformer can then be given by equation 8. Substitution of equations 6 and 7 in equation 8 gives, after rewriting of equation 9, equation 10.

$$\delta H_e^{b,c} = \tfrac{1}{2}\ \delta H_e^{b,c} + \tfrac{1}{2}\ \delta H_e^{b,c} \qquad \text{(eq. 8)}$$

$$= \tfrac{1}{2}\ (\delta H_e^{c,c} - x) + \tfrac{1}{2}\ \delta H_e^{c,c} \qquad \text{(eq. 9)}$$

$$= \delta H_e^{c,c} - \tfrac{1}{2}\ x \qquad \text{(eq. 10)}$$

In the *b,b* conformer both external protons are not deshielded by a proximate bridge as for the *c,c* conformer so their chemical shift ($\delta H_e^{b,b}$) is corrected by subtracting x and can be given by equation 11.

$$\delta H_e^{b,b} = \delta H_e^{c,c} - x \qquad \text{(eq. 11)}$$

The observed chemical shift of the external proton at room temperature can then be given by the weighted average of the chemical shifts of each conformer, in which each chemical shift is again weighted according to the mole fraction of the corresponding conformer (equation 12).

$$\delta H_e^{obs} = \chi^{c,c} \delta H_e^{c,c} + \chi^{b,c} \delta H_e^{b,c} + \chi^{b,b} \delta H_e^{b,b} \qquad \text{(eq. 12)}$$

Substitution of equation 10 for $\delta H_e^{b,c}$ and equation 11 for $\delta H_e^{b,b}$ in equation 12 gives equation 13 which can be rewritten to give equation 14.

$$\delta H_e^{obs} = \chi^{c,c} \delta H_e^{c,c} + \chi^{b,c} (\delta H_e^{c,c} - \tfrac{1}{2} x) + \chi^{b,b} (\delta H_e^{c,c} - x) \qquad \text{(eq. 13)}$$

$$= \delta H_e^{c,c} - x (\tfrac{1}{2} \chi^{b,c} + \chi^{b,b}) \qquad \text{(eq. 14)}$$

If the chemical shifts of the internal and the external protons are compared to a similarly substituted system such as the 5-substituted *meta*-xylene ("half cyclophane") system **12**.

in which the differential steric deshielding effect of the sulfur atoms in the bridges on H_i and H_e is absent, the difference in chemical shift for the internal and the external protons ($\Delta\delta H_i$ and $\Delta\delta H_e$, respectively) can be defined by:

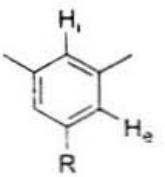

12

Figure 2.08: Structure of *meta*-xylenes **12**.

$$\Delta\delta H_i = \delta H_i^{\text{xylene}} - \delta H_i^{\text{cyclophane}} \qquad \text{(eq. 15)}$$

$$\Delta\delta H_e = \delta H_e^{\text{xylene}} - \delta H_e^{\text{cyclophane}} \qquad \text{(eq. 16)}$$

When equations 5 and 14 are substituted into equations 15 and 16, the $\Delta\delta$ values for H_i and H_e can be given by equation 17 and 19, which can be rewritten to give equations 18 and 20.

$$\Delta\delta H_i = \delta H_i^{\text{xylene}} - [\delta H_i^{c,c} + x\ (\chi^{b,c} + 2\chi^{b,b})] \qquad \text{(eq. 17)}$$

$$= (\delta H_i^{\text{xylene}} - \delta H_i^{c,c}) - x\ (\chi^{b,c} + 2\chi^{b,b}) \qquad \text{(eq. 18)}$$

$$\Delta\delta H_e = \delta H_e^{xylene} - [\delta H_e^{c,c} - x\ (^1/_2\ \chi^{b,c} + \chi^{b,b})] \qquad \text{(eq. 19)}$$

$$= (\delta H_e^{xylene} - \delta H_e^{c,c}) + x\ (^1/_2\ \chi^{b,c} + \chi^{b,b}) \qquad \text{(eq. 20)}$$

The first terms of equations 18 and 20 ($\delta H^{xylene} - \delta H^{c,c}$) shows the difference in chemical shift between the xylene derivative and the *c,c* conformer. This part of the equation is expected to be independent of the ratio of conformers present (mole fractions) and thus independent of the nature of the substituents. It should therefore be constant for the series of compounds studied.

The second term in equation 18 ($-x\ [\chi^{b,c} + 2\chi^{b,b}]$) is opposite in sign to and double the magnitude of the second term in equation 20 ($x\ [^1/_2\ \chi^{b,c} + \chi^{b,b}]$). This part of the equation is dependent on the mole fractions of the *b,c* and the *b,b* conformers. It can be expected to vary with the electronic nature of the substituents, according to the following argument. Differing electronic influences will be expected to affect the relative magnitudes of the dipole moments of the three bridge conformers of **4** and thus, if the dipole moment or some other electronic effect is indeed important (as suggested for **4a**), would lead to different mole fractions of the conformers.

If a *syn*-2,11-dithia[3.3]metacyclophane has a preference for the *b,b* conformation in solution, this should be reflected as a large $\Delta\delta H_t$ value and a small $\Delta\delta H_e$ value compared to a *syn*-2,11-dithia[3.3]metacyclophane that adopts mainly the *c,c* conformation. If the

preference of a *syn*-2,11-dithia[3.3]metacyclophane for one conformer over the other is indeed governed by the electronic nature of the substituents and the magnitude of the $\Delta\delta$ values is directly correlated to the distribution between the conformers (as in equations 18 and 20), it might be possible to correlate the $\Delta\delta$ values to some physical organic parameter that describes the electronic nature of substituent groups on (conformational) processes. In the following Sections, the results of correlation studies of $\Delta\delta$ values will be discussed.

2.4 Results and Discussion

In order to study the bridge conformational behavior of 6,15-disubstituted *syn*-2,11-dithia[3.3]cyclophanes, the synthesis of a large range of cyclophanes and their reference compounds (5-substituted *meta*-xylenes) was required. The compounds that were synthesized are given in Figure 2.09. Samples of several of those compounds were obtained from co-workers[35-40] and their syntheses will not be described. After a short discussion of the syntheses performed by the author, a discussion of the results of the correlation studies will be given.

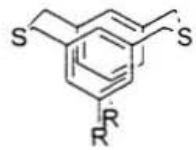

4

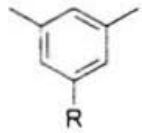

12

Cyclophane	Xylene	R
4a	**12a**	CN
4b	**12b**	H
4c	**12c**	Br
4d	**12d**	CO_2Et
4e	**12e**	CO_2H
4f	**12f**	Me
4g	**12g**	NH_2
4h	**12h**	NHAc
4i	**12i**	NO_2
4j	**12j**	OAc
4k	**12k**	OH
4l	**12l**	OMe
4m	**12m**	SC(O)*t*-Bu
4n	**12n**	SH
4o	**12o**	SMe
4p	**12p**	S(O)Me
4q	**12q**	$S(O)_2Me$

Figure 2.09: Legend for substituents on *syn*-2,11-dithia[3.3]metacyclophanes **4** and *meta*-xylenes **12**

2.4.1 Syntheses of *syn*-2,11-dithia[3.3]metacyclophanes and 5-substituted *meta*-xylenes

The traditional synthesis of *syn*-2,11-dithia[3.3]metacyclophanes **4** involves high dilution coupling of two building blocks: a dithiol **13** and a dibromide **14**, often from a common precursor.[2,13] Dithiols **13** can usually be synthesized from dibromides **14**, which can be formed from *meta*-xylene derivatives **12** *via* free radical benzylic bromination or from isophthalates **16** *via* a reduction-bromination sequence. Alternatively, dibromides **14** can

be reacted with Na_2S/Al_2O_3.[41] This last approach often yields a mixture of dimer (desired products **4**) and trimer (unwanted byproducts **15**), but reduces the number of steps in the synthesis and is compatible with base-sensitive groups, which would require protection if the first approach were used.

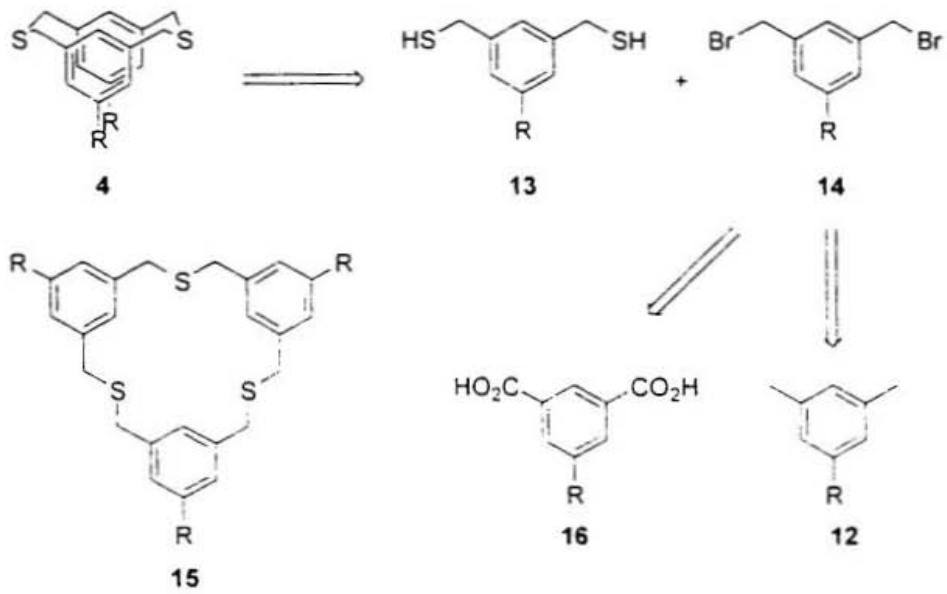

Scheme 2.04: Retrosynthetic analysis of *syn*-2,11-dithia[3.3]metacyclophanes **4**.

Since *meta*-xylenes **12** are required as reference compounds, using these compounds as starting materials would reduce the amount of experimental work involved. Yields of twofold benzylic brominations are often low (especially in the case of electron-rich aromatic rings where ring-bromination is prevalent)[42-45] so this route is not always useful.

The synthesis of *syn*-2,11-dithia[3.3]metacyclophanes **4b**, **4d**, **4e** and **4f** (Scheme 2.05) commenced with the synthesis of the α,α'-dibromo-*meta*-xylene derivatives **14**. For the parent system α,α'-dibromo-*meta*-xylene **14b** is commercially available. In the case of the carboxylic acid derivatives, the *meta*-xylene derivative **12d** was synthesized *via* Fischer-esterification[40] from commercially available 3,5-dimethylbenzoic acid **12e** in 82% yield. Benzylic bromination[42] of **12d** yielded dibromide **14d** in 44% yield.

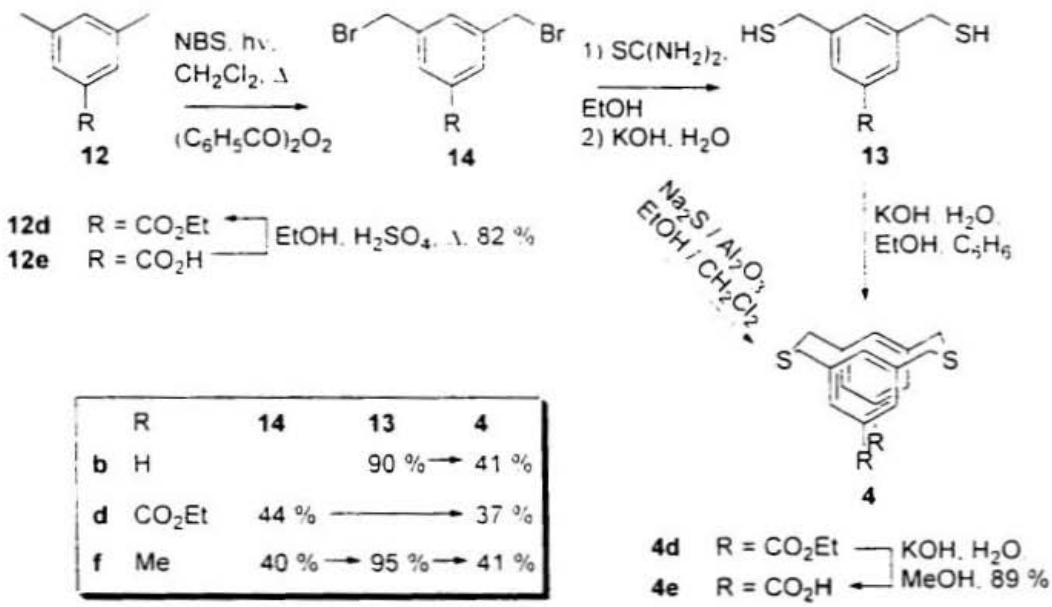

Scheme 2.05: Synthesis of *syn*-2,11-dithia[3.3]metacyclophanes **4**.

α,α'-Dibromo-*meta*-xylenes **14b** and **14f** were converted into their respective dithiols **13** using thiourea to form a bis(isothiouronium) salt, followed by hydrolysis of that salt under basic conditions. Coupling of dithiols **13b** and **13f** with an equimolar amount of the

dibromides **14b** and **14f** under high dilution conditions yielded *syn*-2,11-dithia[3.3]metacyclophanes **4b** and **4f** (41% for each). The diester **4d** was synthesized *via* direct coupling of the dibromide **14d** using Na_2S/Al_2O_3 (37%). Diester **4d** was saponified to give diacid **4e** in 89% yield. An X-ray crystal structure of **4e** was determined and the results will be discussed in Section 2.4.2.

meta-Xylenes **12j** and **12l** were synthesized from commercially available 3,5-dimethylphenol **12k** (Scheme 2.06). 5-Acetoxy-*meta*-xylene **12j** was synthesized in 80% yield upon treatment with Ac_2O/HOAc. 3,5-Dimethylanisole **12l** was synthesized using the reaction of **11k** with iodomethane in DMSO in the presence of KOH (81%).

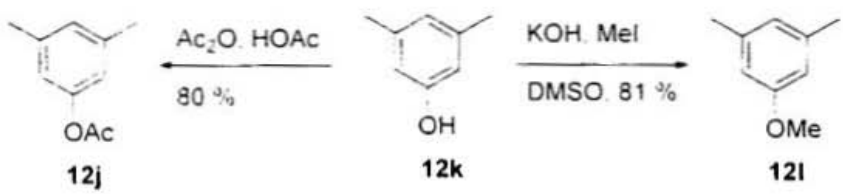

Scheme 2.06: Synthesis of **12j** and **12l** from **12k**.

2.4.2 X-Ray crystal structure of *syn*-2,11-dithia[3.3]metacyclophane-6,15-dicarboxylic acid (4e)

A relatively new theme in the development of chemical sciences has been hydrogen bonding-directed organization of organic molecules to give nanostructured materials.[47-49] The challenge that researchers in this area face is the design of materials that will have

"an energetic bias of sufficient magnitude that discrimination between alternate modes of assembly may be achieved (*ca.* 4 kcal/mol for >99.9% homogeneity)".[49] This energy difference between competitive assemblies is on the same order of magnitude as the strength of the hydrogen bonding interactions, which makes hydrogen bonding a suitable tool for noncovalent synthesis.

In Figure 2.10 some examples of supramolecular assemblies are given. Both examples exist of building blocks that cannot form hydrogen bonds in an intramolecular fashion without adopting a high-energy conformation, which leads to dimer formation in the solid state. *syn*-2,11-Dithia[3.3]metacyclophane-6,15-dicarboxylic acid **4e** also possesses two groups that can form relatively strong hydrogen bonds. In order for **4e** to form intramolecular hydrogen bonds, the carboxylic acid groups would have to adopt highly unfavorable conformations, which led us to believe that **4e** might exhibit intermolecular hydrogen bonding in its solid state.

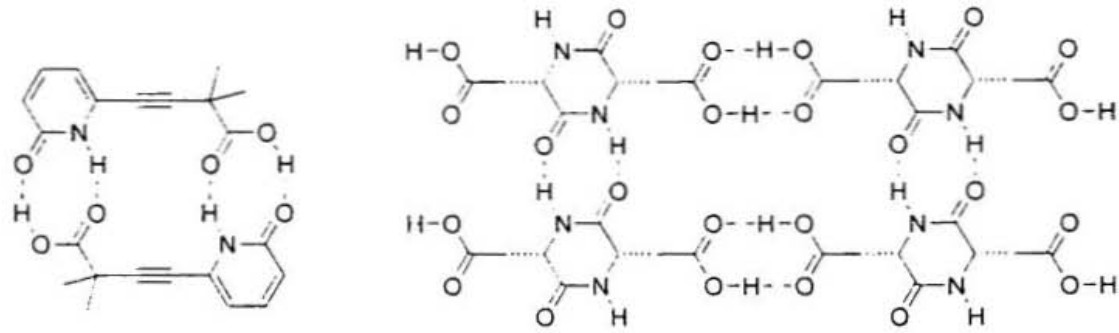

17 **18**

Figure 2.10: Examples of supramolecular assemblies (**17**[50] and **18**).[51]

The three-dimensional structure of diacid **4e** can schematically be represented by structure **I**, which can be seen as a possible building block for supramolecular structures. In the solid state **4e** could form a dimer **II** or an infinite molecular ladder **III**. In order to determine which assembly **4e** would form in the solid state, crystallization of **4e** was attempted.

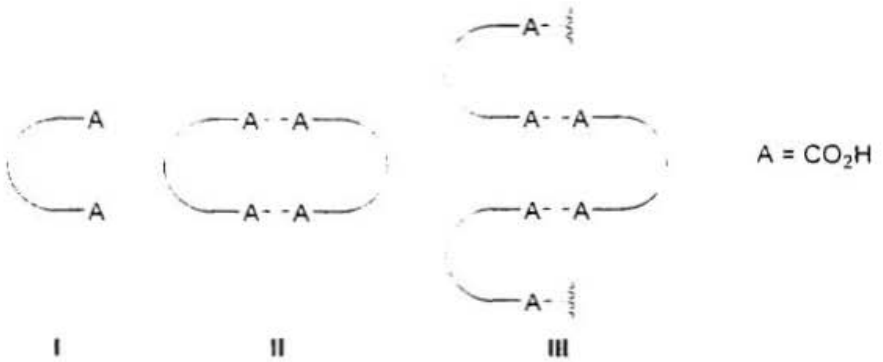

Figure 2.11: Proposed modes of supramolecular assembly for **4e**.

An X-ray structural analysis of crystals of *syn*-2,11-dithia[3.3]metacyclophane-6,15-dicarboxylic acid **4e** obtained from DMF showed formation of a symmetrical hydrogen bonded dimer **II** (Figure 2.12). The thioether bridges in **4e** were arranged in the *pseudo-chair* conformation.

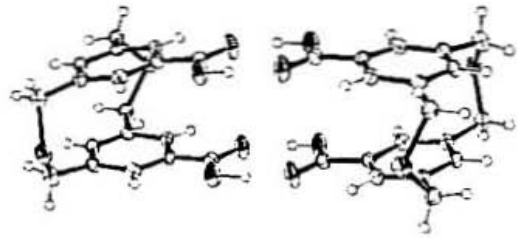

Figure 2.12: ORTEP drawing of the X-ray crystal structure of **4e**.

An interesting feature of the X-ray crystal structure of **4e** is that the carboxylic acid groups in each monomer unit are aligned in such a way, that it has a set of face-to-face oriented carbonyl groups and (automatically) a set of face-to-face hydroxyl groups. The position of the bridging hydrogen atoms was actually determined in the data collection. The positions of the other hydrogen atoms were calculated. The O-H bond length in the hydroxyl groups was 0.962 Å and the distance between the bridging hydrogen atoms and the carbonyl oxygen atoms was 1.551 Å, which is typical for hydrogen bonds.

The formation of a supramolecular structure of **4e** in the solid state suggests that this compound might show some interesting features when co-crystallized with compounds that are capable of hydrogen bonding with **4e**. The *syn*-conformation of **4e** might cause this diacid to act as a "supramolecular clamp" to give assemblies **IV** and **V** when co-crystallized with terephthalic acid (**19**) or trimesic acid (**20**), respectively. Other

compounds containing functionalities capable of forming hydrogen bonding with **4e** might also give rise to interesting structural motifs.

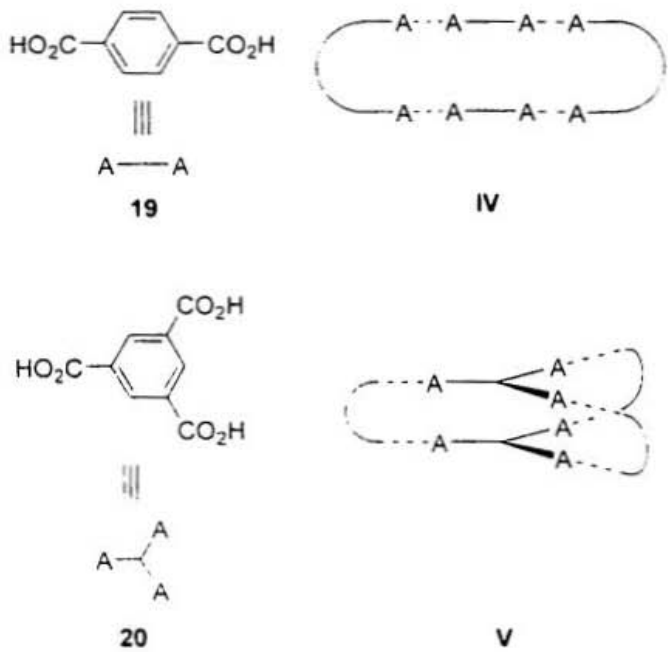

Figure 2.13: Proposed supramolecular structures of **4e** with terephthalic acid (**IV**) and trimesic acid (**V**).

Initial attempts to co-crystallize **4e** with terephthalic acid or trimesic acid have so far failed to give mixed crystals (by ^{1}H NMR). Only DMF has been used as a solvent, so a wide range of crystallization conditions is still to be investigated. Since this project is beyond the scope of this thesis, it was not pursued further. It is a promising project however, and might well be the basis of a new direction in the application of cyclophane chemistry to the area of supramolecular assemblies.

2.4.3 NMR study of *syn*-2,11-dithia[3.3]metacyclophanes

The 300 MHz ^{1}H NMR spectra of all the 6,15-disubstituted cyclophanes **4** and the 5-substituted *meta*-xylenes **12** were recorded at the same concentration (6 mM) and temperature (19°C) in C_6D_6, $CDCl_3$ and DMSO-d_6. The concentration was chosen so as to be as low as possible to still give good quality spectra while minimizing intermolecular interactions. The ^{1}H NMR spectroscopic data of the series of compounds can be found in Tables A-1a-c in Appendix A.

2.4.3.1 Correlation with the Hammett constant σ_m

The experimental $\Delta\delta H_t$ and $\Delta\delta H_e$ values were plotted against several physical organic parameters (Hammett's σ_m (this Section) Taft's dual parameter system (Section 2.4.3.2), Swain and Lupton's dual parameter system (Section 2.4.3.3), electronegativity values of the substituents (Appendix C) and AM1-calculated dipole moments (Appendix C). The first correlation that was studied involved the Hammett constant σ_m, for which the $\Delta\delta$ values for each solvent were plotted directly versus the literature values (Table A-2, Appendix A).[52] The resulting graphs are given in Figures 2.14a-c.* In each plot, the trend lines (calculated by linear regression) are drawn for $\Delta\delta H_t$ and $\Delta\delta H_e$.

---

* Error in $\Delta\delta$ was taken as ± 0.02 ppm.

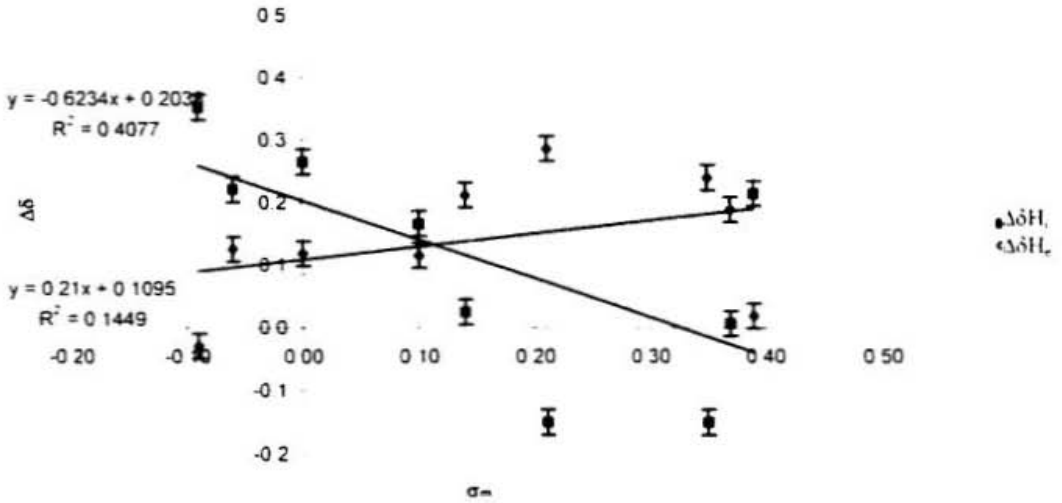

Figure 2.14a: $\Delta\delta H_t$ and $\Delta\delta H_e$ versus σ_m for spectra measured on C_6D_6 solutions.

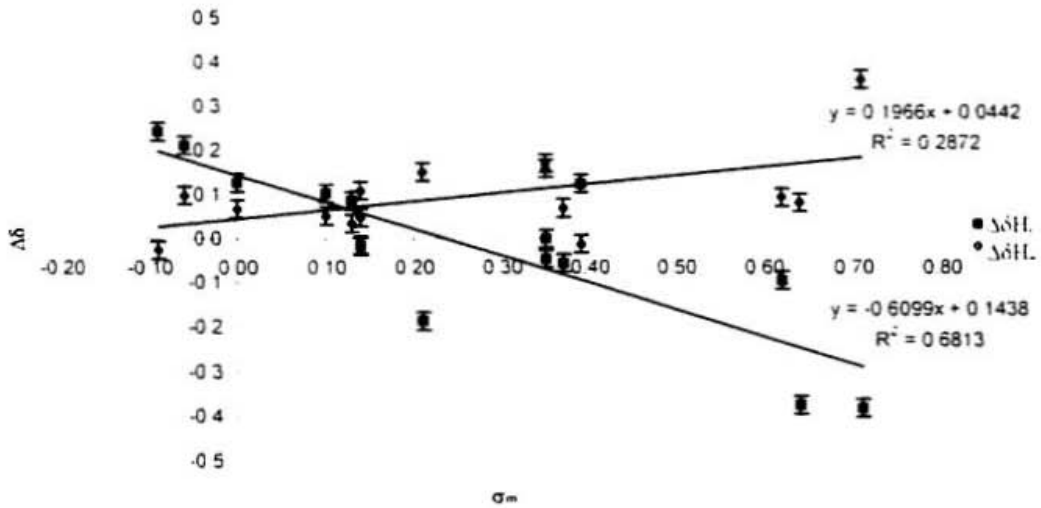

Figure 2.14b: $\Delta\delta H_t$ and $\Delta\delta H_e$ versus σ_m for solutions measured on $CDCl_3$ solutions.

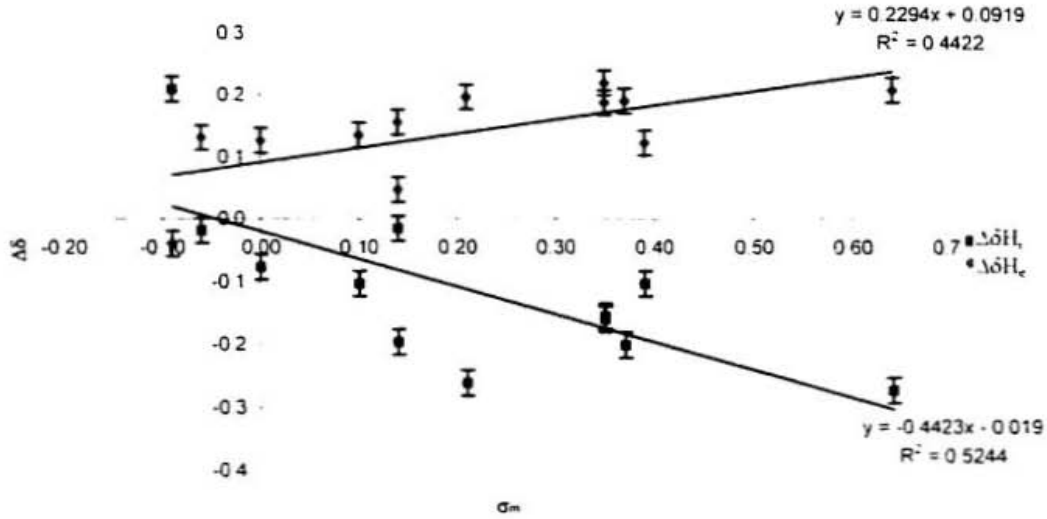

Figure 2.14c: $\Delta\delta H_t$ and $\Delta\delta H_e$ versus σ_m for spectra measured on DMSO-d_6 solutions.

When the graphs and trend lines for the different solvents are compared, several features are apparent. The trend line for $\Delta\delta H_t$ has a negative slope in each solvent and the line for $\Delta\delta H_e$ has a positive slope. Unfortunately, some data points are well off the indicated trend lines. For spectra measured in C_6D_6 solution this is the case for R = OAc (σ_m = 0.39, $\Delta\delta H_t$ = 0.215, $\Delta\delta H_e$ = 0.019). For spectra measured in $CDCl_3$ solution, the points for R = OAc (σ_m = 0.39, $\Delta\delta H_t$ = 0.124, $\Delta\delta H_e$ = -0.013) and R = S(O)Me (σ_m = 0.21, $\Delta\delta H_t$ = -0.187, $\Delta\delta H_e$ = 0.150) are well off the line and for spectra measured in DMSO-d_6 solution, the anomalous points are those for R = NH_2 (σ_m = -0.09, $\Delta\delta H_t$ = 0.210, $\Delta\delta H_e$ = -0.039) and R = S(O)Me (σ_m = 0.21, $\Delta\delta H_t$ = -0.261 only). Despite the presence of some scattering, the trends are unmistakable.

The values for R^2 in Figures 2.14a-c are quite low, so that the correlations can at best be described as a trend. Scattering of data points might be the result of the choice of Hammett's σ_m as physical organic parameter, as it has not been designed to describe conformational processes such as those in the *syn*-2,11-dithia[3.3]metacyclophane system. In trying to explain the scattering of data points, the assumptions that have been made earlier should also be considered. When the hypothesis upon which this work rests was developed, it was assumed that: (a) the only conformers that contribute to the observed ^{1}H NMR spectrum at room temperature are the *c,c*, the *h,c* and the *h,h* conformers, (b) the steric deshielding effect of a sulfur atom in a bridge is equal for each interaction and (c) this steric deshielding effect is additive for each interaction.

The first assumption (that only the *c,c*, the *h,c* and *h,h* conformers should be considered) is probably valid. It is based on reports from Semmelhack[10] and Shinmyozu,[31] who only observed these bridge conformers. In Section 2.4.5 our DNMR studies of cyclophanes **4b**, **4d**, **4g**, **4l**, **4n** and **4r** will be presented. These results were in agreement with Semmelhack and Shinmyozu's results and supported this assumption.

The second assumption, that the steric deshielding effect of a thioether bridge is the same for every interaction, is probably only true by approximation. The amount of steric deshielding that occurs on a proton when steric crowding occurs depends on the distance between (in case of cyclophanes **4**) the thioether bridge and the proton considered. The assumption that the steric deshielding of the internal proton by a *pseudo-boat* bridge is

the same as the steric deshielding of the external proton by a *pseudo-chair* bridge presumes that the distance between these protons and the sulfur atoms in the bridges (or the bond critical points of the C-S bonds) is the same. Although it would be difficult to measure accurately the distance between the sulfur atom in a thioether bridge and a proton in a particular conformer in solution, an estimation of these values can be made based on AM1 level calculations. In Figure 2.15 the AM1-calculated structures and the distances between the thioether bridges and the sterically deshielded aromatic protons are given for the three bridge conformers of the parent system *syn*-2,11-dithia[3.3]metacyclophane **4b**.

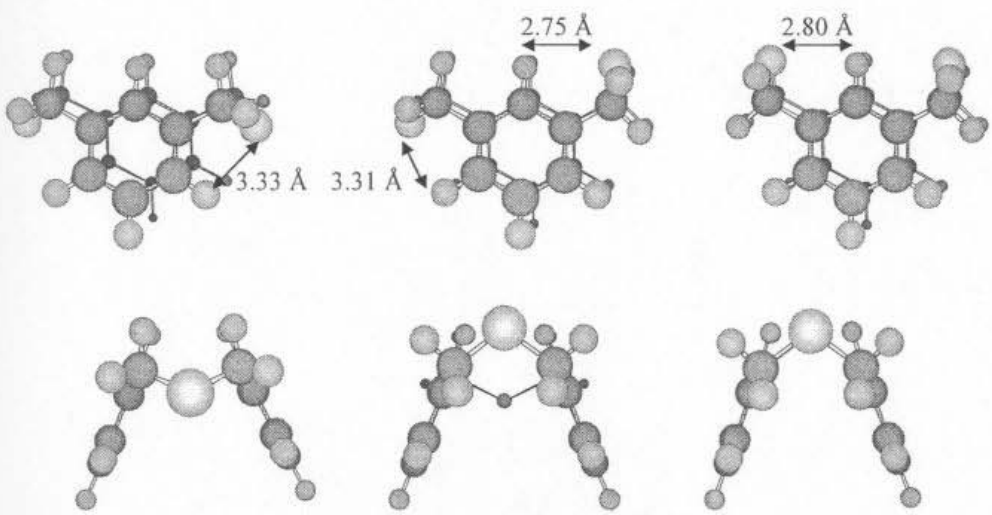

Figure 2.15: AM1 calculated structures and steric deshielding distances in *c,c*-**4b** (left), *b,c*-**4b** (middle) and *b,b*-**4b** (right).

From Figure 2.15 it can be seen that the distance between a *pseudo-boat* bridge and an external proton is calculated to be approximately 3.3 Å, but the distance between an

internal proton and a *pseudo-chair* bridge is calculated to be only about 2.8 Å. This difference in distance can be attributed to the non-coplanarity of the aromatic rings in each calculated structure. The smallest angle between the planes of the aromatic rings (dihedral angle: 48.5° in *c,c*-**4b**, 38.2° in *b,c*-**4b** and 38.2° *b,b*-**4b**) causes the external protons to separate, and, at the same time, to move away from the sulfur atoms in the bridge. For the internal protons the opposite is true, although the effect is not as large. From the published X-ray structure of **4b**[4] (dihedral angle 20.6°) it is obvious that the AM1-calculated dihedral angle is greatly overestimated, but any dihedral angle greater than 0° would cause a difference in distance between the internal and external protons and their corresponding bridges. This difference in distance then leads to a difference in steric deshielding, which would lead to different values for "x" in Section 2.3 for the internal and external protons. As only dihedral angles greater than 0° have ever been observed and or calculated for [3.3]metacyclophanes (Table 2.01) it can also be expected that the steric deshielding effect for the internal proton would be more than twice as large (as previously assumed) as the effect on the external protons, which could lead to the observed ratios of slopes in Figures 2.14a-c.

Compound	R	Dihedral angle (°)
4a	CN	9.0[5]
4b	H	20.6[4]
4c	Br	17.7[53]
4e	CO_2H	9.5[54]
4l	OMe	15.3[53]
4q	SO_2Me	29.0[53]
4r	CO_2Me	18.9[53]
4s	CC-H	29.6[53]

Table 2.01: Dihedral angle in the solid state for selected *syn*-2,11-dithia[3.3]metacyclophanes.

From Table 2.01 it can be seen that a great variation in dihedral angles has been observed in the solid state. No trend is obvious between the value for this angle and any molecular property such as electronic nature or steric bulk of the substituents on the *syn*-2,11-dithia[3.3]metacyclophane structure. If the variation in dihedral angle also occurs in solution it can be expected that the value for "x" (Section 2.3) is not the same for all 6,15-disubstituted *syn*-2,11-dithia[3.3]metacyclophanes. This might explain the significant scattering that was observed in Figures 2.14a-c.

The above discussion of the dependence of the amount of steric deshielding on the dihedral angle might also explain why certain data points in Figures 2.14a-c are well off

the trend lines. This would only hold true if the dihedral angle in these particular compounds is drastically different from the dihedral angle in the majority of the cyclophanes studied. From examination of the structures it is not clear why these particular compounds would exhibit greater dihedral angles than the greater part of the group. The compounds that correspond with the anomalous points do not have substituents that are sterically more demanding than other cyclophanes studied and also electronically these compounds are well within the range of electronic dispositions studied. Unfortunately it does not seem obvious how one would measure the dihedral angle in these systems, so it is not possible to discard the possibility that a drastically different dihedral angle in these systems would cause these particular compounds to show data points well off the expected trend lines. Another explanation for these anomalies can be found based on intramolecular interactions between the substituents and will be discussed after some comments on the remaining assumption from Section 2.3.

After considering the first two assumptions that were made in the development of our hypothesis, the third assumption (additivity of the effect of steric deshielding) should be examined. This assumption was only made for the internal protons in the *b,b* conformer. The internal protons in the *c,c* and *b,c* conformers and the external protons in all three conformers are only deshielded by one proximate bridge. Only if the *b,b* conformer were a major contributor to the conformer mixture of a particular cyclophane in solution at room temperature would the accuracy of this assumption play a role in the error in $\Delta\delta$ values. As the mole fraction of *b,b* conformer is expected to be a function of the

electronic character of the substituent in the 6- and 15- positions (and thus σ_m). deviation from a straight line would be expected only for the compounds with strongly electron withdrawing groups in Figures 2.14a-c if this additivity were not valid. This effect is not observed.

The last effect that remains to be considered is related to the nature of the correlation that is studied. Somewhat arbitrarily, Hammett's σ_m values were chosen for correlation studies of the $\Delta\delta$ values. By making this choice it was automatically assumed that the σ_m value for a given substituent would be equal in the 5-substituted *meta*-xylene and the corresponding *syn*-2,11-dithia[3.3]metacyclophane. This assumption might not hold true if in the cyclophane system significant intramolecular interactions occur between the substituents in the 6- and 15 positions, as these interactions are clearly not accounted for in the *meta*-xylene system. These intramolecular interactions (e.g. intramolecular hydrogen bonding of hydroxyl groups or carboxylic acid groups) might cause the substituent groups to adopt different conformations than in the *meta*-xylene reference compounds. Hammett's σ_m values do not account for such interactions and changes in conformation and as a result the effective σ_m value of these substituents might be different from the published Hammett's σ_m value. This would lead to significant scattering of these particular data points in the plots of $\Delta\delta$ values *versus* σ_m.

2.4.3.2 Correlations with Taft's dual parameter system

When considering the electronic influence of the substituents on the cyclophane system, the question arises whether this effect is a completely inductive effect, or if there might be a resonance component as well. In the literature, several systems have been described that separate the inductive and resonance components in Hammett-like systems. The two systems that will be considered are Taft's[55,56] dual-parameter system and Swain and Lupton's modification.[57-59]

Figure 2.16 shows the results of plotting of $\Delta\delta H_i$ measured in $CDCl_3$ solutions as a function of σ in which $\sigma = \sigma_I + \alpha\sigma^0_R$. Values for σ_I and σ^0_R were taken from published tables[52] and are represented in Appendix A. Eight trend lines (best lines calculated *via* linear regression) have been drawn in the plot, in 0.1 increments for the value of α, ranging from 0.1 – 0.8. For clarity, only the data points for α = 0.1 and α = 0.8 are indicated on the plot, since the data points with intermediate α-values will be located on a straight line, evenly distributed between these two sets of points.

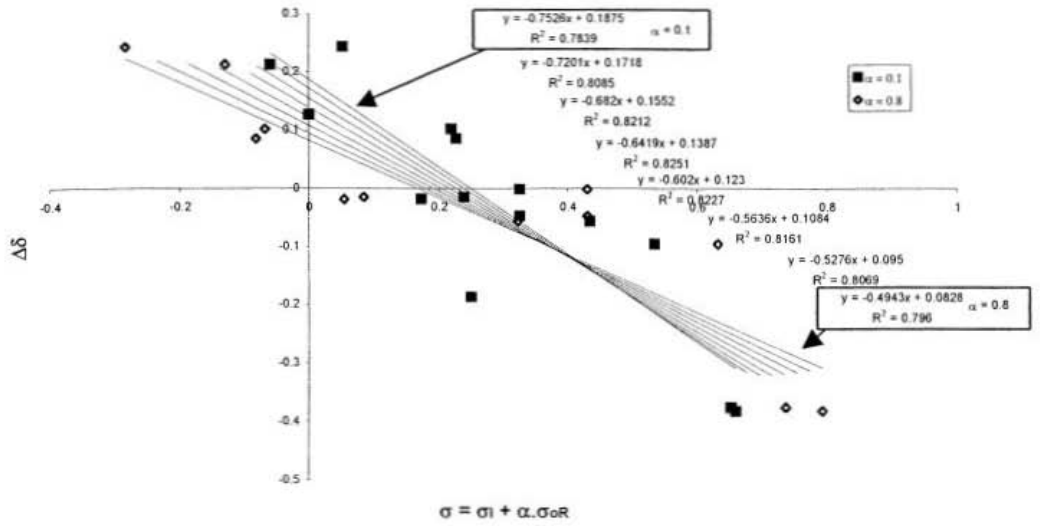

Figure 2.16: $\Delta\delta H_i$ measured in $CDCl_3$ solutions versus $\sigma = \sigma_I + \alpha\sigma^{o}_{R}$.

In Figure 2.16 the best correlations are found for the trend lines where $\alpha = 0.4 - 0.6$. This corresponds to a ratio of inductive to resonance effects of approximately 2:1, which is not surprising, as the resonance effects of the substituent groups would be expected to have less of an impact on the ratio of conformers than the inductive effect. The inductive effect was not expected to have a great impact on the bridge conformational behavior of a *syn*-2,11-dithia[3.3]metacyclophane since no resonance structures could be drawn that greatly prefer one conformation over the other. When the $\Delta\delta H_i$ values in other solvents or the $\Delta\delta H_e$ values are treated in the same manner, very similar results are obtained, with optimal ratios of approximately 2:1 for inductive and resonance effects (Appendix B).

2.4.3.3 Correlation with the Swain-Lupton dual parameter system

A dual-parameter system quite similar to that of Taft is the system developed by Swain and Lupton.[57-59] In this system, the Hammett σ_m is replaced by a new σ, which is defined as $\sigma = f\mathcal{F} + r\mathcal{R}$. The constants $\mathcal{F}$ and $\mathcal{R}$ are constants that describe the field (inductive) and resonance effect of each substituent and were obtained from published tables[52] and are given in Appendix A. Figure 2.17 shows the result of plotting $\Delta\delta H_i$ measured in $CDCl_3$ solution versus σ, where f and r are varied from a ratio $f = 0.70$ / $r = 0.30$ in 0.02 increments for f and –0.02 for r to a final ratio of $f = 0.90$ / $r = 0.10$. In total, 11 lines are indicated on the plot and again only the data points at the extremes for σ are indicated since the other data points lie in between.

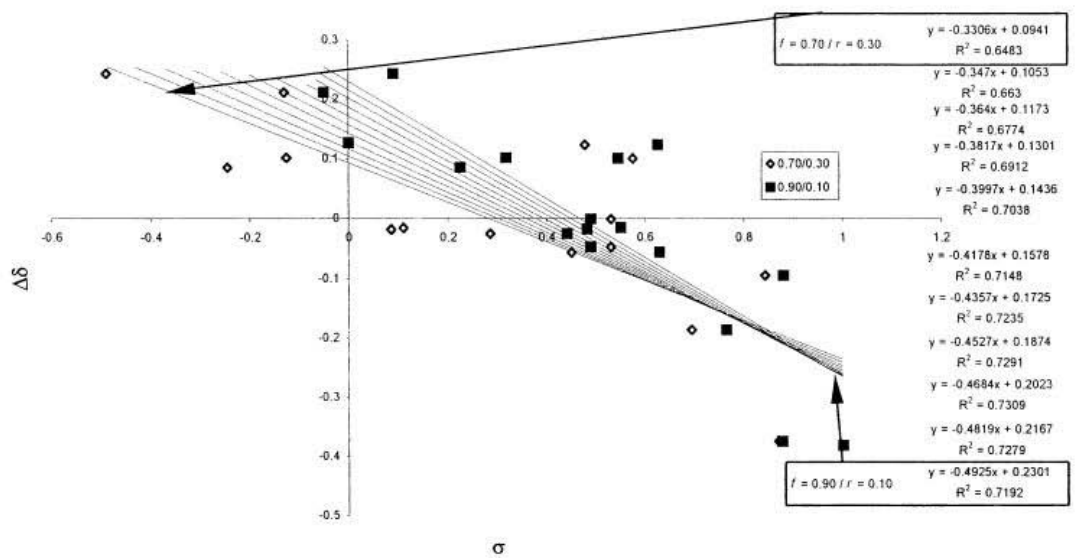

Figure 2.17: $\Delta\delta H_i$ measured on $CDCl_3$ solution versus $\sigma = f\mathcal{F} + r\mathcal{R}$.

The results from Figure 2.17 (Swain and Lupton system) are quite similar to those from Figure 2.16 (Taft's system). Again it can be observed, that the inductive (field) effects are more important in determining the bridge conformational behavior of *syn*-2,11-dithia[3.3]metacyclophanes than resonance effects. In the case of the Swain and Lupton variation a ratio of approximately 0.86 / 0.14 seems to be optimal, giving a ratio of approximately 5:1 of inductive compared to resonance influence. The discrepancy in ratios (2:1 compared to 5:1) between the two dual-parameter systems is not surprising, since the systems define their constants differently. For Taft's system, ^{13}C NMR data are used to determine the values for σ_I and σ^0_R[56] and Swain and Lupton used experimental data from various reactions to try to separate resonance and field effects.[57,58] The importance of the two dual-parameter systems in the case of the bridge conformational behavior of *syn*-2,11-dithia[3.3]metacyclophanes is that they both suggest the inductive effect is more important than the resonance effect.

Other parameters with which the $\Delta\delta$ values might show a correlation were investigated, but no correlations were found when the relation between $\Delta\delta$ values and AM1-calculated dipole moments[59] or group electronegativities[51] was studied. A summary of these results can be found in Appendix C.

2.4.3.4 Solvent Effects

In the plots of $\Delta\delta$ values versus the Hammett constants (Figure 2.14a-c) the slope for $\Delta\delta H_t$ shows some variation with the nature of the solvent (-0.62 in C_6D_6, -0.61 in $CDCl_3$ and –0.44 in DMSO-d_6) and seems to become less negative with increasing polarity of the solvent. For the slope of $\Delta\delta H_e$ no significant difference is observed (0.21 in C_6D_6, 0.20 in $CDCl_3$ and 0.23 in DMSO-d_6). The trend in slopes for $\Delta\delta H_t$ can be explained by invoking the principle that a polar solvent will accommodate a molecule with a large dipole moment better than will a nonpolar solvent.[92] This would cause the substituents to have a less pronounced effect in polar solvents, leading to smaller slopes in the plots of $\Delta\delta$ versus the Hammett constant. This suggests there might be a correlation between the slopes in the different solvents and some constant describing the polarity of the solvent. When the values of the slopes of $\Delta\delta H_t$ and $\Delta\delta H_e$ are plotted against the solvent dielectric constant (ε) the plot in Figure 2.18 arises.

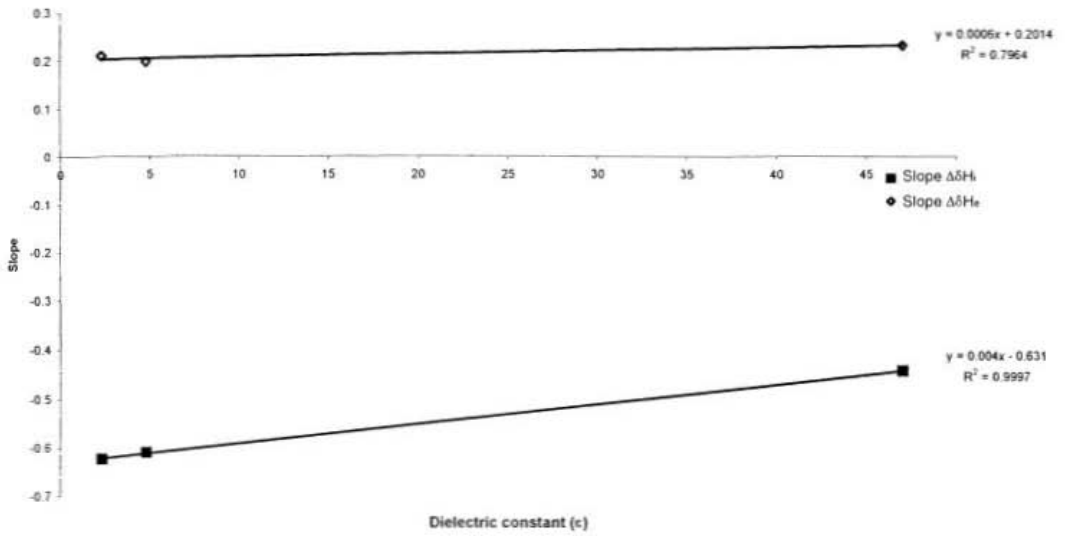

Figure 2.18: Slope of $\Delta\delta H_i$ and $\Delta\delta H_e$ versus dielectric constant (ε).

From the plot in Figure 2.18 it can be seen, that at least for the internal protons, a strong correlation exists between the slope of $\Delta\delta H_i$ versus σ_m and the solvent polarity. For the external protons, this trend seems to be absent. In both cases, care must be taken when interpreting the data, since only three different solvents were used to determine the solvent effect on the $\Delta\delta$ values and two of these have similar values for their dielectric constants. When the slopes from Figures 2.14a-c are plotted versus Reichardt's empirical measure of solvent polarity ($E_T(30)$),[62] the correlation is worse (Figure 2.19). Measurements of these values in more solvents would be necessary to obtain more reliable data, but the small amount of data available so far gives an indication of a correlation between the solvent polarity and the magnitude of the effect of the

substituents of 6,15-disubstituted *syn*-2,11-dithia[3.3]metacyclophanes on the bridge conformational behavior.

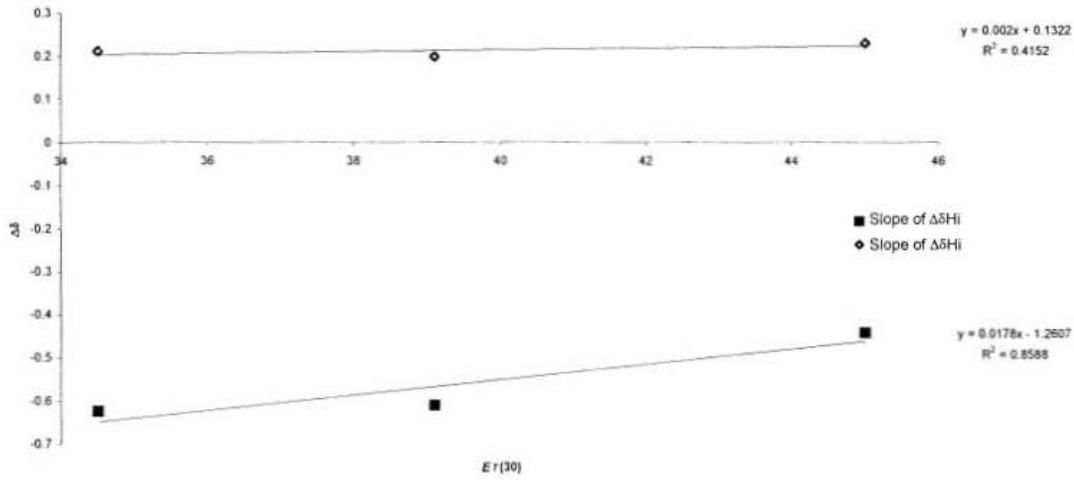

Figure 2.19: Slope of $\Delta\delta H_i$ and $\Delta\delta H_e$ versus Reichardt's $E_T(30)$.

The preceding discussion of the conformational behavior of *syn*-2,11-dithia[3.3]metacyclophanes as a function of the Hammett constant of the substituents in the 6- and 15-positions of the cyclophanes described some noteworthy correlations. Not only does it seem that the electronic properties of the substituents have an influence on the conformational preferences of the sulfur-containing bridges, there also seems to be a solvent effect on the conformational behavior of *syn*-2,11-dithia[3.3]metacyclophanes. Unfortunately, no technique is currently available to determine the actual ratios of the different bridge conformers of *syn*-2,11-dithia[3.3]metacyclophane at room temperature.

If such a technique would be available it would be interesting to compare its results with the results that were presented in this Chapter.

More study is required into the behavior of specific cyclophanes (**4a**, **4j**, **4l** and **4r**) to determine why the data points corresponding to these compounds are well off the trend lines in Figure 2.14a-c. Maybe the situation in these particular cyclophanes is not as the hypothesis contends and the hypothesis might have to be re-examined with this in mind. Additional data for the library of compounds in other solvents are also required, in order to establish with confidence a correlation between solvent polarity and the magnitude of the influence of the substituent groups on the bridge conformational behavior of *syn*-2,11-dithia[3.3]metacyclophanes.

2.4.5 DNMR studies of 6,15-disubstituted *syn*-2,11-dithia[3.3]metacyclophanes

In order to study further the conformational behavior of *syn*-2,11-dithia[3.3]metacyclophanes, some DNMR studies were performed. It was hoped that an explanation could be found using this technique for the scattering of data points that occurred in the plots of $\Delta\delta$H values versus σ_m (Figures 2.14a-c). For the DNMR studies, compounds **4b** (R = H), **4d** (R = CO_2Et), **4g** (R = Me), **4l** (R = OAc), **4n** (R = OMe) and **4r** (R = S(O)Me) were chosen, since the electronic character of the substituent groups ranges from electron-withdrawing (**4d** σ_m = 0.35, **4l** σ_m = 0.39) to electron-donating (**4g**

σ_m = -0.06). All DNMR experiments were performed in CD_2Cl_2 at 500 MHz between 183 and 273 K.

The results from the DNMR studies of each 6,15-disubstituted *syn*-2,11-dithia[3.3]metacyclophane are quite similar. Therefore, the typical results of **4d** will be discussed here first, followed by short discussions of the results from the other cyclophanes.

2.4.5.1 *syn*-6,15-Bis(ethoxycarbonyl)-2,11-dithia[3.3]metacyclophane (4d)

At 273 K the spectrum of **4d** shows two singlets in the aromatic region (7.31 ppm (H_i) and 7.49 ppm (H_e)). Broadening of each signal occurs as the temperature is lowered and at 223 K each signal has resolved into two broad singlets. Integrations suggest that these signals arise from two conformers that are present in a 3:2 ratio.* The major conformer shows a signal at 7.43 ppm for the internal and 7.40 ppm for the external proton (183 K). The corresponding signals of the minor conformer appear at 7.17 ppm and 7.53 ppm (183 K) (Figure 2.20). The same conformer ratio is obtained from the integration of the signals for the benzylic protons in the bridges. The singlet for these protons at room temperature resolves at 203 K to give an AB system for the minor conformer, which is overlapped with a broad singlet for the major conformer (Figure 2.20).

* For this and subsequent DNMR studies the data are consistent with two conformers. There is no evidence for more conformers, although their presence cannot be ruled out.

2.4.5.2 *syn*-6,15-Diacetoxy-2,11-dithia[3.3]metacyclophane (4j)

The results from the DNMR study of *syn*-6,15-diacetoxy-2,11-dithia[3.3]metacyclophane **4j** are quite similar to those of *syn*-6,15-bis(ethoxycarbonyl)-2,11-dithia[3.3]metacyclophane **4d**. At 273 K, the aromatic region showed two singlets (6.68 ppm and 6.85 ppm; integration ratio 2 : 1) and the benzylic protons appeared as a singlet at 3.80 ppm. Upon cooling, all signals broadened and, at lower temperatures, two sets of signals could be observed. The aromatic region showed the presence of two conformers at temperatures below 223 K in a ratio of 2.3 : 1 (Figure 2.21). At the same temperature the signal for the benzylic protons had resolved into an AB system, which was overlapped by a broad singlet (Figure 2.21).

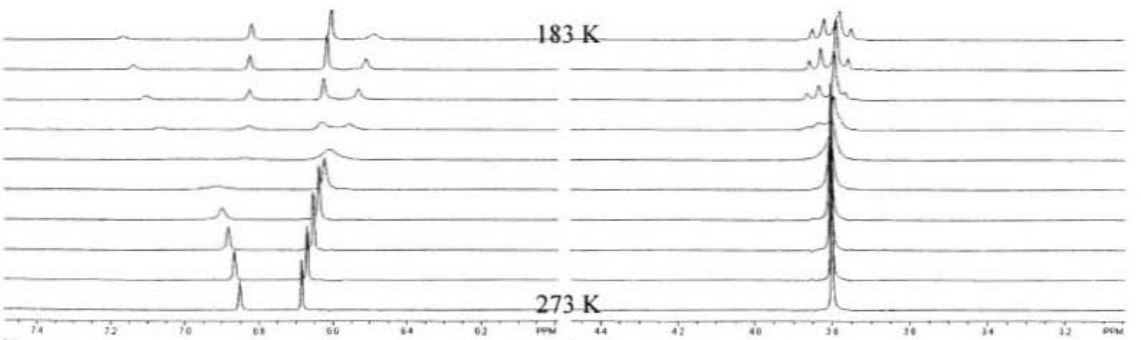

Figure 2.21: DNMR spectra of **4j**.

The major conformer gives rise to the signals at 6.82 ppm (H_i) and 6.61 ppm (H_e) and the AB system for the benzylic signals. Based on the upfield shift of the signal for the internal proton, the major conformer could be assigned the *c,c* conformation (analogous to the results for **4d**). The minor conformer showed signals at 7.13 ppm (H_i), 6.51 ppm

signal (no *pseudo-chair*-like signal is observed). However, calculations on *syn*-2,11-dithia[3.3]metacyclophanes that suggest that the *b,b* conformer is the highest energy conformer[5] so it would be expected that it would be observed in lower concentrations than the *pseudo-boat,pseudo-chair* conformer. The absence of any evidence for the presence of the *b,c* conformer renders this explanation unlikely.

Another explanation is that the signals that are observed for the major conformer are actually the result of a fast interconversion between two conformers, even at 183 K. This would not only explain the broad singlet that appears as the only signal for the benzylic protons, but would also explain why only two signals are observed in the low temperature NMR spectrum. The two interconverting conformers are probably not the *b,c* and *b,b* conformers based on the expectation that the energy barrier (and thus the coalescence temperature) for the interconversion process between these two conformers is similar to that for interconversion between the *c,c* and *b,c* conformers, which would have led to resolution of the signal for the bridge protons at approximately the same temperature (differences in $\Delta\nu$ and J values will lead to only a small difference in T_c).[63] The observation of a broad singlet for the benzylic protons at low temperature can be explained by fast *syn* to *syn'* interconversion of a *b,c* conformer (Scheme 2.07). This interconversion process would exchange the environment of the axial and equatorial protons in the bridges and thus lead to a broad singlet for these protons. The observation of a singlet for the external proton is also consistent with this process. Shinmyozu obtained similar results in his DNMR studies of **d_4-8b** and **d_4-8c**.[31] A notable result in our

study is the ratio of 2 : 3 between the *c,c* and *b,c* conformers in favor of the *b,c* conformer, which was calculated to be 0.3 kcal/mol (1.4 kJ/mol; AM1 level calculations)[93] higher in energy than the (minor) *c,c* conformer. This ratio of *c,c* and *b,c* conformers is consistent with dipole minimization as discussed for *syn*-6,15-dicyano-2,11-dithia[3.3]metacyclophane **4a** (Section 2.1).

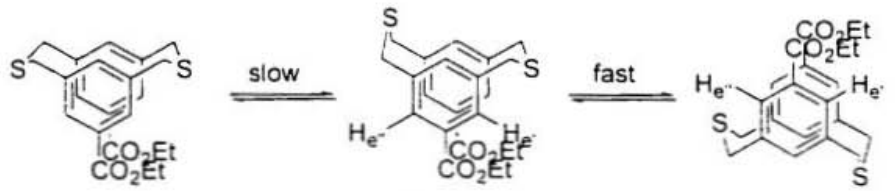

***syn*-c,c-4d** ***syn*-b,c-4d** ***syn'*-b,c-4d**

Scheme 2.07: Some interconversion processes of different conformers of **4d** at 183 K.

For the *c,c* to *b,c* interconversion, the activation energy can be estimated to be 10.2±0.3 kcal mol (42.7±1.1 kJ mol; based on T_c = 213±5 K; $\Delta\nu$ = 55.2±0.2 Hz and ^2J = 15.0±0.2 Hz).[93-95] If the signals for the major conformer can indeed be attributed to a fast *syn* to *syn'* equilibrium, the energy difference between the *c,c* and the *b,c* conformers can be estimated at 0.15 kcal/mol (0.62 kJ/mol) since the *syn*-*b,c* and the *syn'*-*b,c* are degenerate structures.

2.4.5.2 *syn*-6,15-Diacetoxy-2,11-dithia[3.3]metacyclophane (4j)

The results from the DNMR study of *syn*-6.15-diacetoxy-2.11-dithia[3.3]metacyclophane **4j** are quite similar to those of *syn*-6.15-bis(ethoxycarbonyl)-2.11-dithia[3.3]metacyclophane **4d**. At 273 K, the aromatic region showed two singlets (6.68 ppm and 6.85 ppm; integration ratio 2 : 1) and the benzylic protons appeared as a singlet at 3.80 ppm. Upon cooling, all signals broadened and, at lower temperatures, two sets of signals could be observed. The aromatic region showed the presence of two conformers at temperatures below 223 K in a ratio of 2.3 : 1 (Figure 2.21). At the same temperature the signal for the benzylic protons had resolved into an AB system, which was overlapped by a broad singlet (Figure 2.21).

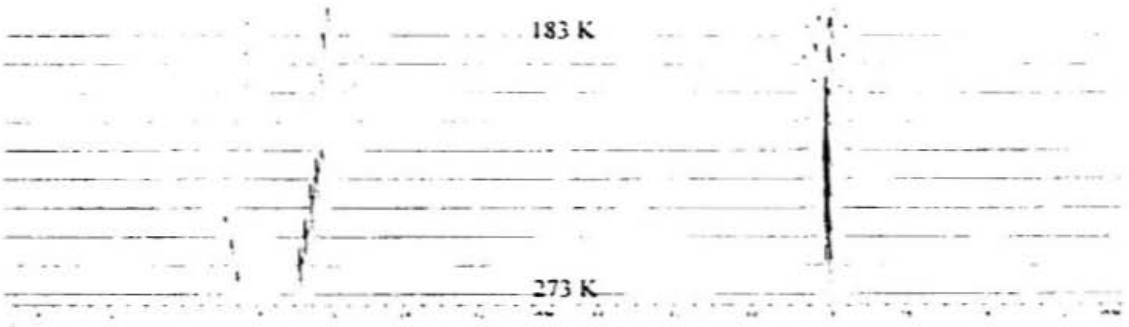

Figure 2.21: DNMR spectra of **4j**.

The major conformer gives rise to the signals at 6.82 ppm (H_t) and 6.61 ppm (H_c) and the AB system for the benzylic signals. Based on the upfield shift of the signal for the internal proton, the major conformer could be assigned the *c,c* conformation (analogous to the results for **4d**). The minor conformer showed signals at 7.13 ppm (H_t), 6.51 ppm

(H_c) and 3.79 ppm (broad singlet for the benzylic protons) and, as for **4d**, is probably the result of a fast *syn* to *syn'* equilibrium for the *b,c* conformer. The ratio of the signals of approximately 2.3:1 in favor of the *c,c* conformer indicates a greater preference of **4j** for the *c,c* conformer than for **4d**, which is consistent with the dipole minimization effect discussed earlier. The energy barrier for the bridge-wobbling process between the *c,c* and the *b,c* conformers can be estimated to be 10.8±0.2 kcal/mol (45.2±1.0 kJ/mol; T_c = 223±5 K; $\Delta\nu$ = 49.7±0.2 Hz; ^2J = 21.9±0.2 Hz) and that the *b,c* conformer is approximately 0.3 kcal/mol (1.3 kJ/mol) higher in energy than the *c,c* conformer.

2.4.5.3 *syn*-6,15-Dimethyl-2,11-dithia[3.3]metacyclophane (4f)

The DNMR study of *syn*-6,15-dimethyl-2,11-dithia[3.3]metacyclophane **4f** was limited by the properties of the solvent, CD_2Cl_2. At the lowest temperature that can be used with this solvent (183 K), the spectrum shows clear signs of resolution into different conformers, but the resolution is not sufficient to draw conclusions (Figure 2.22).

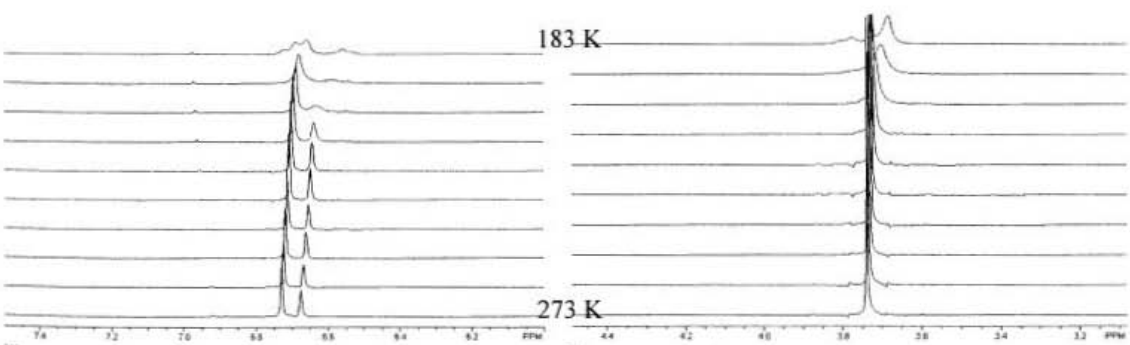

Figure 2.22: DNMR spectra of **4f**.

2.4.5.4 *syn*-6,15-Bis(sulfoxymethyl)-2,11-dithia[3.3]metacyclophane (4p)

The DNMR study of *syn*-6,15-bis(sulfoxymethyl)-2,11-dithia[3.3]metacyclophane **4p** was complicated by the presence of two diastereomers of the cyclophane as a result of the asymmetry at the sulfur atoms in the substituents. As a result, the ^{1}H NMR spectrum of **4p** at 273 K showed a set of signals for each diastereomer (Figure 2.23). At lower temperatures, this led to complicated and overlapping signals in the aromatic region of at least two conformers (each probably with two diastereomers), of which analysis proved too difficult to assign unambiguously the signals to any conformer. The signals for the benzylic protons were not resolved.

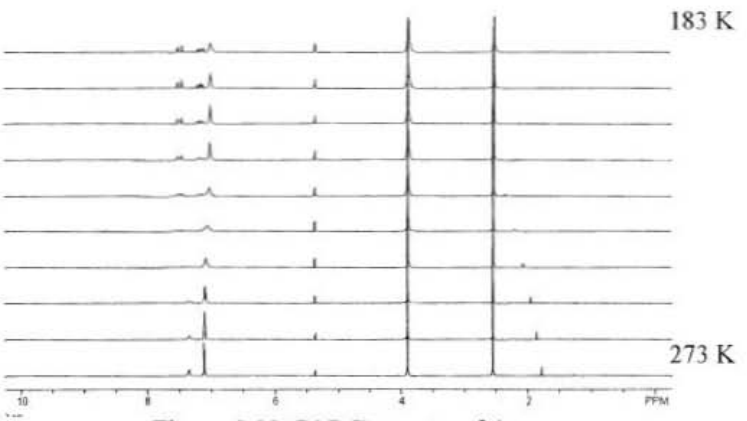

Figure 2.23: DNMR spectra of **4p**.

2.4.5.5 *syn*-6,15-Dimethoxy-2,11-dithia[3.3]metacyclophane (4l)

In its DNMR study, *syn*-6,15-dimethoxy-2,11-dithia[3.3]metacyclophane **4l** showed results similar to **4d** and **4j**. At 183 K, the spectrum showed the presence of at least two conformers, although some overlapping of signals occurred (Figure 2.24). The signal of the benzylic protons, which is a singlet at 3.67 ppm at 273 K, had not resolved into an AB system at 183 K, although considerable broadening was observed. The aromatic region changed from two singlets at 273 K to a set of broad peaks at 183 K. Resolution of the signals at 183 K was not sufficient to draw conclusions.

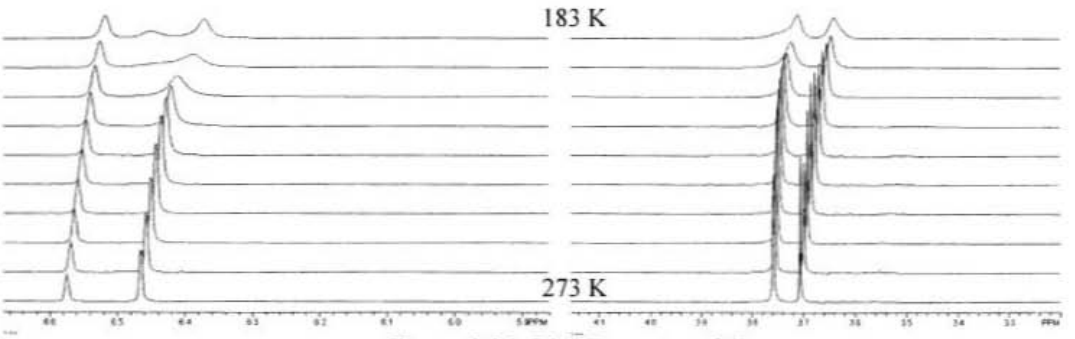

Figure 2.24: DNMR spectra of **4l**.

2.4.5.6 *syn*-2,11-Dithia[3.3]metacyclophane (4b)

DNMR study of the parent system *syn*-2,11-dithia[3.3]metacyclophane **4b** showed similar features to the systems described in the preceding Sections. Since the substituents in the 6- and 15-positions are now hydrogen, the aromatic region (at 273 K) is more complex than cyclophanes with other substituents in these positions. At 273 K, the benzylic protons appeared as a singlet (3.80 ppm). As the temperature was lowered, all signals broadened and resolution of the aromatic region into two conformers occurred below 213 K (Figure 2.23). The signal for the benzylic protons resolved into an AB system, overlapped with a broad singlet in a ratio 1.6 : 1 at that temperature (Figure 2.25). Assignment of the signals in the aromatic region was complicated by the splitting of some of the signals. Based on the results from the previous Sections and the electronic nature of the substituents on the 6- and 15 positions (H), the AB system (of the major conformer) was expected to result from the *c,c* conformer.

The minor conformer (based on the integration of the signals in the benzylic region) gave rise to a singlet at 7.08 ppm (H_i) and a broad singlet at 3.77 ppm for the benzylic protons, which suggests a fast equilibrium between at least two conformers. Based on the observations on the previously discussed cyclophane systems, this equilibrium is probably a fast *syn* to *syn'* equilibrium of the *b,c* conformer. The AB system in the benzylic region can be assigned to the *c,c* conformer and it can then be estimated that the energy barrier for the bridge wobbling process between the *c,c* and the *b,c* conformers is

approximately 10.2±0.3 kcal/mol (42.7±1.0 kJ/mol; T_c = 213±5 K; $\Delta\nu$ = 57.2±0.2 Hz; ^2J = 14.3±0.2 Hz). The energy difference between the *c,c* and the *b,c* conformers can be estimated to be 0.2 kcal/mol (0.7 kJ/mol).

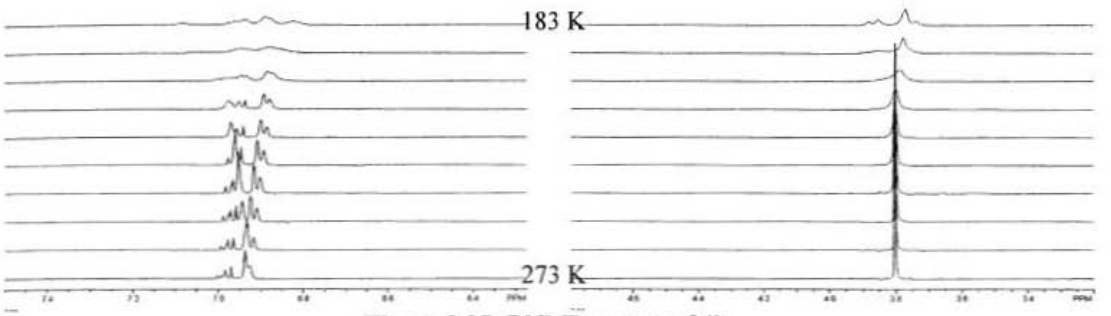

Figure 2.25: DNMR spectra of **4b**.

In order to study further the conformational behavior of **4b** at lower temperatures, a ^{13}C NMR spectrum was collected of the conformer mixture at 183 K (Figure 2.26). Two sets of signals in a ratio of approximately 3:2 were observed, which corresponds to the 1.6 : 1 ratio that was observed in the ^1H NMR spectrum at the same temperature. The major conformer could be assigned the ^{13}C resonances at δ 137.5, 131.6, 128.3, 126.1 (overlap with minor conformer) and 38.7 ppm and the signals at δ 136.7, 130.6, 127.5, 126.1 (overlap with major conformer) and 36.2 ppm can be attributed to the minor conformer (Figure 2.26). The major conformer was assigned the *c,c* conformer based on the results from the ^1H NMR spectrum and the signals of the minor conformer can be attributed to the *b,c* conformer in rapid *syn* to *syn'* equilibrium.

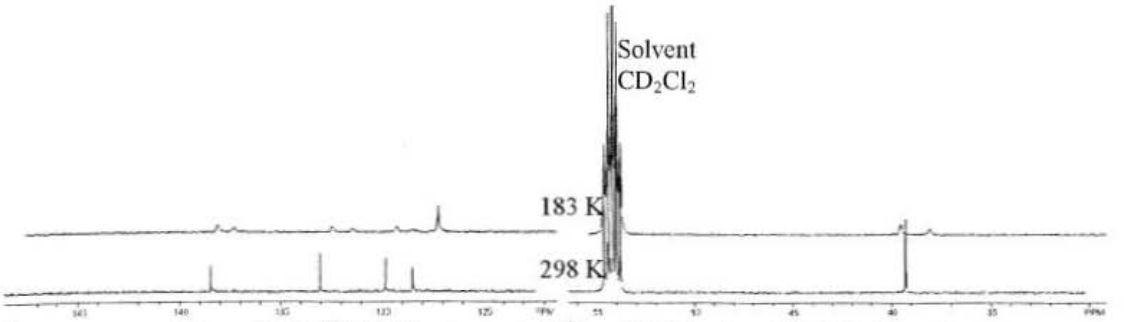

Figure 2.26: ^{13}C NMR spectrum of **4b** at 183K (top) and 298 K (bottom).

2.4.5.7 Conclusions and future work on DNMR studies

In this Section the results of our DNMR studies of 6,15-disubstituted *syn*-2,11-dithia[3.3]metacyclophanes **4** have been presented. To our knowledge this is the first DNMR study of these compounds that has shown resolution of the ^{1}H and ^{13}C NMR spectra at lower temperatures.

The results of the DNMR studies of 6,15-disubstituted *syn*-2,11-dithia[3.3]metacyclophanes (Sections 2.4.5.1-2.4.5.6) show strong similarities. For cyclophanes **4b** (R = H), **4d** (R = CO_2Et) and **4j** (R = OAc), freezing of the *c,c* to *b,c* interconversion was observed. The activation energy for the bridge-wobbling process was estimated to be 10-11 kcal/mol, which is in good agreement with Shinmyozu's estimate of 11.6 kcal/mol for the all-carbon [3.3]metacyclophanes.[30,31] The *b,c* conformers in the frozen mixtures still underwent fast *syn* to *syn'* interconversion similar to Shinmyozu's results.[31] The presence of *b,b* conformers was not observed directly in any case, but could

not be ruled out. In order to observe this conformer, it might be necessary to introduce an extra tether in the cyclophane system (e.g. compound **21**, Figure 2.27), which was the strategy that led to observation of a *b,b* conformer by Shinmyozu.[30]

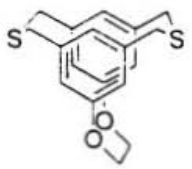

21

Figure 2.27: Tethered cyclophane **21**

A further observation was the preference of *syn*-6,15-bis(ethoxycarbonyl)-2,11-dithia[3.3]metacyclophane **4d** (with electron withdrawing groups) to prefer the *b,c* conformation (*c,c* : *b,c* = 2 : 3), whereas the parent system (*syn*-2,11-dithia[3.3]metacyclophane **4b**) and the more electron rich *syn*-6,15-diacetoxy-2,11-dithia[3.3]metacyclophane **4j** prefer the *c,c* conformation (*c,c* : *b,c* = 1.6 : 1 and 2.3 : 1, respectively). This is again consistent with the hypothesis that the electronic nature of the substituents is an important factor in determining the bridge conformational behavior of *syn*-2,11-dithia[3.3]metacyclophanes. It would be interesting to expand the DNMR studies to cyclophane systems with stronger electron withdrawing properties (e.g. *syn*-6,15-dicyano- and *syn*-6,15-dinitro-2,11-dithia[3.3]metacyclophane **4a** and **4i**), since a considerable preference of these systems for the *b,c* conformer is expected and perhaps

even the *b,b* conformer can be observed. However, low solubility of these systems (in CD_2Cl_2) has so far prevented us from studying these compounds using DNMR.

2.5 Experimental

General. All chemicals were reagent grade and were used as received. Chromatographic separations were performed on Merck silica gel 60 (particle size 40-63 μm, 230-400 mesh). Melting points were determined on a Fisher-Johns apparatus and are uncorrected. Elemental analyses were performed at the MicroAnalytical Service Laboratory, Department of Chemistry, University of Alberta. Mass spectral (MS) data were recorded on a V. G. Micromass 7070HS instrument. ^{1}H NMR (300.1 MHz) and ^{13}C NMR (75.47 MHz) were obtained on a General Electric GE 300-NB spectrometer: ^{1}H shifts are relative to internal tetramethylsilane; ^{13}C shifts are relative to the solvent resonance ($CDCl_3$: δ = 77.0). All experiments with moisture- or air-sensitive compounds were performed in anhydrous solvents under nitrogen unless otherwise noted. Solvents were dried and distilled according to standard procedures.

Ethyl 3,5-dimethylbenzoate (12d)[46]

To a well-stirred solution of 3,5-dimethylbenzoic acid **12e** (17.66 g, 118 mmol) in EtOH (abs.) (400 mL) was added concentrated sulfuric acid (15 mL), and the solution was

refluxed for 24 h. The reaction mixture was cooled, concentrated *in vacuo* to approximately 30% of the original volume and poured into H_2O (150 mL) and EtOAc (150 mL). The aqueous layer was extracted with EtOAc (150 mL). The organic extracts were combined, washed with saturated aqueous $NaHCO_3$ solution (2 x 100 mL), H_2O (100 mL) and saturated aqueous NaCl solution (75 mL), dried ($MgSO_4$) and concentrated *in vacuo* to yield a yellow oil. Purification by vacuum distillation (93 – 95 °C / 4-6 mmHg) yielded **12d** (17.16 g, 96.3 mmol, 82%) as a colorless oil; IR (Nujol, cm^{-1}): 1723 (s), 1609 (m), 1307 (s), 1216 (s), 1115 (m), 1035 (m), 866 (w), 767 (m); ^1H NMR ($CDCl_3$) δ 7.67 (s, 2H), 7.17 (s, 1H), 4.36 (q, 2H, J = 6.8 Hz), 2.36 (s, 6H), 1.39 (t, 3H, J = 6.8 Hz); ^{13}C NMR ($CDCl_3$) δ 166.9, 137.9, 134.4, 130.3, 127.2, 60.8, 21.1, 14.3; EI-MS (70 eV) m/z (%): 178 (26, M^+), 150 (21), 133 (100), 105 (49).

5-Acetoxy-*meta*-xylene (12j)

To a solution of 3,5-dimethylphenol **12k** (6.54 g, 53.5 mmol) in acetic anhydride was added concentrated sulfuric acid (10 drops), and the reaction mixture was stirred under an atmosphere of nitrogen for 6 h. The mixture was poured into ice water (600 mL) and EtOAc (150 mL) was added. The aqueous layer was re-extracted with EtOAc (150 mL). The organic extracts were combined, washed successively with saturated aqueous $NaHCO_3$ solution (3 x 150 mL), water (100 mL) and saturated aqueous NaCl solution (150 mL), dried ($MgSO_4$) and concentrated under reduced pressure. The residue was

distilled *in vacuo* to yield 5-acetoxy-*meta*-xylene **12j** (7.07 g, 43.1 mmol, 80%) as a colorless oil (b.p. 86 - 86.5°C/4-6 mm Hg); IR (Nujol, cm^{-1}) 1766 (s), 1618 (m), 1591 (w), 1296 (w), 1208 (s), 1138 (m), 1032 (m), 948 (w), 899 (w), 869 (w), 835 (w); ^1H NMR ($CDCl_3$) δ 6.86 (s, 1H), 6.69 (s, 2H), 2.31 (s, 6H), 2.27 (s, 3H); ^{13}C NMR ($CDCl_3$) δ 169.7, 150.5, 139.2, 127.6, 119.1, 21.2, 21.1; EI-MS (70 eV) *m/z* (%): 164 (10, M^+), 122 (100), 107 (28).

3,5-Dimethylanisole (12l)

Powdered KOH (10.81 g, 85% purity, 164 mmol) was slurried in DMSO (50 mL) and the mixture was stirred at room temperature for 5 min under an atmosphere of nitrogen. 3,5-Dimethylphenol **12k** (5.00 g, 40.9 mmol) was added, followed by iodomethane (5.1 mL, 82 mmol). After 30 min the reaction mixture was poured out into cold water (100 mL) and extracted with dichloromethane (2 x 75 mL). The combined organic extracts were washed with water (5 x 100 mL) and saturated aqueous NaCl solution (100 mL), dried ($MgSO_4$) and concentrated *in vacuo*. The residual yellow oil was distilled *in vacuo* to yield 3,5-dimethylanisole **12l** (4.50 g, 33 mmol, 81%) as a colorless oil (b.p. 60.5 - 61 °C /20-25 mm Hg; lit:[99] 193 °C); ^1H NMR ($CDCl_3$) δ 6.61 (s, 1H), 6.54 (s, 2H), 3.78 (s, 3H), 2.30 (s, 6H); ^{13}C NMR ($CDCl_3$) δ 159.6, 139.1, 122.4, 111.6, 55.0, 21.4; EI-MS (70 eV) *m/z* (%): 136 (100, M^+), 121 (21).

Ethyl 3,5-bis(bromomethyl)benzoate (14d)

N-Bromosuccinimide (22.97 g, 129.1 mmol) was added in two equal portions to a warm solution of ethyl 3,5-dimethylbenzoate **12d** (10.00 g, 56.11 mmol) in CH_2Cl_2 (175 mL). After each addition, a spatula-tip of benzoyl peroxide was added and the mixture was stirred at reflux while it was irradiated with a 100 W lamp for 2 h. The mixture was cooled to room temperature and washed with H_2O (100 mL), saturated aqueous $NaHCO_3$ solution (2 x 100 mL), H_2O (100 mL) and saturated aqueous NaCl solution (75 mL). The organic layer was dried ($MgSO_4$), concentrated *in vacuo* and crystallized twice from heptane to give **14d** (8.34 g, 24.8 mmol, 44%) as a colorless solid; mp: 88.0 – 89.0 °C; IR (Nujol, cm^{-1}): 1699 (m), 1313 (m), 1228 (w); ^1H NMR ($CDCl_3$) δ 8.00 (s, 2H), 7.62, (s, 1H), 4.51 (s, 4H), 4.40 (q, 2H, J = 6.7 Hz), 1.41 (t, 3H, J = 6.7 Hz); ^{13}C NMR ($CDCl_3$) δ 165.4, 138.9, 133.8, 131.7, 130.0, 61.4, 21.3, 14.3; MS (EI, 70 eV) m/z (%): 335 (5, M^+), 291 (16), 255 (100), 211 (32), 177 (18), 148 (22), 132 (27); Anal. Calc'd for $C_{11}H_{12}Br_2O_2$: C, 39.32; H, 7.86. Found: C, 79.89; H, 8.18.

3,5-Bis(bromomethyl)methylbenzene (14f)

N-Bromosuccinimide (75.21 g, 422.6 mmol) was added in three equal portions to a warm solution of mesitylene **12f** (25.02 g, 208.2 mmol) in CH_2Cl_2 (450 mL). After each addition, a spatula-tip of benzoyl peroxide was added, and the mixture was stirred at reflux while it was irradiated with a 100 W lamp for 2h. The mixture was cooled to room

temperature and washed with saturated aqueous $NaHCO_3$ solution (2 x 200 mL), H_2O (150 mL) and saturated aqueous NaCl solution (150 mL). The organic layer was dried ($MgSO_4$), concentrated *in vacuo* and crystallized from heptane to give an off-white solid that was purified by column chromatography (SiO_2; 10% $CHCl_3$ / hexanes) to yield **14f** (6.53 g, 25.5 mmol, 11%) as a colorless solid. From the heptane mother liquor, additional **14f** (17.0 g, 61 mmol, 29%) could be isolated by extensive column chromatography. For **14f**: mp 63.5 – 65 °C (lit:[97] 62 - 63 °C); ^{1}H NMR ($CDCl_3$) δ 7.23 (s, 1H), 7.16 (s, 2H), 4.46 (s, 4H), 2.36 (s, 3H); ^{13}C NMR ($CDCl_3$) δ 139.3, 138.2, 129.9, 126.7, 33.0, 21.2; EI-MS (70 eV) *m z* (%): 278 (M^+, 9), 197 (100), 118 (79).

1,3-Bis(mercaptomethyl)benzene (13b)

To a solution of α,α'-dibromo-*meta*-xylene **14b** (5.00 g, 18.9 mmol) in EtOH (abs.) (100 mL) was added thiourea (2.96 g, 38.9 mmol) and the mixture was refluxed under an atmosphere of nitrogen for 16 h and concentrated *in vacuo* to give a white solid. The solid was suspended in a degassed solution of KOH (6.25 g, 85% purity, 94.7 mmol) in H_2O (110 mL) and EtOH (420 mL) and the mixture was stirred under reflux overnight. After cooling to room temperature, 9 M H_2SO_4 was added until the mixture became slightly acidic. The mixture was extracted with CH_2Cl_2 (2 x 100 mL). The combined organic layers were washed with H_2O (100 mL) and saturated aqueous NaCl solution (75

mL), dried ($MgSO_4$) and concentrated *in vacuo* to yield **13b** (2.89 g, 17.0 mmol, 90%) as a light yellow oil that was used without further purification in the next step.

3,5-Bis(mercaptomethyl)methylbenzene (13f)

A solution of thiourea (1.25 g, 16.4 mmol) and α,α'-dibromomesitylene **14f** (2.22 g, 7.99 mmol) in degassed EtOH (100 mL) was stirred for 3 h at reflux under an atmosphere of nitrogen. A degassed solution of KOH (2.64 g, 85% purity, 40.0 mmol) in H_2O (25 mL) was added and the reaction mixture was stirred for an additional 3 h under reflux. The mixture was cooled in an ice bath, acidified using 9 M H_2SO_4 and poured into a mixture of CH_2Cl_2 (50 mL) and H_2O (50 mL). The aqueous layer was extracted with CH_2Cl_2 (50 mL), and the combined organic extracts were washed with H_2O (50 mL) and saturated aqueous NaCl solution (50 mL), dried ($MgSO_4$) and concentrated *in vacuo* to yield **13f** (1.40 g, 7.60 mmol, 95%) as a light yellow-brown oil that was used without further purification in the next step.

***syn*-2,11-Dithia[3.3]metacyclophane (4b)**

A degassed solution of dithiol **13b** (1.44 g, 8.45 mmol) and α,α'-dibromo-*meta*-xylene **14b** (2.23 g, 8.45 mmol) in benzene (250 mL) was added by dropping funnel over 2.5 h to a mechanically stirred, degassed solution of KOH (2.79 g, 85% purity, 42.3 mmol) in H_2O (75 mL) and EtOH (250 mL) under an atmosphere of nitrogen. After 15 h the

reaction mixture was concentrated *in vacuo* to a volume of *ca.* 100 mL and then CH_2Cl_2 (100 mL) and H_2O (100 mL) were added. The aqueous layer was extracted with CH_2Cl_2 (100 mL) and the combined organic extracts were washed with H_2O (100 mL) and saturated aqueous NaCl solution (75 mL), dried ($MgSO_4$) and concentrated *in vacuo*. The residue was purified using column chromatography (SiO_2; 50% CH_2Cl_2 / hexanes) to yield **4b** (0.95 g, 3.5 mmol, 41%) as a colorless solid: mp: 118 - 119.5 °C (hexanes) (lit:[1] 119 - 121 °C); ^{1}H NMR (CD_2Cl_2) δ 6.99 (t, 2H, J = 7.4 Hz), 6.94 (d, 4H, J = 7.0 Hz), 6.92 (s, 2H), 3.80 (s, 8H); ^{13}C NMR (CD_2Cl_2) δ 137.7, 132.1, 128.7, 127.3, 38.3; EI-MS (70 eV) *m/z* (%): 272 (68, M^+), 167 (17), 137 (47), 105 (100).

syn-6,15-Bis(ethoxycarbonyl)-2,11-dithia[3.3]metacyclophane (4d)

To a vigorously stirred solution of **12d** (3.40 g, 10.1 mmol) in CH_2Cl_2 (600 mL) and EtOH (abs.) (60 mL), Na_2S/Al_2O_3 (9.02 g, 2.69 mmol/g, 24.3 mmol) was added in 3 portions over 1 h. The reaction mixture was stirred for an additional hour, filtered through a plug of Celite, concentrated *in vacuo* and purified by column chromatography (SiO_2; CH_2Cl_2) followed by crystallization from EtOH to yield **4d** (0.78 g, 1.9 mmol, 37%) as colorless crystals and trimer **15d** (0.35 g, 0.62 mmol, 19%) as colorless crystals.

Dimer **4d**: mp 104.5-106 °C; IR (Nujol, cm^{-1}): 1734 (s), 1285 (m), 1272 (m), 1122 (w), 1072 (w); ^{1}H NMR ($CDCl_3$) δ 7.51 (s, 4H), 7.24 (s, 2H), 4.31 (q, 4H, J = 7.6 Hz), 3.83 (s, 4H), 1.38 (t, 6H, J = 7.6 Hz); ^{13}C NMR ($CDCl_3$) δ 165.7, 137.3, 135.1, 130.5, 128.2, 60.7, 37.4, 14.1; MS (EI, 70 eV) *m/z* (%): 416 (48, M^+), 370 (30), 342 (5), 327 (6), 309

(11), 295 (7), 270 (7), 239 (8), 209 (29), 69 (100): Anal. Calc'd for $C_{22}H_{24}O_4S_2$: C, 63.43; H, 5.81. Found: C, 63.26; H, 5.69.

Trimer **15d**: mp 150-151.5 °C; IR (Nujol, cm^{-1}) 1720 (m), 1304 (w), 1281 (w); ^1H NMR ($CDCl_3$) δ 7.97 (s, 6H), 7.33 (s, 3H), 4.40 (q, 6H, J = 7.0 Hz), 3.61 (s, 12 H), 1.42 (t, 9H, J = 7.0 Hz); ^{13}C NMR ($CDCl_3$) δ 166.1, 138.5, 133.8, 131.6, 129.1, 36.2, 34.9, 14.3; MS (EI, 70 eV) m/z (%): 624 (9, M^+), 578 (42), 532 (37), 468 (22), 447 (19), 415 (36), 401 (35), 371 (60); Anal. Calc'd for $C_{33}H_{36}O_6S_3$: C, 63.43; H, 5.81. Found: C, 63.36; H, 5.44.

syn-2,11-Dithia[3.3]metacyclophane-6,15-dicarboxylic acid (4e)

Cyclophane **4d** (0.43 g, 1.0 mmol) was dissolved in a degassed solution of KOH (0.29 g, 85% purity, 4.4 mmol) in H_2O (20 mL) and EtOH (20 mL), and the reaction mixture was stirred for 16 h at reflux temperature under an atmosphere of nitrogen. The mixture was allowed to cool to room temperature before it was poured into H_2O (20 mL). The mixture was extracted with diethyl ether (2 x 25 mL). The aqueous layer was acidified with 1% HCl and cooled in an ice bath. Suction filtration followed by drying *in vacuo* yielded **4e** (0.33 g, 0.92 mmol, 89%) as a colorless solid, of which a small portion was recrystallized from DMF to give transparent crystals: mp: > 280 °C; IR (Nujol, cm^{-1}): 1699 (m), 1317 (m), 1258 (w), 1238 (w); ^1H NMR (DMSO-d_6) δ 12.6 (bs, 2H), 7.41 (s, 2H), 7.37 (s, 4H), 3.91 (s, 8H); ^{13}C NMR (DMSO-d_6) δ 196.8, 137.9, 135.4, 130.6, 127.8, 36.8; EI-MS (70 eV) m/z (%): 36 (83, M^+), 342 (24), 314 (12), 211 (22), 181 (48), 149 (100).

syn-6,15-Dimethyl-2,11-dithia[3.3]metacyclophane (4f)

A degassed solution of dithiol **12f** (3.50 g, 19.0 mmol) and dibromide **13f** (5.28 g, 19.0 mmol) in benzene (625 mL) was added *via* a dropping funnel over 2.5 h to a mechanically stirred, degassed solution of KOH (6.27 g, 85% purity, 95 mmol) in H_2O (190 mL) and EtOH (975 mL) under an atmosphere of nitrogen. The reaction mixture was stirred for an additional 10 h and the reaction mixture was concentrated *in vacuo* to a volume of ca. 100 mL and CH_2Cl_2 (250 mL) and H_2O (250 mL) were added. The aqueous layer was extracted with CH_2Cl_2 (100 mL) and the combined extracts were washed with H_2O (2500 mL) and brine (150 mL), dried ($MgSO_4$) and concentrated *in vacuo*. The residue was purified using column chromatography (SiO_2: 25% CH_2Cl_2/hexanes) crude **4f** that was crystallized from heptanes to give 6,15-dimethyl-2,11-dithia[3.3]metacyclophane **4f** (2.34 g, 7.79 mmol, 41%) as colorless needles: mp: 103 - 104 °C (lit:[68] 104-105.5 °C); ^{1}H NMR ($CDCl_3$, 500 MHz) δ 6.73 (s, 4H), 6.62 (s, 2H), 3.71 (s, 4H), 2.18 (s, 6H); ^{13}C NMR ($CDCl_3$) δ 137.9, 136.9, 129.0, 127.8, 37.7, 21.0; EI-MS (70 eV) % (*m z*): 300 (58, M^+), 181 (14), 151 (40), 120 (100).

2.6 References

(1) Mitchell, R. H.; Boekelheide, V. *J. Am. Chem. Soc.* **1974**, *96*, 1547-1557.

(2) Mitchell, R. H. *Heterocycles* **1978**, *11*, 563-586.

(3) In this chapter a large number of 6,15-disubstituted *syn*-2,11-dithia[3.3]metacyclophanes **4a-q** will be described. For a complete list of compounds the reader is referred to Figure 2.09.

(4) Anker, W.; Bushnell, G. W.; Mitchell, R. H. *Can. J. Chem.* **1979**, *57*, 3080-3087.

(5) Bodwell, G. J.; Bridson, J. N.; Houghton, T. J.; Yarlagadda, B. *Tetrahedron Lett.* **1997**, *38*, 7475-7478.

(6) Brown, C. J. *J. Chem. Soc.* **1953**, 3278-3285.

(7) Sako, K.; Tatemitsu, H.; Onaka, S.; Takemura, H.; Osada, S.; Wen, G.; Rudzinski, J. M.; Shinmyozu, T. *Liebigs Ann.* **1996**, 1645-1649.

(8) See also Section 2.4.2.

(9) The *c,c* conformer has been calculated as the lowest energy conformer for the parent system *syn*-[3.3]metacyclophane (EFF) and for the *syn*-2,11-dithia[3.3]metacyclophane system (AM1 and 3-21G*).

(10) Semmelhack, M. F.; Harrison, J. J.; Young, D. C.; Guttiérrez, A.; Rafii, S.; Clardy, J. *J. Am. Chem. Soc.* **1985**, *107*, 7508-7514.

(11) Newkome, G. R.; Pappalardo, S.; Fronczek, F. R. *J. Am. Chem. Soc.* **1983**, *105*, 5152-5153.

(12) Sato, T.; Wakabayashi, M.; Kainosho, M.; Hata, K. *Tetrahedron Lett.* **1968**, 4185-4189.

(13) Vögtle, F.; Schunder, L. *Chem. Ber.* **1969**, *102*, 2677-2683.

(14) Wilson, D. J.; Boekelheide, V.; Griffin Jr., R. W. *J. Am. Chem. Soc.* **1960**, *82*, 6302-6304.

(15) Gantzel, P. K.; Trueblood, K. N. *Acta Crystallogr.* **1965**, *18*, 958-968.

(16) Sato, T.; Wakabayashi, M.; Hata, K.; Kainosho, M. *Tetrahedron* **1971**, *27*, 2737-2755.

(17) Boekelheide, V.; Hollins, R. A. *J. Am. Chem. Soc.* **1973**, *95*, 3201-3208.

(18) Ernst, L.; Ibrom, K.; Marat, K.; Mitchell, R. H.; Bodwell, G. J.; Bushnell, G. W. *Chem. Ber.* **1994**, *127*, 1119-1124.

(19) Mitchell, R. H.; Weerawarna, K. S.; Bushnell, G. W. *Tetrahedron Lett.* **1984**, *25*, 907-910.

(20) Lai, Y.-H.; Zhou, Z.-L. *J. Chem. Soc., Perkin Trans. 2* **1994**, 2361-2365.

(21) Mitchell, R. H.; Weerawarna, K. S. *Tetrahedron Lett.* **1988**, *29*, 5587-5588.

(22) Takemura, H.; Kariyazono, H.; Kon, N.; Shinmyozu, T.; Inazu, T. *J. Org. Chem.* **1999**, *64*, 9077-9079.

(23) Hisatome, M.; Yoshihashi, M.; Yamakawa, K.; Iitaka, Y. *Bull. Chem. Soc. Jpn.* **1987**, *60*, 2953-2962.

(24) Ernst, L. *Prog. Nucl. Magn. Reson. Spectrosc.* **2000**, *37*, 47-190.

(25) Shinmyozu, T.; Inazu, T.; Yoshino, T. *Chem. Lett.* **1976**, 1405-1406.

(26) Krois, D.; Lehner, H. *J. Chem. Soc., Perkin Trans. 1* **1982**, 477-481.

(27) Otsubo, T.; Kitasawa, M.; Misumi, S. *Chem. Lett.* **1977**, 977-980.

(28) Otsubo, T.; Kitasawa, M.; Misumi, S. *Bull. Chem. Soc. Jpn.* **1979**, *52*, 1515.

(29) Rossa, L.; Vögtle, F. *J. Chem. Res. (S)* **1977**, 264.

(30) Sako, K.; Hirakawa, T.; Fujimoto, N.; Shinmyozu, T.; Inazu, T.; Horimoto, H. *Tetrahedron Lett.* **1988**, *29*, 6275-6278.

(31) Sako, K.; Shinmyozu, T.; Takemura, H.; Suenaga, M.; Inazu, T. *J. Org. Chem.* **1992**, *57*, 6536-6541.

(32) Mitchell, R. H.; Anker, W. *Tetrahedron Lett.* **1981**, *22*, 5135-5138.

(33) Observed signals for each proton are the weighted averages of the chemical shift values for that proton in each of the conformers. The weighting of each of the chemical shift values depends on the mole fractions of the conformers.

(34) The ^{1}H-NMR-spectra of 6,15-disubstituted *syn*-2,11-dithia[3.3]metacyclophanes at room temperature (300 MHz) show a singlet for the benzylic protons, and two signals for the aromatic region, as well as signals derived from the substituents in the 6- and 15-positions. The signals in the aromatic region often appear as singlets, due to the small value for the *meta*-coupling between the internal and the external protons.

(35) For compound **4c**: Langille, J. M.Sc. Thesis, Memorial University of Newfoundland, **1999**, 111-141.

(36) For compound **4l**: Mannion, M. R. Ph.D. Thesis, Memorial University of Newfoundland, **1999**, 169.

(37) For compounds **4j** and **4k**: Mannion, M. R. *Unpublished results*.

(38) For compounds **4m**, **4n**, **4o**, **4p**, **4q**, **12m**, **12o**, **12p** and **12q**: Li, J. *Unpublished results*.

(39) Compounds **12a**, **12b**, **12c**, **12e**, **12f**, **12g**, **12i**, **12k** and **12n** were purchased from the Aldrich Chemical Company.

(40) For compounds **4g**, **4h** and **4i**: Pottie, I. R. *Unpublished results*.

(41) Bodwell, G. J.; Houghton, T. J.; Koury, H. E.; Yarlagadda, B. *Synlett* **1995**, 751-752.

(42) Djerassi, C. *Chem. Rev.* **1948**, *43*, 271-317.

(43) Konishi, H.; Aritomi, K.; Okano, T.; Kiji, J. *Bull. Chem. Soc. Jpn.* **1989**, *62*, 591-593.

(44) Mistry, A.; Smith, K.; Bye, M. R. *Tetrahedron Lett.* **1986**, *27*, 1051-1054.

(45) Ghaffar, A.; Jabbar, A.; Siddiq, M. *J. Chem. Soc. Pak.* **1994**, *16*, 272-274.

(46) Fischer, L. F.; Speier, A. *Ber. Dtsch. Chem. Ges.* **1895**, *28*, 3252-3258.

(47) Philp, D.; Stoddart, J. F. *Angew. Chem., Int. Ed. Engl.* **1996**, *35*, 1155-1196.

(48) Krische, M. J.; Lehn, J.-M. *Struct. Bond.* **2000**, *94*, 3-30.

(49) Archer, E. A.; Gong, H.; Krische, M. J. *Tetrahedron* **2001**, *57*, 1139-1159.

(50) Walsh, P. L.; Maverick, E.; Chiefari, J.; Lightner, D. A. *J. Am. Chem. Soc.* **1997**, *119*, 3802-3806.

(51) Palmore, G. T. R.; McBride, M. T. *J. Chem. Soc., Chem. Commun.* **1998**, 145-146.

(52) Isaacs, N. S. *Physical Organic Chemistry*; Wiley and Sons: New York, 1987; pp 134-135.

(53) Bodwell, G. J. *Unpublished results.*

(54) This work.

(55) Ehrenson, S.; Brownlee, R. T. C.; Taft, R. W. *Prog. Phys. Org. Chem.* **1973**, *10*, 1-80.

(56) Taft, R. W.; Topsom, R. D. *Prog. Phys. Org. Chem.* **1987**, *16*, 1-83.

(57) Swain, C. G.; Lupton, E. C. *J. Am. Chem. Soc.* **1968**, *90*, 4328-4337.

(58) Swain, C. G.; Unger, S. H.; Rosenquist, N. R.; Swain, M. S. *J. Am. Chem. Soc.* **1983**, *105*, 492-502.

(59) Hansch, C.; Leo, A.; Unger, S. H.; Kim, K. H.; Nikaitani, D.; Lien, E. J. *J. Med. Chem.* **1973**, *16*, 1207.

(60) Calculations were performed using version 5.0a37 of the Chem3D Pro package of software (MOPAC, AM1, closed shell).

(61) Inamoto, N.; Masuda, S. *Chem. Lett.* **1982**, 1003-1006.

(62) Carey, F. A.; Sundberg, R. J. *Advanced Organic Chemistry, Part A: Structure and Mechanisms*; Plenum Press: New York, 1993; pp 232-239.

(63) $\Delta G^{\ddagger} = RT_c(22.96 + \ln T_c - \ln \Delta\nu')$ where $\Delta\nu' = (\Delta\nu^2 + 6J^2)^{\frac{1}{2}}$

(64) Calder, I. C.; Garratt, P. J. *J. Chem. Soc. (B)* **1967**, 660-662.

(65) Mannschreck, A.; Rissmann, G.; Vögtle, F.; Wild, D. *Chem. Ber.* **1967**, *100*, 335-346.

(66) *Aldrich Catalogue and Handbook of Fine Chemicals*; Aldrich Chemical Company, Inc.; Milwaukee, 1996.

(67) von Braun, J.; Engel, O. *Chem. Ber.* **1919**, *58*, 281-285.

(68) Mitchell, R. H.; Carruthers, R. J. *Can. J. Chem.* **1974**, *52*, 3054-3056.

Chapter 3

Attempted Synthesis of

[4](1,4)Benzeno[0](2,7)pyreno[4](1,4)benzenophane

3.1 Introduction

It was anticipated that the synthesis of pyrenophane **1** (Figure 3.01) would represent a significant step forward in our approach to synthesize a Vögtle belt.[1,2] Pyrenophane **1** contains a pyrene unit that could be synthesized using the valence isomerization-dehydrogenation (VID) protocol from biphenylophane diene **2**.[3] Two *para*-phenylene moieties in the tether of **1** constitute the very beginnings of a fully aromatic tether and were chosen in this synthetic target so that the aromatic portion of **1** maps onto the surface of Vögtle belt **4**. The tetramethylene tether in **1** constitutes the remnants of a third *para*-phenylene ring which is present in a more advanced synthetic target **3** (Figure 3.01). The calculated bend angle[4,5] of 114.4° for the pyrene unit in **1** is only slightly larger than that of the "record holder" (1,7-dioxa[7](2,7)pyrenophane: θ_{calcd} = 113.9°, $\theta_{X\text{-ray}}$ = 109.2°) so it seemed to be a reasonable target.

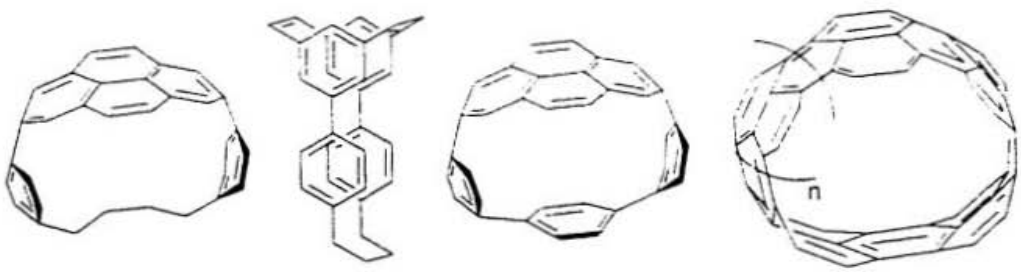

Figure 3.01: Structures of pyrenophanes **1** and **3**, biphenylophane diene **2** and Vögtle belt **4**.

Biphenylophane diene **2**, the direct precursor of **3**, seems to be a viable synthetic target, since other groups have synthesized similar, more strained structures (*vide infra*). In Section 3.1.1 a more detailed discussion of the literature in this area is given. Section 3.1.2 will describe the retrosynthetic analysis of biphenylophane diene **2**.

3.1.1 Biphenylophanes in the literature

Several groups have published syntheses of biphenylophanes and these compounds have received interest from different areas in (organic) chemistry. A small (2,3'-bridged) biphenylophane **5** has been described by Bickelhaupt *et al.* in conjunction with ongoing research in the area of small strained metacyclophanes,[7] and another small (2,2'-bridged) biphenylophane **6** has been described by Vögtle *et al.* as a part of their work in the synthesis of chiral compounds devoid of stereogenic centers.[8] Although both compounds showed some unique properties, in this Section discussion of the literature will remain limited to larger biphenylophanes containing at least two biphenyl units, which more closely resemble biphenylophane diene **2**.

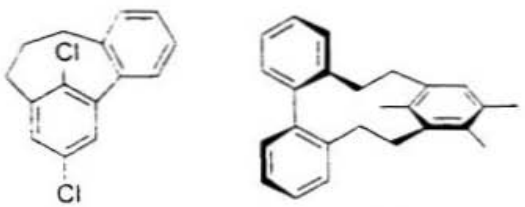

5 **6**

Figure 3.02: Biphenylophanes **5** and **6**.

A number of large biphenylophanes containing more than two biphenyl units has been synthesized by Vögtle *et al.* (Scheme 3.01).[8] Cyclophane **9** was reported in 1996 and was synthesized from compounds **7** and **8** *via* high-dilution coupling. This tube-shaped molecule was characterized by X-ray crystallography, and the molecular structure showed no signs of appreciable strain (i.e., contracted or elongated bond lengths, distorted bond angles, etc.) in the molecule.

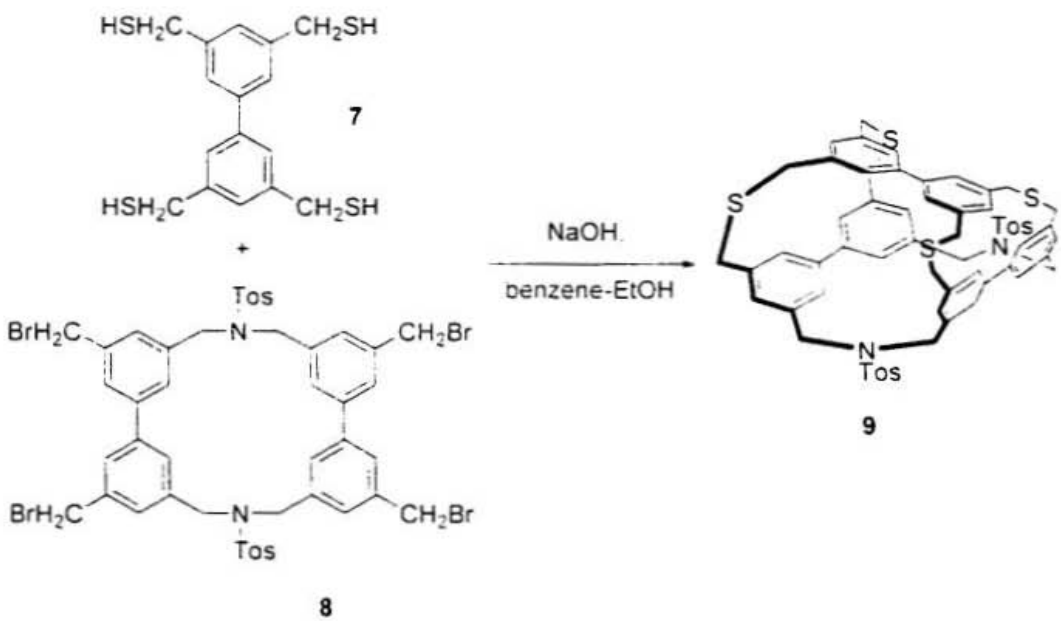

Scheme 3.01: Vögtle's synthesis of biphenylophane **9**.

In the same year Vögtle reported a series of "concave hydrocarbons",[9] some of which are "part of the framework of fullerene C_{60}".[9] Two of the cyclophanes reported were biphenylophane **10** (with three biphenyl subunits) and biphenylophane **11** (with four biphenyl subunits). Both compounds were synthesized *via* sulfur dioxide extrusion from

the bridges. They were tested for ion selective extraction of cations, but were not found to be efficient ligands for any of the metal salts tested.

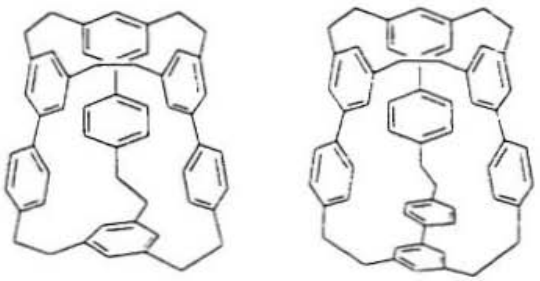

10 **11**

Figure 3.03: Structure of concave cyclophanes **10** and **11**.

Some smaller biphenylophanes have been reported by Iyoda (naphthalene bridged biphenylophane **12**)[10] and Staab ([2.2](4,4')biphenylophane **14**).[11] Both groups were interested in the π,π interactions that occur when the biphenyl units are held in a face-to-face orientation. An X-ray crystal structure of **12** revealed that the aromatic rings were almost planar and ring strain was evident from large β angles. No molecular structure of biphenylophane **14** was reported, but the relatively high yield in the sulfur dioxide extrusion step from **13** (47%) and the relative stability of **14** suggested that biphenylophane **2** was a viable synthetic target.

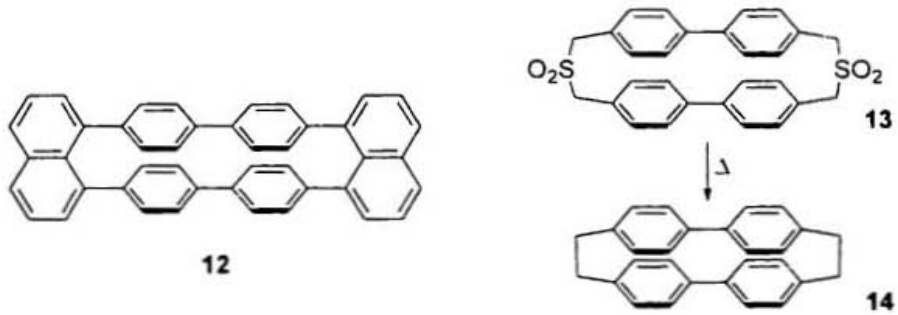

Scheme 3.02: Biphenylophanes **12-14**.

In 1978 Vögtle reported the sythesis of several biphenylophanes with 3 bridges.[12] In the synthetic approach to these systems, thermal sulfur dioxide extrusion as well as Stevens rearrangements were used to ring contract sulfur-containing bridges to give the 2-carbon bridges in **16** and **17**. Biphenylophanes **16** and **17** are structurally quite similar to biphenylophane diene **2**, but their syntheses do not allow for straightforward modification that would permit the introduction of the tetramethylene tether that is required for synthesis of **2**. The success of the three-fold Stevens rearrangement and Hoffmann elimination to form **17** from **15** suggests that formation of biphenylophane diene **2** using this methodology is viable.

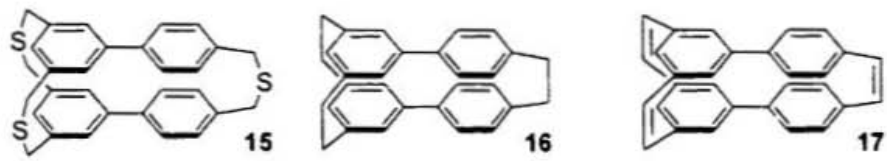

Figure 3.04: Vögtle's biphenylophanes **15** – **17**.

The last biphenylophanes that should be mentioned here are biphenylophanes **20** (Scheme 3.03) and **26** (Scheme 3.04). Biphenylophanes **19** have been reported by Nishimura, who synthesized these compounds *via* intramolecular [2+2] photocyclization of **18** to give **19**. Dissolving-metal reduction of **19** then afforded **20**.[13,14] At the outset of this project, compounds **19** were the only known biphenylophanes containing both a 2-membered bridge and a longer bridge. However, intramolecular [2+2] photocyclization of a derivative of **19** with a tetramethylene tether failed to give the desired product, thus rendering this type of approach less likely to be successful for the synthesis of **2**.

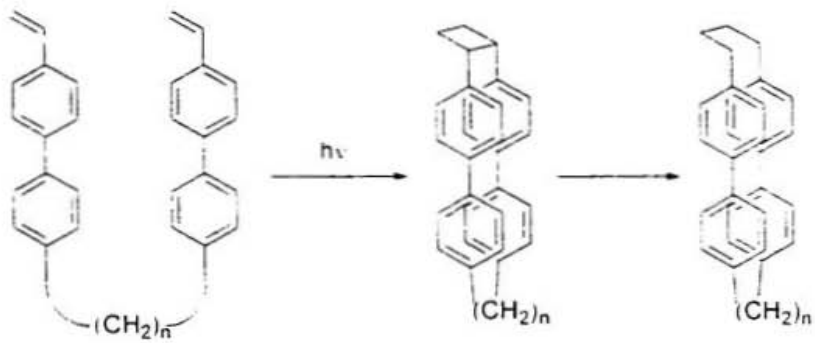

18 **a: n=5** **b: n=6** **19** **a: n=5** **b: n=6** **20** **a: n=5** **b: n=6**

Scheme 3.03: Nishimura's synthesis of biphenylophanes **20**

Biphenylophanes **25** and **26** were reported in 1995 by Tani *et al.* (Scheme 3.04).[15] A mixture of the two biphenylophanes was obtained from photolytic ring contraction of a mixture of the corresponding tetraselenacyclophanes **23** and **24**, which was obtained from high dilution coupling of **21** and **22**. Biphenylophanes **25** and **26** were characterized by

spectroscopic techniques and X-ray crystallography. A similar synthesis with the sulfur analogues was reported to yield only the "crossed" product **29** (Scheme 3.05).[1h]

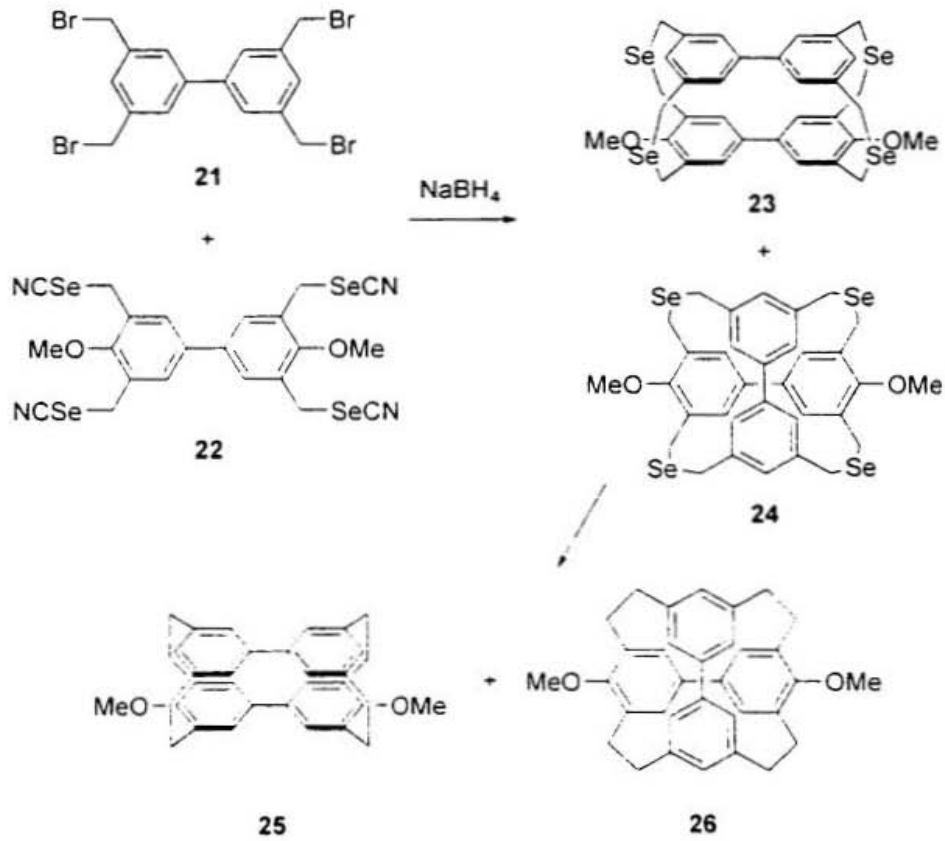

Scheme 3.04: Tani's synthesis of biphenylophanes **25** and **26**.

The X-ray crystal structure of **25** revealed a dihedral angle between the aromatic rings in each biphenyl unit of approximately 25° and a short intramolecular distance of only 2.77 Å as the shortest distance between the internal carbons of the faced biphenyl rings, comparable to the corresponding distance in [2.2]paracyclophane.[17,18] Synthetic target **2** is expected to be less strained than biphenylophane **25**, since, in **2**, two of the

dimethylene bridges of **25** are replaced by a single tetramethylene tether, which by virtue of its greater length, should release much of the strain that is present in **25**.

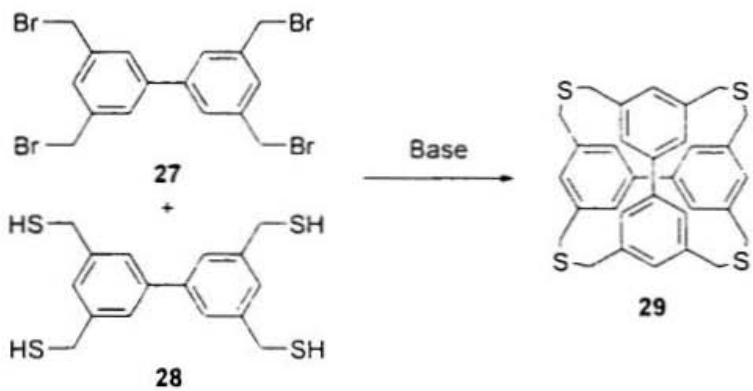

Scheme 3.05: Synthesis of biphenylophane **29**.

3.1.2 Retrosynthetic analysis of pyrenophane 1

The first stages of the retrosynthetic analysis of **1** (Scheme 3.06) are analogous to that of the [*n*](2,7)pyrenophanes discussed in Chapter 1. In the first retrosynthetic step, the key bond in the pyrene unit of **1** was cut using a valence isomerization-dehydrogenation (VID) sequence.[19] For pyrenophanes with longer tethers (9 atoms or more; θ_{calcd} < *ca.* 80°) this sequence has been observed to be spontaneous, but for more strained cyclophanes (less than 9 atoms; θ_{calcd} 87.0 – 113.3°) reflux in benzene in the presence of DDQ has been necessary to accomplish this key conversion.[3] Cyclophanediene **2** could come from dithiacyclophane **30**.[19,20] Tethered dithiacyclophanes with tethers other than

that in **30** have been synthesized previously by our group using the Na_2S/Al_2O_3 reagent,[21] and it was anticipated that this reagent would also be successful in this case, thus leading back to tetrafunctionalized intermediate **31**.

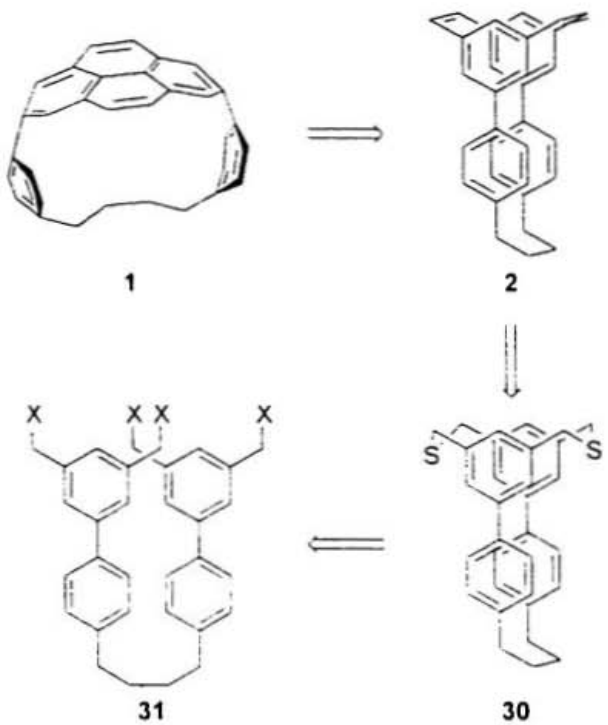

Scheme 3.06: Retrosynthetic analysis of pyrenophane **1**.

For intermediate **31**, various retrosynthetic schemes were considered. Initially an approach based on Wittig-type chemistry was developed (Scheme 3.07). In this approach, tetrafunctionalized compound **31** could be derived from a diene **32**, which could be a mixture of *E*/*Z* isomers, since hydrogenation of the double bonds would give rise to only

a single compound **31**. The biphenyl units in **32** could be formed in a Suzuki-Miyaura coupling[22-27] of a diaryldiene **35** and an arylboronic acid derivative **33**. The latter could be formed by a sequence of functional group interconversions from isophthalic acid **34** and the diene **35** could be derived (using Wittig and / or Horner-Wadsworth-Emmons reactions) from commercially available 4-hydroxybenzaldehyde **36**.

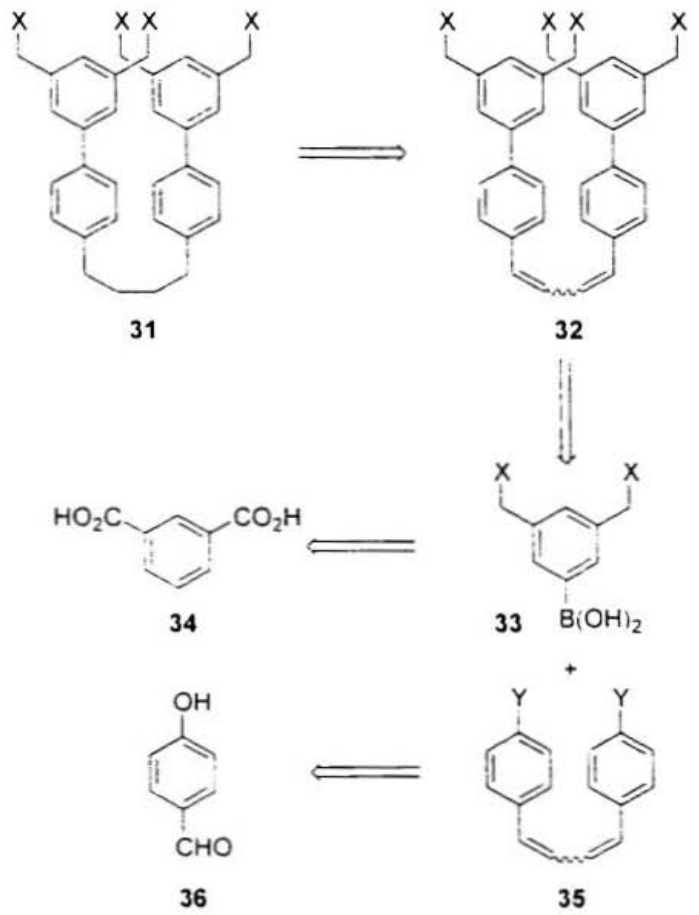

Scheme 3.07: Retrosynthetic analysis of **31** based on Wittig-type chemistry.

In a second retrosynthetic approach (Scheme 3.08), the biphenyl units in **25** were also envisioned as being formed *via* a Suzuki-Miyaura coupling to give, in the retrosynthetic direction, an arylboronic acid **33** and a 1,4-diarylbutane **37**. Compound **37** could be formed from a suitably functionalized *para*-disubstituted aromatic ring **38** and 1,4-dibromobutane **39**.

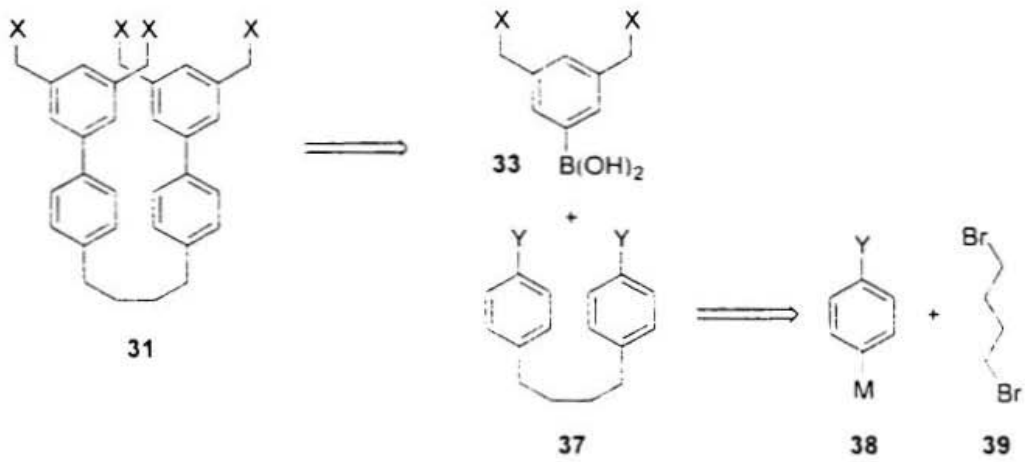

Scheme 3.08: Retrosynthetic analysis of **31** to give **38** and **39**.

Both synthetic approaches to compound **31** were investigated. Since it was anticipated that the conversion of **31** to pyrenophane **1** might not be high yielding, a fast, reliable and high yielding route to compound **31** was required. In the following Sections, the attempts aimed at the synthesis of **1** are described.

3.2 Results and discussion

3.2.1 Initial approach to the synthesis of 31

Synthetic efforts aimed at the total synthesis of pyrenophane **1** commenced with 4-hydroxybenzaldehyde **36**, which was converted to its triflate **40** upon treatment with trifluoromethanesulfonic acid anhydride and pyridine in CH_2Cl_2 (78%). At a later stage in the synthesis, a triflate was required at this position of the aromatic ring for the Suzuki-Miyaura coupling. It was hoped that its introduction at this early stage would also serve to protect the phenolic hydroxyl group. A more common protecting group could have been used if the triflate group proved to be ineffective, but this would require two extra steps in the synthesis. Triflate **40** was then reacted in a Horner-Wadsworth-Emmons reaction with the anion of triethylphosphonoacetate to give α,β-unsaturated ethyl ester **41** (81%). Reduction of ethyl ester **41** was attempted using $LiBH_4$ in methanol,[28] but this gave a mixture of 1,2- and 1,4-reduced products. Reduction of **41** using DIBAL-H in dichloromethane at lower temperatures cleanly yielded the allylic alcohol **42** (92%).

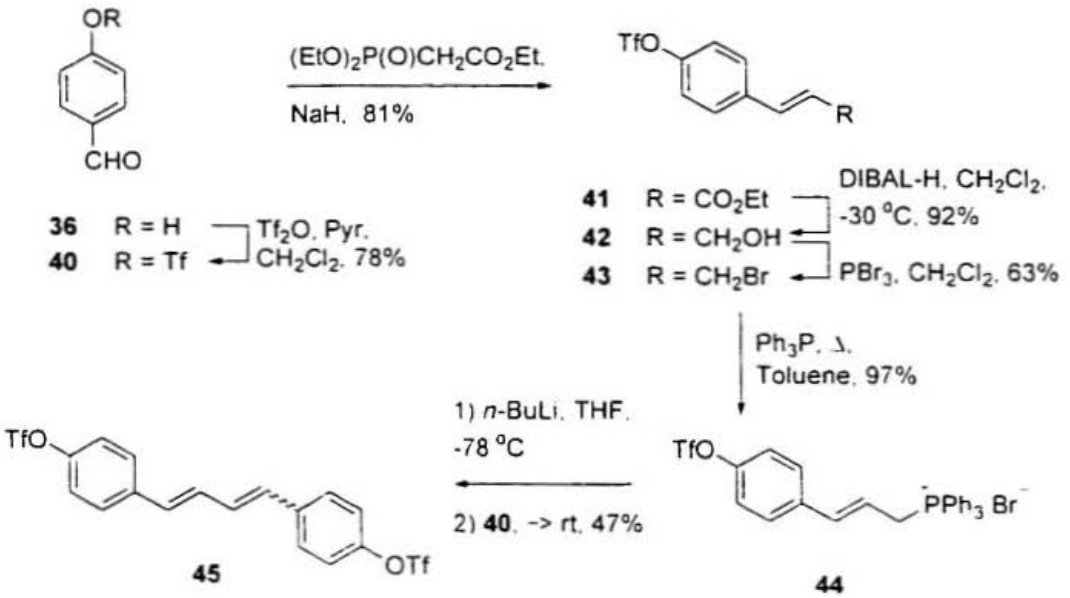

Scheme 3.09: Synthesis of diene **45** from **36**.

Conversion of the alcohol **42** to its allylic bromide **43** was attempted using PPh_3Br_2 (51%)[29] and PPh_3/CBr_4 (43%)[30,31] but the best yield was obtained using PBr_3 (63%). The bromide **43** was then reacted with triphenylphosphine in refluxing toluene to give the desired phosphonium salt **44** in 97% yield. The phosphonium salt **44** was converted to its ylide using *n*-butyllithium and reacted with aldehyde **40** to give only 47% of butadiene **45** (83 : 17 *E,E* : *E,Z* by ^{1}H NMR), which is set up for the anticipated Suzuki-Miyaura coupling. The disappointing yield in this last step prompted the investigation of an alternative approach, in which the complementary version of the Wittig reaction was used (Scheme 3.10).

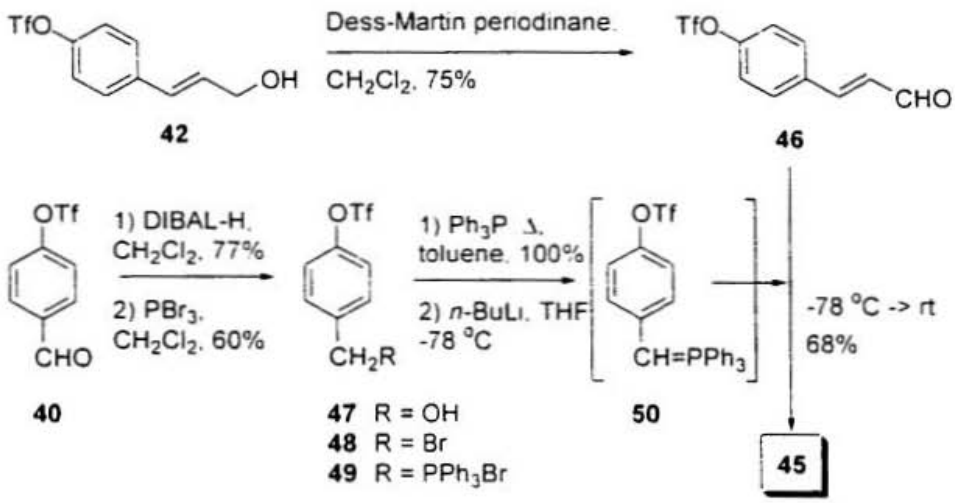

Scheme 3.10: Alternative synthesis of **45**.

Oxidation of allylic alcohol **42** with the Dess-Martin periodinane[32] yielded the desired aldehyde **46** in 75% yield. In a parallel process, aldehyde **40** was reduced to a benzylic alcohol **47** using DIBAL-H in dichloromethane (77%). Treatment of this alcohol with PBr_3 yielded benzylic bromide **48** (68%), which could readily be converted to its triphenylphosphonium salt **49** in quantitative yield. Deprotonation of the triphenylphosphonium salt **49** with *n*-butyllithium, followed by treatment with aldehyde **46** yielded diene **45**, this time in 61% yield (85 : 15 *E,E* : *E,Z* by ^{1}H NMR). A noteworthy feature of both approaches to **45** is that the triflate group proved to be a satisfactory protecting group.

In order to accomplish the anticipated Suzuki-Miyaura coupling, another building block, **55**, had to be synthesized (Scheme 3.11). Synthesis of **55** commenced from commercially

available isophthalic acid **34**, which was brominated at the 5-position in 93% to give 5-bromoisophthalic acid **51**.[33] Fischer esterification[34] of diacid **51** yielded methyl ester **52** in 87% yield. Reduction of the diester **52** with $LiAlH_4$ (89%), followed by methylation of the resulting diol **53** gave the trisubstituted aromatic compound **54** (83%). Boronic acid **55** was formed *via* lithium-halogen exchange on the aromatic bromide **55**, followed by reaction with trimethyl borate to yield a boronic ester, which was not isolated, but was hydrolyzed immediately under mild acidic conditions. Yields of **55** were usually in the range of 80-87% from **54** and due to the short shelf life of **55** (less than two days at −18 °C) it was used directly in the next step. It is important that the halogen-lithium exchange be done at −50 °C. Reaction at higher temperatures gave a mixture of products (probably *ortho*-metallation occurred) and, at lower temperatures, no lithiation occurred.

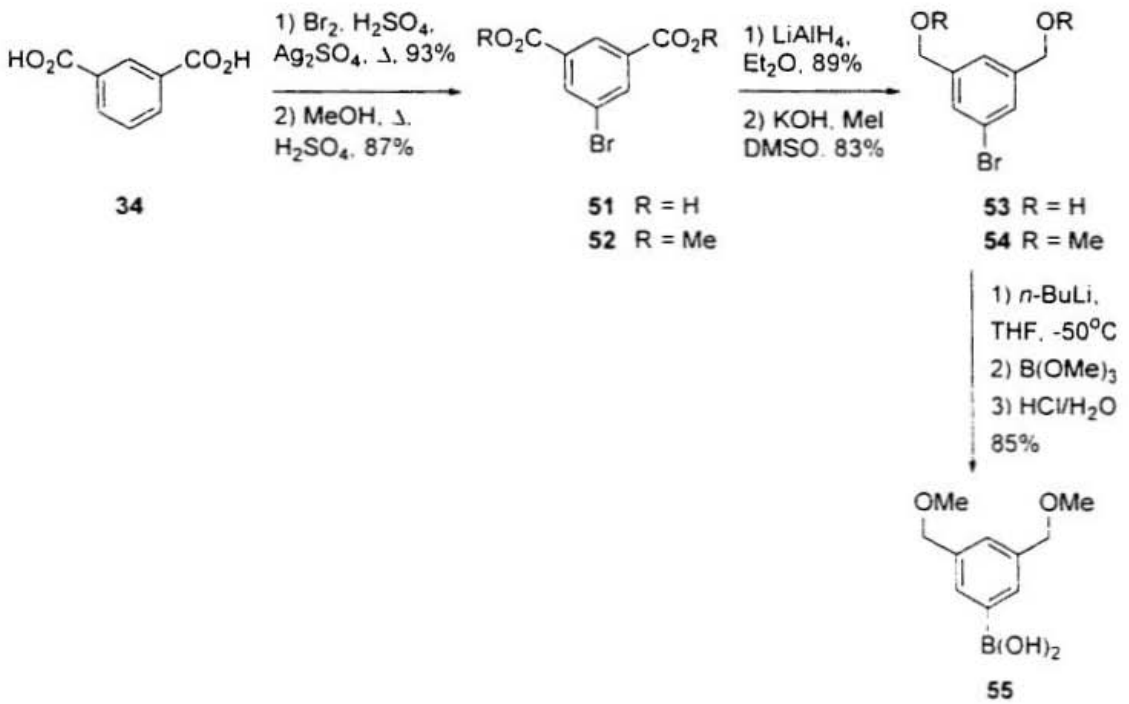

34

51 R = H
52 R = Me

53 R = H
54 R = Me

55

Scheme 3.11: Synthesis of boronic acid **55** from isophthalic acid **34**.

In the next step (Scheme 3.12), boronic acid **55** and ditriflate **45** were coupled to give the desired product **56** in 6% yield using a modified Suzuki-Miyaura coupling with ethyleneglycol dimethyl ether as the solvent. The low isolated yield of this reaction was presumably due to the low solubility of compound **56**. Compound **56** could be hydrogenated in dilute solutions in benzene using Pearlman's catalyst (Pd(OH)/C) together with a drop of glacial acetic acid to give compound **57** (99%), which was much more soluble than **56**. Unfortunately the low solubility of **56** limited the applicability of this synthetic route greatly.

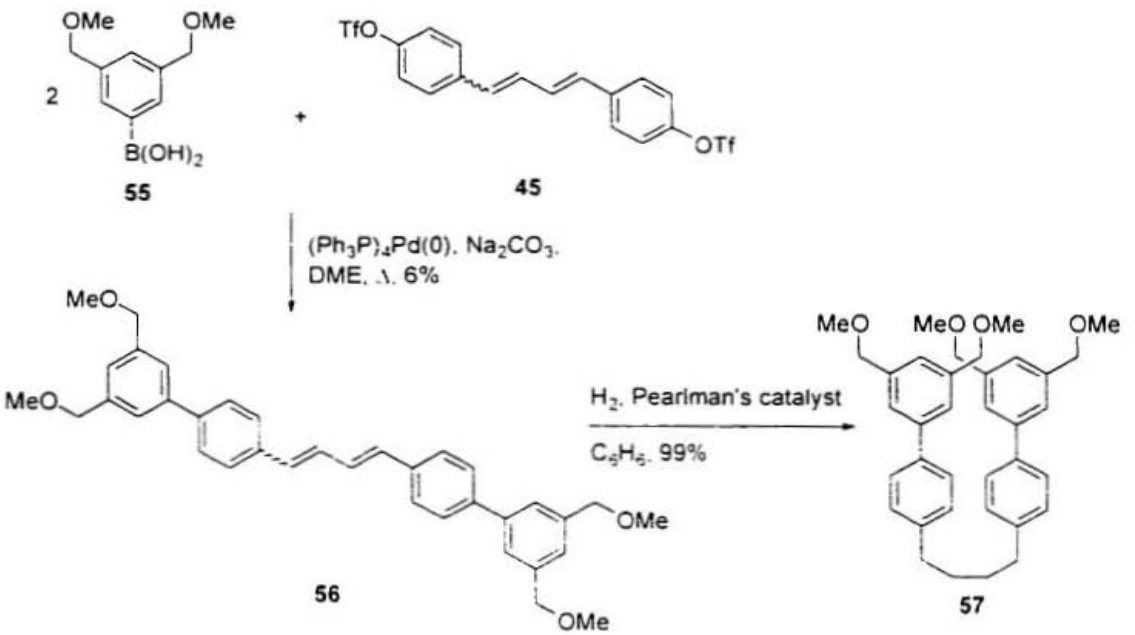

Scheme 3.12: Suzuki-Miyaura coupling of **45** and **55**, and synthesis of **57**.

Due to the poor prospects for the preparation of sufficient quantities of the required synthetic intermediates using the approaches described above, attention was turned to other synthetic routes, which are discussed in the following Section.

3.2.2 Alternative approaches to the synthesis of 57

The first alternative approach that was investigated was the coupling of anisole **58a** or bromobenzene **58b** *via* a two-fold Friedel-Crafts acylation with succinoyl chloride **59** (Scheme 3.13). Attempts to accomplish this conversion failed when using 1,2-

dichloroethane as the solvent or when the reaction was attempted without solvent in the presence of aluminum chloride. The only product that was often isolated after aqueous workup of the reaction mixture was carboxylic acid **61**, which was identical with the reaction product of the Friedel-Crafts acylation of **58a** or **58b** with succinic anhydride **60**.

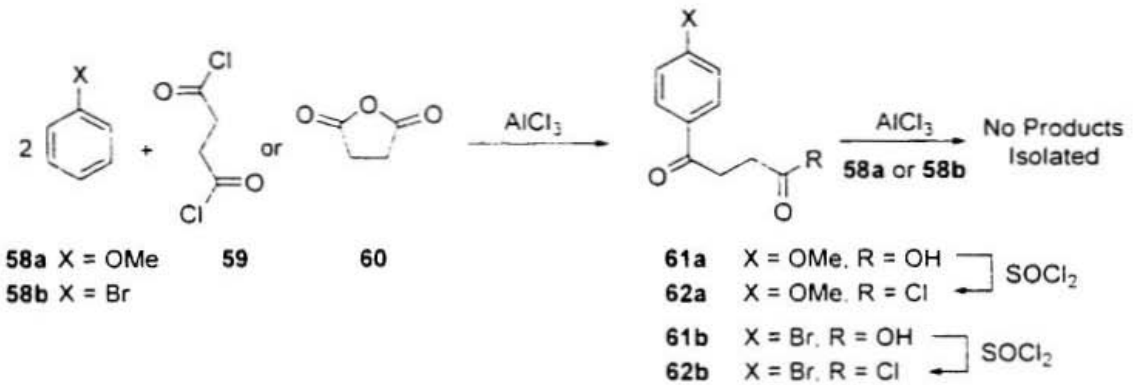

Scheme 3.13: Friedel-Crafts acylations of anisole **58a** and bromobenzene **58b**.

Carboxylic acids **61** were treated with thionyl chloride in order to generate the acid chlorides **62**. The thionyl chloride was removed from the reaction mixture by distillation and a solution of anisole or bromobenzene in 1,2-dichloroethane was added. This initially led to a reaction mixture from which only starting materials could be isolated after aqueous workup. When the reaction mixture was heated to temperatures higher than 30 °C a strongly exothermic reaction took place, after which the reaction mixture solidified to a highly water-sensitive black solid. No product of this reaction was isolated.

Another approach to the synthesis of tetrafunctionalized compound **57** was based on a publication by Mori,[35,36] who described the copper(I)-promoted oxidative homocoupling reaction of substituted trimethylsilylacetylenes to give symmetrically disubstituted butadiynes. This homocoupling reaction must be done in highly polar solvents (DMSO or DMF) under aerobic conditions. Oxygen from the air serves as the oxidant. This homocoupling-based approach is given in Scheme 3.14.

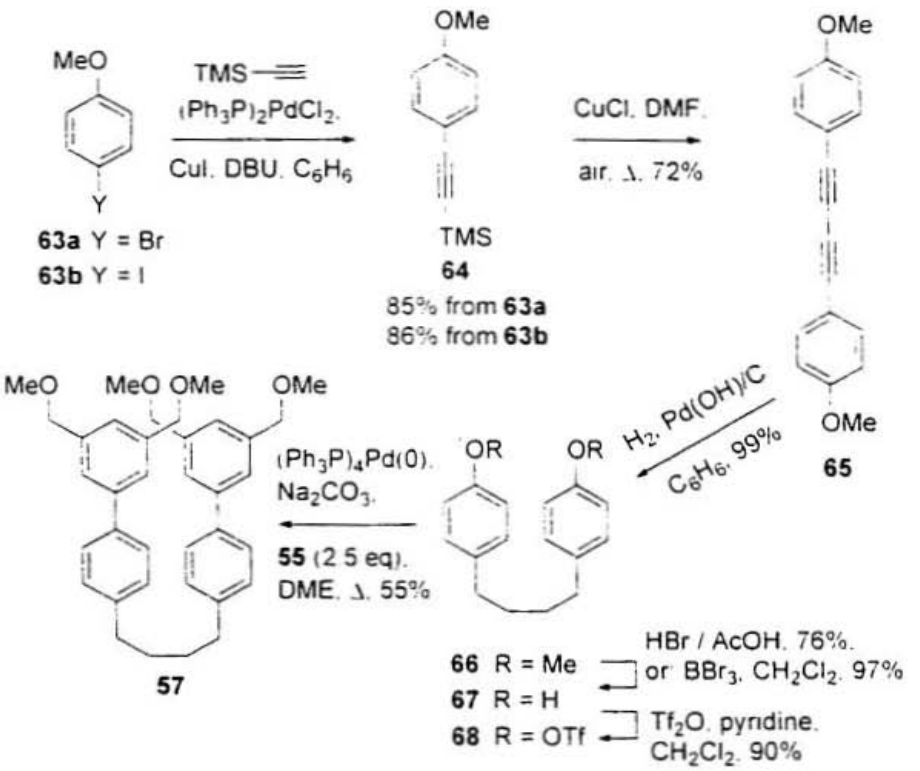

Scheme 3.14: Synthesis of **57** *via* Cu(I) promoted homocoupling of a trimethylsilylacetylene.

The starting material for this approach was either 4-bromoanisole **63a** or 4-iodoanisole **63b**. Sonogashira-Hagihara coupling[37-41] of these anisole derivatives with

trimethylsilylacetylene gave ((4-methoxyphenyl)ethynyl)trimethylsilane **64** (85% from **63a**; 86% from **63b**). When **64** was subjected to the oxidative homocoupling conditions with cuprous chloride in DMF, a yellow solid formed in the reaction mixture, and, after several hours of reaction, a 72% yield of butadiyne **65** was isolated. Unfortunately, this compound was not very soluble in organic solvents, which prevented large amounts of material to be carried through this route. Hydrogenation of slurries of **65** in benzene in the presence of Pearlman's catalyst and a catalytic amount of acetic acid yielded almost quantitative amounts of 1,4-disubstituted butane **66**. Conversion of this compound to the desired tetramethoxy compound **57** was accomplished in 3 steps from **66** by removal of the methyl protecting groups (76% when using HBr-HOAc,[42] 97% with BBr_3), conversion of the resulting bis(phenol) **67** to the ditriflate **68** (81%) and Suzuki-Miyaura coupling with boronic acid **55** to give key intermediate **57** (55%).

Although this synthesis of **50** is shorter and higher yielding than the Wittig-based approaches (Section 3.2.1), the oxidative homocoupling reaction still posed problems due to the low solubility of **65**. This prevented synthesis of large amounts of material through this sequence. While this route was being investigated, another route was designed in which 1,4-diarylbutane derivative **66** might be formed in a single step from a Grignard reagent derived from 4-bromoanisole **63a** and 1,4-dibromobutane **39** (Scheme 3.15).

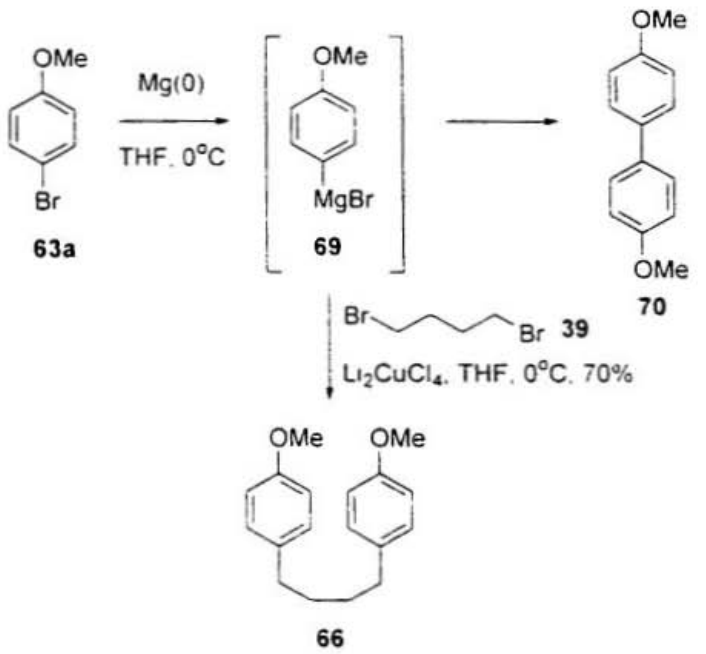

Scheme 3.15: Synthesis of **66** using the coupling of Grignard reagent **69** with 1,4-dibromobutane **39**.

Initial attempts to accomplish this conversion failed and often the only isolable product was 4,4'-dimethoxybiphenyl **70**. This product was likely formed as soon as 4-bromoanisole **63a** was treated with magnesium, even before Grignard reagent **69** could be reacted with 1,4-dibromobutane **39**. It was soon found that formation of this side product could be minimized when activated magnesium turnings[43] were used, instead of commercially-available magnesium. Activation with iodine prior to use, followed by thermal activation (5 minutes at 150 °C) proved to be sufficient, and no more than approximately 15% 4,4'-dimethoxybiphenyl was formed when this type of magnesium was used. When organomagnesium compound **69** was reacted with 1,4-dibromobutane **39**, it was found that in order to obtain the desired reaction product, **69** had to be added

slowly at 0 °C to a well-stirred solution of 1,4-dibromobutane **39** and dilithium tetrachlorocuprate.[44] This catalyst can be formed *in situ* by dissolving lithium chloride and cuprous chloride in dry THF. When the addition was performed slowly, yields of 70-73% of **66** were obtained. The reaction was scaled up to yield several grams of product. When the temperature was not controlled carefully or the addition was performed too fast, the reaction products were similar to those obtained when the reaction was performed without catalyst (probably due to elimination of HBr from 1,4-dibromobutane **39** or reaction intermediates).

3.2.3 Attempted synthesis of pyrenophane 1

Using the methodology described in Sections 3.2.1 and 3.2.2, multigram quantities of **57** were available and attention was focused on the next task: synthesis of a cyclophanediene **2**, the direct synthetic precursor of pyrenophane **1**. Scheme 3.16 shows the synthetic approach aimed at accomplishing these conversions.

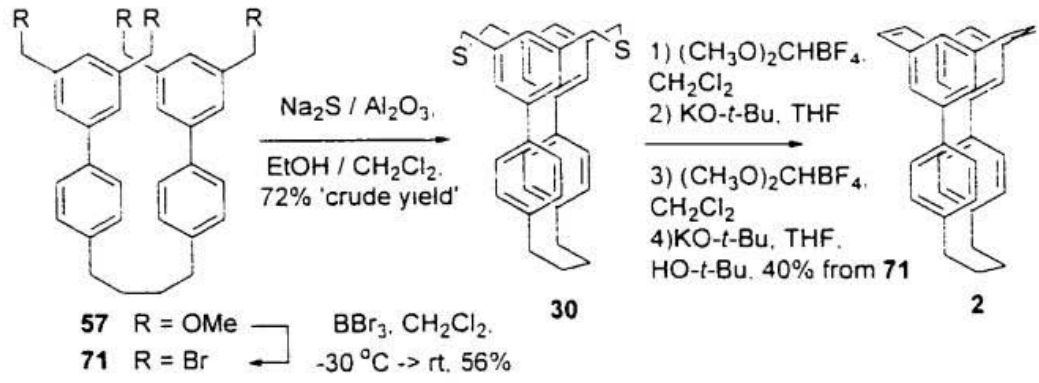

Scheme 3.16: Synthesis of cyclophanediene **2**.

Tetramethoxy compound **57** was converted to the corresponding tetrabromide **71** using BBr_3 in dichloromethane in 56% yield. For this reaction it was important that it was not left longer than required, since the product decomposed slowly under the reaction conditions at room temperature. Treatment of tetrabromide **64** with Na_2S/Al_2O_3[21] gave **30**. However, dithiacyclophane **30** could not be purified using column chromatography, due to decomposition of the cyclophane under these conditions. Recrystallization of crude samples of **30** did not lead to greater purities of the samples. Fortunately, fast filtration of the concentrated reaction mixture through a short plug of silica using CH_2Cl_2 as the eluent yielded dithiacyclophane **30** of sufficiently high purity to be used in the next steps (72% crude yield).

Crude **30** was then subjected to the standard sequence of reactions to form cyclophanediene **2**. During this 4-step process, characterization of the intermediates was not attempted (analogous to other syntheses by our group),[3] since all intermediates are present as mixtures of isomers and some intermediates are poorly soluble tetrafluoroborate salts. In the first step, **30** was treated with Borch reagent[45] ($(CH_3O)_2CHBF_4$) and the resulting bis(methylsulfonium) salt was subjected to Stevens rearrangement conditions[46,47] (KO-*t*-Bu, THF) to yield a mixture of thioethers. Treatment of this mixture with Borch reagent, followed by Hoffman elimination[19] using KO-*t*-Bu gave cyclophanediene **2** in 40% yield (4 steps) from tetrabromide **71**. Unfortunately, no crystals of **2** that were suitable for X-ray analysis could be obtained.

Cyclophane diene **2** showed accidental chemical shift degeneracy of some of its aromatic protons in the ^{1}H NMR spectra when $CDCl_3$ was used as the solvent. The 300 MHz spectrum of **2** in C_6D_6 showed a single peak for its internal protons at δ 6.80 and a single peak at δ 6.78 for the protons *meta* to the internal protons. The *para*-phenylene ring of **2** showed an AA'BB' system centered at δ 7.00 and δ 6.67 in benzene. These data are in good agreement with other tethered cyclophanedienes that have been synthesized by our group.[48,49]

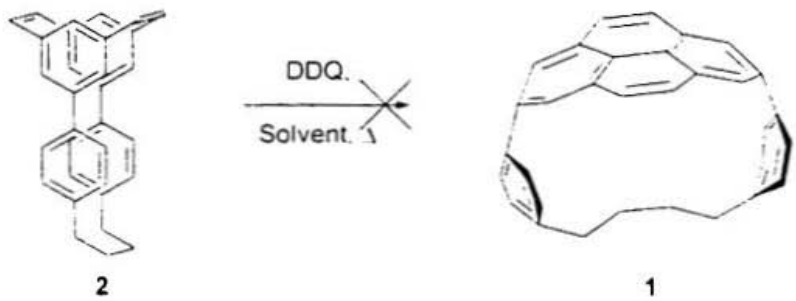

Scheme 3.17: Attempted synthesis of pyrenophane **1**.

Cyclophanediene **2** is only one step away from the target compound pyrenophane **1** by the VID protocol.[3] When solutions of cyclophanediene **2** in benzene or toluene were treated with DDQ at reflux temperatures, not even trace amounts of the desired pyrenophane **1** were isolated and slow decomposition of the starting material to intractable materials was observed. Unfortunately, it has not been possible to determine whether this decomposition process was a result of initial formation of the dihydropyrene or the pyrenophane **1**, followed by decomposition or if cyclophanediene **2** decomposed

via other routes. The desired transformation was also attempted photochemically (irradiation with a mercury lamp (254 nm) in the presence of air as the oxidant)[50] and pyrolytically (flame sublimation[48] or continuous flow flash vacuum pyrolysis).[51] No products could be isolated from the irradiation experiments (starting material was consumed) and the pyrolytic methods led to almost quantitative recovery of starting material. The mass spectrum of cyclophanediene **2** showed the molecular ion of **2** to be the most abundant species (*m/z* 410). No trace of the molecular ion of **1** was observed (*m/z* 408).

In order to explain the reluctance of cyclophanediene **2** to give pyrenophane **1**, semi-empirical (AM1) calculations were performed on both systems.[52] The first factor that might contribute is the expected high bend angle of the pyrene unit in pyrenophane **1** (θ_{calcd} = 114.4°). This angle for the pyrene unit is slightly higher than that calculated for the most bent pyrenophane that has yet been isolated by our group (O-$(CH_2)_5$-O tether: θ_{calcd} = 113.3°, $\theta_{X\text{-}ray}$ = 109.2°[53]). It is possible that the actual bend angle is too large for **1** to be formed using the VID protocol.

The *para*-phenylene units in the calculated structure of **1** showed α angles of *ca.* 10° and β angles of 16.7° at the positions that are linked to the pyrene moiety. In the calculated structure of cyclophanediene **2** these angles were considerably smaller (α < 5°, β = 6.1°). This suggested that in going from **2** to **1**, the strain in these *para*-phenylene units increased considerably. In the computation-based prediction that pyrenophanes with θ_{calcd}

smaller than *ca.* 115° - 120° might be synthesized using the VID approach (Section 1.5), the formation of other strained aromatic nuclei was not taken into account. The actual borderline value for θ_{calcd} in systems like **1** might very well be lower than for the [*n*](2,7)pyrenophanes. Synthesis of systems with lower θ_{calcd} values will have to be undertaken to investigate the limitations of the VID approach towards the synthesis of this class of pyrenophanes.

Another factor that might limit the reactivity of **2** towards the VID reactions is the dihedral angle around the biaryl bonds, i.e., twist in the biphenyl systems. This twist was calculated to be approximately 18° and the closest distance between the hydrogen atoms *ortho* to this bond was calculated to be 1.9 – 2.1 Å. By comparison, AM1 calculations on a single biphenyl unit gave 41° for the dihedral angle and 2.3 Å for the distance between the *ortho* hydrogens. In the VID process, the aromatic portion of the molecule moves towards the adoption of a belt-like structure. In such a situation the two *para*-phenylene units become increasingly boat-shaped. In order to adopt most effectively this geometric requirement, both biphenyl units in **2** must adopt unfavorable *coplanar* conformations (0° dihedral angles). If the VID sequence were to proceed with each biphenyl unit in its preferred twisted arrangement, then the *para*-phenylene groups of **1** would be required to form with in-plane distortions. This entails bond length distortions, which are much more demanding energetically than the bend angle distortions associated with the adoption of boat conformations.

The reluctance of cyclophanediene **2** to form pyrenophane **1** might very well be a combination of the effects described above. In order to overcome the first problem (too much bend in the pyrene unit) a cyclophane diene with a longer tether could be synthesized, which might undergo the VID reactions more easily to give a pyrenophane. Pyrenophanes **72**, **73** and **74** (Figure 3.05) appear to be reasonable synthetic targets. They have slightly longer tethers than pyrenophane **1** and, as a result, their calculated bend angles are smaller (θ_{calcd} 108.9°, 110.1° and 111.1° respectively). With the smaller calculated bend angles for **72** - **74** than for **1**, these synthetic targets might provide the necessary data to develop meaningful cut-off values in computational methods to predict the limitations of the VID protocol for synthesis of (2.7)pyrenophanes with two *para*-phenylene units in the tether.

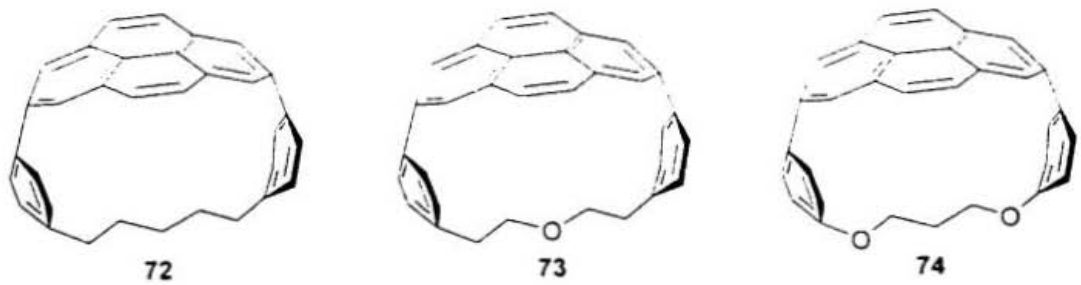

Figure 3.05: Structures for future synthetic targets **72** - **74**.

The other way to facilitate the desired VID reactions would be to try and reduce the dihedral angle in the biaryl units of the cyclophanedienes. This can be done by placing ethano bridges on the biaryl units. Cyclophanedienes **75** and **77** (Scheme 3.18) then present themselves as promising candidates for this modification. The additional ethano bridges that are present in **75** and **77** should dehydrogenate under the conditions used for the VID reactions. Through this dehydrogenation the biaryl units in **2** are effectively replaced by phenanthrene (**75**) and pyrene (**77**) units, which reduces the dihedral angles (the corresponding dihedral angles in phenanthrene and pyrene are calculated to be 0°).[52] Not only do the new ethano bridges serve to reduce the dihedral angle of the biaryl moieties, but they also manifest themselves in the Vögtle belts **4**. As a further point of interest, the transoid orientation of the phenanthrene units in **75** and **76** introduces an element of chirality to the system. A similar system with a cisoid orientation of the phenanthrene units can also be proposed, but this is achiral.

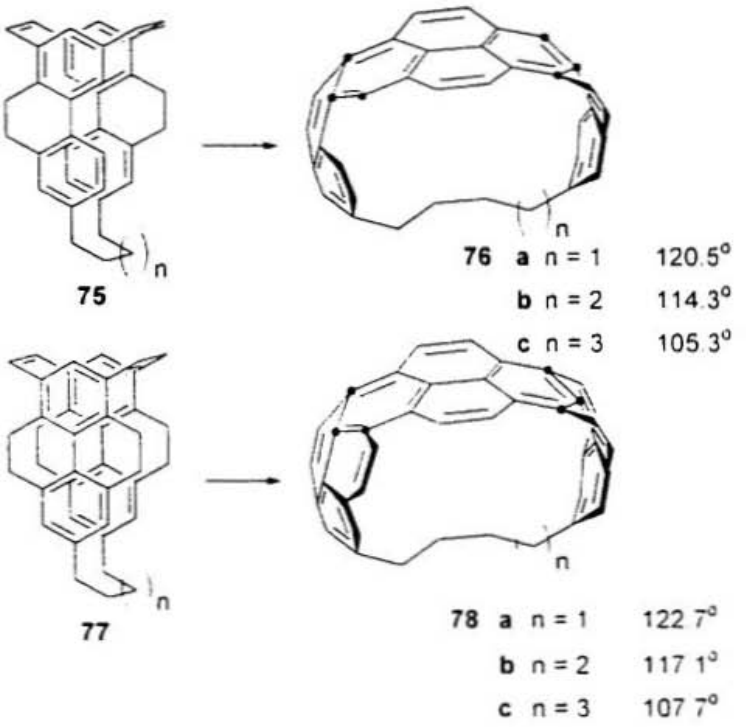

Scheme 3.18: Future synthetic targets **76** and **78** and their AM1-calculated bend angles for the highlighted (•) pyrene units.

3.2.4 Retrosynthetic analysis of 76 and 78

From Scheme 3.18 it can be seen that synthesis of **76** and **78** requires first that cyclophane dienes **75** and **77** be synthesized. Scheme 3.19 shows a retrosynthetic analysis of phenanthrenophane diene **75**.

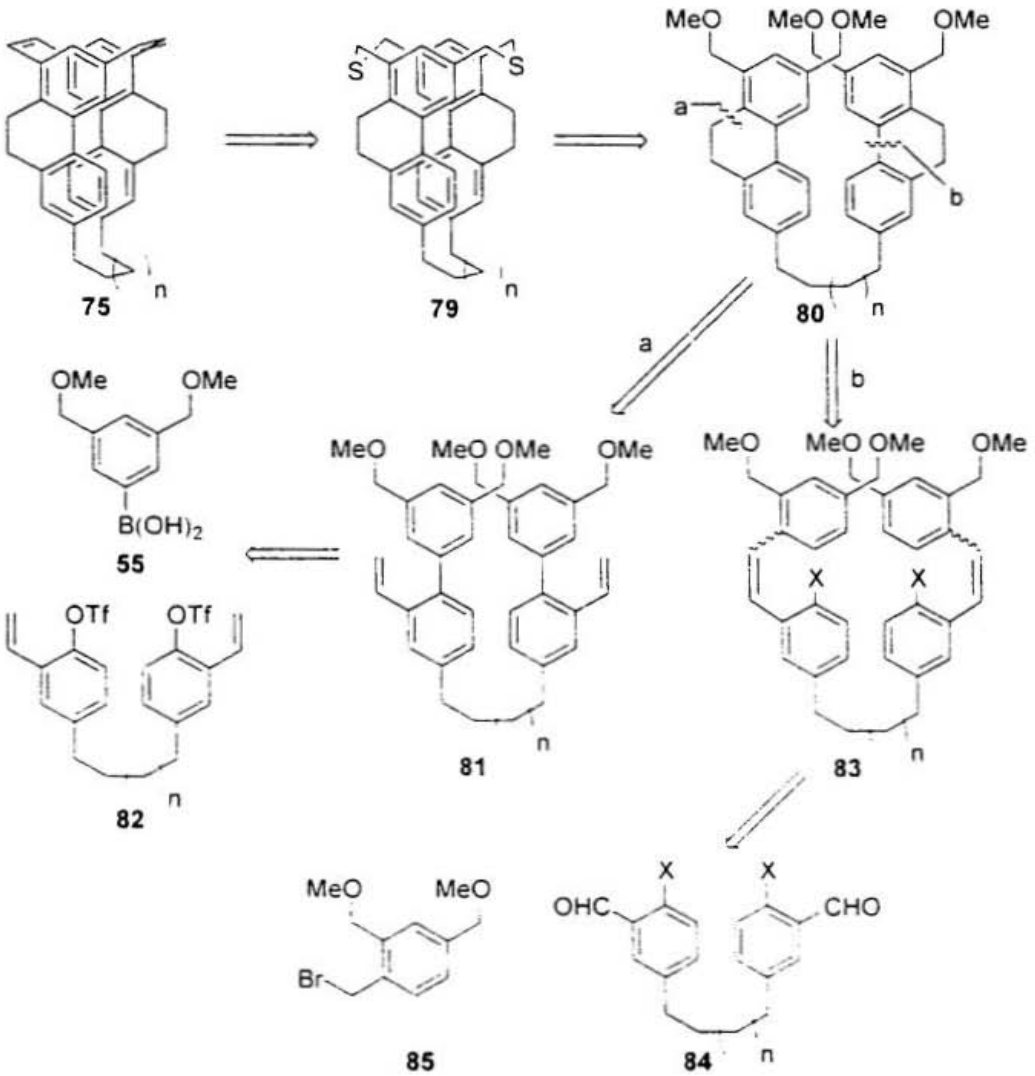

Scheme 3.19: Retrosynthetic analysis of phenanthrenophane diene **75**.

Analogous to the retrosynthetic approach for pyrenophane **1**, a retrosynthesis for phenanthrenophane **75** could lead back to a tetramethoxy compound **80** *via* a dithiacyclophane **79**. Cutting of the bonds connecting the ethanobridges to the biaryl system in compound **80** (path a) gives **81**, which could be envisioned as the Suzuki-

Miyaura coupling product of ditriflate **82** and boronic acid **55**. The ring closure from **81** to **80** might be achieved photochemically[54-56] or using a palladium-catalyzed cyclization reaction.[57] In the latter case, it might be possible to convert ditriflate **82** and **55** in a one-pot process to compound **80**. Cutting of the central biaryl bonds in **80** in a complementary retrosynthetic approach (path b) could lead back to compound **83**. Compound **83** can come from Wittig-type olefination of a dialdehyde **84** with a phosphorous ylide derived from bromide **85**. The substituent "X" on compounds **83** and **84** could be used as a directing group for the installation of the formyl groups in **84**. In the cyclization step to form **80**, this substituent will be eliminated as "HX".

Dithiacyclophane **79**, phenanthrenophanediene **75** and pyrenophane **76** all possess an element of planar chirality. Unfortunately, this means that in the ring-closing step in which the dithiacyclophane **79** is formed (and the element of chirality is introduced) two diastereomers could be produced: an achiral dithiacyclophane **86** and the C_2 symmetric dithiacyclophane **79**. This may cause problems with purification and characterization, but **86** could conceivably also be brought through to a partial belt.

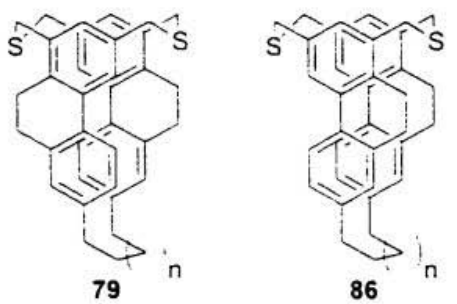

79 **86**

Figure 3.06: Structures of dithiacyclophanes **79** (C_2 symmetry) and **86** (achiral).

Nishimura *et al.* have synthesized compounds akin to distyryl compound **82**.[58,59] but they used anisole derivatives. which placed methoxy groups where triflate groups are required. Due to the sensitivity to acid of the styrene units in the product. functional group interconversions to give the desired ditriflate **82** are likely to be problematic so another approach was investigated.

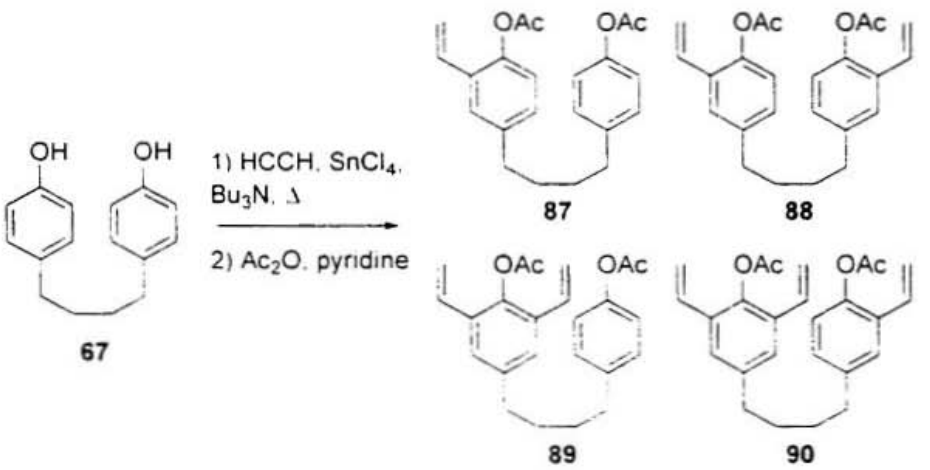

Scheme 3.20: Attempted *ortho*-vinylation of **67**.

Attempts to synthesize distyrylbutanes like **82** have so far been unsuccessful (Scheme 3.20). When an *ortho*-vinylation reaction described by Yamaguchi[49,50] was used to attempt divinylation of bis(phenol) **67** (corresponding to the synthesis of **76** and **78** with n = 1) several small fractions of what was thought to be a mixture of vinylated compounds (at least 3) was obtained from column chromatography of the reaction mixture. In Scheme 3.20 several possible structures are shown. although no direct evidence for any of these products has been obtained. Most chromatographic fractions obtained from this

reaction proved to be very unstable and polymerized readily even under refrigeration at – 18 °C, forming transparent, gel-like material. The low yield of isolated material, together with the instability of the products made this approach unattractive, so an alternative synthesis of **80** was investigated (Scheme 3.21).

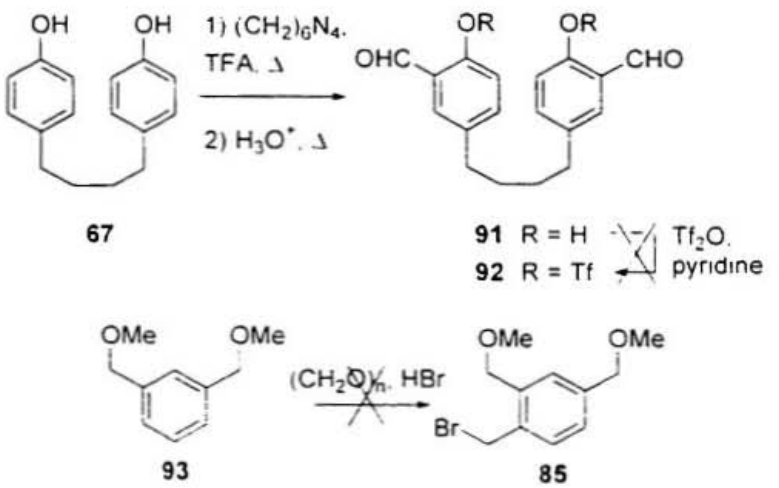

Scheme 3.21: Attempted syntheses of **84** and **85**.

For this approach, two coupling partners for a Wittig-type olefination had to be synthesized: a derivative of dialdehyde **84** (where X is a leaving group) and a benzylic bromide **85**. Initial attention went to the synthesis of a suitable derivative of **84**, where introduction of X as a triflate group was anticipated (compound **92**). Formation of precursor **91** from bis(phenol) **67** was accomplished in approximately 60% yield using the Duff reaction.[61,62] (Purification of dialdehyde **91** proved difficult due to low solubility and instability.) Unfortunately, reaction of **91** with triflic anhydride was sluggish and the

only material that was recovered from the reaction mixture was a small amount of starting material.

Synthesis of benzylic bromide **85** was attempted using several conditions for bromomethylation of electron-rich aromatic rings, but in no case was the desired compound isolated. The only product isolated was often α,α'-dibromo-*meta*-xylene, resulting from nucleophilic displacement of the methoxy groups on starting material **93**. Due to the failure of this route as well as the previous route, this project was set aside in favor of more promising targets. For completeness, a short discussion of a proposed synthesis of cyclophanediene **77** will be given here. This project has not been pursued by the author.

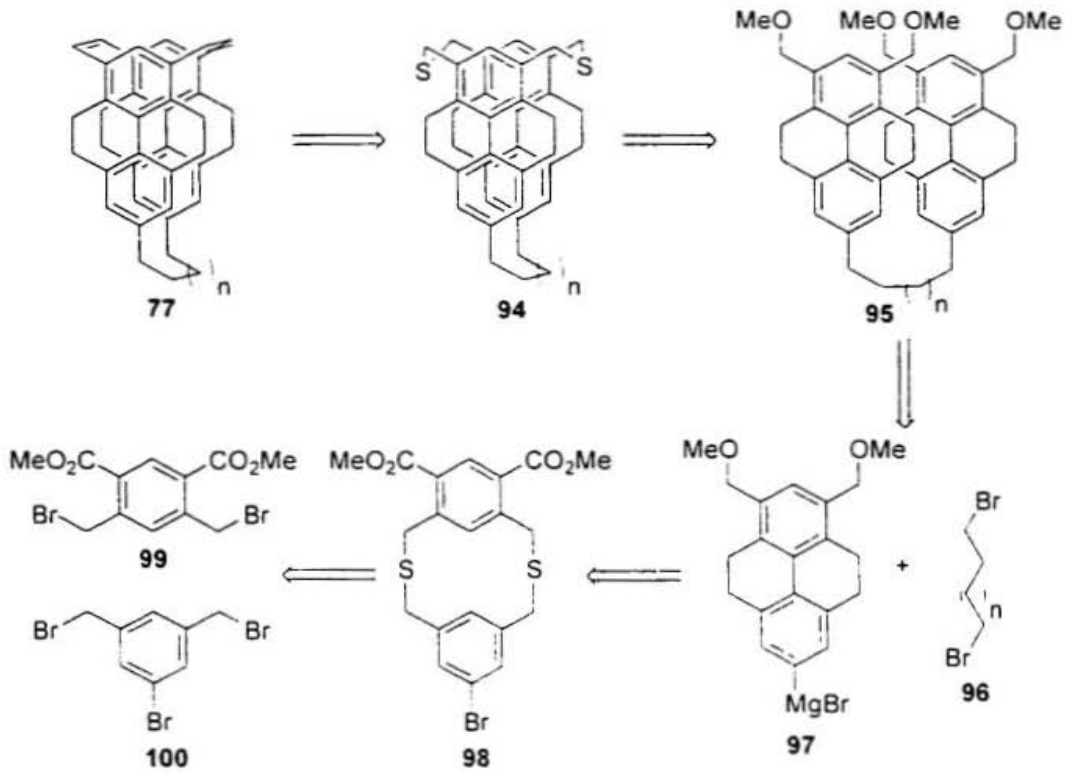

Scheme 3.22: Retrosynthetic analysis of pyrenophanediene [77]

A retrosynthetic analysis of cyclophanediene **77** (Scheme 3.22) proceeds, along the same route as the one for phenanthrenophane **75** to a tetramethoxy compound **95**, which could be derived from an organomagnesium compound **97** and 1,*n*-dibromoalkane **96**. Compound **97** could possibly be derived from a dithiacyclophane **98** using established procedures. First a [2.2]metacyclophane could be formed, whose central bond is closed using iron filings and bromine to give a tetrahydropyrene.[93] Dithiacyclophane **98** could be formed from a coupling between diester **99** and tribromide **100**.

Pyrenophane **78**, if its synthesis were successful, would contain a curved aromatic surface with 36 sp^2-hybridized carbon atoms that would map onto the surfaces of D_{5h} C_{70}, D_{5d} C_{80} and D_{6h} C_{84}. Curved aromatic surfaces of this size have not yet been synthesized using cyclophane methodology and accomplishment of this synthesis would constitute a landmark in the field of cyclophane chemistry. Preliminary work in this area by another researcher in this group has led to the synthesis of a small amount of dithiacyclophane **98**.[64] Obviously, large quantities of this compound will be required in order to accomplish its transformation into **77** and **78**, but the groundwork has been laid for a serious assault on a very challenging target.

3.3 Experimental

General. All chemicals were reagent grade and were used as received. Chromatographic separations were performed on Merck silica gel 60 (particle size 40-63 μm, 230-400 mesh). Melting points were determined on a Fisher-Johns apparatus and are uncorrected. Elemental analyses were performed at the MicroAnalytical Service Laboratory, Department of Chemistry, University of Alberta. Mass spectroscopic (MS) data were obtained on a V. G. Micromass 7070HS instrument. ^{1}H NMR (300.1 MHz) and ^{13}C NMR (75.47 MHz) were obtained on a General Electric GE 300-NB spectrometer: ^{1}H shifts are relative to internal tetramethylsilane; ^{13}C shifts are relative to the solvent resonance ($CDCl_3$: δ = 77.0). All experiments with moisture- or air-sensitive compounds were

performed in anhydrous solvents under nitrogen unless otherwise stated. Solvents were dried and distilled according to standard procedures.

4-(Trifluoromethylsulfonyloxy)benzaldehyde (40).[75] To a stirred 0 °C solution of 4-hydroxybenzaldehyde **36** (25.00 g, 204.7 mmol) and pyridine (17.8 mL, 17.4 g, 220 mmol) in dichloromethane (500 mL) was added triflic anhydride (28. 6 mL, 47.9 g, 170 mmol) by syringe through a septum over 15 min. The reaction was allowed to warm to room temperature before it was quenched with 2.5% aqueous HCl solution (100 mL). The aqueous layer was extracted with dichloromethane (2 x 100 mL). The combined organic layers were washed with saturated aqueous Na_2CO_3 solution (2 x 100 mL), water (100 mL) and brine (75 mL), dried ($MgSO_4$) and concentrated *in vacuo*. The residue was purified by column chromatography (SiO_2; CH_2Cl_2) to yield triflate **40** (33.63 g, 132.4 mmol, 78%) as a colorless oil; IR (cm^{-1}): 2725 (w), 1716 (s), 1597 (s), 1434 (s), 1217 (s), 1142 (s), 1015 (m), 884 (s), 732 (m); ^1H NMR ($CDCl_3$) δ 10.08 (s, 1H), 8.04 (d, 2H, J = 8.5 Hz), 7.50 (d, 2H, J = 8.3 Hz); ^{13}C NMR ($CDCl_3$) δ 190.2, 153.2, 135.9, 131.7, 122.1, 118.6 (q, J = 332 Hz); EI-MS (70 eV) m/z (%): 254 (61, M^+), 189 (100), 161 (14).

Ethyl (*E*)-3-(4-(trifluoromethylsulfonyloxy)phenyl)propenoate. To a stirred 0 °C suspension of NaH (1.71 g, 60% in mineral oil, 42.6 mmol) in dry THF (200 mL) was added triethylphosphonoacetate (7.81 mL, 8.82 g, 39.4 mmol). After stirring for 10 min, a

solution of **40** (8.33 g, 32.8 mmol) in dry THF (25 mL) was added, and the mixture was stirred at 0 °C for 1 h, then under reflux for 20 h. The mixture was cooled to room temperature, 2% aqueous HCl solution (50 mL) was added and the mixture was concentrated to *ca.* 1/3 of the original volume under reduced pressure. Dichloromethane (100 mL) was added and the aqueous layer was extracted with dichloromethane (100 mL). The combined extracts were washed with water (100 mL), dried ($MgSO_4$) and concentrated *in vacuo* to yield a brown oil that was purified by column chromatography (SiO_2; CH_2Cl_2) to yield **41** (8.58 g, 26.5 mmol, 81%) as a light-yellow oil: IR (cm^{-1}) 1724 (m), 1644 (m), 1503 (m), 1532 (s), 1215 (s), 1143 (s); ^1H NMR ($CDCl_3$) δ 7.67 (d, 1H, J = 16.5 Hz), 7.61 (d, 2H, J = 8.5 Hz), 7.32 (d, 2H, J = 8.6 Hz), 6.45 (d, 2H, J = 16.1 Hz), 4.29 (q, 2H, J = 7.1 Hz), 1.36 (t, 3H, J = 7.5 Hz); ^{13}C NMR ($CDCl_3$) δ 166.4, 150.2, 142.1, 134.8, 129.7, 121.9, 120.1, 118.6 (q, J = 319), 60.8, 14.3; EI-MS (70eV) m/z (%): 324 (56, M^+), 296 (14), 279 (88), 191 (69), 163 (100), 146 (47); HRMS Calc'd for $C_{12}H_{11}F_3O_5S$: 324.0278, found 324.02625.

(*E*)-3-(4-(Trifluoromethylsulfonyloxy)phenyl)-2-propen-1-ol (42). To a solution of ethyl ester **41** (1.00 g, 3.08 mmol) in dry CH_2Cl_2 (30 mL) at –35°C under an atmosphere of nitrogen was added diisobutylaluminium hydride (1 M solution in hexanes). The reaction mixture was stirred for 1.5 h while it was allowed to warm slowly. Aqueous HCl solution (3 M, 20 mL) was added, and the aqueous layer was extracted with dichloromethane (30 mL). The organic layers were combined, washed with brine (30

mL), dried ($MgSO_4$) and concentrated *in vacuo*. The residue was purified by column chromatography (SiO_2: CH_2Cl_2) to yield alcohol **42** (0.80 g, 2.8 mmol, 92%) as a yellow oil: ^1H NMR ($CDCl_3$) δ 7.42 (d, 2H, J = 9.5 Hz), 7.21 (d, 2H, J = 9.5 Hz), 6.61 (d, 1H, J = 15.6 Hz), 6.37 (dt, 1H, J = 15.4 Hz, 6.0 Hz), 4.33 (d, 2H, J = 5.9 Hz), 2.25 (br s, 1H); ^{13}C NMR ($CDCl_3$) 148.7, 137.1, 130.8, 128.7, 128.0, 121.5, 118.7, 63.3; EI-MS (70 eV) m/z (%): 282 (65), 240 (10), 226 (6), 175 (9), 149 (35), 55 (100).

(*E*)-1-Bromo-3-(4-trifluoromethylsulfonyloxy)phenyl-2-propene (43). A solution of PBr_3 (0.32 g, 1.2 mmol) in dichloromethane (10 mL) was added slowly to a solution of alcohol **42** (0.66 g, 2.3 mmol) in dichloromethane (25 mL). After 30 min the reaction was quenched with water (10 mL). The organic layer was washed with water (4 x 15 mL) and brine (15 mL), dried ($MgSO_4$) and concentrated *in vacuo*. The residue was purified by column chromatography (SiO_2: CH_2Cl_2) to yield bromide **43** (0.51 g, 1.5 mmol, 63%) as a colorless oil: ^1H NMR ($CDCl_3$) δ 7.46 (d, 2H, J = 9.0 Hz), 7.25 (s, 2H, J = 9.0 Hz), 6.64 (d, 1H, 15.5 Hz), 6.42 (dt, 1H, J = 15.5 Hz, 7.7 Hz), 4.15 (d, 2H, J = 7.7 Hz); ^{13}C NMR ($CDCl_3$) δ 149.1, 136.2, 132.3, 128.3, 127.4, 121.6, 118.7 (q, J = 320.0 Hz), 32.4; EI-MS (70 eV) m/z (%): 346 (1, M^+), 344 (1), 265 (70), 131 (100), 115 (68).

(*E*)-[3-(4-Trifluoromethylsulfonyloxy)allyl]triphenylphosphonium bromide (44). A solution of bromide **43** (1.47 g, 4.26 mmol) and triphenylphosphine (1.23 g, 4.69 mmol) in toluene (15 mL) was stirred at reflux under an atmosphere of nitrogen for 1.5 h. The resulting mixture was concentrated to approximately 5 mL under reduced pressure. The

product was isolated by suction filtration, washed with petroleum ether (bp. 30-60 °C) and dried *in vacuo* to give phosphonium salt **44** (2.50 g, 4.12 mmol, 97%) as a white solid that was used without purification.

(*E*,*E*)- And (*E*,*Z*)-1,4-Bis(4-(trifluoromethylsulfonyloxy)phenyl)-1,3-butadiene (45). To a –78 °C suspension of phosphonium salt **44** (1.29 g, 2.12 mmol) in dry THF (30 mL) was added *n*-BuLi (1.08 M in hexanes, 1.8 mL, 1.9 mmol). The reaction mixture was slowly warmed to room temperature, and a solution of aldehyde **40** (0.59 g, 2.3 mmol) in dry THF (5 mL) was added. The mixture was stirred at room temperature for 1 hour, and water was added (10 mL) followed by dichloromethane (100 mL). The aqueous layer was extracted with dichloromethane (2 x 50 mL). The organic extracts were combined and washed with brine (50 mL). After drying ($MgSO_4$), the organic layer was concentrated *in vacuo* and the residue was purified by column chromatography (SiO_2; 50% CH_2Cl_2 – petroleum ether (bp. 30-60 °C)) to yield diene **45** (0.50 g, 1.0 mmol, 47%) as a light yellow solid: mp 111.0 - 113.0 °C; IR (Nujol, cm^{-1}): 1497 (w), 1422 (w), 1210 (s), 1138 (s), 994 (w), 891 (m), 859 (w); ^1H NMR (Only signals for *E,E*-isomer are listed; $CDCl_3$) δ 7.51 (m, 4H), 7.26 (m, 4H), 6.94 (m, 2H), 6.70 (m, 4H); ^{13}C NMR (Only signals for *E,E*-isomer are listed; $CDCl_3$) δ 148.1, 137.4, 131.8, 130.4, 128.0, 121.7, 120.8, 118.4 (q, J = 318 Hz); EI-MS (70 eV) *m/z* (%): 502 (59), 369 (100), 236 (66); HRMS Calc'd for $C_{18}H_{12}F_6O_6S_2$: 501.9978, found 501.9894.

(*E*)-3-(4-Trifluoromethylphenyl)propenal (46). To a solution of alcohol **42** (1.10 g, 3.90 mmol) in dichloromethane (20 mL) under an atmosphere of nitrogen was added over 10 min a suspension of the Dess-Martin periodinane (2.35 g, 5.39 mmol). After stirring for 30 min the reaction mixture was washed with 1.3 M aqueous KOH solution (3 x 20 mL), water (30 mL) and brine (25 mL). After the organic layer was dried ($MgSO_4$) it was concentrated *in vacuo*, and the residue was passed through a plug of SiO_2 to give aldehyde **46** (0.82 g, 2.9 mmol, 74%) as a light yellow oil; ^1H NMR ($CDCl_3$) δ 9.85 (d, 1H, J = 6.7 Hz), 7.78 (d, 2H, J = 8.4 Hz), 7.59 (d, 1H, J = 15.1 Hz), 7.47 (d, 2H, J = 8.4 Hz), 6.83 (dd, 1H, J = 15.3 Hz, 6.9 Hz); ^{13}C NMR ($CDCl_3$) δ 193.1, 150.9, 149.7, 134.3 130.2, 130.1, 122.2, 118.7 (q, 320.6 Hz); EI-MS (70 eV) m/z (%): 324 (5, M^+), 280 (19), 147 (76), 91 (100).

4-(Hydroxymethyl)-1-(trifluoromethylsulfonyloxy)benzene (47). To a –30°C solution of aldehyde **40** (1.00 g, 3.93 mmol) in dichloromethane (15 mL) under an atmosphere of nitrogen was added diisobutylaluminium hydride (1 M solution in hexanes, 5.9 mL, 5.9 mmol) over 5 min. The reaction mixture was allowed to warm to room temperature and was quenched with 3 M aqueous HCl solution (15 mL). The aqueous layer was extracted with dichloromethane (2 x 10 mL), and the combined organic extracts were washed with brine, dried ($MgSO_4$) and concentrated *in vacuo*. The residue was purified by column chromatography (SiO_2; CH_2Cl_2) to yield **47** (0.78 g, 0.30 mmol, 77%) as a colorless oil, that was used directly in the next step: ^1H NMR ($CDCl_3$) δ 7.44 (d, 2H, J = 8.9 Hz), 7.26 (d, 2H, J = 8.9 Hz), 4.71 (s, 2H), 2.16 (br s, 1H); ^{13}C NMR ($CDCl_3$) δ 148.7, 141.3,

128.4, 121.3, 118.7 (q, J = 320 Hz), 64.0; EI-MS (70 eV) m/z (%): 256 (51, M^+), 227 (3), 191 (5), 175 (4), 123 (28), 107 (29), 67 (100).

4-(Bromomethyl)-1-(trifluoromethylsulfonyloxy)benzene (48). To a solution of alcohol **47** (9.46 g, 36.9 mmol) in dichloromethane (100 mL) was added a solution of PBr_3 (2.5 mL, 7.2 g, 26 mmol) in dichloromethane (15 mL) over 3 min. After 45 min the reaction mixture was quenched with water (25 mL). The organic layer was washed with water (3 x 25 mL), dried ($MgSO_4$) and concentrated *in vacuo* and purified by column chromatography (SiO_2; 25% CH_2Cl_2 / petroleum ether (bp. 30-60 °C)) to give **48** (7.62 g, 23.9 mmol, 65%) as a colorless oil; ^1H NMR ($CDCl_3$) δ 7.49 (d, 2H, J = 8.4 Hz), 7.26 (d, 2H, J = 8.5 Hz), 4.48 (s, 2H); ^{13}C NMR ($CDCl_3$) δ 149.1, 138.3, 130.9, 121.7, 118.7 (q, J = 324 Hz), 31.4; EI-MS (70 eV) m/z (%): M^+ not observed, 239 (100), 175 (53).

(*E*,*E*)- And (*E*,*Z*)-1,4-di(4-(trifluoromethylsulfonyloxy)phenyl)-1,3-butadiene (45). To a solution of benzylic bromide **48** (2.20 g, 6.89 mmol) in toluene (10 mL) was added triphenylphosphine (1.81 g, 6.90 mmol) and the reaction mixture was stirred under an atmosphere of nitrogen at reflux for 1.5 h. The reaction mixture was concentrated *in vacuo* to give phosphonium salt **49** (4.00 g, 6.88 mmol, 100%) that was used without purification in the next step.

Phosphonium salt **49** (4.00 g, 6.88 mmol) was suspended in dry THF (50 mL) and cooled to –78 °C. At that temperature was added *n*-BuLi (1.08 M solution in hexanes, 6.1 mL, 6.1 mmol). The reaction mixture was warmed up to room temperature over 30 min and a

solution of aldehyde **46** (1.95 g, 6.96 mmol) in dry THF (25 mL) was added. The reaction mixture was stirred for 65 h, concentrated and 0.1 M aqueous HCl solution (50 mL) and dichloromethane (100 mL) were added. The aqueous layer was extracted with dichloromethane (50 mL) and the organic extracts were combined, washed (100 mL water and 75 mL brine), dried ($MgSO_4$) and concentrated *in vacuo*. The residue was purified using column chromatography (SiO_2; CH_2Cl_2) to give diene **45** (2.08 g, 4.14 mmol, 68% *E,E*- and *E,Z*-mixture) as a colorless solid.

5-Bromoisophthalic acid (51). To a 2 L 3-necked round-bottommed flask, equipped with a mechanical stirrer and a reflux condenser with calcium chloride drying tube, containing isophthalic acid (36.51 g, 210 mmol), silver sulfate (40.01 g, 128 mmol) and bromine (15 mL) was added concentrated sulfuric acid (500 mL). The mixture was stirred at reflux for 48 h. The mixture was allowed to cool to room temperature, and it was carefully poured onto 750 mL of crushed ice. The precipitate was filtered by suction filtration, washed with water, dissolved in saturated aqueous $NaHCO_3$ solution and suction filtered into 6 M aqueous sulfuric acid, after which the crude product was isolated by suction filtration. Recrystallization from acetone/water yielded **51** (41.25 g, 77%) as colorless needles: mp: > 280 °C (lit:[33] 282 - 283 °C); IR (Nujol, cm^{-1}) 3540 (m), 1715 (s), 1296 (m), 1255 (w), 1213 (s), 1164 (w); ^1H NMR (acetone-d_6) δ 8.64 (t, 1H, J = 2.4 Hz), 8.38 (d, 2H, J = 2.3 Hz); ^{13}C NMR (acetone-d_6) δ 123.1, 130.3, 134.1, 137.2, 165.6; EI-MS (70 eV) m/z (%): 244 (100, M^+), 227 (66), 199 (19), 143 (19), 75 (39).

Dimethyl 5-bromoisophthalate (52).[66] To a solution of 5-bromoisophthalic acid **51** (41.13 g, 168 mmol) in methanol (500 mL) in a 1 L round-bottomed flask, equipped with a dropping funnel and a reflux condenser with drying tube was added concentrated H_2SO_4 (20 mL) via the dropping funnel. The resulting solution was refluxed overnight. After cooling to room temperature, the reaction mixture was concentrated under reduced pressure, dissolved in ethyl acetate (500 mL) and washed with water (350 mL), saturated aqueous $NaHCO_3$ solution (2 x 300 mL), water (250 mL) and brine (200 mL), dried ($MgSO_4$) and concentrated under reduced pressure to yield **52** (39.85 g, 87%) as colorless crystals; mp: 86 – 86.5 °C (lit:[66] 88 - 89 °C); IR (Nujol, cm^{-1}): 1726 (s), 1575 (m), 1260 (s), 1003 (m), 958 (w), 753 (m), 733 (m); ^1H NMR ($CDCl_3$) δ 8.60 (t, 1H, J = 1.5 Hz), 8.34 (d, 2H, J = 1.5 Hz), 3.96 (s, 6H); ^{13}C NMR ($CDCl_3$) δ 164.9, 136.6, 132.2, 129.2, 122.5, 52.7; EI-MS (70 eV) m/z (%): 272 (36, M^+), 241 (100), 213 (22), 198 (37).

1-Bromo-3,5-bis(hydroxymethyl)benzene (53).[66] To a vigorously stirred, 0 °C suspension of $LiAlH_4$ (4.17 g, 110 mmol) in dry diethyl ether (100 mL) in a 1 L 3-necked round-bottomed flask, equipped with a reflux condenser under nitrogen and a dropping funnel, was added a solution of dimethyl 5-bromoisophthalate **52** (15.02 g, 55 mmol) in dry diethyl ether (500 mL), over *ca.* 30 min. The reaction mixture was allowed to warm to room temperature and after 16 h, the mixture was cooled in an ice/water bath and ethyl acetate (100 mL) was carefully added *via* the dropping funnel, followed by dropwise addition of water (50 mL). The mixture was poured into 3 M aqueous HCl solution (100 mL) and the

aqueous layer was extracted with diethyl ether (3 x 100 mL). The combined organic layers were washed with aqueous HCl solution (3 M, 100 mL), water (2 x 100 mL) and brine (100 mL) and dried ($MgSO_4$). Concentration under reduced pressure yielded a white solid, which could be recrystallized from methanol to give **53** (10.55 g, 88%) as colorless needles: mp: 79 - 80.5 °C (methanol) (lit:[66] 90 – 91 °C); IR (Nujol, cm^{-1}): 3220 (s), 1576 (m), 1238 (m), 1061 (m), 1012 (m), 863 (m), 807 (m), 706 (m); ^1H NMR (acetone-d_6) δ 7.42 (s, 2H), 7.31 (s, 1H), 4.62 (s, 4H), 3.86 (s, 2H); ^{13}C NMR (acetone-d_6) δ 146.2, 128.6, 124.2, 122.6, 64.0; EI-MS (70 eV) *m/z* (%): 216 (43, M^+), 199 (8), 185 (21), 169 (12), 138 (37), 107 (59), 91 (100), 79 (96), 77 (87); Anal. Calc'd for $C_8H_9BrO_2$: C, 44.27; H, 4.18. Found: C, 44.68; H, 4.16.

1-Bromo-3,5-bis(methoxymethyl)benzene (54). To a round-bottomed flask containing powdered KOH (9.71 g, 173 mmol) in DMSO (80 mL) was added 1-bromo-3,5-bis(hydroxymethyl)benzene **53** (5.00 g, 23.0 mmol), followed by iodomethane (12.28 g, 86.5 mmol). The reaction mixture was stirred for 1 h at room temperature and poured into water (100 ml). Dichloromethane was added and the aqueous layer was extracted with another portion of dichloromethane (100 mL). The combined organic layers were washed with water (5 x 100 mL), brine (75 mL), dried ($MgSO_4$) and concentrated under reduced pressure. Vacuum distillation (145 - 149 °C 5 – 7 mmHg) yielded **54** (4.38 g, 78%) as a colorless oil: ^1H NMR ($CDCl_3$) δ 7.40 (s, 2H), 7.21 (s, 1H), 4.40 (s, 4H), 3.38 (s, 6H); ^{13}C

NMR ($CDCl_3$) δ 140.8, 129.8, 125.3, 122.7, 73.9, 58.5; EI-MS (70 eV) *m* z (%): 244 (11, M^+), 199 (27), 165 (44), 104 (51), 45 (100).

3,5-Bis(methoxymethyl)phenylboronic acid (55). To a –50 °C solution of 1-bromo-3,5-bis(methoxymethyl)benzene **54** (8.64 g, 35 mmol) in dry THF (50 ml) was added *n*-BuLi (1.6 M solution, 24.23 mL, 39 mmol) over 10 min, and the reaction mixture was stirred for 15 min. At –50 °C, trimethylborate (12.0 mL, 106 mmol) was added over 10 minutes and the reaction mixture was stirred overnight, slowly warming up to room temperature. The reaction mixture was quenched with 5% aqueous HCl solution until pH 6 and the solvent was removed under reduced pressure. The residue was dissolved in dichloromethane, washed with brine, dried over $MgSO_4$ and concentrated *in vacuo*, yielding crude **55** as a foamy white solid (7.13 g, 33.9 mmol 96%), which was used without purification in the next step.

(*E*,*E*)-1,4-Bis-4-(3,5-bis(methoxymethyl)phenyl)phenyl-1,3-butadiene (56). Ditriflate **45** (2.06 g, 4.10 mmol) was added to a solution of $Pd(PPh_3)_4$ (0.28 g, 0.25 mmol) in degassed ethylene glycol dimethyl ether (50 mL) in a 3-necked round-bottomed flask with reflux condenser under an atmosphere of nitrogen. After 5 min, a solution of boronic acid **55** (2.58 g, 12.3 mmol) in a minimum of degassed ethanol was added, followed by a solution of Na_2CO_3 (1.74 g, 16.4 mmol) in H_2O (9 mL) and the resulting mixture was refluxed for 18 h. After cooling the reaction mixture to room temperature, it was concentrated *in vacuo*,

$CHCl_3$ (250 mL) was added and the mixture was washed with saturated aqueous NH_4Cl solution (2 x 50 mL), water (50 mL) and brine (50 mL). The organic layer was dried ($MgSO_4$), concentrated *in vacuo* and the residue was purified using column chromatography to yield **56** as a light yellow solid (0.13 g, 0.24 mmol, 6%, *E,E*- and *E,Z* mixture): mp. 188.0 – 191.5 °C ($CHCl_3$): ^1H NMR (Only signals for *E,E*-isomer are listed: $CDCl_3$) δ 7.61 (m, 4H), 7.53 (s, 4H), 7.52 (m, 4H), 7.30 (s, 2H), 7.03 (m, 2H), 6.74 (m, 2H), 4.54 (s, 8H), 3.44 (s, 12H): ^{13}C NMR (Only signals for *E,E*-isomer are listed: $CDCl_3$) δ 141.0, 139.9, 139.0, 136.5, 132.4, 129.4, 127.4, 126.8, 125.9, 125.5, 74.6, 58.3; EI-MS (70 eV) *m/z* (%): 534 (100, M^+), 520 (9), 457 (5), 355 (4), 255 (17); HRMS Calc'd for $C_{36}H_{38}O_4$: 534.2768, found 534.2764.

1,4-Bis(4-(3,5-bis(methoxymethyl)phenyl)phenyl)butane (57). To a solution of diene **56** (0.11 g, 0.21 mmol) in degassed C_6H_6 (200 mL) was added a spatula-tip Pearlman's catalyst, followed by 3 drops of glacial acetic acid. The mixture was stirred vigorously under an atmosphere of hydrogen (1.1 bars) for 1 h and nitrogen was bubbled through the mixture to displace the hydrogen gas. Filtration over a plug of $MgSO_4$ followed by *in vacuo* concentration of the reaction mixture yielded **57** (0.11 g, 0.20 mmol, 99%) as a colorless solid: mp: 71.0 – 72.0 °C (ethyl acetate / hexanes): ^1H NMR ($CDCl_3$) δ 7.50 (s, 4H), 7.40 (A_2B_2 system, 8H), 4.52 (s, 8H), 3.43 (s, 12H), 2.70 (br m, 4H), 1.73 (br m, 4H); ^{13}C NMR ($CDCl_3$) δ 141.8, 141.4, 138.8, 138.3, 128.8, 127.0, 125.6, 74.6, 58.2, 35.4, 31.0; EI-MS (70 eV) *m/z* (%): 538 (1, M^+), 506 (24), 491 (19), 474 (25), 459 (13),

445 (9), 429 (10), 358 (8), 255 (46), 45 (100); Anal. Calc'd for $C_{36}H_{42}O_4$: C, 80.26; H, 7.86. Found: C, 79.89; H, 8.18.

[(4-Methoxyphenyl)ethynyl]trimethylsilane (64). To a suspension of bis(triphenylphosphine)palladium(II) chloride (0.27 g, 0.4 mmol) and CuI (0.27 g, 1.4 mmol) in dry benzene (50 mL) in a 100 mL 3-necked round-bottomed flask with condenser under nitrogen was added 4-iodoanisole (1.80 g, 7.7 mmol), followed by DBU (1.76 g, 11.5 mmol) and trimethylsilylethyne (1.13 g, 98.22 mmol). The mixture was stirred at room temperature for 14 h, and the reaction mixture was poured in petroleum ether (bp. 30-60 °C, 50 mL), filtered and concentrated *in vacuo*. To the residue was added petroleum ether (bp. 30-60 °C, 75 mL), and the solution was washed with 3 M aqueous HCl solution (3 x 50 mL), water (2 x 30 mL) and brine, dried over $MgSO_4$ and concentrated under reduced pressure. After column chromatography (2% ethyl acetate/petroleum ether (bp. 30-60 °C), vacuum distillation yielded **64** (1.16 g, 74%) as a colourless oil.[36] bp 110 -112 °C 7 mmHg; ^{1}H NMR ($CDCl_3$) δ 7.70 (d, 2H, J = 9.0 Hz), 6.53 (d, 2H, J = 9.1 Hz), 3.81 (s, 3H), 0.25 (s, 9H); ^{13}C NMR δ 133.4, 113.8, 105.2, 92.4, 55.2, 0.1; EI-MS (70 eV) m/z (%): 204 (27, M^+), 189 (100), 174 (8), 146 (13); Anal. Calc'd for $C_{12}H_{16}OSi$: C, 70.53; H, 7.89. Found: C, 70.34; H, 8.12.

1,4-Bis(4-methoxyphenyl)butadiyne (65).[37] To a solution of **64** (1.62 g, 7.9 mmol) in DMF (40 mL, was added copper(I) chloride (0.86 g, 8.7 mmol) and the flask was equipped

with a condenser. The mixture was stirred vigorously overnight at 60 °C and allowed to cool to room temperature. Approximately 5 g of citric acid was added, followed by water (10 mL) and the mixture was stirred for an additional 1 h at room temperature, after which diethyl ether (30 mL) was added. The aqueous layer was extracted with diethyl ether (20 mL) and the combined organic layers were washed with 5% aqueous citric acid solution (25 mL), water (25 mL) and brine (25 mL), dried over $MgSO_4$ and concentrated under reduced pressure to yield **65** as a yellow solid (1.93 g, 93% crude), which could be recrystallized from ethanol/water mixtures to give **65** (1.79 g, 86%) as slightly yellow needles. mp: 137.5 - 139.0 °C; IR (Nujol, cm^{-1}): 2137 (w), 1598 (m), 1504 (m), 1294 (m), 1255 (s), 1167 (m), 1027 (m), 841 (m); ^1H NMR ($CDCl_3$) δ 7.48 (d, 4H, J = 8.7 Hz), 6.88 (d, 4H, J = 8.8 Hz), 3.84 (s, 6H); ^{13}C NMR δ 160.2, 134.0, 114.1, 116.9, 81.2, 72.9, 55.3; EI-MS (70 eV) m/z (%): 262 (100, M^+), 247 (58), 219 (14), 176 (18); Anal. Calc'd for $C_{18}H_{14}O_2$: C, 82.42; H, 5.38. Found: C, 82.00; H, 5.16.

1,4-Bis(4-methoxyphenyl)butane (66).[58] To a solution of 1,4-bis(4-methoxyphenyl)butadiyne **66** (2.03 g, 7.7 mmol) in benzene (50 mL), was added 20 % Pd(OH)/C (Pearlman's catalyst, approximately 0.3 g), followed by glacial acetic acid (2 drops). The mixture was degassed and placed under an atmosphere of hydrogen (1.1 bar). Once hydrogen consumption ceased, the reaction mixture was filtered and the filtrate was concentrated *in vacuo* to yield 1,4-di(4-methoxyphenyl)butane **66** (2.09 g, 100%) as a white solid, mp 75-76.5 °C (ethyl acetate / hexanes); ^1H NMR ($CDCl_3$) δ 7.08 (d, 4H, J =

8.6 Hz), 6.82 (d, 4H, J = 8.8 Hz), 3.79 (s, 6H), 2.57 (br m, 4H), 1.62 (br m, 4H); ^{13}C NMR δ 157.6, 134.7, 129.2, 113.6, 55.2, 34.8, 31.3; EI-MS (70 eV) m/z (%) 270 (11, M^+), 121 (100).

1,4-Bis(4-methoxyphenyl)butane (66). Iodine (0.70 g, 2.8 mmol) was added to a 100 mL 3-necked round-bottomed flask containing magnesium turnings (1.58 g, 65.0 mmol) in dry benzene (30 mL) and dry diethyl ether (2.0 mL) equipped with a distillation head under an atmosphere of nitrogen. The mixture was stirred vigorously for 15 min and most of the color disappeared. The solvent was distilled off under an atmosphere of nitrogen. The residue was stirred at 150 °C for 5 min and was allowed to cool to room temperature. Dry THF (10 mL) was added, the mixture was cooled to 0 °C, and a solution of 4-bromoanisole **63a** (7.45 g, 39.8 mmol) in dry THF (40 mL) was added over 1 h and the cooling-bath was removed. The suspension was added dropwise over 30 minutes to a 0 °C solution of 1,4-dibromobutane **39** (2.15 g, 9.96 mmol), LiCl (0.04 g, 1 mmol) and $CuCl_2 \cdot 2\,H_2O$ (0.08 g, 0.5 mmol) in dry THF (40 mL) under an atmosphere of nitrogen. The mixture was stirred for 16 h at room temperature, quenched with H_2O (10 mL) and concentrated *in vacuo* to a volume of *ca.* 25 mL. The residue was slurried in diethyl ether (75 mL) and filtered, washing the residue with diethyl ether (50 mL). The filtrate was washed with water (75 mL) and brine (50 mL), dried ($MgSO_4$) and concentrated *in vacuo*. The residue was purified by column chromatography (SiO_2; 5% diethyl ether/hexanes) to yield **66** (1.89 g, 6.97 mmol, 70%) as a colorless solid.

1,4-Bis(4-hydroxyphenyl)butane (67).[59] To a –30 °C (dry ice/acetone bath) solution of 1,4-di(4-methoxyphenyl)butane **66** (1.46 g, 5.4 mmol) in dichloromethane (30 mL) in a 50 mL 3-necked flask under nitrogen, was added borontribromide (1.53 mL, 16 mmol) dropwise over 10 min. The mixture was allowed to warm to room temperature, and, after stirring for 3 h at room temperature, ethanol (5 mL) was added, followed by water (15 mL). The aqueous layer was extracted with dichloromethane (30 mL). The combined organic layers were extracted with 3 M aqueous KOH solution (2 x 30 mL) and the combined alkaline layers were acidified using 6 M aqueous HCl solution. The mixture was then extracted with diethyl ether (2 x 50 mL). The combined organic layers were washed with water (25 mL) and brine (25 mL), dried over $MgSO_4$ and concentrated under reduced pressure. Column chromatography of the residue (SiO_2; 60% ethyl acetate hexanes) yielded **67** as a white solid (1.23 g, 94%), mp 152-153.5 °C (ethyl acetate); IR (Nujol, cm^{-1}): 3405 (s), 1511 (s), 1236 (m), 815 (m); ^1H NMR (acetone-d_6) δ 7.01 (d, 4H, J = 8.4 Hz), 6.74 (d, 4H, J = 8.4 Hz), 3.83 (s, 2H), 2.54 (br m, 4H), 1.59 (br m, 4H); ^{13}C NMR (acetone-d_6) δ 152.4, 130.4, 126.4, 112.16, 31.83, 28.5; EI-MS (70 eV) m/z (%): 242 (12, M^+), 186 (16), 107 (100).

1,4-Bis(4-(trifluoromethanesulfonyloxy)phenyl)butane (68). To a solution of 1,4-bis(4-hydroxyphenyl)butane **67** (1.27 g, 5.24 mmol) and pyridine (0.93 mL, 11.5 mmol) in dichloromethane (30 mL) at 0 °C, was added triflic anhydride (1.94 mL, 11.5 mmol) dropwise over 10 min under nitrogen. After addition was complete the reaction mixture

was stirred for 2 h at room temperature and 5% aqueous HCl solution (10 mL) was added. The organic layer was washed with 5% aqueous HCl, water and brine, dried over $MgSO_4$ and concentrated *in vacuo*. Column chromatography (25% ethyl acetate/hexanes) of the residue yielded **68** (2.38 g, 4.70 mmol, 90%) as a white solid, mp: 84.0 – 86.0 °C (ethyl acetate / hexanes); IR (Nujol, cm^{-1}): 1504 (m), 1248 (w), 1213 (m), 1174 (w), 1143 (m), 892 (m), 717 (w); ^1H NMR ($CDCl_3$) δ 7.21 (AA'BB', 8H), 2.67 (br m, 8H), 1.67 (br m, 8H); ^{13}C NMR δ 147.7, 142.8, 130.0, 121.1, 118.7 (q, J = 320 Hz), 35.0, 30.7; EI-MS (70eV) m/z (%): 506 (26, M^+), 373 (15), 279 (19), 239 (100), 175 (82). Anal. Calc'd for $C_{18}H_{16}F_6O_6S_2$: C, 42.69; H, 3.18. Found: C, 42.65; H, 2.93.

1,4-Bis(4-(3,5-bis(methoxymethyl)phenyl)phenyl)butane (57). To a suspension of tetrakistriphenylphosphine palladium(0) (0.15 g, 0.13 mmol) in dry anhydrous dimethoxyethane (35 mL) in a 50 mL 3-necked round bottom flask equipped with magnetic stirrer and reflux condenser under nitrogen, was added **68** (2.22 g, 4.41 mmol), followed after 10 min by DBU (2.6 mL, 18 mmol) and a solution of 3,5-bis(methoxymethyl)phenylboronic acid **55** (3.64 g, 17.3 mmol) in 5 mL anhydrous ethanol. The mixture was refluxed for 20 h, and allowed to cool to room temperature. The reaction mixture was filtered and the filtrate was concentrated *in vacuo*, dichloromethane (20 mL) was added and the organic solution was washed with 3 M aqueous HCl solution (2 x 25 mL), water (25 mL) and brine, dried over $MgSO_4$ and concentrated under reduced pressure.

The residue was subjected to column chromatography (SiO_2; 75% CH_2Cl_2/hexanes) to yield **57** (1.29 g, 55%) as a white solid.

1,4-Bis-4-(3,5-bis(bromomethyl)phenyl)phenyl)butane (71). To a –30 °C solution of **57** (1.36 g, 2.5 mmol) in dichloromethane (20 mL) under nitrogen, was added dropwise borontribromide (1.9 mL, 20 mmol). The reaction mixture was allowed to warm slowly to *ca.* –10 °C. When no more starting material could be detected by TLC, ethanol (5 mL) was added followed by water (10 ml). The organic layer was washed with water and brine, dried ($MgSO_4$) and concentrated under reduced pressure. Column chromatography (50% dichloromethane/hexanes) yielded **71** (0.97 g, 52%) as a white solid: mp: 143 – 145 °C (dec.): ^{1}H NMR ($CDCl_3$) δ 7.54 (s, 4H), 7.50 (d, 4H, J = 8.1 Hz), 7.38 (s, 2H), 7.27 (d, 4H, J = 7.9 Hz), 4.53 (s, 8H), 2.71 (br m, 4H), 1.73 (br m, 4H); ^{13}C NMR ($CDCl_3$) δ 142.5, 142.4, 138.9, 137.3, 129.0, 128.1, 127.8, 127.0, 35.4, 32.9, 31.0; EI-MS (70 eV) *m/z* (%): M^+ not observed, 573 (3), 493 (3), 413 (2), 353 (9), 287 (18), 193 (32), 80 (100); Anal. Calc'd for $C_{32}H_{30}Br_4$: C, 52.35; H, 4.12. Found: C, 52.48; H, 4.05.

18,33-Dithia[4.3.3](4',3,5)biphenylophane (30). To a vigorously stirred solution of **71** (1.11 g, 1.5 mmol) in dichloromethane (540 mL) and absolute ethanol (60 mL) in a 1 L Erlenmeyer flask was added Na_2S/Al_2O_3 (1.36 g, 2.44 mmol/g) over 15 minutes. When all of the starting material was consumed (TLC), the reaction mixture was filtered and

concentrated under reduced pressure. Filtering through a short plug of silica (60% ethyl acetate/hexanes) yielded **30** (0.54 g, 75% crude) as an off-white solid that was immediately used in the next step: ^{1}H NMR ($CDCl_3$) δ 7.17 (s, 2H), 7.03 (s, 4H), 7.02 (d, 4H, J = 8.0 Hz), 6.75 (d, 4H, J = 8.1 Hz), 3.89 (narrow AB system, 8H), 2.41 (br m, 4H), 1.75 (br m, 4H); ^{13}C NMR ($CDCl_3$) δ 140.7, 140.3, 137.4, 136.9, 130.1, 128.8, 125.8 (2C), 38.4, 35.5, 28.7;

[4.2.2](4',3,5)Biphenylophane-17,31-diene (2). To a solution of dithiabiphenylophane **30** (0.50 g, 1.0 mmol) in dichloromethane (50 mL) under nitrogen, was added Borch reagent (0.42 mL, 4.2 mmol). After stirring for 5 h, the solvent was removed under reduced pressure, 80% aqueous methanol was added (5 mL) and the precipitate was collected by suction filtration as a beige-white solid (0.59 g, 83% crude) that was used without purification. The solid was suspended in dry THF (75 mL). Potassium *tert*-butoxide (0.29 g, 2.6 mmol) was added, and the mixture was stirred under nitrogen for 5 h. The reaction was quenched with saturated aqueous NH_4Cl solution (10 mL), and the mixture was concentrated under reduced pressure. The residue was dissolved in dichloromethane and washed with saturated aqueous NH_4Cl, water and brine, dried ($MgSO_4$) and concentrated under reduced pressure, which yielded a yellow foamy solid, which was used immediately in the next step.

The yellow solid was dissolved in dry dichloromethane (75 mL). Borch reagent (0.26 mL, 2.6 mmol) was added and the mixture was stirred for 1.5 h. The solvent was removed under reduced pressure. A solution of 5% methanol in ethyl acetate was added and the mixture was concentrated *in vacuo*, to give a brown oil, which was immediately used in the next step.

To a suspension of the brown oil in 1:1 *tert*-butanol and dry THF (50 mL) was added potassium *tert*-butoxide (0.75 g 6.7 mmol), and the mixture was stirred overnight under nitrogen. The reaction was quenched with saturated aqueous NH_4Cl, and the solvent was removed under reduced pressure. The residue was dissolved in dichloromethane and washed with saturated aqueous NH_4Cl, water and brine, dried over $MgSO_4$ and concentrated *in vacuo*. Column chromatography (50% dichloromethane/hexanes) yielded **2** (0.25 g, 48% from crude **30**, 40% from tetrabromide **71**) as a colorless solid: mp: > 270 °C (dec.): ^{1}H NMR ($CDCl_3$) δ 7.35 (s, 4H), 7.08 (d, 4H, J = 8.3 Hz), 6.78 (d, 4H, J unresolved), 6.77 (s, 6H), 2.41 (br m, 4H), 1.70 (br m, 4H); ^{1}H NMR (C_6D_6) δ 7.14 (s, 4H), 7.00 (d, 4H, J = 8.4 Hz), 6.80 (s, 2H), 6.78 (s, 4H), 6.67 (d, 4H, J = 8.4 Hz); ^{13}C NMR ($CDCl_3$) δ 141.2, 139.0, 137.6, 136.4, 128.4, 125.2, 125.1, 120.3, 34.9, 29.5; ^{13}C NMR (C_6D_6) 139.9, 138.1, 136.8, 136.7, 136.5, 135.5, 127.4, 124.2 (2C), 33.9, 28.5; MS (EI, 70 eV) m/z (%): 410 (100, M^+), 381 (7), 363 (2), 291 (41); HRMS Calc'd for $C_{32}H_{26}$: 410.2033, found 410.2027.

Attempts to synthesize [4](1,4)benzeno[0](2,7)pyreno[0](1,4)benzeno<3>phane (1). Cyclophane diene **2** was dissolved in dry and degassed solvent (benzene or toluene) and DDQ (1-3 equivalents) was added. The flask was equipped with a reflux condenser and the mixture was refluxed under nitrogen while reaction progress was monitored by TLC. The mixture was concentrated (after 6 h for benzene, 4 h for toluene) under reduced pressure, and the residue was filtered through a plug of silica using 50% dichloromethane/hexanes to give cyclophane diene **2** as the only identifiable component.

Attempted *ortho*-vinylation of 67. In a 250 mL 3-necked round-bottom flask under an atmosphere of nitrogen chlorobenzene (75 mL) was cooled to −50 °C using a dry ice acetone bath and $SnCl_4$ was added (7.7 mL, 66 mmol) followed by Bu_3N (15.7 mL, 65.9 mmol) and ethyne was bubbled through the reaction mixture for 30 min at this temperature. Bis(phenol) **60** (2.00 g, 8.25 mmol) was added, the ethyne flow was stopped and the mixture was heated at 60 °C for 1.5 hours. Methanol was added and the mixture was kept at 60 °C for 30 min and cooled to room temperature. The mixture was poured into diethyl ether (150 mL) and saturated aqueous $KHSO_4$ solution (100 mL) and filtered through Celite. The aqueous layer was re-extracted with diethyl ether (2 x 75 mL) and the organic extracts were washed (75 ml brine), dried ($MgSO_4$) and the diethyl ether was removed under reduced pressure. Acetic anhydride (20 mL) and pyridine (20 mL) were added to the concentrate and the mixture was stirred overnight under an atmosphere of nitrogen. The reaction mixture was poured into saturated $KHSO_4$ solution (100 mL) and EtOAc (100 mL)

was added. The aqueous layer was extracted with EtOAc (100 mL), the organic extracts were combined, washed with saturated $NaHCO_3$ solution (2 x 100 mL), brine (100 mL), dried ($MgSO_4$) and concentrated under reduced pressure. The residue was subjected to column chromatography (10-35% EtOAc/hexanes) and several fractions were collected. All fractions were yellow oils and were mixtures of several compounds and formed insoluble gel-like substances within hours of isolation.

1,4-Bis(3-formyl-4-hydroxyphenyl)butane (91). To a suspension of **67** (2.11 g, 9.12 mmol) in trifluoroacetic acid (70 mL), hexamethylenetetramine (2.56 g, 18.2 mmol) was added and the mixture was refluxed for 90 min. After cooling to room temperature, the mixture was poured into 3 M aqueous HCl solution (300 mL) and stirred overnight. Dichloromethane (150 mL) was added, and the aqueous layer was re-extracted with dichloromethane (150 mL). The combined organic extracts were washed with 3 M aqueous HCl solution (2 x 150 mL) and extracted with 3 M aqueous KOH solution (3 x 100 mL). After separation the basic aqueous layers were acidified with 6 M aqueous HCl solution and extracted with EtOAc (3 x 250 mL). The combined EtOAc extracts were washed with saturated aqueous NaCl solution (100 mL), dried ($MgSO_4$) and concentrated under reduced pressure to yield crude **91** as a sparingly soluble waxy yellow substance (1.72 g, 5.50 mmol, 60%): ^{1}H NMR ($CDCl_3$) δ 10.87 (s, 2H), 9.87 (s, 2H), 7.34 (d, 2H, J = 7.9 Hz), 7.33 (s, 2H), 6.93 (d, 2H, J = 7.9 Hz), 2.64 (br m, 4H), 1.66 (br m, 4H); ^{13}C NMR ($CDCl_3$) δ 196.5, 159.8, 137.3, 133.7, 132.8, 120.3, 117.5, 34.5, 30.8.

3.4 References

(1) Bodwell, G. J.; Miller, D. O.; Vermeij, R. J. *Org. Lett.* **2001**, *3*, 2093-2096.

(2) The name Vögtle belt has been proposed by us for a (so far hypothetical) fully aromatic belt like **4**. For a more detailed discussion refer to Section 4.1 and references therein.

(3) Bodwell, G. J.; Fleming, J. J.; Mannion, M. R.; Miller, D. O. *J. Org. Chem.* **2000**, *65*, 5360-5370.

(4) In Section 1.4 a more detailed discussion of AM1 calculations on [*n*](2,7)pyrenophanes can be found.

(5) Bend angles of pyrene units in pyrenophanes were calculated using the Chem3D package of software (MOPAC, AM1, closed shell).

(6) van Eis, M. J.; de Kanter, F. J. J.; de Wolf, W. H.; Bickelhaupt, F. *J. Am. Chem. Soc.* **1998**, *120*, 3371-3375.

(7) Laufenberger, S.; Feuerbacher, N.; Pischel, I.; Börsch, O.; Nieger, M.; Vögtle, F. *Liebigs Annalen-Recueil* **1997**, 1901-1906.

(8) Breidenbach, S.; Harren, J.; Neumann, S.; Nieger, M.; Rissanen, K.; Vögtle, F. *J. Chem. Soc., Perkin Trans. 1* **1996**, 2061-2067.

(9) Gross, J.; Harder, G.; Siepen, A.; Harren, J.; Vögtle, F.; Stephan, H.; Gloe, K.; Ahlers, B.; Cammann, K.; Rissanen, K. *Chem. Eur. J.* **1996**, *2*, 1585-1595.

(10) Iyoda, M.; Kondo, T.; Nakao, K.; Hara, K.; Kuwatani, Y.; Yoshida, M.; Matsuyama, H. *Org. Lett.* **2000**, *2*, 2081-2083.

(11) Staab, H. A.; Haenel, M. *Chem. Ber.* **1973**, *106*, 2190-2202.

(12) Vögtle, F.; Steinhagen, G. *Chem. Ber.* **1978**, *111*, 205-212.

(13) Nishimura, J.; Ohbayashi, A.; Ueda, E.; Oku, A. *Chem. Ber.* **1988**, *121*, 2025-2028.

(14) Nishimura, J.; Okada, Y.; Inokuma, Y.; Gao, S. R. *Synlett* **1994**, 884-894.

(15) Tani, K.; Seo, H.; Maeda, M.; Imagawa, K.; Nishiwaki, N.; Ariga, M.; Tohda, Y. *Tetrahedron Lett.* **1995**, *36*, 1883-1886.

(16) Vögtle, F.; Hohner, G.; Weber, E. *J. Chem. Soc., Chem. Commun.* **1973**, 366.

(17) Brown, C. J. *J. Chem. Soc.* **1953**, 3265-3270.

(18) Hope, H.; Bernstein, J.; Trueblood, K. N. *Acta Crystallogr.* **1972**, *B28*, 1733-1743.

(19) Mitchell, R. H.; Boekelheide, V. *J. Am. Chem. Soc.* **1974**, *96*, 1547-1557.

(20) Mitchell, R. H. *Heterocycles* **1978**, *11*, 563-586.

(21) Bodwell, G. J.; Houghton, T. J.; Koury, H. E.; Yarlagadda, B. *Synlett* **1995**, 751-752.

(22) Suzuki, A. *Acc. Chem. Res.* **1982**, *15*, 178-184.

(23) Suzuki, A. *Pure Appl. Chem.* **1985**, *57*, 1749-1758.

(24) Suzuki, A. *Pure Appl. Chem.* **1986**, *58*, 629-638.

(25) Suzuki, A. *Pure Appl. Chem.* **1991**, *63*, 419-422.

(26) Miyaura, N.; Yamada, K.; Suginome, H.; Suzuki, A. *J. Am. Chem. Soc.* **1985**, *107*, 972-985.

(27) Miyaura, N.; Ishiyama, T.; Sasaki, H.; Ishikawa, M.; Satoh, M.; Suzuki, A. *J. Am. Chem. Soc.* **1989**, *111*, 314-321.

(28) Soai, K.; Ookawa, A. *J. Org. Chem.* **1986**, *51*, 4000.

(29) Wiley, G. A.; Hershkowitz, R. L.; Rein, B. M.; Chung, B. C. *J. Am. Chem. Soc.* **1964**, *86*, 964-965.

(30) Appel, R. *Angew. Chem., Int. Ed. Engl.* **1975**, *14*, 801-811.

(31) Cadogan, J. I. G.; Mackie, R. K. *Chem. Soc. Rev.* **1974**, *3*, 87-137.

(32) Dess, D. B.; Martin, J. C. *J. Org. Chem.* **1983**, *48*, 4155-4156.

(33) Crandan, E. W.; Harris, L. *Org. Prep. Proc. Int.* **1969**, *1*, 147-156.

(34) Fischer, L. F.; Speier, A. *Ber. Dtsch. Chem. Ges.* **1895**, *28*, 3252-3258.

(35) Ikegashira, K.; Nishihara, Y.; Hirabayashi, K.; Mori, A.; Hiyama, T. *J. Chem. Soc., Chem. Commun.* **1997**, 1039-1040.

(36) Nishihara, Y.; Ikegashira, K.; Hirabayashi, K.; Ando, J. I.; Mori, A.; Hiyama, T. *J. Org. Chem.* **2000**, *65*, 1780-1787.

(37) Sonogashira, K.; Tohda, Y.; Hagihara, N. *Tetrahedron Lett.* **1975**, 4467-4470.

(38) Sonogashira, K. *Comprehensive Organic Chemistry*; Pergamon Press: New York, 1991; p 521.

(39) Cassar, L. *J. Organomet. Chem.* **1975**, *93*, 253-257.

(40) Dieck, H. A.; Heck, F. R. *J. Organomet. Chem.* **1975**, *93*, 259.

(41) Ratovelomana, V.; Linstrumelle, G. *Synth. Commun.* **1981**, *11*, 917-923.

(42) Kawasaki, I.; Matsuda, K.; Kaneko, T. *Bull. Chem. Soc. Jpn.* **1971**, *44*, 1986-1987.

(43) Lai, Y.-H. *Synthesis* **1981**, 585-604.

(44) Tamura, M.; Kochi, J. *Synthesis* **1971**, 303-305.

(45) Borch, R. F. *J. Org. Chem.* **1969**, *34*, 627-629.

(46) Thomson, T.; Stevens, T. S. *J. Chem. Soc.* **1932**, 69-73.

(47) Baldwin, J. E.; Erickson, W. F.; Hackler, R. E.; Scott, R. M. *J. Chem. Soc., Chem. Commun.* **1970**, 576-578.

(48) Houghton, T. J. Ph.D. Dissertation, Memorial University of Newfoundland, **1999**.

(49) Mannion, M. R. Ph.D. Dissertation, Memorial University of Newfoundland, **1999**.

(50) Mitchell, R. H.; Carruthers, R. J. *Can. J. Chem.* **1974**, *52*, 3054-3056.

(51) Brown, R. F. C. *Pyrolytic Methods in Organic Chemistry*; Academic Press: New York, 1980.

(52) Calculations were performed using version 5.0a37 of the Chem3D Pro package of software (MOPAC, AM1, closed shell).

(53) Bodwell, G. J.; Bridson, J. N.; Houghton, T. J.; Kennedy, J. W. J.; Mannion, M. R. *Chem. Eur. J.* **1999**, *5*, 1823-1827.

(54) Flammang-Barbieux, M.; Nasielski, J.; Martin, R. H. *Tetrahedron Lett.* **1967**, 743-744.

(55) Laarhoven, W. H.; Cuppen, T. J. H. M.; Nivard, R. J. F. *Recl. Trav. Chim. Pays-Bas* **1968**, *87*, 687-698.

(56) Laarhoven, W. H.; Cuppen, T. J. H. M.; Nivard, R. J. F. *Tetrahedron* **1970**, *26*, 4865-4881.

(57) Bringmann, G.; Pabst, T.; Henschel, P.; Kraus, J.; Peters, K.; Peters, E. M.; Rycroft, D. S. *J. Am. Chem. Soc.* **2000**, *122*, 9127-9133.

(58) Okada, Y.; Mabuchi, S.; Kurahayashi, M.; Nishimura, J. *Chem. Lett.* **1991**, 1345-1348.

(59) Okada, Y.; Sugiyama, K.; Wada, Y.; Nishimura, J. *Tetrahedron Lett.* **1990**, *31*, 107-110.

(60) Yamaguchi, M.; Arisawa, M.; Omata, K.; Kabuto, K.; Hirama, M.; Uchimaru, T. *J. Org. Chem.* **1998**, *63*, 7298-7305.

(61) Smith, K. *J. Org. Chem.* **1972**, *37*, 3972.

(62) Ogata, Y.; Kawasaki, A.; Suguira, F. *Tetrahedron* **1968**, *24*, 5001-5010.

(63) Umemoto, T.; Kawashima, T.; Sakata, Y.; Misumi, S. *Tetrahedron Lett* **1975**, 1005-1006.

(64) Hurley, P. B.Sc. Hounours Dissertation, Memorial University of Newfoundland, **2000**.

(65) Lumma Jr., W. C. *J. Org. Chem.* **1981**, *46*, 3668-3671.

(66) Sherrod, S. A.; da Costa, R. L.; Barnes, R. A.; Boekelheide, V. *J. Am. Chem. Soc* **1974**, *96*, 1565-1577.

(67) Galamb, V.; Gopal, M.; Alper, H. *Organometallics* **1983**, *2*, 801-805.

Chapter 4

Attempted Synthesis of a Vögtle Belt

4.1 Introduction

Our group has proposed the name "Vögtle Belts"[1,2] for fully aromatic belts like **1** since Vögtle[3,4] was the first to propose this class of molecules as synthetic targets. Aromatic belts such as **1** map directly onto the equators of the D_{5h}-C_{70} and D_{6h}-C_{84} fullerenes. Upon the recognition of a repeating pyrene unit in **1** it was anticipated that the pyrene-forming VID methodology might be applied to its synthesis.

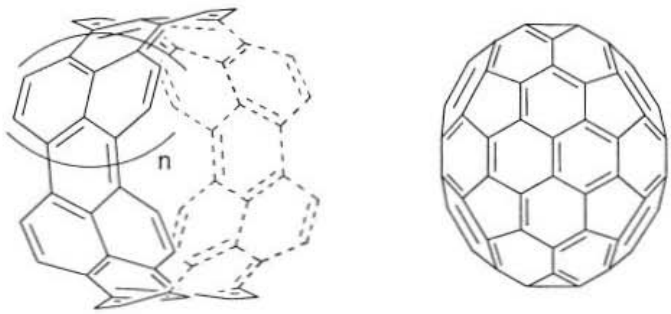

1 **2**

Figure 4.01: Structures of a "Vögtle belts" **1** and D_{6h}-C_{84} **2**.

When investigations toward the synthesis of model compounds for the Vögtle belts failed (Chapter 3) it came to mind that, rather than attempting to synthesize partial aromatic belts, at least one attempt should be made to synthesize a fully aromatic belt. The relatively low calculated bend angle ($\theta_{calcd} = 90.3°$) for each of the pyrene units in **1** (n = 1) suggested that the VID protocol might be applicable for its synthesis. As the "tether" in **1** consists entirely of pyrene units (indistinguishable from the cyclophane pyrene

nucleus) the dihedral angles around the biaryl bonds are expected to be small, which makes this synthetic target a logical step forward from the synthetic targets that were proposed in Section 3.2.4.

4.1.1 Molecular belts in the literature

Since the initial proposal of molecular structures like **1**, not much progress toward the synthesis of **1** or related compounds has been reported. Some reports on attempted syntheses of similar structural motifs describe projects aimed toward the [*n*]cyclacenes **3**. Several approaches have been followed and have led to the synthesis of advanced intermediates (e.g. **4**-**6**; Figure 4.02).[5-11]

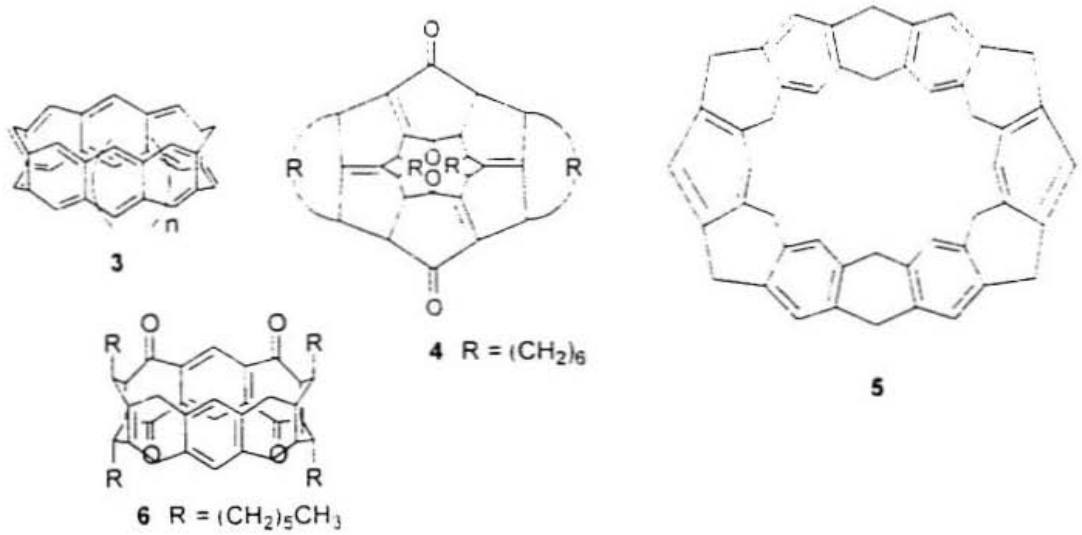

Figure 4.02: Structure of [*n*]cyclacene **3** and possible precursors **4**,[4] **5**[5-7] and **6**[10,11].

Another structural motif that falls under the category of belt-like molecules is the cyclic oligo-*para*-phenylene motif. Several approaches have been reported in this area and have led to the synthesis of macrocycles **7** – **9** (Figure 4.03).

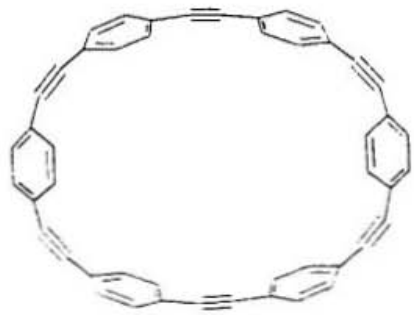

7

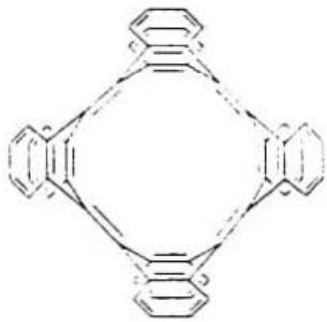

8

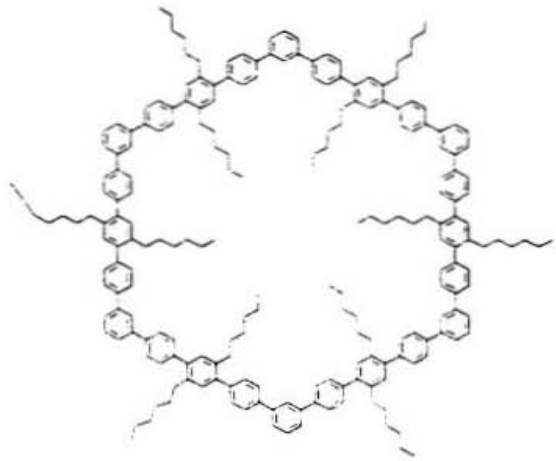

9

Figure 4.03: Belt-shaped molecules **7**,[12,13] **8**[14] and **9**[15].

Vögtle *et al.*[16,17,17,18] have described syntheses of several tube-shaped molecules. Their approach is based on high-dilution coupling of two (or more) partners to form macrocyclic structures that should, in principle, after ring contraction, lead to possible precursors for **1**. In 1991 the synthesis of cyclophane **10** was described,[19] although no

unequivocal proof for this structure was provided. DNMR study of **10** showed the presence of (at least) two conformers at room temperature, which was ascribed to the slow (*syn* to *syn'*-like) equilibrium between conformers **10a** and **10b** with an activation barrier of 15-17 kcal/mol (65-70 kJ/mol). A notable feature of cyclophane **10** is that it contains both nitrogen and sulfur atoms in the bridges. For the conformers of **10** it was not determined which bridge contained which heteroatom.

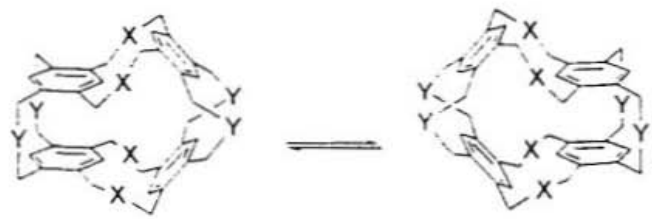

Scheme 4.01: Structure and conformational interconversion of cyclophane **10**

Later, the Vögtle group published the synthesis and molecular structures of some smaller tube-shaped molecules (**11**[17] and **12**[17]) and a larger cyclophane **13**[18] (Figure 4.04). So far, only cyclophanes with tosylamine-containing bridges have been reported, together with some pyridine-based tube-shaped cyclophanes.[19] Synthesis of the tube-shaped cyclophanes with sulfur atoms as the only heteroatoms in the bridges and benzene rings as the only aromatic units has not been successful due to the reported instability of some of the intermediates.[16,20] Compound **13** is a precursor to a Vögtle belt **1** (n = 0). Ring contraction of the sulfur-containing bridges seems feasible, since it has been used

successfully in many cases, but ring-contraction of the nitrogen-containing bridges appears to be a nontrivial task.

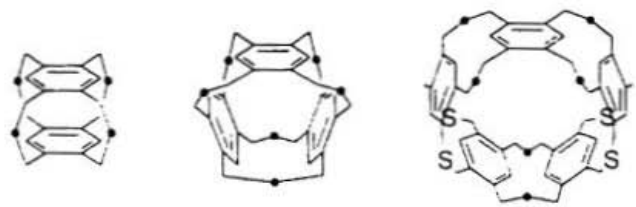

11 **12** **13**

• = N-Tos

Figure 4.04: Tube-shaped cyclophanes **11** – **13**.

4.1.2 Retrosynthetic analysis of a Vögtle belt

In the first part of the retrosynthesis of Vögtle belt **1**, two pyrene units in the belt are broken down to dithiacyclophane moieties to give a tetrathiacyclophane **14**. Compound **14** contains tetrahydropyrene units rather than pyrene units, since the former are expected to impart greater solubility to **14** and its precursors.[21] Dehydrogenation of the tetrahydropyrene units[22] was expected to be accomplished in the last step of the synthesis, during which DDQ is used to accomplish the conversion of the cyclophane diene systems to the pyrene units.

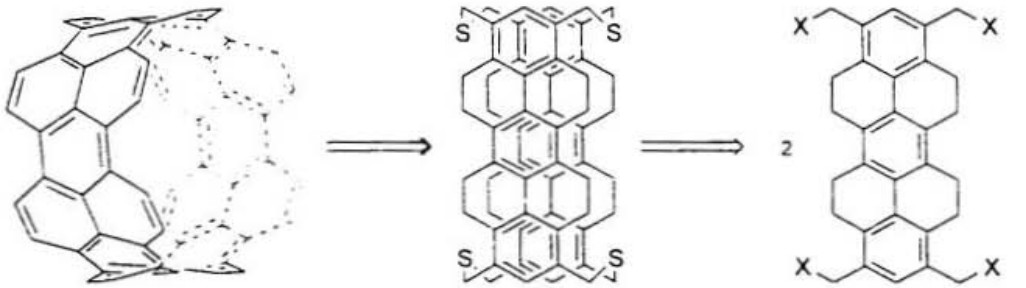

1 **14** **15a** X = Br
15b X = SH

Scheme 4.02: Retrosynthetic analysis of a Vögtle belt – Part 1.

Tetrathiacyclophane **14** could be formed from a coupling reaction of a tetrathiol (**15b**; X = SH) with a tetrabromide (**15a**; X = Br) under high dilution conditions. The tetrathiol (**15b**; X = SH) can be formed from the precursor tetrabromide (Scheme 4.03).

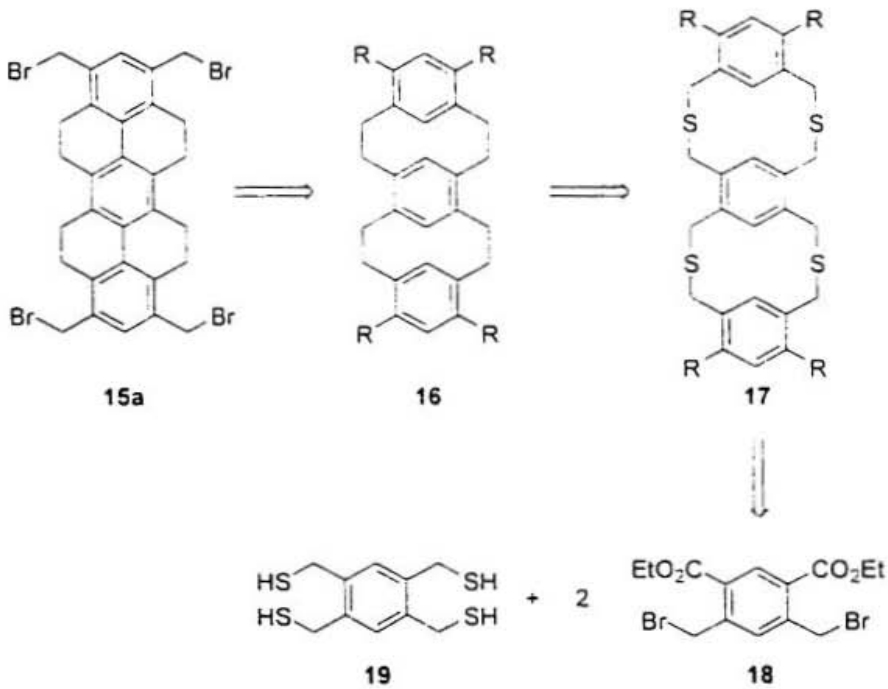

15a **16** **17**

19 **18**

Scheme 4.03: Retrosynthetic analysis of a Vögtle belt – Part 2.

Compound **15a** contains two tetrahydropyrene units. This type of structural feature can usually be formed in high yield from [2.2]metacyclophanes using iron filings and bromine in the dark[22] or using pyridinium perbromide.[23] These conditions are sufficiently mild to not dehydrogenate the product.

Metacyclophanes containing four dimethylene bridges like **16** are known for R = H and have previously been synthesized[24] by building up the two cyclophane units separately. For our purposes, this synthetic route would be too long and low yielding, since appreciable quantities of building block **16** are needed. A shorter approach to the synthesis of **16** would be to form the two metacyclophane units at the same time. This can be done using the Stevens rearrangement for ring contraction followed by reductive removal of the sulfur-containing groups or *via* pyrolysis of the sulfones or photolysis of the sulfide linkages. In all cases, retrosynthetic analysis of metacyclophane **16** leads back to tetrathiabenzeno-<3>phane **17**.[25]

Tetrathiabenzeno-<3>phane **17** could be formed in a single step from the tetrathiol **19** (derived from tetrabromodurene) and a dibromide **18** in a high-dilution coupling. Couplings of this type have been described by Vögtle *et al.*, who have described the synthesis of compounds similar to **17** using coupling of **18** and **19**.[16,20] For the synthesis of **17** it was decided to apply Vögtle's approach, but with some minor modifications.

4.2.1 Synthesis of tetrathiabenzeno<3>phanes

Vögtle's synthesis[16,20] started with dichloride **20b**, which was oxidized using $KMnO_4$ under basic conditions to yield diacid **21** in 71%, presumably *via* the diol **20c** that is formed *in situ*. We chose to use dibromide **20d** as starting material, as it was readily available from other research projects. It was synthesized in 56% yield by the double bromomethylation of *meta*-xylene.[26] However, the oxidation of **20d** under conditions that were reported for **20a** was found to be problematic, since yields varied (20-45%).[27] In order to increase the reactivity of dibromide **20d**, it was decided to synthesize diacetate **20e** (99% from **20d**), which could form diol **20c** by saponification of the ester moieties. This saponification was expected to be more effective than the nucleophilic substitution that is required to convert dibromide **20d** to diol **20c**. Oxidation of diacetate **20e** under basic conditions yielded the desired diacid **21** in 80% yield. Although the overall yield of this process is not higher than Vögtle's process,[20] the results were reproducible.

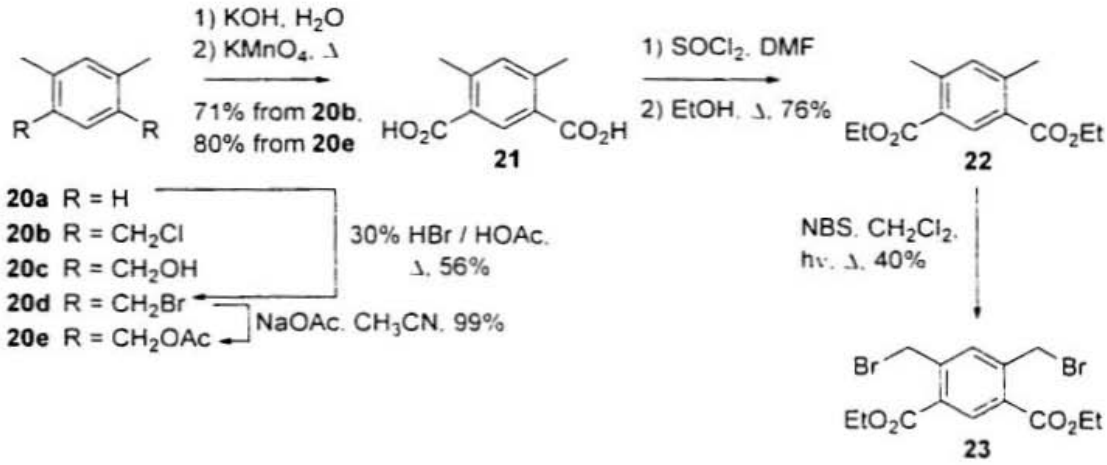

Scheme 4.04: Synthesis of intermediate **23**

Diacid **21** was esterified to provide diester **22** in 76% yield *via* the bisacid chloride). When Fischer esterification conditions were used in this step (reflux in EtOH with catalytic H_2SO_4), the diester was formed in only 57%.[27] Double free radical benzylic bromination of **22** yielded **23** in 40% yield. The yields for these steps (**21** -> **22** -> **23**) were comparable to those reported by Vögtle.

Building block **23** is one of the partners required for the coupling reaction to form the required tetrathiacyclophanes. The other building block is tetrabromodurene **26**, which is commercially available. It can also be synthesized by the fourfold free radical benzylic bromination of durene **27**[28] or by a reduction-bromination sequence from pyromellitic acid derivatives, e.g. **24** (Scheme 4.05). It was decided to apply the second synthetic approach.

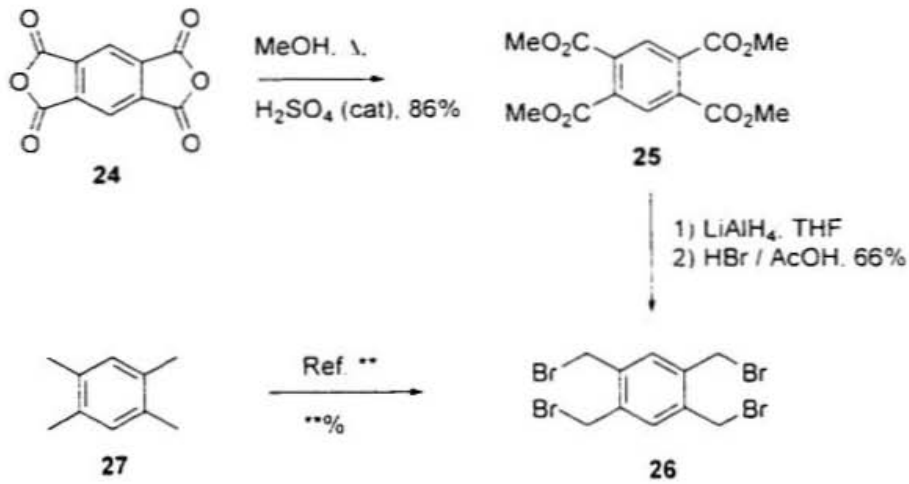

Scheme 4.05: Synthesis of tetrabromodurene **26**.

In the first step, pyromellitic anhydride **24** was converted to tetramethyl pyromellitate in 86% using Fischer esterification conditions.[29] The tetramethyl ester **25** was reduced using $LiAlH_4$ and workup of the reaction mixture without isolating the intermediate 1,2,4,5-tetrakis(hydroxymethyl)benzene with concentrated hydrogen bromide in acetic acid yielded the desired tetrabromodurene **26** (66%).

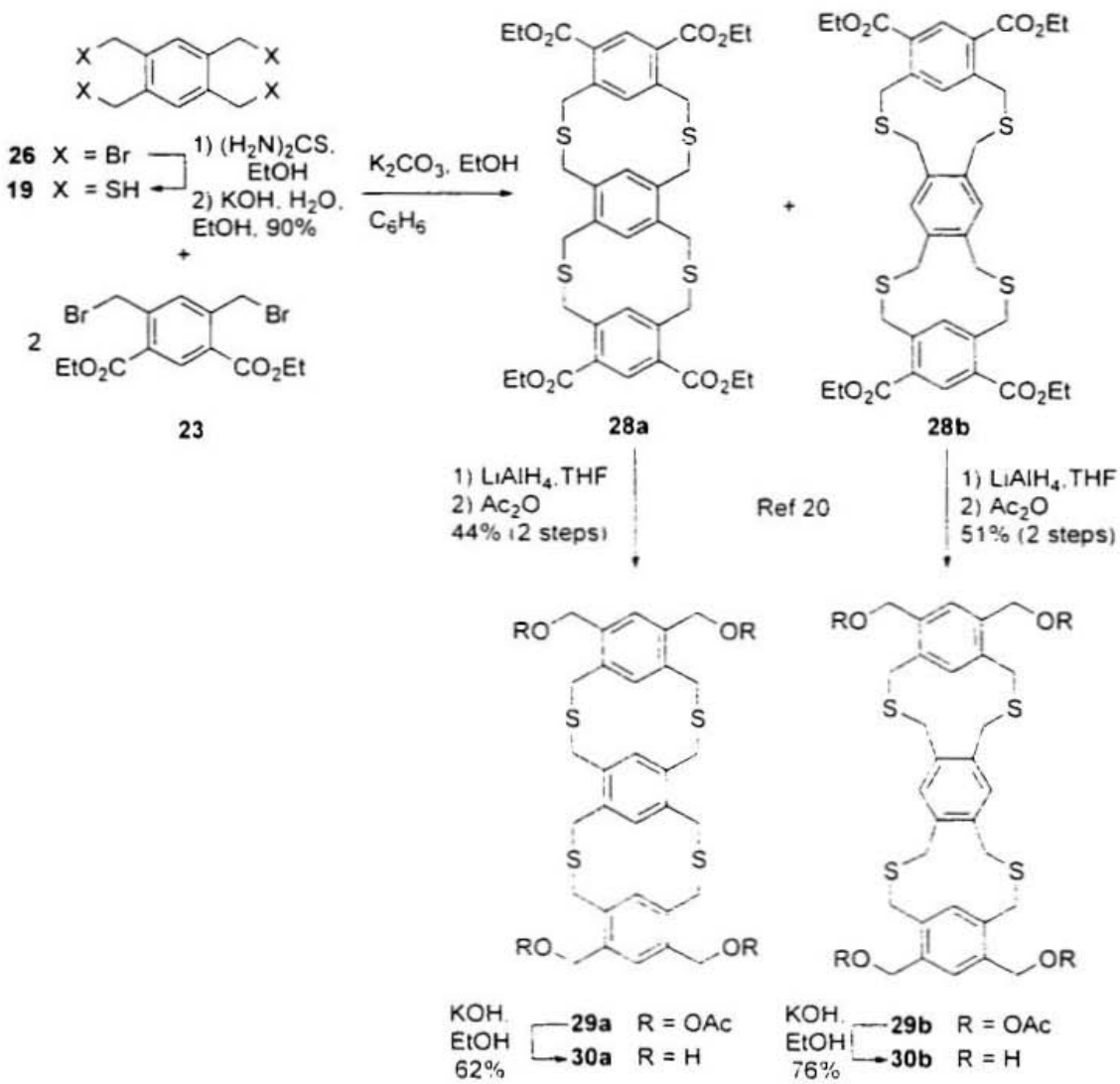

Scheme 4.06: Synthesis of tetrathiabenzeno[3]phanes **28**

Tetrabromodurene **26** was converted into tetrathiol **19** by converting it into tetrakis(isothiouronium) salt, followed by hydrolysis to give **19** (90%). Coupling of this tetrathiol with **23** under high dilution conditions in the presence of a base yielded a mixture of both possible isomers, **28a** and **28b**, which could be separated using column

chromatography to give 13% of the desired cyclophane **28a** and 19% of the unwanted orthometacyclophane **28b**. (Differentiation between the isomers could be made based on ^{1}H NMR data.[20]) This outcome is similar to that described by Vögtle *et al.* (**28a** : **28b** = 18% : 27%).[20] The same group described the conversion of tetraesters **28a** and **28b** to tetraacetates **29a** and **29b** and tetraalcohols **30a** and **30b**. However, other functional group interconversions (PBr_3 or $SOBr_2$) were reported to be unsuccessful, due to acid sensitivity of cyclophanes **28** - **30**. This suggested that the required functional group interconversions on the ester functionalities would be better left until a later stage in the synthesis and ring contraction of cyclophane **28a** should be performed first. For future synthetic applications, this might obviate the need to separate **28a** and **28b**, since ring contraction of dithia[3.3]orthometacyclophanes (**28b**) should lead to mainly other (decomposition) products.[20]

4.2.2 Attempted ring contraction of tetrathiabenzeno<3>phane 28a

4.2.2.1 General

Several known routes are available for the ring contraction of dithia[3.3]metacyclophanes to give [2.2]metacyclophanes.[31,32] A route that is used often is the "pyrolysis route," in which the sulfur atoms in the bridges are first oxidized to sulfones. SO_2 is then extruded with concomitant ring contraction using flash vacuum pyrolysis techniques.[32] This methodology has some major drawbacks when applied to our system. The oxidation step

should produce intermediates that contain one or more sulfoxide or sulfone functionalities before forming tetrakis(sulfone) **31**. As sulfoxides and sulfones are usually not very soluble, the reaction might not proceed to completion due to precipitation of some of the reaction intermediates. The second (pyrolytic) step often suffers from low yields, especially when two or three bridges are contracted. In case of **31**, four sulfone groups are to be extruded. The last drawback is the anticipated low volatility of **31**, which might make flash vacuum pyrolysis an inappropriate technique for synthesis of appreciable amounts of **32**.

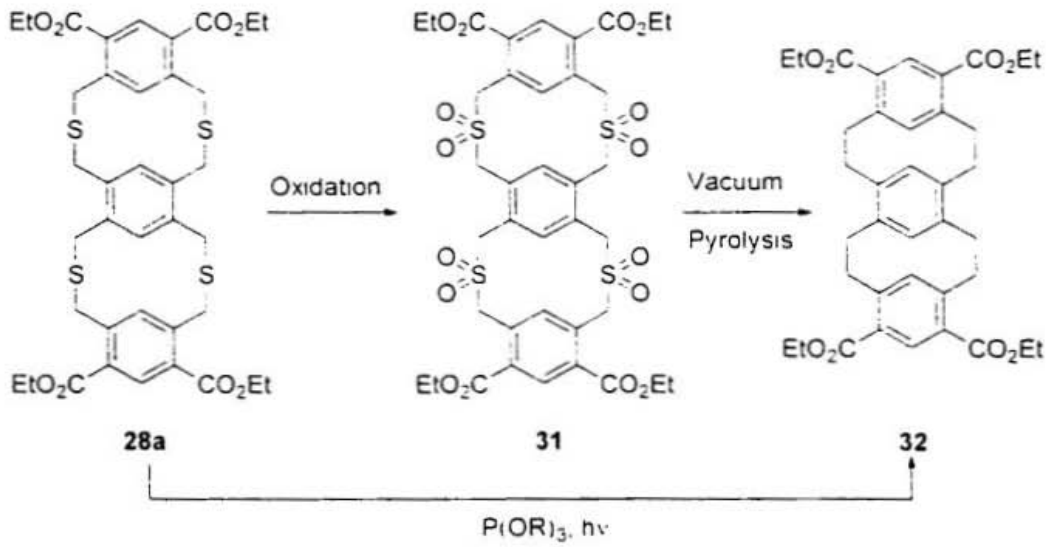

Scheme 4.07: The proposed routes to form **32** from **28a**.

The conversion of tetrathiabenzeno<3>phane **28a** to benzeno<3>phane **32** could also be achieved using the photolysis of sulfide linkages to give C-C bonds.[33-37] In this procedure

triethylphosphite acts as a thiophilic reagent (formation of $(EtO_3)P{=}S$) as well as the solvent.

Other routes that can be followed is to ring contract the dithiacyclophane **28a** using a Stevens[31,38] or Wittig[31,39,40] rearrangement. Both routes lead to the same product, but are complementary in mechanism. For the Stevens rearrangement, the sulfur atoms in the bridges are methylated, after which a base (e.g. KO-*t*-Bu) can induce the rearrangement to yield **33**. When a thiacyclophane is treated directly with a strong base (e.g. BuLi), Wittig rearrangement can occur. The rearranged product is then methylated to give the same product as the Stevens rearrangement (**33**). Both approaches are expected to yield a mixture of isomeric thioethers (**33**), which can be carried through without separation. Reductive cleavage of the thioether groups of such mixtures with Raney nickel has proved to be effective in related systems[41] and should not reduce the ester functionalities that are present in **33** and **32**.[42]

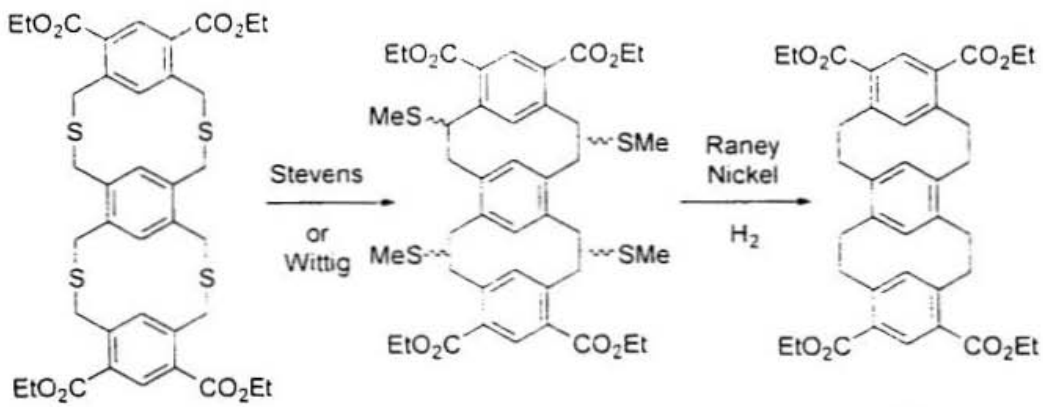

Scheme 4.08: Proposed conversion of **28a** to **32** using Stevens or Wittig rearrangements.

The problem with the Wittig rearrangement of **28a** could be the choice of a suitable base. Alkyllithium species, which are normally used, are not appropriate, since the starting material has four ester functional groups that are susceptible to reaction with strong nucleophiles such as alkyllithium reagents. Less nucleophilic bases like LDA or LHMDS might be required. Another potential problem in this approach might be intramolecular reaction of the intermediate thiolate ions with proximate ester groups (Scheme 4.09: **34** -> **35**). Deprotonation of a thioether bridge in **28a** is expected to occur preferentially at the benzylic position *ortho* to an ester group, which leads to the precursor for this intramolecular cyclization. Obviously this side reaction could also occur in an intermolecular manner, which would lead to oligomerization.

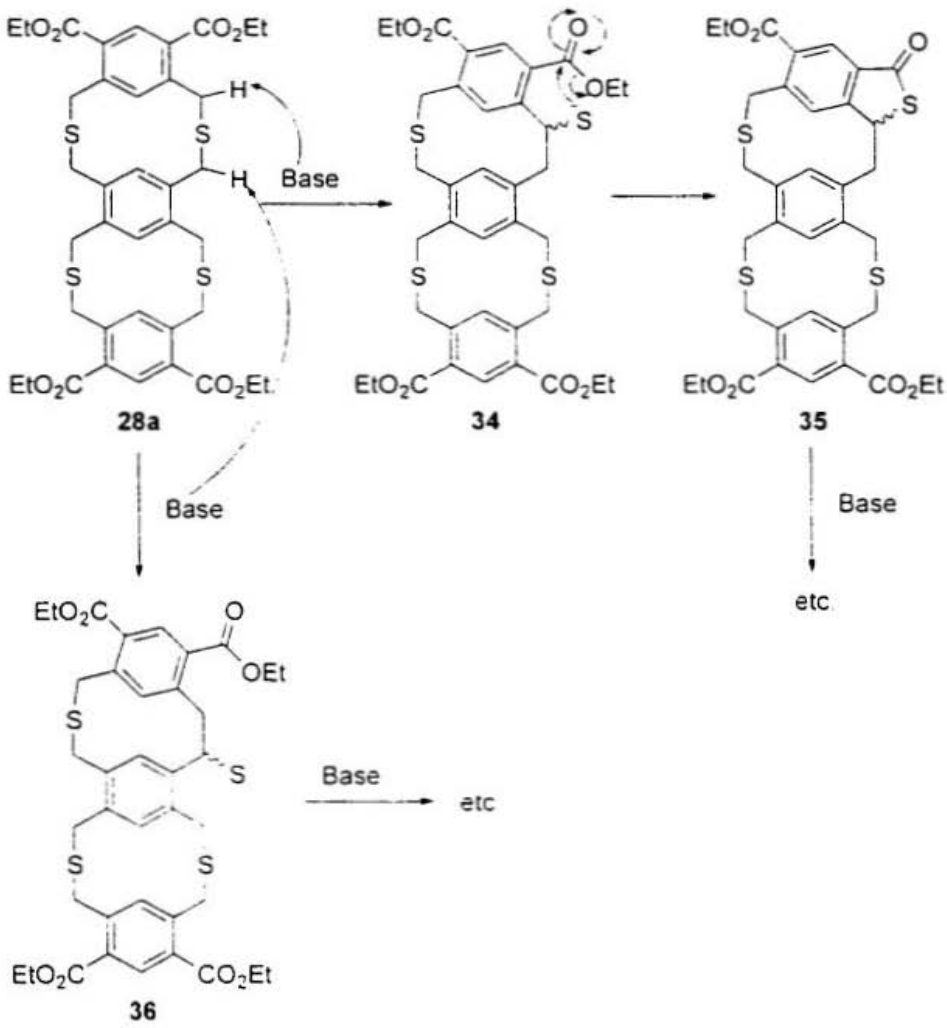

Scheme 4.09: Possible side reactions in the Wittig rearrangement of **28a**.

Raney nickel desulfurization of the reaction products should yield **32**. In **28a**, however, four reductions are taking place as opposed to only one or two, which will probably be reflected in the yield. If one of the rearrangements did not go to completion (i.e., one or more of the bridges in the cyclophane system still contains the original thioether), this thioether will be cleaved the Raney nickel reduction, yielding methylbenzene moieties.

A further complication arises when **32** is actually formed. Layered cyclophanes, such as **32**, have been described to exist in (at least) two distinct conformations, namely the "up,up" and the "up,down" conformers (Scheme 4.10).[24] Formation of this mixture will complicate separation and characterization of **32**. However, in the anticipated synthesis both conformers should, ultimately, lead to the formation of a single compound **37**.

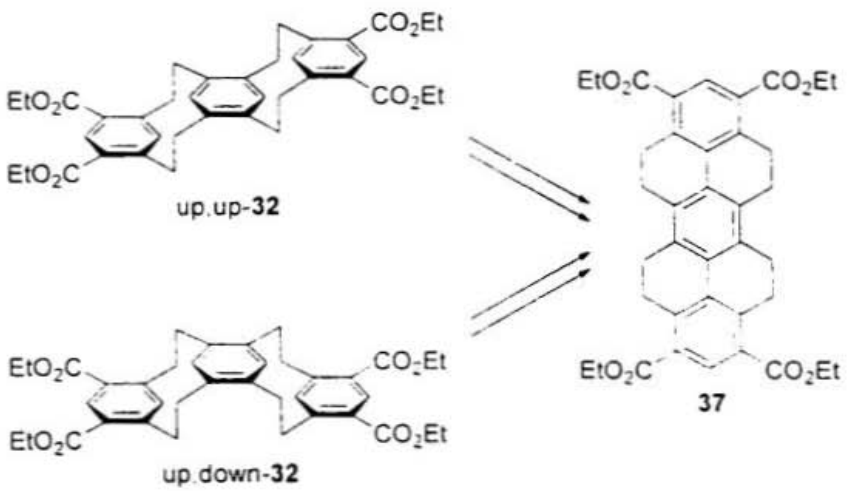

Scheme 4.10: Structures of "up-up"-**32**, "up-down"-**32** and compound **37**

Based on the preceding discussion, it was expected that the projected ring contraction would not be accomplished easily. Most projected complications seem to arise from solubility problems, so one alternative to the Stevens and Wittig methodology described above was also considered as an option. In 1975 Boekelheide described the benzyne-Stevens rearrangement as a useful alternative for the ring-contraction of dithia[3.3]cyclophanes.[43,44] This reaction was performed on several known

[3.3]cyclophane systems and it was concluded that this methodology was superior in the case of cyclophanes containing *ortho*- and *para*-substituted rings. For metacyclophanes, this methodology gave slightly lower yields than the traditional conditions for the Stevens rearrangement (29% with benzyne-Stevens vs. 33% using Stevens rearrangement and 33% using Wittig rearrangement for formation of pyrene from 2,11-dithia[3.3]metacyclophane **38**).[51]

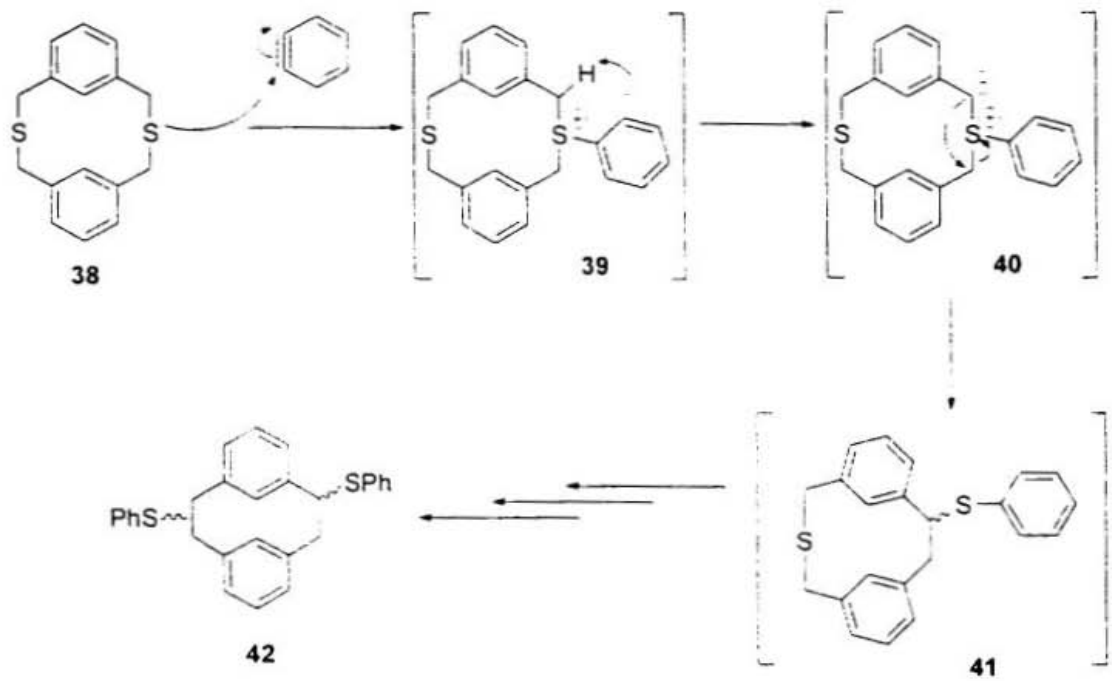

Scheme 4.11: Benzyne-Stevens rearrangement of **38**.

No mechanistic study has been reported to date for the benzyne-Stevens rearrangement. A likely mechanism would be a similar order of events as for the regular Stevens rearrangement[45] and a schematic representation is given in Scheme 4.11 for the 2,11-

dithia[3.3]metacyclophane system **38**. A key feature of the benzyne-Stevens rearrangement is, that for each individual bridge contraction from a neutral starting material, neutral products are formed, even though the reaction might proceed *via* a series of zwitterionic species (i.e. **39** or **40**). In this manner, the formation of multiply charged reaction intermediates and/or products is avoided. Therefore the anticipated solubility problems for the Stevens and Wittig rearrangements probably do not apply to this procedure. After the bridges in a dithiacyclophane have undergone ring contractions, the thiophenyl substituents can also be desulfurized using Raney nickel to give the desired cyclophane products.

4.2.2.2 Results and discussion

Irradiation of a well-stirred saturated solution of cyclophane **28a** in trimethylphosphite did not lead to formation of **32**. Instead, starting material was consumed to give a complex mixture of compounds, from which no single product was isolated. When cyclophane **28a** was subjected to methylation using Borch reagent in dichloromethane or chloroform at room temperature or reflux, a yellow or sometimes black oil would form. After treatment of this oil with base to initiate the Stevens rearrangement, it could be seen from the ^{1}H NMR spectrum that a complex mixture of products was produced as expected. No conclusions regarding nature of the mixture could be drawn from the spectroscopic data. Unfortunately, attempted reduction of the mixture with Raney nickel did not yield even trace amounts of **32**, but rather another complex mixture of products.

from which no single compound could be isolated. The problematic step in this reaction sequence is presumably the methylation. The low solubility of the di- and trimethylated intermediates in this reaction might cause them to precipitate from solution and not react further to give the desired tetramethylated intermediates.

Wittig rearrangement of cyclophane **28a** was attempted by treatment with LDA in THF, followed by treatment with iodomethane. This gave (by ^{1}H NMR) a complex mixture of products comparable to that formed in the Stevens rearrangement. Again attempted desulfurization with Raney Nickel did not lead to the formation of any of the desired products.

After the disappointing results that were obtained using the photolytic extrusion of sulfur from the bridges and the Stevens and Wittig rearrangements, attention was focused on the benzyne-Stevens rearrangement. When cyclophane **28a** was subjected to the conditions for the benzyne-Stevens rearrangement as described by Boekelheide using 5 equivalents of benzyne (from anthranilic acid and excess isoamylnitrite), a mixture of compounds was formed. Desulfurization of this mixture again led to the formation of a complex mixture of compounds. In this case, column chromatographic separation of this mixture led to the isolation of a single compound. However, its ^{1}H NMR spectrum did not correspond to either conformer of structure **32**. In the mass spectrum, this new compound **43** showed a peak at m/z 704. From the results from ^{1}H NMR, ^{13}C NMR and the mass spectroscopic data, structure **43** was proposed (Figure 4.05). This structure was later

confirmed by X-ray crystallography, although the quality of the data set was low.[46] When 5 – 15 equivalents of benzyne were used, the yield of **43** was 15-18%.

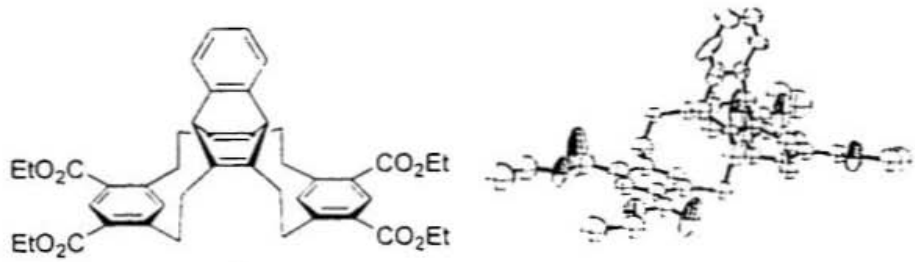

43

Figure 4.05: Structure of compound **43**

Structure **43** seems to be the result of a Diels-Alder reaction between the central aromatic ring in the desired product up,down-**32** (or precursor thereof) and benzyne (Scheme 4.12). In going from **28a** to **32**, the strain in the system (specifically in the central aromatic ring) increases with each consecutive ring contraction. At a certain stage during the ring contractions the energy loss due to loss of aromaticity that occurs during the Diels-Alder reaction, will be offset by the energy that is gained upon relief of the strain that occurs in the Diels-Alder reaction. [4+2] Cycloaddition reactions of benzyne with aromatic rings has been described quite extensively[47-52] and an example of an intramolecular benzyne cycloaddition in the [3.3]paracyclophane system has been reported.[53] Apparent Diels-Alder reaction of some [5]metacyclophanes with other dienophiles has also been reported.[54] The proposed Diels-Alder reaction to form **43**, can only occur if the reacting cyclophane adopts the "up,down" conformation. In this

conformation the central aromatic ring is expected to possess a boat-like geometry[24] and the Diels-Alder reaction can occur at the internal carbon atoms of this cyclophane.

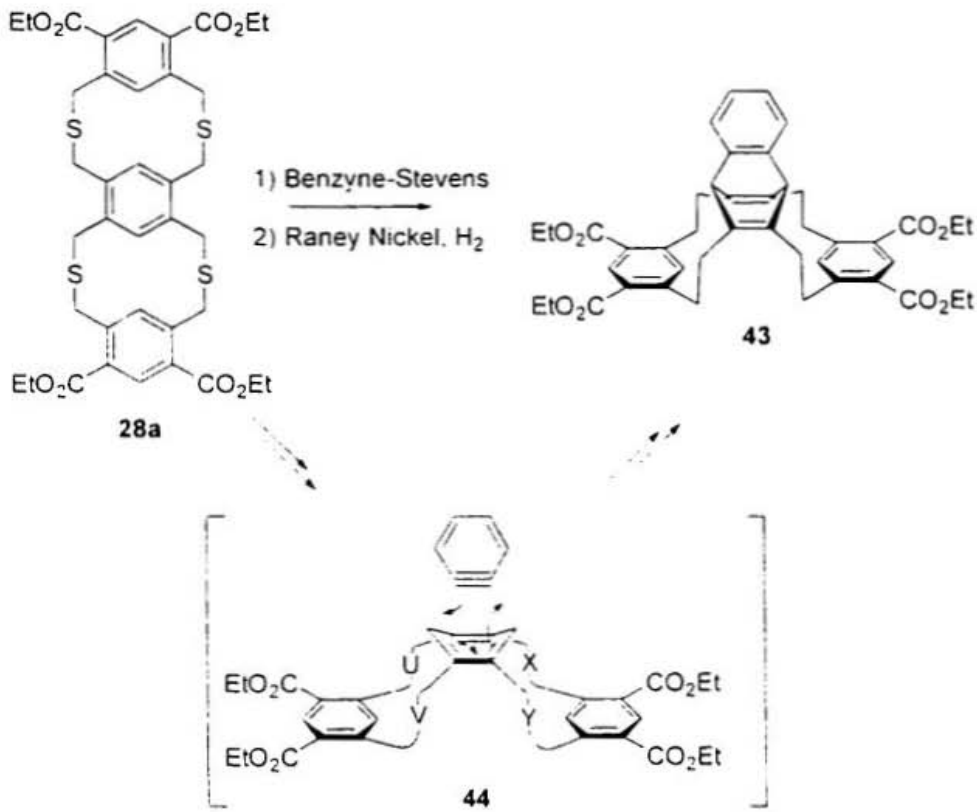

Scheme 4.12: Formation of compound **43** from **28a**.

4.3 Conclusions and future work

In this Chapter a novel approach to the synthesis of a "Vögtle belt" has been proposed. Unfortunately, the inability to cause **28a** to undergo the desired ring contraction has so far greatly limited the application of this approach to the synthesis of advanced

intermediates. A novel structure **43** was found to be the only isolable product from benzyne-Stevens rearrangement of **28a** after desulfurization of the reaction mixture. The approach has not led to the synthesis of an aromatic belt so far, so the viability if the VID approach for the synthesis of Vögtle belts has not been determined.

In order to attempt further application of this approach to the synthesis of a fully aromatic belt, compounds of the general structure **15** (Scheme 4.03) are required. As the approach described in this Chapter has failed, an alternative approach would be to form a fourfold bromomethylated cyclophane **46** from cyclophane **45** *via* free radical bromination with NBS (Scheme 4.13). This type of selective bromination of [2.2]metacyclophanes has been described in the literature.[55] However, synthesis of cyclophane **45** might suffer from the same complications that have been described in this Chapter. Its synthesis might have to be performed in a more classical (and low-yielding) stepwise approach,[24] but as stated earlier multigram quantities are required for serious attempts to the synthesis of aromatic belts. Future work in this area should therefore be directed toward the development of better methodology to synthesize [2.2]metacyclophanes. All of the currently used methodology was discovered in the 60's and 70's and it is not easily applied to the multi-gram scale synthesis of cyclophanes such as **32** and **46**. The use of more modern reactions for the synthesis of [2.2]metacyclophanes might therefore be a fruitful area of future research.

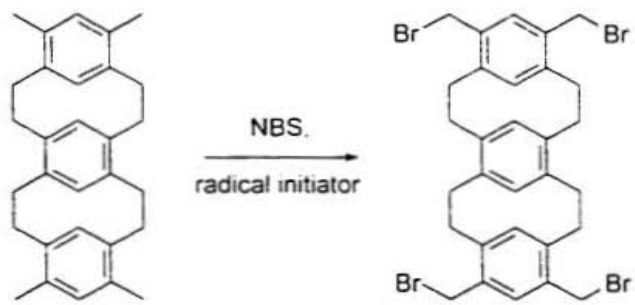

45 **46**

Scheme 4.13: Proposed synthesis of cyclophane **46**

4.4 Experimental

General. All chemicals were reagent grade and were used as received. Chromatographic separations were performed on Merck silica gel 60 (particle size 40-63 μm, 230-400 mesh). Melting points were determined on a Fisher-Johns apparatus and are uncorrected. Elemental analyses were performed at the MicroAnalytical Service Laboratory, Department of Chemistry, University of Alberta. Mass spectroscopic (MS) data were obtained on a V. G. Micromass 7070HS instrument. ^{1}H NMR (300 MHz) and ^{13}C NMR (75.47 MHz) were obtained on a General Electric GE 300-NB spectrometer: ^{1}H shifts are relative to internal tetramethylsilane; ^{13}C shifts are relative to the solvent resonance ($CDCl_3$: δ = 77.0). All experiments with moisture- or air-sensitive compounds were performed in anhydrous solvents under nitrogen unless otherwise stated. Solvents were dried and distilled according to standard procedures.

1,3-Bis(bromomethyl)-4,6-dimethylbenzene (20d). *meta*-Xylene **20a** (12.21 mL, 0.100 mol), paraformaldehyde (6.15 g, 0.200 mol), glacial acetic acid (50 mL) and concentrated hydrogen bromide in acetic acid (30%, 40 mL) were stirred at approximately 85 °C for 8 h. The reaction mixture was cooled and poured into water (150 mL). The resulting yellow precipitate was collected by suction filtration and crystallized from heptane to give **20d** (16.4 g, 56.2 mmol, 56%) as colorless needles: mp 104-106 °C; ^{1}H NMR ($CDCl_3$) δ 7.27 (s, 1H), 7.03 (s, 1H), 4.49 (s, 4H), 2.38 (s, 6H); ^{13}C NMR ($CDCl_3$) δ 138.3, 134.0, 133.6, 131.7, 32.0, 18.7; EI-MS *m* / *z* (%): 290 (8, M^+ $^{79}Br^{81}Br$), 211 (100), 132 (80), 115 (15), 91 (17); Anal. Calc. For $C_{10}H_{12}Br_2$: C 41.13, H 4.14; found C 41.03, H 3.91.

1,3-Bis(acetoxymethyl)-4,6-dimethylbenzene (20e). To a solution of dibromide **20d** (5.00 g, 17.1 mmol) in acetonitrile (150 mL) was added sodium acetate (11.65 g, 85.6 mmol), and the mixture was stirred at reflux temperature for 24 h. The mixture was concentrated *in vacuo*, and ethyl acetate and water were added until all material dissolved. The aqueous layer was extracted with ethyl acetate (2 x 100 mL). The combined organic layers were washed with water (100 mL), saturated $NaHCO_3$ solution (100 mL), water (100 mL) and saturated aqueous NaCl solution (100 mL), dried ($MgSO_4$) and concentrated under reduced pressure to yield **20e** (4.24 g, 17.0 mmol, 99%) as a light yellow oil that was used without further purification: ^{1}H NMR ($CDCl_3$) δ 7.28 (s, 1H), 7.05 (s, 1H), 5.09 (s, 4H), 2.32 (s, 6H), 2.09 (s, 6H); ^{13}C NMR ($CDCl_3$) δ 171.0, 137.6, 132.7, 131.6, 130.9, 64.5, 21.1, 18.6; EI-MS *m* / *z* (%): M^+ not observed, 190 (33), 130 (48), 119 (24), 115 (16), 91 (28), 43 (100).

4,6-Dimethylisophthalic acid (21). To a solution of potassium hydroxide (85% purity, 4.33 g, 65.6 mmol) in water (200 mL) was added diacetate **20e** (4.10 g, 16.4 mmol). The flask was equipped with a reflux condenser and the mixture was stirred vigorously for 6 h at reflux temperature. The heat source was removed, the mixture was stirred for 10 min and potassium permanganate (6.86 g, 43.1 mmol) was slowly added (fast addition led to a strong exotherm!). The mixture was stirred at room temperature for 18 h and filtered using suction filtration to produce a clear colorless filtrate that was acidified to pH ~1 with concentrated hydrochloric acid. The precipitate was collected by suction filtration and recrystallized from ethanol to yield **21** (2.56 g, 13.1 mmol, 80%) as a colorless solid: mp 295 - 297 °C (lit.[56] > 320 °C); ^{1}H NMR (DMSO-d_6) δ 8.39 (s, 1H), 7.25 (s, 1H), 2.56 (s, 6H); ^{13}C NMR (DMSO-d_6) δ 167.9, 143.4, 135.1, 133.0, 127.7, 21.3; EI-MS *m z* (%): 194 (94, M^+), 176 (100), 148 (27), 103 (12), 91 (13).

Diethyl 4,6-dimethylisophthalate (22). Thionyl chloride (40.0 mL, 462 mmol) was added dropwise to diacid **15** (17.04 g, 87.8 mmol) in a 100 mL 3-necked round-bottomed flask equipped with condenser and calcium chloride drying tube. Three drops of *N,N*-dimethylformamide were added, and the mixture was stirred at reflux temperature for 4 h. Excess thionyl chloride was removed using distillation and absolute ethanol (25 mL, 426 mmol) was added carefully while the mixture was cooled in an ice-water bath. After the addition was complete, the mixture was stirred at reflux temperature for 20 min, cooled to room temperature and concentrated under reduced pressure to give a yellow-brown solid that was crystallized from methanol to yield **22** (16.7 g, 66.7 mmol, 76%) as colorless

needles: mp 59.5 – 61 °C (lit.[20] 60 - 61°C); ^{1}H NMR ($CDCl_3$) δ 8.49 (s, 1H), 7.13 (s, 1H), 4.37 (q, 4H, J = 7.3 Hz), 2.61 (s, 6H), 1.41 (t, 6H, J = 7.3 Hz); ^{13}C NMR ($CDCl_3$) δ 166.8, 144.0, 135.2, 133.1, 127.3, 60.8, 21.6, 14.3; EI-MS (70 eV) m/z (%): 250 (35, M^+), 221 (14), 205 (100), 193 (17), 177 (42).

Diethyl 4,6-bis(bromomethyl)isophtalate (23). To a solution of diester **22** (3.50 g, 14.0 mmol) and NBS (3.50 g, 19.7 mmol) in dichloromethane (50 mL) was added a spatula tip benzoyl peroxide. The mixture was stirred at reflux temperature for 3 h while it was irradiated with a 100 W halogen lamp. Another portion of NBS (2.28 g, 12.8 mmol) was added followed by a spatula tip of benzoyl peroxide, and the mixture was stirred with irradiation at reflux temperature for 2.5 h and then cooled to room temperature. The reaction mixture was washed with water (200 mL), saturated aqueous sodium carbonate solution (2 x 100 mL), water (100 mL) and saturated aqueous sodium chloride solution (100 mL), dried ($MgSO_4$) and concentrated *in vacuo* to give an orange solid that was crystallized from cyclohexane to yield **23** (2.29 g, 7.88 mmol, 40%) as colorless crystals: mp 78-80 °C (lit.[20] 78-81°C); IR (Nujol, cm^{-1}): 1719 (s), 1366 (m), 1296 (s), 1236 (m), 1137 (w), 1101 (m), 1044 (w); ^{1}H NMR ($CDCl_3$) δ 8.52 (s, 1H), 7.55 (s, 1H), 4.92 (s, 4H), 4.43 (q, 4H, J = 7.2 Hz), 1.43 (t, 6H, J = 7.2 Hz); ^{13}C NMR ($CDCl_3$) δ 165.6, 143.3, 135.0, 134.5, 129.6, 62.0, 30.2, 14.4; EI-MS m/z (%): 408 (12, M^+ $^{79}Br^{81}Br$), 363 (27), 299 (100), 192 (45), 148 (36) 134 (18), 102 (28), 91 (36).

Tetramethyl 1,2,4,5-benzenetetracarboxylate (25). To a well-stirred suspension of pyromellitic anhydride **24** (20.06 g, 91.97 mmol) in methanol (700 mL) in a 1000 mL 3-necked round-bottomed flask equipped with a reflux condenser with $CaCl_2$ drying tube was carefully added H_2SO_4 (concentrated, 20 mL) and the reaction mixture was stirred at reflux temperature for 18 h. The reaction mixture was cooled in an ice bath. Suction filtration and washing with small amounts of cold methanol yielded **25** (24.52 g, 79.03 mmol, 86%) as colorless crystals; mp: 138 – 139 °C; IR (Nujol, cm^{-1}): 1732 (s), 1303 (s), 1103 (s), 953 (m), 918 (m), 796 (m), 742 (m); ^1H NMR ($CDCl_3$) δ 8.09 (s, 2H), 3.96 (s, 12H); ^{13}C NMR ($CDCl_3$) δ 166.3, 134.1, 129.5, 53.0; EI-MS (70 eV) *m z* (%) 310 (3, M^+), 279 (100).

1,2,4,5-Tetrakis(bromomethyl)benzene (26). To a well-stirred slurry of $LiAlH_4$ (3.94 g, 104 mmol) in dry THF (200 mL), was added dropwise a solution of **25** (7.04 g, 22.7 mmol) in dry THF (150 mL). The reaction mixture was stirred at reflux temperature for 5.5 h and cooled in an ice-bath. Carefully, EtOAc (100 mL) was added and the mixture was concentrated under reduced pressure to give a gray solid. To the solid was added dropwise 48% aqueous HBr (200 mL) (caution: vigorous exotherm), followed by concentrated H_2SO_4 (100 mL; caution: exotherm). The reaction mixture was stirred at reflux temperature for 1.5 h, cooled in an ice bath, poured into ice water (500 mL) and extracted with CH_2Cl_2 (3 x 100 mL). The combined organic extracts were washed with water (2 x 100 mL), saturated aqueous $NaHCO_3$ solution (2 x 150 mL), water (150 mL) and saturated aqueous NaCl solution (100 mL). After drying ($MgSO_4$) the organic layers

were concentrated *in vacuo* and the residue was crystallized from toluene to yield **26** (6.74 g, 15.0 mmol, 66%) as slightly brown crystals that were pure enough for further synthetic purposes: mp 150 – 151.5 °C; ^{1}H NMR ($CDCl_3$) δ 7.38 (s, 2H), 4.61 (s, 8H); ^{13}C NMR ($CDCl_3$) δ 137.6, 133.6, 28.7; EI-MS (70 eV) *m/z* (%) 450 (3, M^+ ($^{79}Br)_2(^{81}Br)_2$), 369 (100), 290 (24), 209 (47).

1,2,4,5-Tetrakis(thiomethyl)benzene (19). Thiourea (6.24 g, 82.0 mmol) was added to a well-stirred suspension of tetrabromide **26** (9.00 g, 20.0 mmol) in absolute ethanol (250 mL) in a 500 mL round bottom flask. The mixture was stirred at reflux temperature for 6 h and concentrated under reduced pressure. To the residue was added a solution of potassium hydroxide (85 % purity, 13.21 g, 200.1 mmol) in degassed water (150 mL), and the mixture was heated at reflux temperature under an atmosphere of nitrogen for 16 h. After cooling to room temperature, the mixture was acidified using 9 M aqueous sulfuric acid and extracted with dichloromethane (3 x 75 mL). The organic layers were combined and washed with water (100 mL) and saturated aqueous sodium chloride solution (100 mL), dried ($MgSO_4$) and concentrated under reduced pressure to yield **19** (4.73 g, 18.0 mmol, 90%) as a yellow-brown solid that was used without purification in the next step.

5,7,23,25-Tetrakis(ethoxycarbonyl)-2,11,20,29-tetrathia[3.3](1,3)(1,3)[3.3](4,6)(1,3)-benzeno<3>phane (28a) and 5,7,23,25-Tetrakis(ethoxycarbonyl)-2,11,20,29-tetrathia[3.3](1,3)(1,2)[3.3](4,5)(1,3)benzeno<3>phane (28b). Tetrathiol **19** (0.90 g, 3.4 mmol) and dibromide **13** (2.80 g, 6.86 mmol) were washed into a 3000 mL 3-necked round bottom flask using 2000 mL 1:1 degassed absolute ethanol and degassed benzene. The solution was stirred vigorously using a mechanical stirrer and potassium carbonate (1.90 g, 13.7 mmol) was added. The mixture was stirred for 2.5 d and concentrated *in vacuo* onto silica gel (3.1 g). Column chromatography of the residue (SiO_2; 2.5 % EtOAc $CHCl_3$) first yielded **28b** (0.61 g, 0.81 mmol, 19%, colorless solid) followed by **28a** (0.34 g, 0.45 mmol, 13%, colorless solid).

28a: mp: 215 - 217.5 °C (lit.[20] 209-211 °C); IR (Nujol, cm^{-1}) 1723 (s), 1709 (s), 1244 (s); ^1H NMR ($CDCl_3$) δ 7.79 (s, 2H), 6.96 (s, 2H), 6.57 (s, 2H), 4.29 (q, 8H, J = 7.6 Hz), 4.05 (br s, 8H), 3.85 (br s, 8H), 1.36 (t, 12H, J = 7.4 Hz); ^{13}C NMR ($CDCl_3$) δ 166.6, 142.3, 135.7, 135.5, 133.3, 133.2, 128.1, 61.2, 37.5, 36.1, 14.2; EI-MS m/z (%): M^+ not observed, 730 (1), 713 (4), 505 (22), 473 (28), 191 (100).

28b mp: 248 - 251 °C (dec.) (lit.[20] 250-252 °C); IR (Nujol, cm^{-1}) 1707 (s), 1287 (m); ^1H NMR ($CDCl_3$) δ 8.53 (s, 2H), 8.07 (s, 2H), 6.40 (s, 2H), 4.42 (q, 8H, J = 7.0 Hz), 4.10 (br s, 8H), 3.34 (s, 8H), 1.43 (t, 12H, J = 7.0 Hz); ^{13}C NMR ($CDCl_3$) δ 165.7, 142.5, 136.6, 135.3, 134.6, 130.3, 127.9, 61.4, 33.4, 28.8, 14.3; EI-MS m/z (%): M^+ not observed, 713 (3), 704 (1), 506 (3), 473 (100).

Attempted ring contraction of 28a: photolytic method. Cyclophane **28a** (0.35 g, 0.46 mmol) was dissolved as well as possible in freshly distilled trimethylphosphite (15 mL) and filtered to remove undissolved material. The solution was placed in a quartz tube in a photolysis apparatus (Rayonet Photochemical Reactor) and was stirred while being irradiated (254 nm, 112 W) for 22 h. The mixture was concentrated *in vacuo* and subjected to column chromatography. A small amount of starting material was recovered (< 0.02 g) together with several fractions of unidentified materials.

Attempted ring contraction of 28a: Wittig rearrangement. Cyclophane **28a** (0.50 g, 0.66 mol) was dissolved in dry tetrahydrofuran (50 mL) under an atmosphere of nitrogen and cooled in an ice water bath. A solution of LDA (1.5 M in cyclohexane, 2.2 mL, 3.3 mmol) was added over 10 minutes, the reaction mixture was allowed to warm up to room temperature and stirred for 2 h. A drop of water was added, followed directly by iodomethane (0.25 mL, 4.0 mmol) and the reaction mixture was concentrated *in vacuo*. Dichloromethane (50 mL) was added and the mixture was washed with water (25 mL) and saturated sodium chloride solution (25 mL), dried ($MgSO_4$) and concentrated under reduced pressure to give a yellow-brown oil. Absolute ethanol (25 mL) was added and the mixture was heated to reflux temperature. Freshly prepared Raney Nickel (3 spatula tips) was added and the mixture was stirred at reflux temperature for 20 min. Two more portions of Raney Nickel (3 spatula tips each) were added and after each addition the mixture was stirred at reflux temperature for 20 min. The mixture was cooled to room temperature and the solid was removed using suction filtration and washed with ethyl

acetate (2 x 5 mL). The filtrate was concentrated under reduced pressure and the residue was subjected to column chromatography to yield several fractions of unidentified composition.

Attempted ring contraction of 28a: Stevens rearrangement. To a solution of cyclophane **28a** (0.50 g, 0.66 mmol) in dichloromethane (50 mL) was added Borch reagent (1.08 g, 6.7 mmol) and the reaction mixture was stirred for 14 h under an atmosphere of nitrogen. The mixture was concentrated *in vacuo* and ethyl acetate (10 mL) and methanol (2 mL) were added and again the mixture was concentrated *in vacuo*. To the residue was added dry tetrahydrofuran (50 mL), followed by potassium *tert*-butoxide (0.38 g, 3.4 mmol) and the mixture was stirred at room temperature for 16 h under an atmosphere of nitrogen. Saturated aqueous ammonium chloride solution (1 mL) was added and the mixture was concentrated under reduced pressure. Saturated aqueous ammonium chloride solution (25 mL) and dichloromethane (50 mL) were added and the aqueous layer was extracted with dichloromethane (50 mL). The organic layers were combined and washed with water (50 mL) and saturated aqueous sodium chloride solution (50 mL). After drying ($MgSO_4$) and concentration under reduced pressure the residue was passed through a plug of silica using dichloromethane and the eluent was concentrated under reduced pressure. To the residue was added absolute ethanol (25 mL), and the mixture was heated to reflux temperature. Raney nickel (3 spatula tips) was added and after each addition the reaction mixture was stirred at reflux temperature for 20 min. The reaction mixture was cooled to room temperature and the solid was removed

using suction filtration and washed using ethyl acetate. The mother liquor was concentrated under reduced pressure to yield an inseparable mixture of unidentified compounds. (No indication was found for formation of the desired product **32**.) Several variations to this procedure were attempted, varying solvent (dichloromethane or chloroform for the first step, ethanol or ethyl acetate for the desulfurization), temperature (room temperature to reflux), amount of reagent used (10 or 20 equivalents Borch reagent, 5, 7 or 10 equivalents potassium *tert*-butoxide, 3, 7 or 10 additions of Raney Nickel) and reaction times (1-24 hours). Results were comparable for each variation and no indication of formation of **32** was observed.

Attempted ring contraction of 28a: benzyne-Stevens rearrangement. A solution of anthranilic acid (0.30 g, 2.2 mmol) in 1,2-dichloroethane (50 mL) was added dropwise over 1 h to a refluxing solution of cyclophane **28a** (0.33 g, 0.44 mmol) and isoamylnitrite (1.1 mL, 7.9 mmol) in 1,2-dichloroethane (35 mL). The reaction mixture was stirred at reflux temperature for an additional 30 min, concentrated under reduced pressure, filtered over a plug of silica using 5% ethyl acetate chloroform and concentrated again under reduced pressure. The residue was dissolved in a refluxing mixture of ethanol (70 mL) and ethyl acetate (10 mL) and Raney Nickel (2 spatula tips) was added and the mixture was heated at reflux temperature for 5 min. The mixture was cooled to room temperature, filtered using suction filtration (the residue was washed with ethyl acetate) and the residue was concentrated under reduced pressure. Hexanes was added to the residue and a colorless precipitate formed that was isolated using suction filtration and dried to yield **43**

(~ 0.05 g, 0.071 mmol, ~15 %): mp > 280 °C; IR (Nujol, cm^{-1}) 1712 (s), 1558 (w), 1290 (s), 1232 (m), 1169 (m), 1137 (s); ^1H NMR ($CDCl_3$) δ 8.60 (s, 2H), 7.20 (s, 2H), 6.70 (AA'BB' system, 4H), 4.45 (q, 8H, J = 6.5 Hz), 4.07 (m, 4H), 2.88 (s, 2H), 2.74 (m, 8H), 1.94 (m, 4H), 1.46 (t, 12H, J = 6.8 Hz); ^{13}C NMR ($CDCl_3$) δ 166.9, 148.2, 146.5, 145.6, 136.0, 134.1, 126.1, 122.7, 120.9, 63.0, 61.1, 35.5, 33.8, 14.3; EI-MS m/z (%): 704 (26, $(M+2)^+$), 657 (15), 453 (17), 407 (16), 279 (100); HRMS Calc'd for $(C_{44}H_4O_8)^+$: 703.3268, found: 703.3271.

4.5 References

(1) The name Vögtle belt has been proposed by us for a (so far hypothetical) fully aromatic belt like **4**. For a more detailed discussion refer to Section 4.1 and references therein.

(2) Bodwell, G. J.; Miller, D. O.; Vermeij, R. J. *Org. Lett.* **2001**, *3*, 2093-2096.

(3) Vögtle, F. *Top. Curr. Chem.* **1983**, *115*, 1-40.

(4) Schröder, A.; Mekelburger, H.-B.; Vögtle, F. *Top. Curr. Chem.* **1994**, *172*, 179-201.

(5) Kohnke, F. H.; Slawin, A. M. Z.; Stoddart, J. F.; Williams, D. J. *Angew. Chem., Int. Ed. Engl.* **1987**, *26*, 892-894.

(6) Ashton, P. R.; Isaacs, N. S.; Kohnke, F. H.; Slawin, A. M. Z.; Spencer, C. M.; Stoddart, J. F.; Williams, D. J. *Angew. Chem., Int. Ed. Engl.* **1988**, *27*, 966-969.

(7) Kohnke, F. H.; Mathias, J. P.; Stoddart, J. F. *Top. Curr. Chem.* **1993**, *165*, 1-69.

(8) Kang, H. C.; Hanson, A. W.; Eaton, B.; Boekelheide, V. *J. Am. Chem. Soc.* **1985**, *107*, 1979-1985.

(9) Godt, A.; Enkelmann, V.; Schlüter, A.-D. *Angew. Chem., Int. Ed. Engl.* **1989**, *28*, 1680-1682.

(10) Cory, R. M.; McPhail, C. L.; Dikmans, A. J.; Vittal, J. J. *Tetrahedron Lett.* **1996**, *37*, 1983-1986.

(11) Cory, R. M.; McPhail, C. L. *Tetrahedron Lett.* **1996**, *37*, 1987-1990.

(12) Kammermeier, S.; Jones, P. G.; Herges, R. *Angew. Chem., Int. Ed. Engl.* **1996**, *35*, 2669-2671.

(13) Kammermeier, S.; Jones, P. G.; Herges, R. *Angew. Chem., Int. Ed. Engl.* **1996**, *36*, 2200-2202.

(14) Kawase, T.; Darabi, H. R.; Oda, M. *Angew. Chem., Int. Ed. Engl.* **1996**, *35*, 2664-2666.

(15) Müller, P.; Usón, I.; Henseler, D.; Schlüter, A.-D.; Sheldrick, G. M. *Helv. Chim. Acta* **2001**, *84*, 778-785.

(16) Vögtle, F.; Schröder, A.; Karbach, D. *Angew. Chem., Int. Ed. Engl.* **1991**, *30*, 575-577.

(17) Josten, W.; Neumann, S.; Vögtle, F.; Hägele, K.; Przybylski, M.; Beer, F.; Müllen, K. *Chem. Ber.* **1994**, *127*, 2089-2096.

(18) Josten, W.; Karbach, D.; Nieger, M.; Vögtle, F.; Hägele, K.; Svoboda, M.; Przybylski, M. *Chem. Ber.* **1994**, *127*, 767-777.

(19) Breidenbach, S.; Ohren, S.; Herbst-Irmer, R.; Kotila, S.; Nieger, M.; Vögtle, F. *Liebigs Ann.* **1996**, 2115-2121.

(20) Schröder, A.; Karbach, D.; Güther, R.; Vögtle, F. *Chem. Ber.* **1992**, *125*, 1881-1887.

(21) Reiss, J. A. In *Cyclophanes, Vol. II*; Keehn, P. M., Rosenfeld, S., eds.; Academic Press: New York, 1983; pp 443-484.

(22) Umemoto, T.; Kawashima, T.; Sakata, Y.; Misumi, S. *Tetrahedron Lett.* **1975**, 1005-1006.

(23) Umemoto, T.; Kawashima, T.; Sakata, K.; Misumi, S. *Tetrahedron Lett.* **1975**, 463-466.

(24) Misumi, S. Multilayered Cyclophanes; In *Cyclophanes, Vol II*; Keehn, P. M., Rosenfeld, S., eds.; Academic Press: New York, 1983; pp 573-628.

(25) For a more detailed discussion on the use of angular brackets <> in cyclophane nomenclature see Section 1.3.1 and references therein.

(26) Van der Made, A. W.; Van der Made, R. H. *J. Org. Chem.* **1993**, *58*, 1262-1263.

(27) Hurley, P. B.Sc. Hounours Dissertation, Memorial University of Newfoundland, **2000**.

(28) Ried, W.; Bodem, H. *Chem. Ber.* **1956**, *89*, 2328-2331.

(29) Fischer, L. F.; Speier, A. *Ber. Dtsch. Chem. Ges.* **1895**, *28*, 3252-3258.

(30) Bodwell, G. J. Ph.D. Dissertation, Technischen Universität Braunschweig, **1989**.

(31) Mitchell, R. H. *Heterocycles* **1978**, *11*, 563-586.

(32) Vögtle, F.; Schunder, L. *Chem. Ber.* **1969**, *102*, 2677-2683.

(33) Boekelheide, V.; Reingold, I. D.; Tuttle, M. *J. Chem. Soc., Chem. Commun.* **1973**, 406-407.

(34) Bruhin, J.; Jenny, W. *Tetrahedron Lett.* **1973**, 1215-1218.

(35) Umemoto, T.; Otsubo, T.; Misumi, S. *Tetrahedron Lett.* **1974**, 1573-1576.

(36) Fukazawa, Y.; Aoyagi, M.; Ito, S. *Tetrahedron Lett.* **1978**, 1067-1070.

(37) Corey, E. J.; Block, E. *J. Org. Chem.* **1969**, *34*, 1233-1240.

(38) Mitchell, R. H.; Boekelheide, V. *J. Am. Chem. Soc.* **1974**, *96*, 1547-1557.

(39) Mitchell, R. H.; Otsubo, T.; Boekelheide, V. *Tetrahedron Lett.* **1975**, 219-222.

(40) Boekelheide, V.; Tsai, C.-H. *Tetrahedron* **1976**, *32*, 423-425.

(41) Welch, S. C.; Gruber, J. M. *J. Org. Chem.* **1982**, *47*, 385-389.

(42) Dauben, W. G.; Kessel, C. R.; Takemura, K. H. *J. Am. Chem. Soc.* **1980**, *102*, 6893-6894.

(43) Otsubo, T.; Boekelheide, V. *Tetrahedron Lett.* **1975**, *45*, 3881-3884.

(44) Otsubo, T.; Boekelheide, V. *J. Org. Chem.* **1977**, *42*, 1085-1087.

(45) Baldwin, J. E.; Erickson, W. F.; Hackler, R. E.; Scott, R. M. *J. Chem. Soc., Chem. Commun.* **1970**, 576-578.

(46) The quality of the structural data is not optimal since an incomplete dataset was collected due to time constraints. Inclusion of solvent molecules and the presence of 2 conformers of **43** caused complications in the calculation of the structure as well.

(47) Friedman, L. *J. Am. Chem. Soc.* **1967**, *89*, 3071-3073.

(48) Stiles, M.; Burckhardt, H.; Freund, G. *J. Org. Chem.* **1967**, *32*, 3718-3719.

(49) Friedman, L.; Lindlow, F. *J. Am. Chem. Soc.* **1968**, *90*, 2329-2333.

(50) Brewer, J. P. N.; Heaney, H. *Tetrahedron Lett.* **1965**, 4709-4712.

(51) Brewer, J. P. N.; Eckhard, I. F.; Heaney, H.; Marples, B. A. *J. Chem. Soc. C* **1968**, 664-676.

(52) Pittman Jr., C. U.; Saebo, S.; Xu, H. *J. Org. Chem.* **2000**, *65*, 6620-6626.

(53) Longone, D. T.; Gladysz, J. A. *Tetrahedron Lett.* **1976**, 4559-4562.

(54) Bickelhaupt, F.; Dewolf, W. H. *J. Phys. Org. Chem.* **1998**, *11*, 362-376.

(55) Umemoto, T.; Otsubo, T.; Sakata, Y.; Misumi, S. *Tetrahedron Lett.* **1973**, 593-596.

(56) Schnapauff, E. *Ber. Dtsch. Chem. Ges.* **1886**, *19*, 2508-2511.

Chapter 5

Synthesis of

[2]Paracyclo[2](2,7)pyrenophane

and

[2]Metacyclo[2](2,7)pyrenophane

5.1 Introduction

After the failed attempt to synthesize a fully aromatic belt **1** (Chapter 4) and the failed model study of a (2.7)pyrenophane **2** with two *para*-phenylene rings in the tether (Chapter 3) it was decided to focus attention to the synthesis of a simpler model compound, **3**. This (2.7)pyrenophane contains one *para*-phenylene ring in the tether, which is connected to the pyrene unit *via* dimethylene bridges. Part of the tether consists of a *para*-phenylene ring and **3** is a model compound for **4**, which maps onto the surface of aromatic belt **1** (n = 0).

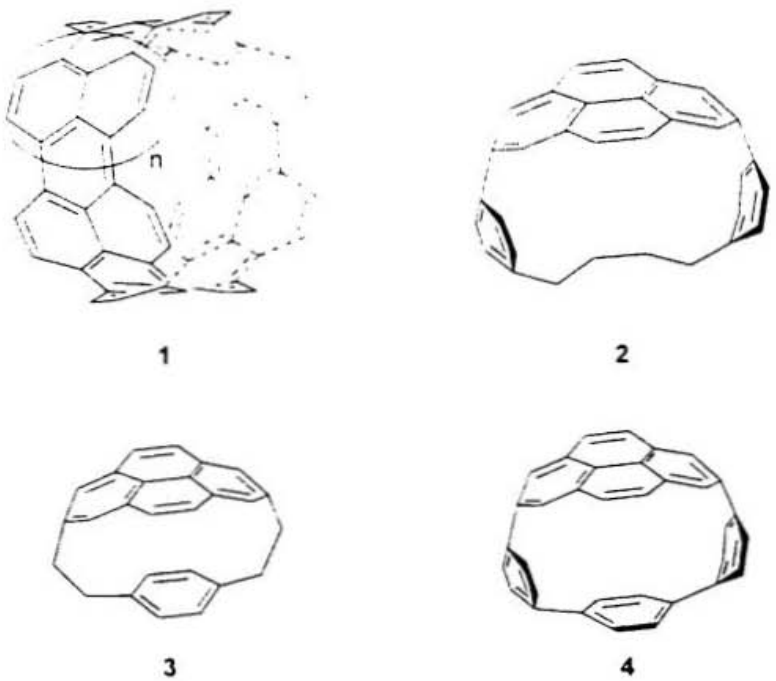

Figure 5.01: Synthetic targets **1** - **4**.

AM1 level calculations show a bend angle (θ_{calcd}) of the pyrene unit in **3** of 100.4°.[1] This suggests that (2.7)pyrenophane **3** should synthetically be accessible using the valence isomerization-dehydrogenation (VID) protocol.[2-4] Using the same calculations for a constitutional isomer of **3**, with a *meta*-phenylene unit in the tether (Figure 5.02: compound **5**) the bend angle was calculated to be 106.6°. As this is still a smaller angle than for some of the most strained (2.7)pyrenophanes that have been synthesized by our group,[1,3,4] cyclophane **5** was also identified as a synthetic target. Due to the *meta* positioning of the tethers in **5** this compound does not map onto the surface of fullerenes or aromatic belts. Nonetheless it was considered an interesting target in the context of our ongoing research in the areas of novel cyclophanes and nonplanar aromatic compounds. The *ortho*-phenylene isomer **6** has a θ_{calcd} of 130.4°, which is well beyond the estimated cut-off value (115° - 120°) for the VID approach, so its synthesis was not considered worth pursuing.

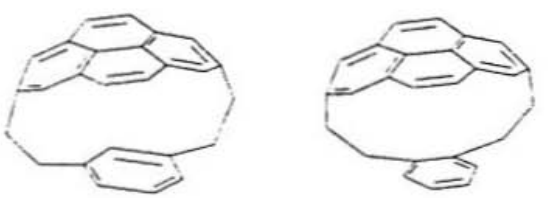

5 **6**

Figure 5.02: Structure of pyrenophanes **5** and **6**.

Cyclophanes containing a *para*-phenylene, *meta*-phenylene or pyrene unit that is bridged with two tethers of equal length with another aromatic unit have been described quite

extensively in the literature. Figure 5.03 contains some examples of cyclophanes with dimethylene tethers.[5]

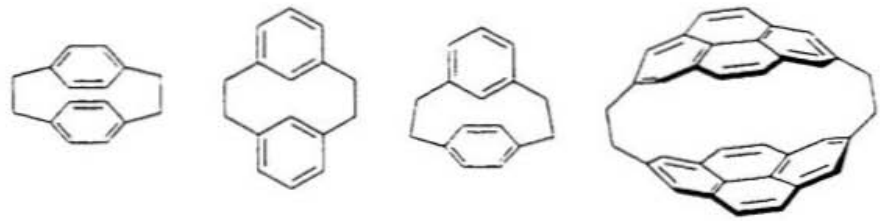

7 **8** **9** **10**

Figure 5.03: Some cyclophanes containing 2 aromatic units.

The [2.2]cyclophanes that have been described in the literature most extensively are probably [2.2]paracyclophane **7**,[7-8] [2.2]metacyclophane **8**[9,10] and [2.2]metaparacyclophane **9**.[11] [2.2](2,7)Pyrenophane **10**[12-14] is also a relevant example when cyclophanes **3** and **5** are considered. To our knowledge, no examples of mixed cyclophanes with two dimethylene tethers bridging a (2,7)pyrene unit with another aromatic unit have been described. Pyrenophanes **3** and **5** would then constitute the first examples of this class of compounds.

The syntheses of cyclophanes **7** – **10** involve formation of the dimethylene bridges in the last (or a very late) step either *via* [6+6] dimerization of *para*-xylylene (for **7** only)[15], Wurtz coupling (for **7** and **8**)[16-19] or SO_2 extrusion from a dithia[3.3]cyclophane.[12-14,20,21] None of these cyclophanes has been synthesized by forming one of the aromatic units in

the last step, which is the approach our group has applied to the synthesis of several pyrenophanes by forming the pyrene unit in these systems *via* the VID sequence.[3,4]

5.1.1 Retrosynthetic analysis

Since the retrosynthetic analyses of [2]paracyclo[2](2,7)pyrenophane **3** and [2]metacyclo[2](2,7)pyrenophane **5** differ only in the substitution pattern of one of the starting materials, these analyses are presented together (Scheme 5.01).

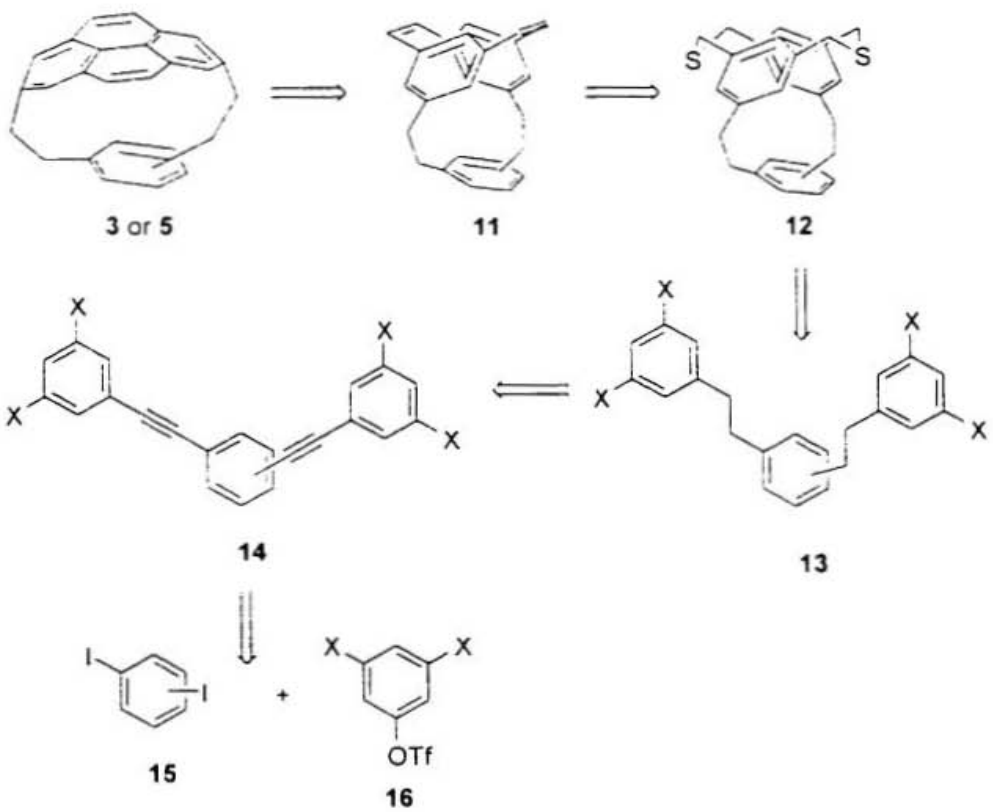

Scheme 5.01: Retrosynthetic analysis of pyrenophanes **3** and **5**.

Using the VID protocol that has proven successful for many (2.7)pyrenophanes, compounds **3** and **5** could retrosynthetically be derived from cyclophanedienes **11**.[3,4] Cyclophane dienes then lead back to *syn*-dithiacyclophanes **12** *via* ring contraction methods.[22] *syn*-Dithiacyclophanes like **12** have previously been synthesized successfully using our Na_2S/Al_2O_3 reagent,[23] thus leading back to a tetrafunctionalized precursor **13**. In this compound, the dimethylene tethers that ultimately become the bridges in the target compound are already present, making this approach a conceptually novel one. The dimethylene tethers in **13** could be derived from alkyne units, i.e., **14**. An advantage of this retrosynthetic step is that unsymmetrically substituted alkynes like **14** are readily synthesized using Sonogashira chemistry,[24-27] thus leading back to compounds **15** and **16**.

5.2 Results and discussion

For the synthesis of [2]paracyclo[2](2.7)pyrenophane **3**, two complementary routes starting from 1,4-diiodobenzene **17** and triflate **21**[28] were initially investigated. One of these routes was ultimately applied to the successful synthesis of **5**. Therefore the synthesis of **3** will be discussed first, followed by the synthesis of **5**.

5.2.1 Synthesis of [2]paracyclo[2](2,7)pyrenophane 3

Sonogashira coupling of 1,4-diiodobenzene **17** with two equivalents of trimethylsilylacetylene **18** gave diyne **19** (95%), which was protodesilylated to yield 1,4-diethynylbenzene **20** (77%). Due to the volatility of **20**, it was purified using sublimation at atmospheric pressure. When performed carefully on a small scale, this sublimation was successful. However, in one case where purification was attempted with approximately 4 g of material, an explosive decomposition took place. Compound **20** was subjected to Sonogashira conditions using two equivalents of triflate **21**[28] to form tetraester **22** in 57% yield. The low solubility of diyne **22** complicated its purification. This might be the reason for the relatively low recovery of product in this step.

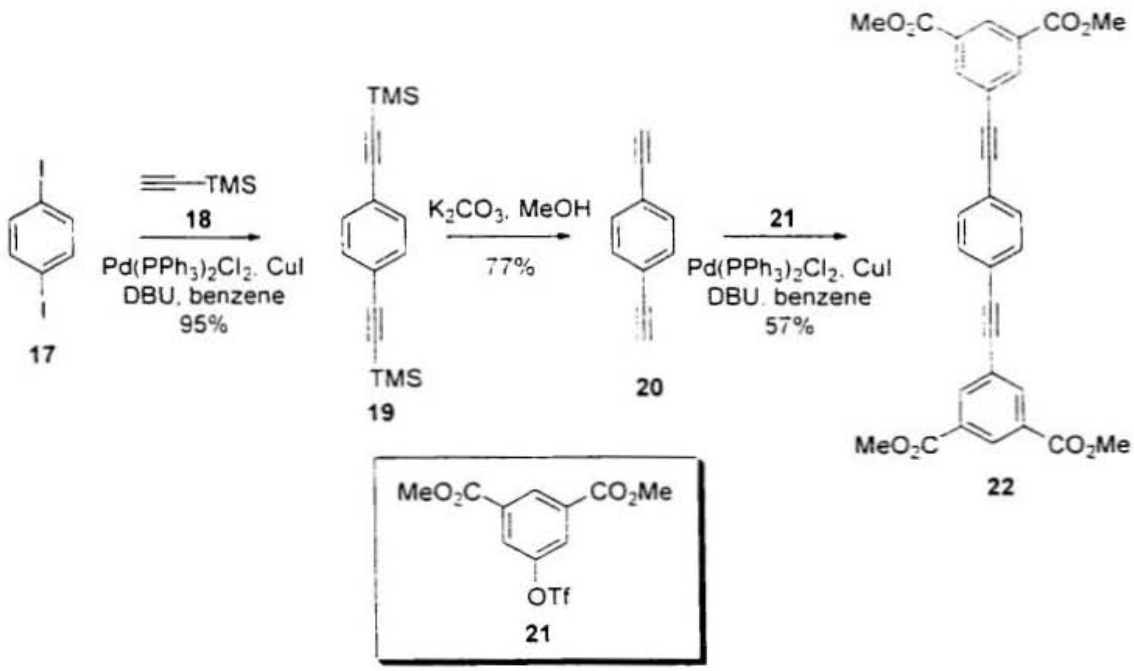

Scheme 5.02: Synthesis of **22** from 1,4-diiodobenzene **17**.

Due to the explosive character of 1,4-diethynylbenzene **20**, an alternative route to **22** was investigated in which the order of the Sonogashira couplings was reversed (Scheme 5.03). Starting from triflate **21**, Sonogashira coupling with trimethylsilylacetylene yielded compound **23** in 71% yield. Protodesilylation gave terminal alkyne **24** (91%), which was coupled with 1,4-diiodobenzene **17** under Sonogashira conditions to yield diyne **22** in 91% yield (based on 1,4-diiodobenzene). Again, the low solubility of **22** complicated purification of the material, but the crude mixture from this particular Sonogashira coupling was of higher purity than in the initial route, which made the second approach the preferred method to produce large quantities of **22**.

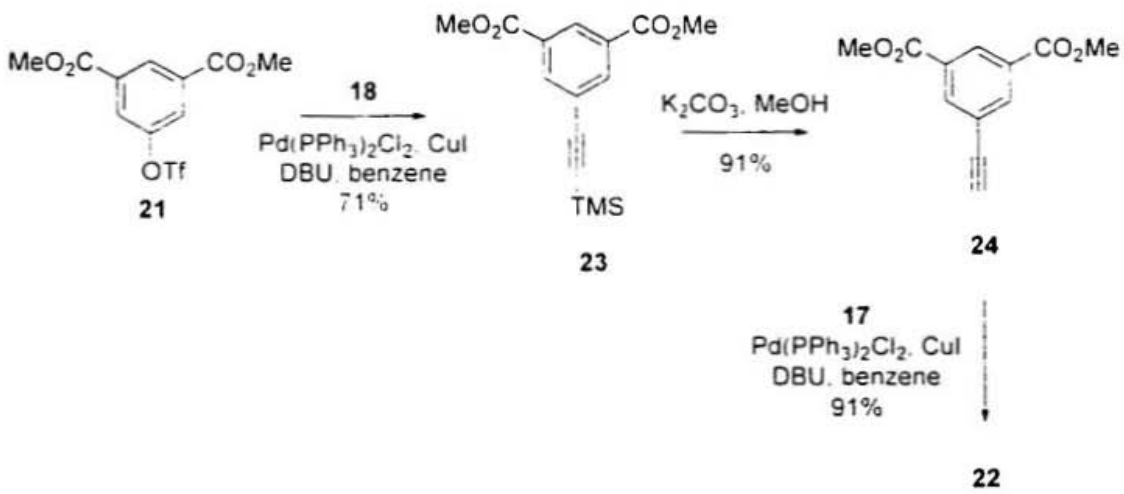

Scheme 5.03: Alternative synthesis of diyne **22**.

With a convenient synthesis of **22** in hand, attention was focused on the functional group interconversions of **22** that were necessary to form the appropriate dithiacyclophane (Scheme 5.04). Catalytic hydrogenation of the alkyne units in **22** gave tetraester **25**

(95%), which contained the dimethylene tethers that would ultimately become the bridges of pyrenophane **3**. The hydrogenation of **22** was somewhat problematic due to its low solubility. Small-scale hydrogenations could be performed using saturated (dilute) solutions of **22** in THF or benzene, but when larger amounts of **25** were required this method became impractical due to the large volumes of solvent required. For the catalytic hydrogenation of larger quantities of **22**, slow addition of a slurry of **22** in THF to a suspension of catalyst in THF under an atmosphere of hydrogen proved to be the most convenient method (both methods gave **25** in approximately 95% yield). Tetraester **25** was reacted with excess $LiAlH_4$ in THF followed by HBr/HOAc to provide tetrabromide **26** (85%). This method has previously been used by our group for the synthesis of similar tetrabromides.[3,28,29] When tetrabromide **26** was subjected to standard conditions (Na_2S, Al_2O_3) to form dithiacyclophane **27**,[23] less than a 3% yield of **27** was obtained in low purity (~25% of an unidentified impurity by ^1H NMR). However, when the reaction was performed at reflux temperature, dithiacyclophane **27** was formed in 28% yield. Changing the solvent mixture from CH_2Cl_2/EtOH to $CHCl_3$/EtOH in order to increase the reflux temperature did not increase the yield.

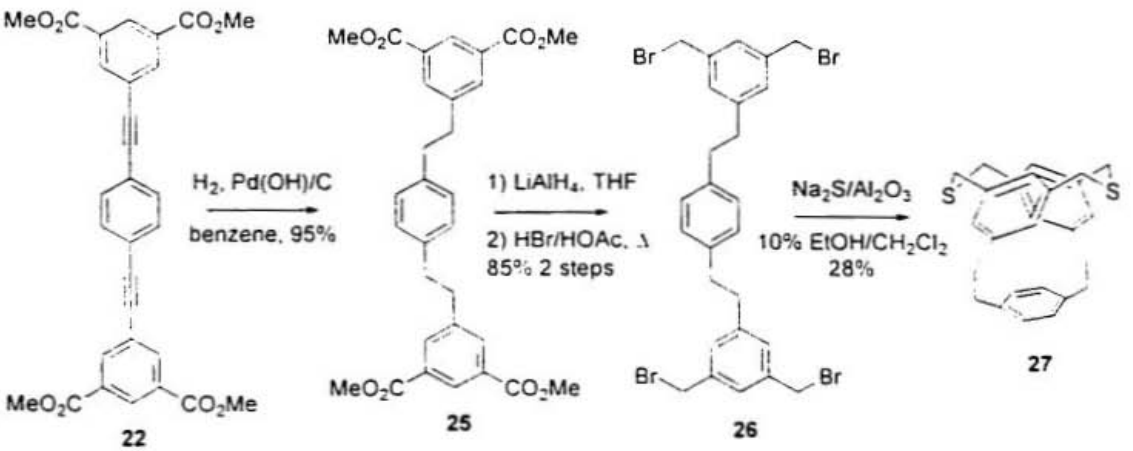

Scheme 5.04: Synthesis of dithiacyclophane **27**.

Bridge contraction of dithiacyclophane **27** was accomplished by methylation of the sulfur atoms in **27** using Borch reagent, followed by treatment of the resulting bis(methylsulfonium) salt with potassium *tert*-butoxide to induce Stevens rearrangement. This yielded **28** as a mixture of isomers (70% crude from **27**). Methylation of the sulfur atoms in **28** (Borch reagent) followed by Hofmann elimination gave a mixture (*ca.* 1 : 1 by ^{1}H NMR) of cyclophanediene **29** and the desired [2]paracyclo[2](2,7)pyrenophane **3**. The mixture could be converted cleanly to pyrenophane **3** by treatment of the mixture with DDQ in benzene to yield **3** in 14% overall yield from dithiacyclophane **27**. Crystals of **3** were obtained from heptane, and its molecular structure was determined using X-ray crystallography. This will be discussed together with its ^{1}H NMR spectrum in Section 5.2.3.

The spontaneous formation of **3** in the Hofmann elimination step was somewhat surprising, since the formation of pyrenophanes with comparable calculated bend angles (Section 1.4) usually requires treatment of the corresponding cyclophanediene with DDQ in hot benzene. The reactivity of **29** can be explained by the presence of the rigid *para*-phenylene unit in the tether, which forces open the *syn*-[2.2]metacyclophanediene unit relative to those present in the precursors to the [*n*](2,7)pyrenophanes. The resulting increase in the inter-ring angle, moves the internal C atoms closer to one another and presumably lowers the activation energy to the formation of a bond between them.

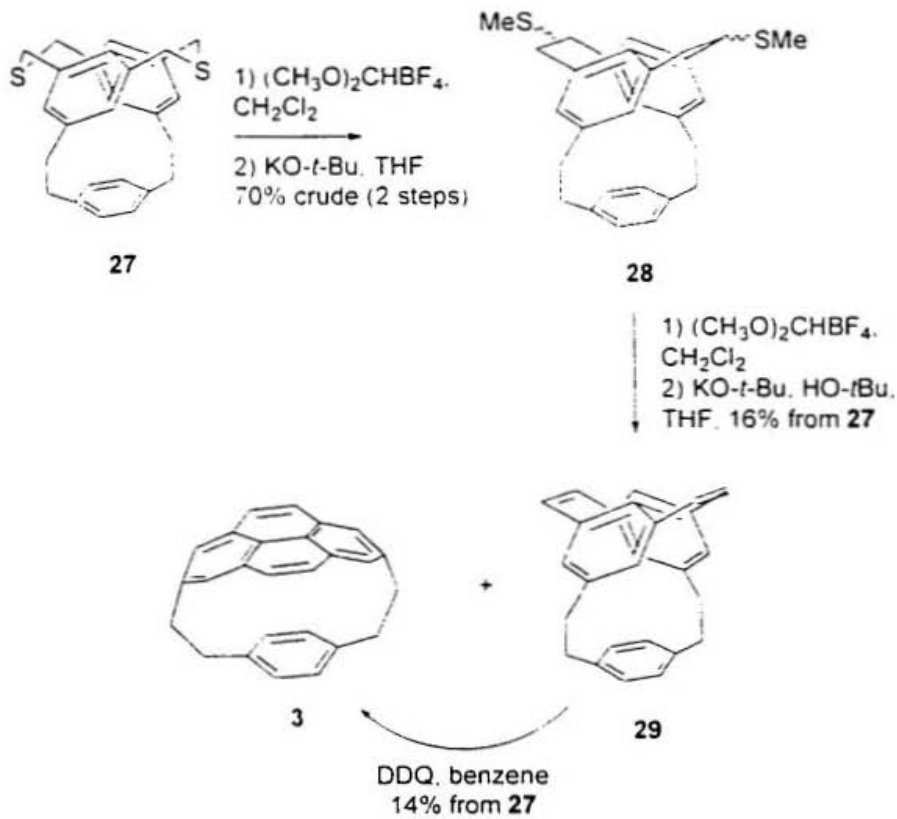

Scheme 5.05: Synthesis of [2]paracyclo[2](2,7)pyrenophane **3**.

The overall yield of the synthesis of **3** from triflate **21** is a disappointingly low 2% (longest linear sequence: 3% from **17**). The low yield of this synthesis can be traced back to two particular synthetic transformations: the cyclization to furnish dithiacyclophane **27** and the methylation-Hofmann elimination sequence to form the mixture of **29** and **3**. The cyclization step has been somewhat optimized, but needs closer examination. As many examples of dithiacyclophanes with different tether lengths are known to form with Na_2S/Al_2O_3 under standard conditions, it can be assumed that the presence of the *para*-phenylene unit in the tether somehow causes the low yield in this key step. Perhaps the rigidity of this unit prevents easy initial cyclization of tetrabromide **26** to form an intermediate like **30** (Scheme 5.06). Another effect could be that the second step in this transformation (ring closure of **30** to give **27**) has an unexpectedly high energy barrier due to the rigidity of the *para*-phenylene unit, which forces the two aromatic systems in **30** away from each other.

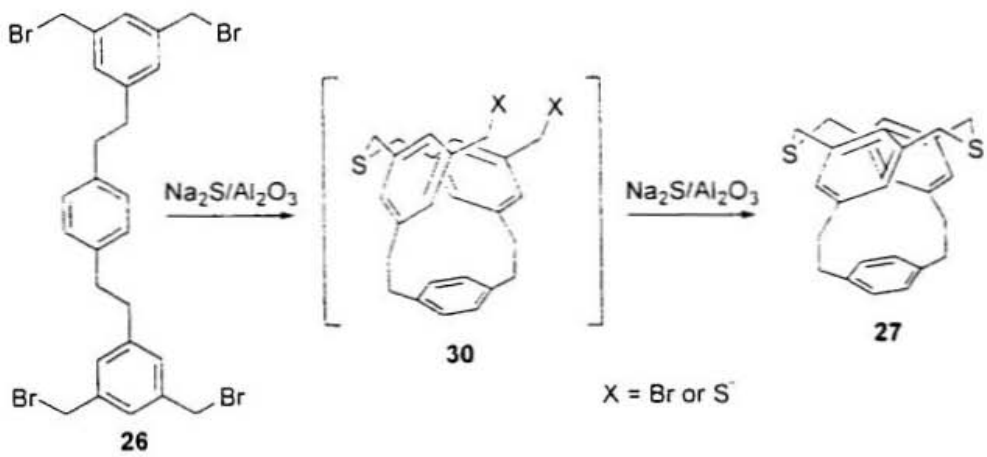

Scheme 5.06: Formation of dithiacyclophane **27** *via* intermediate **30**.

The second stumbling block in the synthesis was the methylation-Hofmann elimination sequence. This problem has also been observed in the synthesis of other (but not all) pyrenophanes that have been prepared in this group, and it is not clear what causes the yields in this transformation to be so erratic. Other groups[22,30,31] have observed that in similar eliminations, by-products are found that are derived from Stevens rearrangement of the methylated intermediates. In our case, this Stevens rearrangement of bis(methylsulfonium) salt **31** would form intermediate **33**, which could undergo Hofmann elimination to form **33** or a second Stevens rearrangement to form **34**. Compound **34** could also be formed by sequential Hofmann elimination and Stevens rearrangement of **30** *via* intermediate **32**. No particular effort was made in order to detect by-products **34** or **35**, as attention was focused on the isolation of the desired product only.

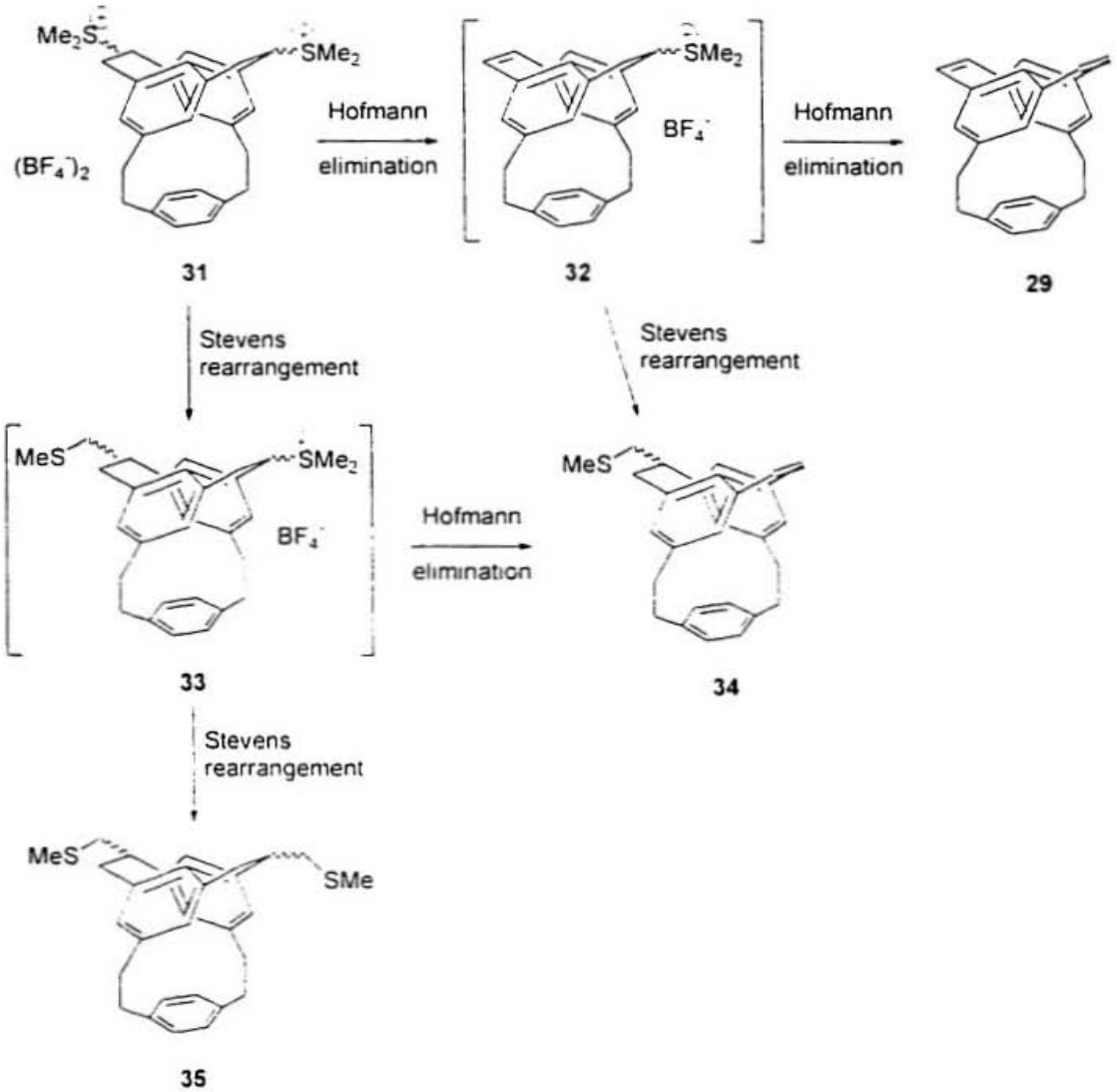

Scheme 5.07: Proposed side reactions in the Hofmann elimination of **31**.

Despite the low overall yield, it was highly gratifying to obtain the targeted pyrenophane **3**. A very important feature of the synthesis is the novel way in which the dimethylene bridges were installed. This clearly establishes the viability of the approach, which has great potential for the synthesis of related compounds.

5.2.2 Synthesis of [2]metacyclo[2](2,7)pyrenophane

The synthesis of **3** began with Sonogashira coupling of 1,3-diiodobenzene **36** with alkyne **24**, which proceeded in 76% yield to give diyne **37**. Fortunately, diyne **37** is more soluble than its constitutional isomer **22**, so it could easily be purified using column chromatography. Catalytic hydrogenation of the product proceeded smoothly to yield tetraester **38** in quantitative yield.

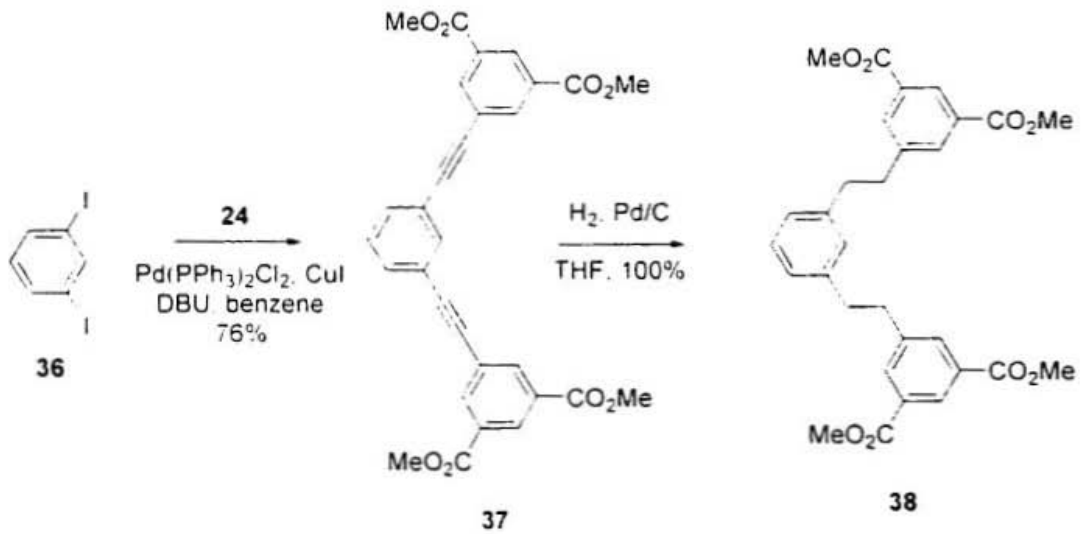

Scheme 5.08: Synthesis of tetraester **38**.

Reduction of **38** with excess $LiAlH_4$ in THF, followed by treatment of the reaction mixture with HBr/HOAc yielded tetrabromide **39** in 54% yield. When tetrabromide **39** was subjected to standard cyclization conditions using Na_2S/Al_2O_3,[23] dithiacyclophane **40** formed smoothly in 68%. This result is in line with the results that our group has

observed for cyclization of other tetrabromides and suggests that the geometric requirements of the *para*-phenylene unit in **26** are probably the cause for the low yield in the cyclization of **26** to give **27**.

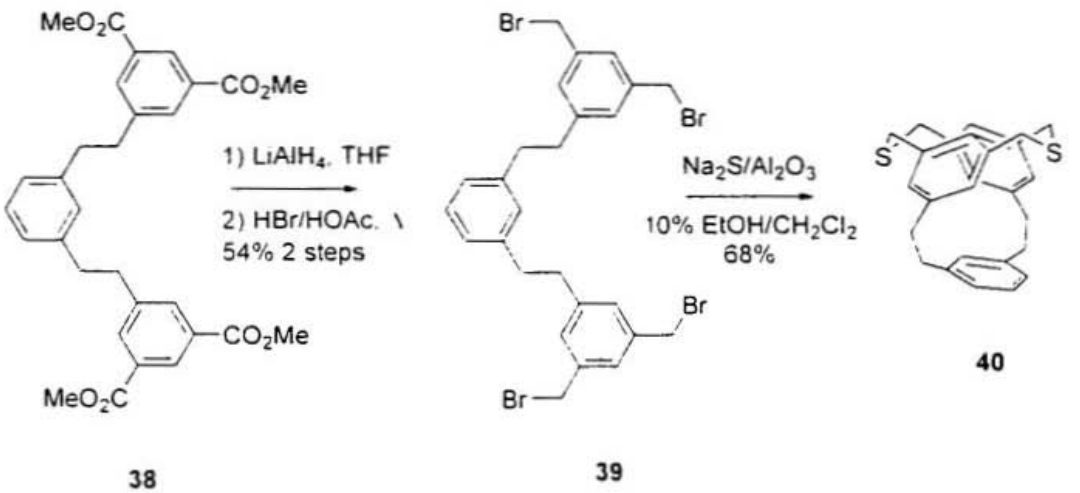

Scheme 5.09: Synthesis of dithiacyclophane **40**.

Methylation of the sulfur atoms in the bridges of dithiacyclophane **40** with Borch reagent followed by treatment of the resulting bis(methylsulfonium) salt with potassium *tert*-butoxide yielded **41** as a mixture of isomers in 88% crude yield from **40**. After treatment of the isomer mixture **41** with Borch reagent to methylate the sulfur atoms, the bis(methylsulfonium) salt was treated with potassium *tert*-butoxide (Hofmann elimination) to form cyclophanediene **42** in 61% yield from dithiacyclophane **40**. Although this yield is not very high, it is considerably better than the yield that was obtained for the system with the *para*-phenylene unit in the tether. Another notable result in this particular project is that, in the formation of cyclophanediene **42**, not even trace

amounts of pyrenophane **5** were observed in the ^{1}H NMR spectrum. Treatment of a solution of cyclophanediene **42** in benzene led to clean formation of the desired [2]metacyclo[2](2,7)pyrenophane **5** (97%), even at room temperature. The ^{1}H NMR spectrum of pyrenophane **5** will be discussed in Section 5.2.3. In that Section the results of the X-ray crystal structure of **5** will also be discussed.

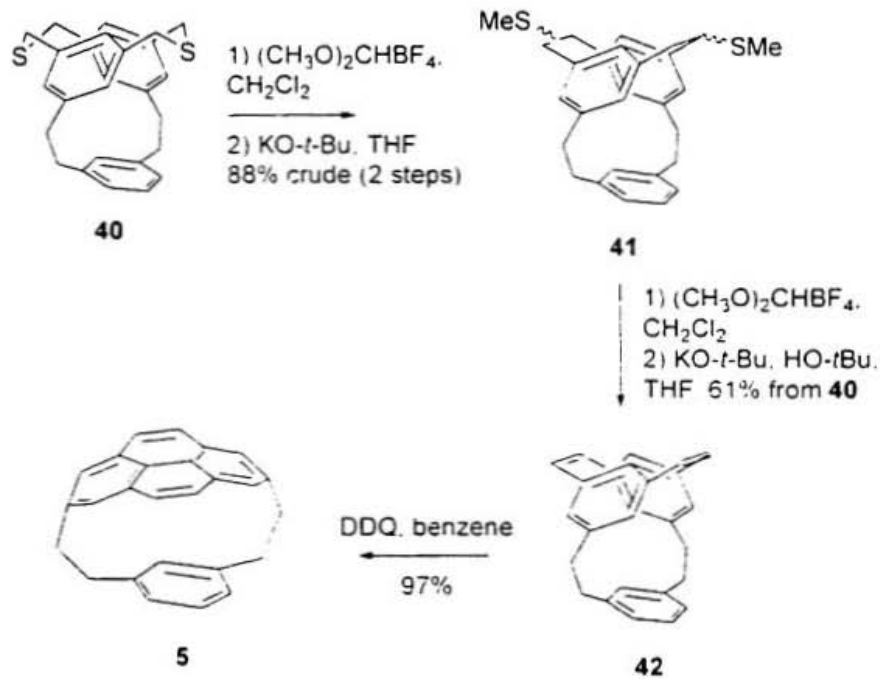

Scheme 5.10: Synthesis of [2]metacyclo[2](2,7)pyrenophane **5**.

A notable feature of the synthesis of **5** is, that it was accomplished in a single run. Without any optimization, the overall yield was 17% from 1,3-diiodobenzene **36**. This bodes well for the use of the use of this approach for the synthesis of related systems (Section 5.3).

5.2.3 Molecular structure of pyrenophanes 3 and 5

5.2.3.1 X-ray crystallography

Fortunately it proved to be possible to obtain crystals of pyrenophanes **3** (from heptane) and **5** (from toluene) that were suitable for X-ray crystallographic analysis. In Appendices F and G full crystallographic details are given. For the discussion of the structures in this Section, the crystallographic numbering of the carbon atoms will be used, which is different from the systematic numbering.

For pyrenophane **3** a bend angle $\theta_{X\text{-}ray}$ of 89.7° was determined and the curvature is spread out quite evenly over the pyrene surface. The bend angle is an anomalously 10.7° less than the AM1 calculated value (θ_{calcd} = 100.4°). In the [*n*](2,7)pyrenophanes this difference is usually only 4 – 7°. The β angles were measured to be 16.1° (for C(26)) and 16.3° (for C(17)), which is more than the usually observed values for β in the solid state (< 9.0°)[3,4,28,32,33] or those in the AM1 calculated structure (11.0°).

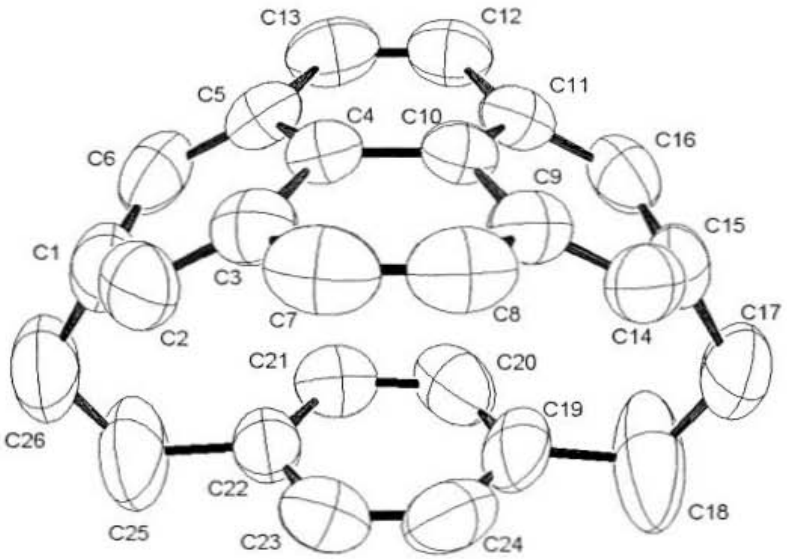

Figure 5.04: ORTEP representation of **3** in the crystal.[34]

The isolated benzene ring in **3** has very small α values (α < 1°) and, thus, is essentially planar. Considerable β angles were observed ($\beta_{C(25)}$ = 4.0° and $\beta_{C(17)}$ = 4.6°), indicating a distortion of the *para*-xylylene unit. The direction of this distortion from planarity, although subtle, is in the direction of the concave face of the pyrene unit. So far, this is the first and only example of such a "spoons-like" arrangement of the areas in one molecule. Usually the aromatic units are bowed away from one another (e.g. in compounds **7** and **10** in Figure 5.03). The dimethylene bridges are close to being fully eclipsed, with a torsion angle about the central C-C axis of 1(1)° and 7(7)°, which causes the pyrene and benzene decks to be almost perfectly aligned.

The most striking feature of the bridges in the molecular structure of **3** is the unusually large bond angles at the carbon atoms benzylic to the benzene ring (123.7(5)° and 124.8(6)°). Another unusual feature is the unusually short bond lengths of the central bonds of the dimethylene bridges (1.468(9) Å and 1.439(8) Å). The thermal ellipsoids at C(25) and (especially) C(18) are large and the exact values for these bond angles and bond lengths should not be viewed with a high degree of confidence. There is little doubt however, that the bond angles are indeed quite large and the bond lengths unusually short. The AM1 level calculations do not predict these large bond angles or short bond lengths. Normal tetrahedral angles at C(25) and C(18) would push the benzene deck well into the concave face of the pyrene deck and cause the benzene ring to adopt a nonplanar conformation. Repulsions between the π clouds of the opposing arene decks presumably disfavor the adoption of this arrangement. The short bond lengths in the dimethylene tethers can be explained by the rigid nature of the *para*-phenylene unit in the tether. If the lengths of these bonds would be in the range of normal C-C bonds, the distance between C(18) and C(25) would decrease. The result of this would be a curved or compressed *para*-phenylene unit.

In the X-ray crystal structure of **5** two slightly different molecules (**5a** and **5b**; Figure 5.05) are present in the unit cell. The bend angles are $\theta_{X\text{-}ray}$ = 97.1° for **5a** and $\theta_{X\text{-}ray}$ = 96.9° for **5b**, only 7.4° (average) less than the AM1 calculated value (θ_{calcd} = 104.4°). This is in line with previously observed values.[3,4,28,32,33] The β angles (**5a** $\beta_{C(17)}$ = 17.7°

and $\beta_{C(26)}$ = 16.5°; **5b** $\beta_{C(43)}$ = 17.3° and $\beta_{C(52)}$ = 16.8°) are even larger than in **3** and the [*n*](2,7)pyrenophanes.

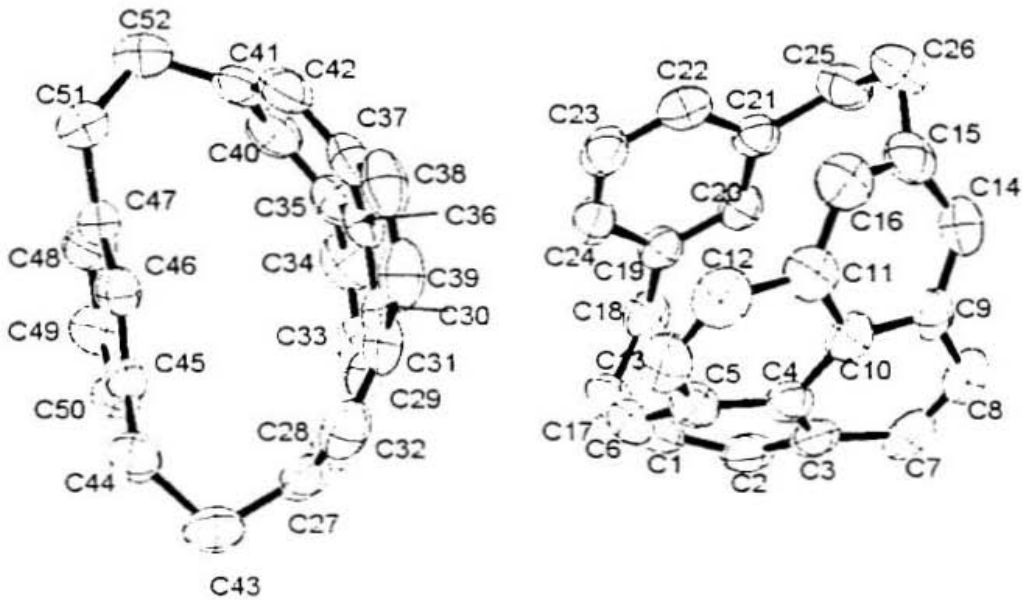

Figure 5.05: ORTEP representation of **5** in the crystal.[35]

The isolated aromatic ring in **5** is, similar to that in **3**, essentially planar (α < 2.5°, $\beta_{5a(C18)}$ = 3.9°, $\beta_{5a(C25)}$ = 3.3°, $\beta_{5b(C44)}$ = 7.0° and $\beta_{5b(C51)}$ = 3.6°) and bowed towards the concave face of the pyrenophane deck. The bridges in **5** are in a staggered conformation, with a torsional angle around the dimethylene bond of 51°, and the aromatic decks are not perfectly aligned, but rather slightly offset from one another.

5.2.3.2 NMR spectroscopy

In the 500 MHz ^{1}H NMR spectrum of **3**, the signal for the protons on the isolated aromatic ring (δ 5.54) were observed *ca.* 1.5 ppm upfield from the corresponding signal of *para*-xylene (δ 7.07). This indicated that the isolated aromatic ring in **3** is located in the shielding cone of the pyrene unit, which was also apparent from the X-ray crystal structure. Due to the difference in size between the pyrene deck and the isolated benzene rings, only the shielding effect of the pyrene rings on the protons of the isolated aromatic rings could be observed; the protons on the pyrene unit appeared to experience little magnetic anisotropy from the benzene ring. The signals of protons on the pyrene system of **3** appeared at δ 7.67 and 7.40, which was comparable to those of [8](2,7)pyrenophane (δ 7.84 and 7.59; $\theta_{X\text{-ray}}$ = 80.8°) and 1,8-dioxa[8](2,7)pyrenophane (δ 7.84 and 7.44; $\theta_{X\text{-ray}}$ = 87.8°). This observation fitted well with the previously observed trend that increased curvature of the pyrene unit caused an upfield shift of the signals of the protons on that pyrene unit (Table 5.02).

Pyrenophane **5** showed more signals in its 500 MHz ^{1}H NMR spectrum than initially might be expected. The pyrene deck showed four signals instead of the usual two, and four signals could be observed for the protons on the dimethylene bridges. This chemical inequivalence could be attributed to "freezing" of the conformational flip of the isolated benzene ring on the NMR time scale to give two degenerate conformers (Scheme 5.11).

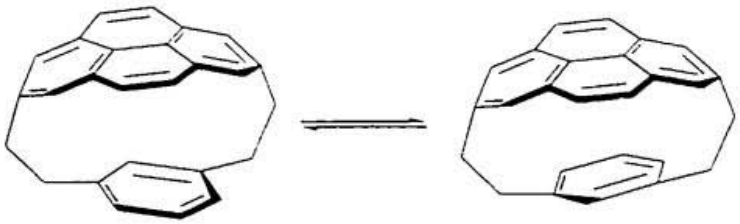

Scheme 5.11: Conformational flipping in pyrenophane **5**.

The internal proton in **5** was located in the shielding cone of the pyrene unit and its signal appeared at δ 4.18. This is almost identical with that of anti[2.2]metacyclophane **8**.[36] A smaller shielding effect was observed for the remaining protons on the isolated aromatic ring, which were observed as a triplet at δ 6.56 and a doublet at δ 6.31. A shielding effect was also observed for one of the protons on the dimethylene bridges (ddd at δ 1.21: *vide infra*). The appearance of four signals for the protons on the pyrene system in **5** was the result of the restricted flip of the isolated benzene ring. This caused the isolated benzene ring to shield the protons one side of the pyrene unit (H_h and H_i) more than the others (Figure 5.07). Using several NMR experiments, the signals in the ^{1}H NMR spectrum of **5** could be assigned as indicated in Figure 5.06 and 5.07.

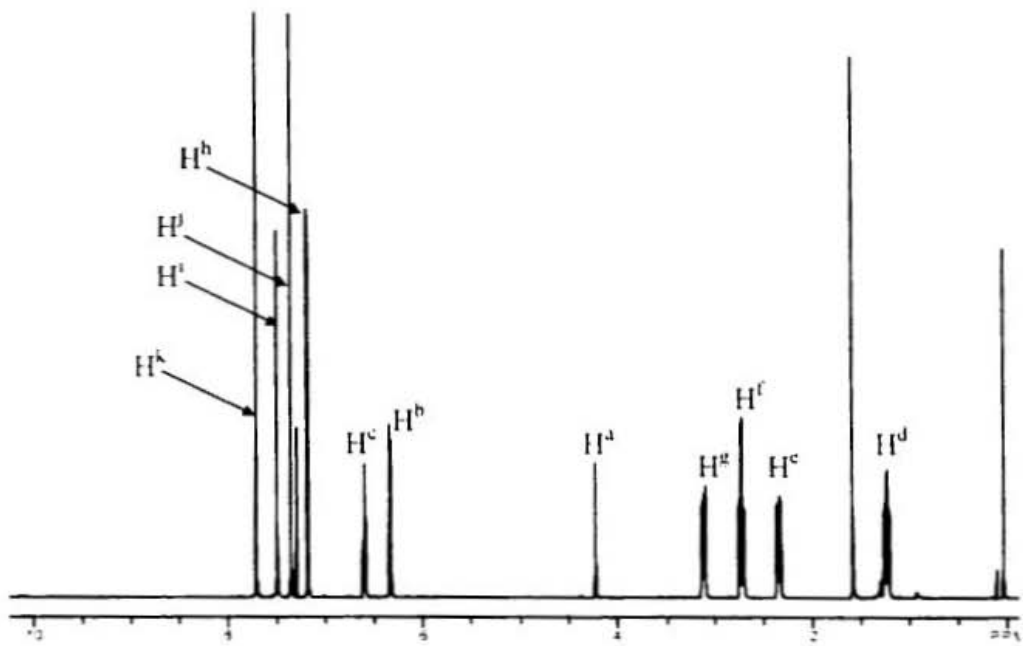

Figure 5.06: The 500 MHz ^{1}H NMR spectrum of **5**.

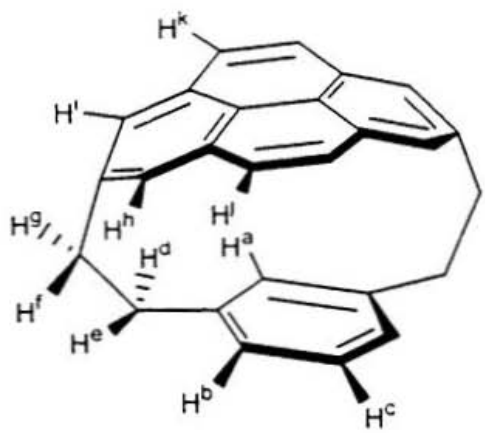

H^a	4.18	s
H^b	6.31	d
H^c	6.56	t
H^d	1.21	ddd
H^e	2.31	ddd
H^f	2.69	ddd
H^g	3.09	ddd
H^h	7.15	s
H^i	7.47	s
H^j	7.32	s
H^k	7.68	s

Figure 5.07: Assignment of the signals in the ^{1}H NMR spectrum of **5**.

Based on the chemical shift of the internal proton on the isolated benzene ring (H^a) and the multiplicity of the signals of the other protons on that ring (H^b and H^c), these signals could be assigned directly. One of the bridge protons was observed as a ddd around δ 1.21, which indicated it was shielded by one of the aromatic units. When a three-dimensional structure of **5** was examined, only H^d was situated in the shielding cone of the pyrene unit, and the ddd that appeared at unusually high field (δ 1.21) could tentatively be assigned to this proton. This assignment was later confirmed by a 2.6% enhancement of the signal for H^a when the signal for H^d was irradiated in a NOESY experiment (1.7% for the reverse experiment). Using HMQC correlation data, it could then be deduced that H^d (ddd at δ 2.31) was bonded to the same carbon atom as H^c, since both H^d and H^c showed a cross peak with the signal at δ 38.0 in the ^{13}C NMR spectrum.

When the signal for H^n was irradiated in an NOESY experiment an enhancement was observed for three signals (δ 7.15, δ 2.69 and δ 2.31). The signal for H^c (δ 2.31) showed an enhancement of 1.5%, confirming the assignment for that proton. The ddd at δ 2.69 was enhanced by 2.0%, indicating that this signal might be assigned to H^f. The enhancement of 1.2% of the singlet at δ 7.15 made it possible to assign this signal one of the protons on the "front" side of the pyrene unit (most likely H^h; Figure 5.07). Based on the small coupling of the signal at δ 7.15 with the signal at δ 7.47, these signals must belong to H^h and H^i. In conjunction with the previous NOESY data, H^h could thus be assigned to the signal at δ 7.15. That the chemical shift value for H^h is at higher field than

that for H^f can be explained by the situation of H^h in the shielding cone of the *meta*-phenylene group.

The last NMR experiment necessary for complete assignment of the signals of **5** was NOESY irradiation of the signal for H^f at δ 7.47. Irradiation experiment of this signal showed an enhancement of 1.9% of the ddd around δ 3.09, which could then be assigned to H^g. This also confirms the assignment of H^f. Irradiation of the signal for H^i also showed an enhancement of the singlet at δ 7.68 by 1.2%, which allowed for assignment of this signal to H^k and, by elimination, the signal at δ 7.32 could be assigned to H^j. This assignment was in line with the shielding of H^j by the shielding cone of the isolated benzene ring compared to H^k

The slow flipping motion of the isolated aromatic ring in **5** led us to further study this effect by a DNMR study. In the flipping process the environments of H^d and H^e, H^f and H^g, H^i and H^h, and H^j and H^k are exchanged. At temperatures above the coalescence temperature for this process, each set of protons (i.e. H^d and H^e, etc.) is expected to show one signal at approximately the average chemical shift of the contributing values. The signals for H^a, H^b and H^c are not expected to undergo coalescence, as their environments in the two conformers are the same.

For the DNMR experiment, a solution of [2]metacyclo[2](2,7)pyrenophane in DMSO-d_6 was warmed up slowly from room temperature to 120 °C, while a 500 MHz ^{1}H NMR

spectrum was collected every 10 °C (Figure 5.08). At temperatures above approximately 70 °C, considerable broadening of the signals in the ^{1}H NMR spectra was observed, but no coalescence of signals occurred when the temperature limit of the spectrometer had been reached (120 °C). The broadening of the signals indicated, however that conformational interconversion of the two conformers of **5** was occurring at increasing rates. As expected, the signals for the protons on the *meta*-phenylene ring did not show any significant broadening.

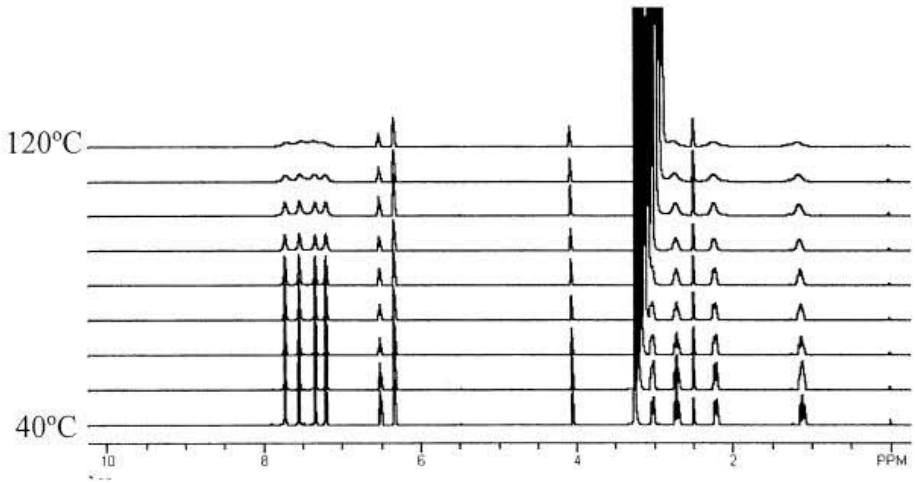

Figure 5.08: DNMR spectra of **5**.

From the shapes of the signals it was estimated that the coalescence temperature for this process probably lies in the range 130-160 °C, but unfortunately the equipment available does not allow for acquisition at these temperatures. Using equations 1 and 2[37,38] and the ^{1}H NMR data of H^d and H^e ($\Delta\nu_{Ha,Hb}$ = 560 Hz, J = 13.5 Hz), an activation barrier for the interconversion process of approximately 19 kcal/mol (80 kJ/mol) was calculated.

$$\Delta G^{\ddagger} = RT_c(22.96 + \ln T_c - \ln \Delta\nu') \qquad \text{Equation 1}$$

$$\Delta\nu' = (\Delta\nu_{Ha,Hb}^{\ 2} + 6J^2)^{1/2} \qquad \text{Equation 2}$$

From the same equations it can be determined that if the same experiment were to be performed on a 60 MHz instrument, these estimated values would correspond to a coalescence temperature of 100-130°C, which is within the limits of such an instrument. Unfortunately this capability was not available to our group.

5.3 Conclusions and future work

In Section 5.2 the successful syntheses of [2]paracyclo[2](2,7)pyrenophane **3** and [2]metacyclo[2](2,7)pyrenophane **5** were described. The overall yield for the synthesis of **3** was quite low at only 3%. The low yield is due primarily to two low-yielding steps in the synthesis. For the synthesis of **5** the overall yield was a satisfying 17%, which can probably be increased by optimizing the reaction conditions for some steps. The successful syntheses of **3** and **5** demonstrate the use of a novel approach to the formation of ethano-bridged cyclophanes, and further establishes the VID protocol as a powerful method for the formation of nonplanar pyrene containing systems.

The molecular structures of **3** and **5** were determined by X-ray crystallography. Both cyclophanes exhibit an unprecedented "spoons-like" arrangement with the isolated

aromatic ring in each cyclophane bowed *toward* the pyrene deck. The bend angles of the pyrene units in **3** and **5** are 89.7° and 97.0°, respectively, and unusually large β angles were observed for both compounds.

The 500 MHz ^{1}H NMR spectrum of pyrenophane **3** displayed no unusual features. Due to the shielding effect of the pyrene ring, the signal of the protons on the *para*-xylyl ring appear at a chemical shift of δ 5.54. With cyclophane **5** this shielding effect causes the "internal" proton of the *meta*-xylyl ring to appear at δ 4.18. The most striking feature of the ^{1}H NMR spectrum of **5** is probably the observation of restricted interconversion between two degenerate conformers. The energy barrier for this interconversion was estimated to be approximately 19 kcal mol (80 kJ mol) by extrapolation of the DNMR results.

The unusual bond angles and bond lengths in the bridges of **3** indicated that these bridges might be less strained if the carbon atoms in these bridges are sp^2-hybridized (pyrenophanediene **43**: Figure 5.09). The AM1-calculated bend angle of this pyrenophane is 102.6°, only 2.2° more than the calculated value for **3**. The shorter-than-usual bond lengths and bond angles in the X-ray crystal structure of **3** suggest that the formation of pyrenophanediene **43** should be feasible.

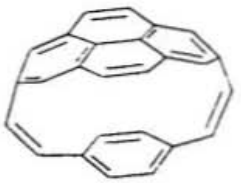

43

Figure 5.09: Structure of pyrenophanediene **43**.

Another project would be the synthesis of diketones **44** and **46** (Scheme 5.12). The keto/enol ratios in **44** and **46** should display the relative stability of the double C-C bond (enol) *versus* the single C-C bond (ketone). It is anticipated that, even though the aromatic units are orthogonal to the keto and enol π-systems, the enol form might be preferred. Based on the large bond angle that was observed in the X-ray crystal structure of **3** it can be expected that the **44** will enolize more readily than **46**.

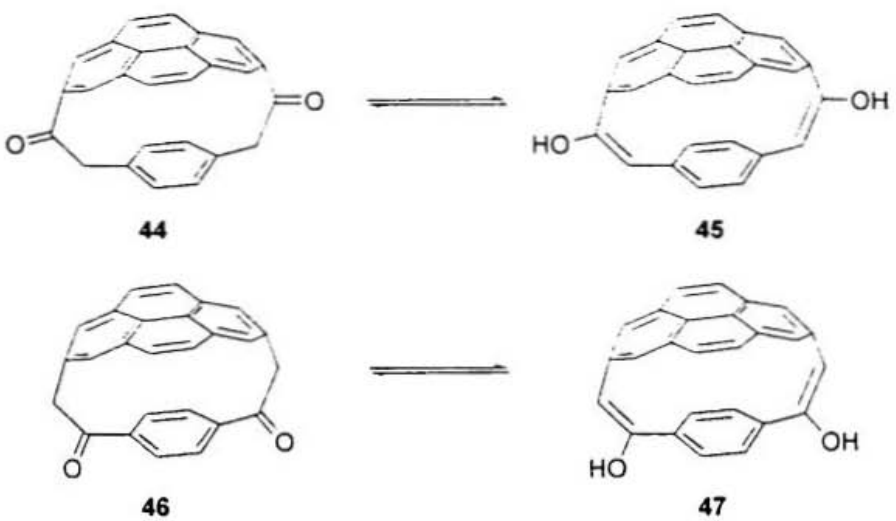

44 **45**

46 **47**

Scheme 5.12: Keto-enol equilibria of **44** and **46**.

Other synthetic targets that can be derived from [2]paracyclo[2](2,7)pyrenophane **3** are given in Figure 5.10. Cyclophane **48** has Dewar benzene units in the positions where pyrenophane **3** had dimethylene bridges and is a direct precursor of aromatic belt **4** (Figure 5.01). Synthesis of **48** is expected to be quite challenging, however.

Pyrenophane **49** is an example of a cyclophane with planar chirality. If in **49** the substituent R is a chiral substituent, with the same absolute configuration in (***S***)-**49** and (***R***)-**49**, two diastereomers are created. Since these compounds should be distinguishable by ^{1}H NMR spectroscopy, these compounds would provide an elegant opportunity to study the rotation of the *para*-phenylene unit in the cyclophane. (This "skipping rope"-type rotation would interconvert the two diastereomers). A notable feature of pyrenophane **3** is that substitution at *any* of the carbon atoms renders a chiral cyclophane. Substitution on the bridges leaves a stereogenic center and substitution on any of the aromatic carbons gives a cyclophane of planar chirality.

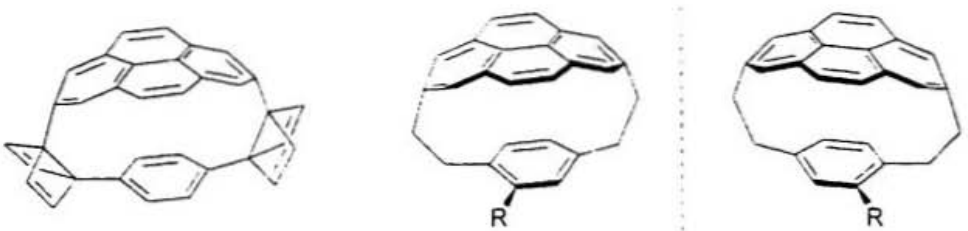

48 (***S***)-**49** (***R***)-**49**

Figure 5.10: Future synthetic targets based on the [2]paracyclo[2](2,7)pyrenophane system.

Based on the successful synthesis of [2]metacyclo[2](2,7)pyrenophane **5** some similar future synthetic targets can be proposed (Figure 5.11). The pyrenophanediene **50** can be proposed, similar to **43** and has an AM1 calculated bend angle of 115.1°, which is 8.5° more than the value calculated for **5**. This suggests that introduction of the double bonds in the metacyclophane **50** structure has a much greater effect than in the paracyclophane structure **43**. This is supported by the X-ray crystal structures of **3** and **5**, since introduction of double bonds in the dimethylene tethers would drastically change their conformation in **5**, but not as much in **3**, which already shows short bond lengths and large bond and torsion angles. Similar to the substitution of pyrenophane **3**, substitution on cyclophane **5** can render a cyclophane of planar chirality like ***S*-51**.

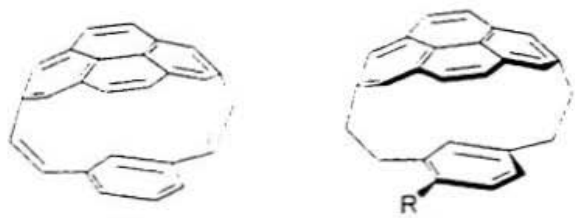

50 **(*S*)-51**

Figure 5.11: Future synthetic targets **50** and **51**.

Using similar methodology as for the synthesis of **3** and **5**, it should be possible to synthesize pyrenophanes **52** and **54** (Scheme 5.13). If sufficient amounts of these materials can be made available, it might be possible to build up larger structures like **53** and **55**. For **53** other isomers can be drawn, but they have been omitted for clarity. Compound **55** should still undergo a "skipping-rope" motion of the pyrene units around

the central aromatic ring, which would make it an interesting topic for dynamic studies. Both compounds can be seen as fullerene isosteres, although they are calculated (AM1) to contain pyrene units at greater intramolecular distance (8.2 - 11.7 Å) than D_{5h}-C_{70} (6.82 Å).[39]

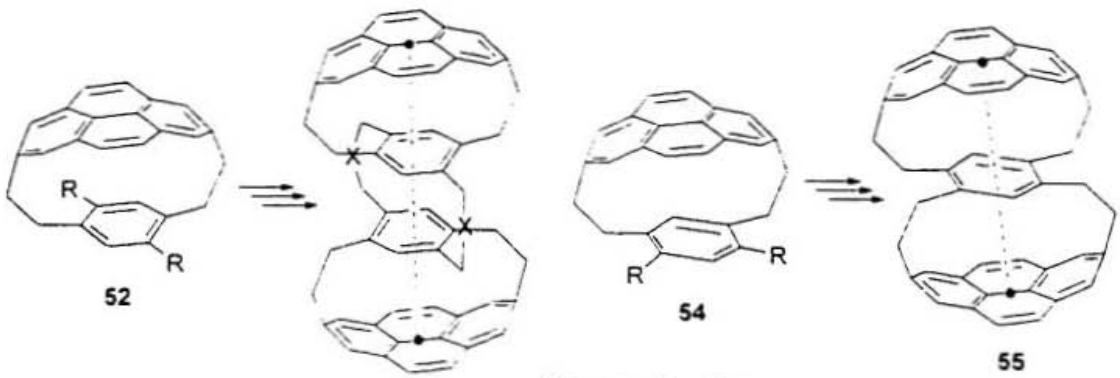

Compound	Distance • · · •
53a X = S	11.7 A
53b X = bond	11.4 A
55	8.2 A

Scheme 5.13: Future synthetic targets **52** - **55**

5.4 Experimental

General. All chemicals were reagent grade and were used as received. Chromatographic separations were performed on Merck silica gel 60 (particle size 40-63 μm, 230–400 mesh). Melting points were determined on a Fisher-Johns apparatus and are uncorrected. Elemental analyses were performed at the MicroAnalytical Service Laboratory, Department of Chemistry, University of Alberta. Mass spectroscopic (MS) data were

obtained on a V. G. Micromass 7070HS instrument. ^{1}H NMR (500 MHz) and ^{13}C NMR (126 MHz) were obtained on a Bruker spectrometer: ^{1}H shifts are relative to internal tetramethylsilane; ^{13}C shifts are relative to the solvent resonance ($CDCl_3$: δ = 77.0). All experiments with moisture- or air-sensitive compounds were performed in anhydrous solvents under nitrogen unless otherwise stated. Solvents were dried and distilled according to standard procedures.

1,4-Bis(trimethylsilylethynyl)benzene (19).[40]

To a solution of 1,4-diiodobenzene **17** (10.25 g, 31.07 mmol) in degassed benzene (225 mL) under a nitrogen atmosphere, were added $(Ph_3P)_2PdCl_2$ (1.05 g, 1.50 mmol) and CuI (1.00 g, 5.25 mmol), followed after 5 min by trimethylsilylacetylene **18** (7.65 g, 77.9 mmol) and DBU (14.19 g, 93.21 mmol). The reaction mixture was stirred at room temperature for 2 h, washed with saturated aqueous NH_4Cl solution (100 mL), water (2 x 100 mL) and saturated aqueous NaCl solution (100 mL), dried ($MgSO_4$) and concentrated under reduced pressure. The residue was purified by column chromatography (hexanes, silica) to give **19** (7.99 g, 29.5 mmol, 95%) as colorless crystals: mp 118 – 119 °C (hexanes) (lit.[40] 122 °C); IR (nujol, cm^{-1}) 2155 (s), 1492 (m), 1246 (s); ^{1}H NMR (500 MHz, $CDCl_3$) δ 7.40 (s, 4H), 0.25 (s, 18H); ^{13}C NMR (126 MHz, $CDCl_3$) δ 131.7, 123.1, 104.6, 96.3, -0.1; EI-MS (70 eV) *m z* (%): 270 (27, M^+), 255 (100).

1,4-Diethynylbenzene (20).[40]

K_2CO_3 (3.54 g, 25.61 mmol) and 1,4-bis(trimethylsilylethynyl)benzene **19** (2.77 g, 13.3 mmol) were added to methanol (50 mL) and the reaction mixture was stirred for 1 h. The mixture was poured into ice water (100 mL) and filtered under suction. The residue was sublimed at atmospheric pressure (*ca.* 95 °C oil bath; CAUTION: in one instance this procedure led to explosive decomposition of the material !) to give **20** (0.99 g, 77%) as colorless plates; mp: 94 – 95 °C (sublimes slowly above 76 °C) (lit.[40] 95 – 96 °C); ^{1}H NMR (300 MHz, $CDCl_3$) δ 7.45 (s, 4H), 3.18 (s, 2H); ^{13}C NMR (75 MHz, $CDCl_3$) δ 132.0, 122.5, 82.9, 79.2.

1,4-Bis(3,5-bis(methoxycarbonyl)phenylethynyl)benzene (22).

To a solution of triflate **21** (3.22 g, 9.41 mmol) in degassed benzene (80 mL) under a nitrogen atmosphere, were added $(Ph_3P)_2PdCl_2$ (0.08 g, 0.1 mmol) and CuI (0.08 g, 0.4 mmol), followed after 5 min by 1,4-diethynylbenzene **20** (0.54 g, 4.3 mmol) and DBU (1.95 g, 12.8 mmol). The reaction mixture was refluxed for 18 h, concentrated under reduced pressure, and the residue was dissolved in $CHCl_3$ (250 mL), and saturated aqueous NH_4Cl solution (100 mL). The aqueous layer was extracted with $CHCl_3$ (100 mL) and the combined organic layers were washed with water (2 x 100 mL) and saturated aqueous NaCl solution (100 mL), dried ($MgSO_4$) and concentrated under reduced pressure. The residue was purified by column chromatography (chloroform,

silica) to give **22** (1.25 g, 57%) as an off-white solid: mp: decomposes > 290 °C (chloroform); IR (nujol, cm^{-1}): 1732 (s), 1247 (m); ^1H NMR (500 MHz, $CDCl_3$) δ 8.66 (s, 2H), 8.39 (s, 4H), 7.56 (s, 4H), 3.99 (s, 12H); ^{13}C NMR (126 MHz, $CDCl_3$) δ 165.6, 136.5, 131.7, 131.1, 130.1, 124.1, 122.9, 90.7, 89.4, 52.5; EI-MS (70 eV) *m z* (%): 510 (100, M^+), 479 (10), 224 (10); HRMS Calc'd for $C_{30}H_{22}O_8$: 510.1313, found 510.1334

Alternative route (preferred):

To a solution of 1,4-diiodobenzene (6.03 g, 18.28 mmol) in 400 mL degassed benzene under a nitrogen atmosphere, was added $(Ph_3P)_2PdCl_2$ (0.64 g, 0.91 mmol) and CuI (0.35 g, 1.8 mmol), followed after 5 min by dimethyl 5-ethynylisophtalate **24** (9.98 g, 45.7 mmol) and DBU (8.35 g, 54.8 mmol). The reaction mixture was stirred for 2.5 h, concentrated under reduced pressure and the residue was dissolved in $CHCl_3$ (1000 mL) and saturated aqueous NH_4Cl solution (500 mL). The aqueous layer was extracted with $CHCl_3$ (500 mL) and the combined organic layers were washed with water (2 x 500 mL) and saturated aqueous NaCl solution (500 mL), dried ($MgSO_4$) and concentrated under reduced pressure. The residue was purified by column chromatography (chloroform, silica) to give **22** (8.51 g, 16.7 mmol, 91%) as an off-white solid.

Dimethyl 5-(trimethylsilylethynyl)benzene-1,3-dicarboxylate (23).

To a solution of $(Ph_3P)_2PdCl_2$ (2.57 g, 3.66 mmol) and CuI (1.39 g, 7.30 mmol) in degassed benzene (400 mL), was added triflate **21** (25.07 g, 73.25 mmol), followed, after 10 min, by a solution of trimethylsilylacetylene **18** (10.07 g, 102.5 mmol) in degassed benzene (200 mL) and DBU (16.70 g, 109.7 mmol). The mixture was stirred under a nitrogen atmosphere for 2 h, concentrated under reduced pressure and dissolved in chloroform (250 mL) and saturated NH_4Cl solution (200 mL). The aqueous layer was extracted with chloroform (150 mL). The organic extracts were combined and washed successively with water (200 mL) and saturated aqueous NaCl solution (200 mL), dried ($MgSO_4$), concentrated *in vacuo*, and purified by column chromatography (SiO_2, 10% ethyl acetate-hexanes) to yield **23** (14.92 g, 51.38 mmol, 70%) as a colorless solid: mp: 100 – 101.5 °C; IR (nujol, cm^{-1}) 2159 (w), 1734 (s), 1593 (w), 1332 (m), 1242 (s); ^1H NMR (500 MHz, $CDCl_3$) δ 8.61 (s, 1H), 8.30 (s, 2H), 3.96 (s, 6H), 0.27 (s, 9H); ^{13}C NMR (126 MHz, $CDCl_3$) δ 165.5, 136.8, 130.8, 130.3, 124.2, 102.7, 96.7, 52.5, -0.22; EI-MS (70 eV) *m z* (%): 290 (10, M^+), 275 (100), 259 (9), 201 (10).

Dimethyl 5-ethynylbenzene-1,3-dicarboxylate (24).

Dimethyl 5-(trimethylsilylethynyl)benzene-1,3-dicarboxylate **23** (14.92 g, 51.38 mmol) and K_2CO_3 (9.23, 66.8 mmol) were weighed into a 1 L round-bottom flask and 650 mL methanol was added. The mixture was stirred under a nitrogen atmosphere for 1.5 h and poured into 1 L water. Dimethyl 5-ethynylisophthalate **24** (10.19 g, 46.70 mmol, 91%) was isolated by suction filtration, washed with water (2 x 100 mL) and dried *in vacuo* as a colorless powder; mp: 127 – 128 °C; ^{1}H NMR (500 MHz, $CDCl_3$) δ 8.53 (s, 2H), 8.07 (s, 4H), 7.11 (s, 4H), 3.95 (s, 12H), 3.04-2.97 (m, 4H), 2.96-2.89 (s, 4H); ^{13}C NMR (126 MHz, $CDCl_3$) δ 166.4, 142.9, 138.9, 133.9, 130.6, 128.6 (2C), 52.3, 37.6, 37.2; EI-MS (70 eV) *m z* (%): 218 (50, M$^+$), 187 (100), 159 (28), 144 (22).

1,4-Bis(2-(3,5-bis(methoxycarbonyl)phenyl)ethyl)benzene (25).

To a solution of diyne **22** (0.64 g, 1.3 mmol) in degassed benzene (300 mL) was added Pd(OH) C (Pearlman's catalyst, 0.40 g), and the suspension was stirred vigorously under an atmosphere of hydrogen for 2 h. The flask was subjected to reduced pressure and let down to nitrogen several times before being filtered through a plug of Celite. Removal of solvent under reduced pressure afforded tetraester **25** (0.62 g, 95%) as a colorless solid; mp: 146 – 147.5 °C (chloroform / hexanes); ^{1}H NMR (500 MHz, $CDCl_3$) δ 8.56 (s, 2H), 8.10 (s, 4H), 7.14 (s, 4H), 3.98 (s, 8H), 3.04 (m, 4H), 2.96 (m, 4H); ^{13}C NMR (126 MHz, $CDCl_3$) δ

166.4, 142.7, 138.8, 133.9, 130.6, 128.5 (2C), 52.3, 37.6, 37.2; EI-MS (70 eV) *m/z* (%): 518 (6, M^+), 486 (55), 426 (5), 311 (33), 281 (100), 207 (79), 104 (45).

1,4-Bis(2-(3,5-bis(bromomethyl)phenyl)ethyl)benzene (26).

A solution of tetraester **25** (2.16 g, 4.17 mmol) in THF (100 mL) was added dropwise to a well-stirred suspension of $LiAlH_4$ (1.90 g, 50.1 mmol) in THF at 0 °C under nitrogen. The mixture was stirred at reflux for 16 h, cooled in an ice-bath and quenched with ethyl acetate (10 mL). The mixture was concentrated under reduced pressure, suspended in glacial acetic acid (100 mL), 30% HBr HOAc (10 mL, 50 mmol) was added and the mixture was refluxed for 30 min. After cooling to room temperature, the mixture was poured into water (200 mL) and extracted with CH_2Cl_2 (2 x 200 mL). The combined organic layers were washed with water (2 x 150 mL), saturated aqueous $NaHCO_3$ solution (2 x 150 mL), water (100 mL) and saturated aqueous NaCl solution (100 mL), dried ($MgSO_4$) and concentrated under reduced pressure. The residue was purified by column chromatography (50% $CHCl_3$ / hexanes, silica) to afford tetrabromide **26** (2.33 g, 85%) as a white solid: mp 142.5-143.5 °C (hexanes); ^1H NMR (500 MHz, $CDCl_3$) δ 7.26 (overlapped with solvent, s, 2H), 7.13 (s, 4H), 7.09 (s, 4H), 4.45 (s, 8H), 2.89 (s, 8H); ^{13}C NMR (126 MHz, $CDCl_3$) δ 143.1, 138.9, 138.3, 129.3, 128.5, 127.2; EI-MS (70 eV) *m/z* (%): 658 (5, M^+ ($^{81}Br)_3(^{79}Br)_2$), 497 (17), 417 (27), 381 (100); HRMS Calc'd for $C_{30}H_{22}(^{79}Br)_4$: 653.8765, found 653.8772.

Belta-2,11-dithia[3.3](1,3)(1,3)[2](5)(1)[2](4)(5)benzeno<3>phane (27).

To a well-stirred refluxing solution of tetrabromide **26** (2.48 g, 3.77 mmol) in degassed 10% ethanol (abs)/CH_2Cl_2 (825 mL) was added $Na_2S{\cdot}Al_2O_3$[23] (7.83 g, 19.4 mmol) in three roughly equal portions over 1 h. After stirring for 1.5 h at reflux temperature, the reaction mixture was cooled to room temperature, suction filtered through a plug of Celite and concentrated under reduced pressure. Column chromatography (25% $CHCl_3$/hexanes) afforded dithiacyclophane **27** (0.43 g, 28%) as a colorless, foamy solid: mp > 280 °C; ^{1}H NMR (500 MHz, $CDCl_3$) δ 6.96 (br s, 2H), 6.87 (s, 4H), 6.52 (s, 4H), 3.71 (narrow AB system, 8H), 2.99 (t, J = 7.0 Hz, 4H), 2.86 (t, J = 6.9 Hz, 4H); ^{13}C NMR (126 MHz, $CDCl_3$) δ 140.4, 137.2, 137.0, 129.1, 128.7, 128.0, 40.5, 34.9, 32.8; EI-MS (70 eV) m/z (%): 402 (100, M^+), 369 (27), 338 (36); HRMS Calc'd for $C_{26}H_{26}S_2$: 402.1475, found 402.1493.

Belta[2.2](1,3)(1,3)[2](5)(1)[2](4)(5)benzeno<3>phane-1,9-diene (29) and [2]paracyclo[2](2,7)pyrenophane (3).

To a stirred solution of dithiacyclophane **27** (0.60 g, 1.5 mmol) in degassed CH_2Cl_2 (120 mL) under an atmosphere of nitrogen, was added $(MeO)_2CHBF_4$ (1.21 g, 7.47 mmol) and after 3 h the mixture was concentrated under reduced pressure. Ethyl acetate (50 mL) was added to the residue, the mixture was stirred for 5 min and suction filtered to give a beige solid that was washed with ethyl acetate (2 x 3 mL) and dried *in vacuo* to yield a

bis(sulfonium tetrafluoroborate) salt. This was slurried in degassed THF (120 mL) under nitrogen and *t*-BuOK (0.50 g, 4.5 mmol) was added. The reaction mixture was stirred overnight, saturated aqueous NH_4Cl solution (50 mL) was added and the mixture was concentrated under reduced pressure. The residue was taken up in degassed CH_2Cl_2 (100 mL) and washed with saturated aqueous NH_4Cl solution (50 mL), water (50 mL) and brine (50 mL), dried ($MgSO_4$) and concentrated under reduced pressure. The residue was passed through a plug of silica ($CHCl_3$), and concentration of the eluents afforded a mixture of bis(methylthio)cyclophane isomers (0.45 g, 70% from **27**) as a foamy, light yellow solid. The solid was dissolved in degassed CH_2Cl_2 (100 mL) under an atmosphere of nitrogen and slowly $(MeO)_2CHBF_4$ (0.85 g, 5.3 mmol) was added, and after 3 h the mixture was concentrated under reduced pressure. Ethyl acetate (15 mL) and methanol (5 mL) were added, the mixture was stirred for 5 min and concentrated under reduced pressure to give a brown oil. This oil was slurried in degassed 1:1 *t*-BuOH:THF (100 mL) under nitrogen and to this mixture *t*-BuOK (0.35 g, 3.1 mmol) was added. After stirring for 16 h, saturated aqueous NH_4Cl solution (20 mL) was added and the mixture was concentrated under reduced pressure. The residue was taken up in degassed CH_2Cl_2 (100 mL) and saturated aqueous NH_4Cl solution (75 mL) and the aqueous layer was extracted with degassed CH_2Cl_2 (50 mL). The combined organic layers were washed with water (100 mL) and saturated aqueous NaCl solution (100 mL), dried ($MgSO_4$) and concentrated under reduced pressure. The residue was concentrated under reduced pressure to afford a mixture of cyclophanediene **29** and [2]paracyclo[2](2,7)pyrenophane **3** (0.08 g, 16% from **27**) as a colorless solid. The mixture was dissolved in degassed

benzene (25 mL) under nitrogen. DDQ was added (0.04 g, 0.2 mmol) and after 10 min the mixture was concentrated under reduced pressure and purified by preparative TLC (silica, 60% $CHCl_3$/hexanes) to yield [2]paracyclo[2](2,7)pyrenophane **3** (0.07 g, 14% from **27**) as a colorless solid, that was crystallized from heptane: mp 216 – 219 °C; ^1H NMR (500 MHz, $CDCl_3$) δ 7.67 (s, 4H), 7.40 (s, 4H), 5.54 (s, 4H), 2.99 (t, J = 7.3 Hz, 4H), 2.32 (t, J = 7.2 Hz, 4H); ^{13}C NMR (126 MHz, $CDCl_3$) 135.7, 134.2, 131.3, 129.3, 128.6, 128.0, 126.1, 36.5, 33.8; EI-MS (70 eV) m/z (%): 332 (11, M^+), 228 (100).

1,3-Bis(3,5-bis(methoxycarbonyl)phenylethynyl)benzene (37)

To a solution of $(Ph_3P)_2PdCl_2$ (0.39 g, 0.56 mmol) and CuI (0.39 g, 2.0 mmol) in degassed benzene (250 mL) under nitrogen, was added 1,3-diiodobenzene **36** (3.66 g, 11.1 mmol), followed after 5 min by a solution of **24** (5.33 g, 24.4 mmol) in degassed benzene (150 mL) and DBU (4.23 g, 27.8 mmol). The reaction mixture was stirred at room temperature under an atmosphere of nitrogen for 3 h, concentrated under reduced pressure and dissolved in $CHCl_3$ (200 mL) and saturated aqueous NH_4Cl solution (100 mL). The aqueous layer was extracted with $CHCl_3$ (150 mL) and the combined organic layers were washed with saturated aqueous NH_4Cl (100 mL), water (100 mL), brine (100 mL), dried ($MgSO_4$) and concentrated *in vacuo*. The residue was subjected to column chromatography (SiO_2, 2% EtOAc / $CHCl_3$) to yield **37** (4.31 g, 8.44 mmol, 76%) as a beige solid that was crystallized from EtOH / $CHCl_3$: mp: 176 – 177.5 °C (ethanol / chloroform); IR (nujol, cm^{-1}): 2216 (w), 1734 (s), 1290 (w), 1249 (m), 1008 (w), 751 (w);

^{1}H NMR (500.1 MHz; $CDCl_3$): δ 8.65 (s, 2H), 8.38 (s, 4H), 7.76 (s, 1H), 7.56 (d, J = 7.9 Hz, 2H), 7.04 (t, J = 7.7 Hz, 1H), 3.98 (s, 12H); ^{13}C NMR (126 MHz; $CDCl_3$): δ 165.6, 136.5, 134.9, 131.9, 131.0, 130.3, 128.7, 124.1, 123.0, 90.2, 88.1, 52.6; EI-MS (70 eV) m/z (%): 510 (100, M$^+$), 479 (25), 224 (25); HRMS Calc'd for $C_{30}H_{22}O_8$: 510.1313, found 510.1295.

1,3-Bis(2-(3,5-bis(methoxycarbonyl)phenyl)ethyl)benzene (38)

To a solution of **37** (4.31 g, 8.44 mmol) in degassed benzene (700 mL), was added 20% Pd/C (0.35 g) and acetic acid (0.1 mL), and the suspension was stirred under a H_2-atmosphere for 16 h. The reaction mixture was degassed by bubbling nitrogen through the mixture for 20 min, filtered through a plug of $MgSO_4$ and concentrated *in vacuo* to yield **38** (4.37 g, 8.44 mmol, 100%) as a colorless oil, that solidified upon standing; mp: 150 – 151.5 °C (benzene); ^{1}H NMR (500.1 MHz; $CDCl_3$): δ 8.53 (s, 2H), 8.05 (s, 4H), 7.22 (t, J = 7.4 Hz, 1H), 7.04 (d, J = 7.6 Hz, 2H), 6.98 (s, 1H), 3.94 (s, 9H), 2.99 (m, 4H), 2.92 (m, 4H); ^{13}C NMR (126 MHz; $CDCl_3$): δ 166.4, 142.6, 141.1, 133.9, 130.6, 128.7, 128.6, 128.5, 126.3, 52.3, 37.6; EI-MS (70 eV) m/z (%): 518 (6, M$^+$), 486 (83), 311 (22), 281 (100), 207 (50), 177 (10), 104 (17).

1,3-Bis(2-(3,5-bis(bromomethyl)phenyl)ethyl)benzene (39)

A solution of **38** (4.33 g, 8.35 mmol) in dry THF (150 mL) was added over 45 min to a well-stirred, 0 °C suspension of $LiAlH_4$ (3.80 g, 10.0 mmol) in dry THF (200 mL) under a nitrogen atmosphere. The mixture was stirred at room temperature for 22 h, cooled in an ice-bath, quenched with ethyl acetate (20 mL) and concentrated *in vacuo*. HBr in acetic acid (30%, 125 mL) was carefully added to the residue, and the mixture was heated to reflux, cooled and poured into ice water (300 mL). CH_2Cl_2 (100 mL) was added, and the aqueous layer was extracted with CH_2Cl_2 (2 x 100 mL). The combined organic extracts were washed with saturated aqueous $NaHCO_3$ solution (3 x 100 mL), water (100 mL) and saturated aqueous NaCl solution (100 mL), dried ($MgSO_4$) and concentrated under vacuum. The residue was purified by column chromatography to yield **39** (2.95 g, 4.48 mmol, 54%) as a white solid: mp: 109 - 111.5 °C ($CHCl_3$-hexanes); ^1H NMR (500.1 MHz; $CDCl_3$): δ 7.27 (s, 2H), 7.22 (t, J = 7.5 Hz, 1H), 7.14 (s, 4H), 7.02 (d, J = 7.5 Hz, 2H), 6.94 (s, 1H), 4.45 (s, 8H), 2.89 (s, 8H); ^{13}C NMR (126 MHz; $CDCl_3$): δ 143.1, 141.3, 138.4, 129.3, 128.7, 128.5, 127.2, 126.2, 37.6, 37.5, 33.0; EI-MS (70 eV) *m/z* (%): 658 (5, M^+ ($^{81}Br)_2(^{79}Br)_2$), 577 (3), 497 (59), 417 (87), 381 (100), 335 (29), 219 (43).

Beta-2,11-dithia[3.3](1,3)(1,3)[2](5)(1)[2](3)(5)benzeno<3>phane (40)

To a vigorously stirred solution of **39** (2.35 g, 3.57 mmol) in ethanol (abs; 200 mL) and CH_2Cl_2 (1800 mL) was added Na_2S / Al_2O_3 (12.01 g, 4.0 mmol; 3.0 mmol/g) in three

approximately equal portions over 30 min. The reaction mixture was stirred for 1.5 h, filtered over a plug of celite and concentrated *in vacuo*. The residue was subjected to column chromatography (50% SiO_2, $CHCl_3$ / hexanes) to yield **40** (0.98 g, 2.4 mmol, 68%) as a colorless crystalline solid: mp: > 218 °C (dec.) ($CHCl_3$/hexanes): ^1H NMR (500.1 MHz; $CDCl_3$): δ 7.25 (t, J = 7.6 Hz, 1H), 7.10 (s, 2H), 7.06 (d, J = 7.8 Hz 2H), 6.56 (s, 4H), 6.31 (s, 1H), 3.74 (m, 8H), 2.96 (m, 4H), 2.80 (m, 4H); ^{13}C NMR (126 MHz; $CDCl_3$): δ 140.5, 140.3, 136.9, 129.3, 129.0, 128.0, 127.0, 125.9, 39.3, 35.1, 34.2; EI-MS (70 eV) *m/z* (%): 402 (100, M^+), 369 (23), 338 (25), 217 (14), 119 (29); HRMS Calc'd for $C_{26}H_{26}S_2$: 402.1475, found 402.1479.

Belta[2.2](1,3)(1,3)[2](5)(1)[2](3)(5)benzeno<3>phane-1,9-diene (42)

To a well-stirred solution of **40** (0.98 g, 2.4 mmol) in CH_2Cl_2 (200 mL) was added Borch reagent (1.18 g, 7.3 mmol). After 10 h the reaction mixture was concentrated *in vacuo*, quenched with ethyl acetate (5 mL) and suction filtered, to yield (after drying *in vacuo*) a white solid (1.41 g) that was suspended in THF (200 mL). KO-*t*-Bu (1.37 g, 12.2 mmol) was added and the mixture was stirred vigorously. After 3.5 h, saturated aqueous NH_4Cl solution (5 mL) was added, and the mixture was concentrated *in vacuo*. The residue was dissolved in CH_2Cl_2 (75 mL) and H_2O (25 mL), and the aqueous layer was extracted with CH_2Cl_2 (30 mL). The organic extracts were combined and washed with H_2O (50 mL) and saturated aqueous NaCl solution (50 mL), dried over $MgSO_4$ and concentrated *in vacuo*.

The residue was passed through a plug of silica gel using $CHCl_3$ to yield the isomeric mixture **41** (0.92 g, 2.1 mmol, 88% crude from **40**) as a light yellow solid.

The solid was dissolved in CH_2Cl_2 (200 mL) and Borch reagent (1.04 g, 6.4 mmol) was added dropwise over 5 min, while the mixture was stirred vigorously. After 2 h the mixture was concentrated *in vacuo*, quenched with ethyl acetate (5 mL) and methanol (1 mL) and concentrated again. The residue was slurried into THF (200 mL) and HO-*t*-Bu (2 mL) and KO-*t*-Bu (1.20 g, 10.7 mmol) were added. The mixture was stirred vigorously for 3.5 h and the reaction was quenched with saturated aqueous NH_4Cl solution (5 mL). The reaction mixture was concentrated and CH_2Cl_2 (50 mL) and H_2O (25 mL) was added. The aqueous layer was extracted with CH_2Cl_2 (40 mL), the organic extracts were combined and washed with H_2O (25 mL) and saturated aqueous NaCl solution (20 mL), dried ($MgSO_4$), concentrated and subjected to column chromatography (SiO_2, 25% $CHCl_3$/hexanes) to yield **42** (0.50 g, 1.4 mmol, 61% from **40**) as a colorless crystalline solid: mp 204 –205 °C (chloroform / hexanes); ^{1}H NMR (500.1 MHz; $CDCl_3$): δ 7.67 (s, 2H), 7.16 (t, J = 7.5 Hz, 1H), 7.11 (s, 4H), 6.96 (d, J = 7.5 Hz, 2H), 6.27 (s, 4H), 5.95 (s, 1H), 2.81 (m, 4H), 2.71 (m, 4H); ^{13}C NMR (126 MHz; $CDCl_3$): δ 140.3, 137.1, 135.6, 135.5, 132.6, 131.4, 128.0, 125.6, 125.5, 36.3, 35.5; EI-MS (70 eV) *m/z* (%): 334 (36, M^+), 229 (100), 215 (67); HRMS Calc'd for $C_{26}H_{22}$: 334.1720, found 334.1726.

[2]Metacyclo[2](2,7)pyrenophane (5)

To a solution of **42** (0.26 g, 0.78 mmol) in degassed benzene (20 mL) was added a solution of DDQ (0.19 g, 0.86 mmol) in degassed benzene (5 mL) over 10 min. The reaction mixture was stirred for an additional 5 min, concentrated *in vacuo* and the residue was filtered over a plug of silica using $CHCl_3$ to yield **5** (0.25g, 0.75 mmol, 97%) as a crystalline slightly yellow solid, that could be recrystallized from heptanes: mp: 184 –186 °C (chloroform); ^{1}H NMR (500.1 MHz; $CDCl_3$): δ 7.68 (s, 2H), 7.47 (s, 2H), 7.32 (s, 2H), 7.15 (s, 2H), 6.56 (t, *J* = 7.5 Hz, 1H), 6.31 (d, *J* = 7.5 Hz, 2H), 4.18 (s, 1H), 3.09 (ddd, *J* = 13.0 Hz, *J* = 1.9 Hz, *J* = 5.8 Hz, 2H), 2.69 (ddd, *J* = 13.0 Hz, *J* = 5.3 Hz, *J* = 13.3 Hz, 2H), 2.31 (ddd, *J* unresolved, 2H), 1.21 (ddd, *J* = 13.3 Hz, *J* = 5.8 Hz, *J* = 13.9 Hz, 2H); ^{13}C NMR (126 MHz; $CDCl_3$): δ 137.4, 134.0, 133.0, 131.3, 130.3, 129.8, 129.4, 127.9, 126.2, 126.0, 125.1, 125.1, 38.0, 35.3; EI-MS (70 eV) *m/z* (%): 332 (100, M^+), 317 (10), 228 (97), 213 (8), 202 (7), 166 (17); HRMS Calc'd for $C_{26}H_{20}$: 332.1564, found 332.1562.

5.5 References

(1) Calculations were performed using version 5.0a37 of the Chem3D Pro package of software (MOPAC, AM1, closed shell).

(2) In Section 1.4 a more detailed discussion of AM1 calculations on [*n*](2,7)pyrenophanes can be found.

(3) Bodwell, G. J.; Fleming, J. J.; Mannion, M. R.; Miller, D. O. *J. Org. Chem.* **2000**, *65*, 5360-5370.

(4) Bodwell, G. J.; Fleming, J. J.; Miller, D. O. *Tetrahedron* **2001**, *57*, 3577-3585.

(5) *Cyclophanes, Vols. 1 and 2*; Keehn, P. M., Rosenfeld, S. M., eds.; Academic Press: New York, 1983.

(6) Brown, C. J.; Farthing, A. C. *Nature* **1949**, *164*, 915-916.

(7) Brown, C. J. *J. Chem. Soc.* **1953**, 3265-3270.

(8) De Meijere, A.; König, B. *Synlett* **1997**, 1221-1232.

(9) Brown, C. J. *J. Chem. Soc.* **1953**, 3278-3285.

(10) Gantzel, P. K.; Trueblood, K. N. *Acta Crystallogr.* **1965**, *18*, 958-968.

(11) Cram, D. J.; Helgeson, R. C.; Lock, D.; Singer, L. A. *J. Am. Chem. Soc.* **1966**, *88*, 1324-1325.

(12) Irngartinger, H.; Kirrstetter, R. G. H.; Krieger, C.; Rodewald, H.; Staab, H. A. *Tetrahedron Lett.* **1977**, 1425-1428.

(13) Mitchell, R. H.; Carruthers, R. J.; Zwinkels, J. C. M. *Tetrahedron Lett.* **1976**, 2585-2588.

(14) Umemoto, T.; Satani, S.; Sakata, K.; Misumi, S. *Tetrahedron Lett.* **1975**, 3159-3162.

(15) Wynberg, H. E.; Fawcett, F. S.; Mochel, W. E.; Theobald, C. W. *J. Am. Chem. Soc.* **1960**, *83*, 1428-1435.

(16) Pellegrin, M. *Recl. Trav. Chim. Pays-Bas* **1899**, *18*, 457.

(17) Baker, W.; McOmie, J. F. W.; Norman, J. M. *J. Chem. Soc.* **1951**, 1114-1118.

(18) Burri, K.; Jenny, W. *Helv. Chim. Acta* **1967**, *50*, 1978-1993.

(19) Flammang, R.; Figeys, H. P.; Martin, R. H. *Tetrahedron* **1968**, *24*, 1171-1185.

(20) Vögtle, F.; Schunder, L. *Chem. Ber.* **1969**, *102*, 2677-2683.

(21) Vögtle, F. *Angew. Chem., Int. Ed. Engl.* **1969**, *8*, 274.

(22) Mitchell, R. H. *Heterocycles* **1978**, *11*, 563-586.

(23) Bodwell, G. J.; Houghton, T. J.; Koury, H. E.; Yarlagadda, B. *Synlett* **1995**, 751-752.

(24) Tsuji, J. *Palladium Reagents and Catalysts*; Wiley: New York, 1995.

(25) Stang, P. J.; Diederich, F. *Modern Cross-Coupling Reactions*; VCH: Weinheim, 1997.

(26) Ritter, K. *Synthesis* **1993**, 735-762.

(27) De Meijere, A.; Meyer, F. E. *Angew. Chem., Int. Ed. Engl.* **1994**, *33*, 2379-2411.

(28) Mannion, M. R. Ph.D. Dissertation, Memorial University of Newfoundland, **1999**.

(29) Houghton, T. J. Ph.D. Dissertation, Memorial University of Newfoundland, **1999**.

(30) Boekelheide, V.; Hollins, R. A. *J. Am. Chem. Soc.* **1973**, *95*, 3201-3208.

(31) Jessup, P. J.; Reiss, J. A. *Aust. J. Chem.* **1977**, *30*, 843-850.

(32) Bodwell, G. J.; Bridson, J. N.; Houghton, T. J.; Kennedy, J. W. J.; Mannion, M. R. *Angew. Chem., Int. Ed. Engl.* **1996**, *35*, 1320-1321.

(33) Bodwell, G. J.; Bridson, J. N.; Houghton, T. J.; Kennedy, J. W. J.; Mannion, M. R. *Chem. Eur. J.* **1999**, *5*, 1823-1827.

(34) The crystallographic numbering shown differs from the systematic numbering. The crystallographic data for **3** can be found in Appendix F.

(35) The crystallographic numbering shown differs from the systematic numbering. The crystallographic data for **5** can be found in Appendix G.

(36) Wilson, D. J.; Boekelheide, V.; Griffin Jr., R. W. *J. Am. Chem. Soc.* **1960**, *82*, 6302-6304.

(37) Calder, I. C.; Garratt, P. J. *J. Chem. Soc. (B)* **1967**, 660-662.

(38) Mannschreck, A.; Rissmann, G.; Vögtle, F.; Wild, D. *Chem. Ber.* **1967**, *100*, 335-346.

(39) Balch, A. L.; Catalano, V. J.; Lee, J. W.; Olmstead, M. M.; Parkin, S. R. *J. Am. Chem. Soc.* **1991**, *113*, 8953-8955.

(40) Takahashi, S.; Kuroyama, Y.; Sonogashira, K.; Hagihara, N. *Synthesis* **1980**, 627-630.

Appendix A

Table A-1a: NMR Data for 6,15-disubstituted *syn*-2,11-dithia[3.3]metacyclophanes and 5-substituted *meta*-xylenes in C_6D_6.

Compound	$\delta H_i^{cyclophane}$	$\delta H_e^{cyclophane}$	δH_i^{xylene}	δH_e^{xylene}	$\Delta\delta H_i$	$\Delta\delta H_e$
(a)	*	*				
(b)	6.59	6.78	6.85	6.90	0.26	0.12
(c)	6.51	6.83	6.51	7.02	0.00	0.19
(d)	6.97	7.69	6.82	7.93	-0.15	0.24
(e)	*	*				
(f)	6.50	6.60	6.72	6.72	0.22	0.12
(g)	*	*				
(h)	6.05	6.09	6.40	6.06	0.35	-0.03
(i)	*	*				
(j)	6.39	6.72	6.60	6.74	0.21	0.02
(k)	*	*				
(l)	6.37	6.48	6.53	6.59	0.16	0.11
(m)	*	*				
(n)	**	**				
(o)	6.56	7.68	6.59	6.89	0.03	0.21
(p) ***	6.80	6.85	6.65	7.14	-0.15	0.29
(q)	*	*				

Table A-1b: NMR Data for 6,15-disubstituted *syn*-2,11-dithia[3.3]metacyclophanes and 5-substituted *meta*-xylenes in $CDCl_3$.

Compound	$\delta H_i^{cyclophane}$	$\delta H_e^{cyclophane}$	δH_i^{xylene}	δH_e^{xylene}	$\Delta\delta H_i$	$\Delta\delta H_e$
(a) ****	7.32	7.19	7.23	7.28	-0.09	0.09
(b)	6.86	6.95	6.98	7.01	0.12	0.06
(c)	6.97	7.07	6.91	7.14	-0.06	0.07
(d)	7.24	7.51	7.19	7.67	-0.05	0.15
(e)	*	*				
(f)	6.63	6.74	6.84	6.84	0.21	0.10
(g)	6.19	6.37	6.43	6.35	0.24	-0.02
(h)	6.68	7.15	6.67	7.19	-0.01	0.04
(i) ****	7.71	7.50	7.33	7.86	-0.38	0.36
(j)	6.75	6.72	6.88	6.71	0.13	-0.01
(k)	6.51	6.44	6.60	6.47	0.09	0.03
(l)	6.51	6.49	6.61	6.54	0.10	0.05
(m)	6.93	6.99	7.03	7.03	0.10	0.04
(n)	6.79	6.86	6.76	6.89	-0.03	0.03
(o)	6.80	6.79	6.78	6.90	-0.02	0.11
(p) ***	7.33/7.31	7.12	7.13	7.27	-0.19	0.15
(q)	7.67	7.50	7.30	7.58	-0.37	0.08

Table A-1c: NMR Data for 6,15-disubstituted *syn*-2,11-dithia[3.3]metacyclophanes and 5-substituted *meta*-xylenes in DMSO-d_6.

Compound	$\delta H_i^{cyclophane}$	$\delta H_e^{cyclophane}$	δH_i^{xylene}	δH_e^{xylene}	$\Delta\delta H_i$	$\Delta\delta H_e$
(a) ****	****	****	7.47	7.38		
(b)	7.08	6.84	7.00	6.97	-0.08	0.13
(c)	7.21	7.01	7.01	7.20	-0.20	0.19
(d)	7.45	7.36	7.29	7.58	-0.16	0.22
(e)	7.41	7.37	7.25	7.56	-0.16	0.19
(f)	6.79	6.64	6.78	6.78	-0.01	0.14
(g)	5.93	6.21	6.14	6.17	0.21	-0.04
(h)	6.68	7.15	6.67	7.19	-0.01	0.04
(i) ****	****	****	7.51	7.88		
(j)	7.00	6.61	6.90	6.74	-0.10	0.13
(k)	*****	*****	6.41	6.37		
(l)	6.68	6.41	6.57	6.55	-0.11	0.14
(m)	7.18	6.81	7.09	7.00	-0.09	0.19
(n)	6.88	6.80	6.75	6.90	-0.13	0.10
(o)	6.97	6.71	6.77	6.87	-0.20	0.16
(p) ***	7.43	7.09	7.17	7.28	-0.26	0.19
(q)	7.66	7.35	7.39	7.56	-0.27	0.21

* Compound not soluble enough to collect a ^{1}H NMR spectrum.

** Overlap of the signals with the signals of an unidentified impurity does not allow for unambiguous assignment.

*** Mixture of diastereomers. Average values are given for $\delta H_i^{cyclophane}$ and $\delta H_e^{cyclophane}$.

**** Impurity present.

***** Not enough material available to obtain spectrum of reasonable quality.

Table A-2: Values for Hammett's σ_m {Isaacs 1987 533 /id} and for the dual parameter systems of Taft (σ_I and σ^0_R) {Isaacs 1987 533 /id} and Swain and Lupton ($\mathcal{F}$ and $\mathcal{R}$). {Carroll 1998 772 /id} {Isaacs 1987 533 /id}

Compound	Hammett	Taft		Swain / Lupton	
	σ_m	σ_I	σ^0_R	$\mathcal{F}$	$\mathcal{R}$
(a)	0.62	0.52	0.14	0.90	0.71
(b)	0	0	0	0	0
(c)	0.37	0.45	-0.16	0.72	-0.18
(d)	0.35	0.31	0.15	0.47	0.67
(e)	0.35	0.31	0.15	0.44	0.66
(f)	-0.06	-0.05	-0.10	-0.01	-0.41
(g)	-0.09	0.1	-0.48	0.38	-2.52
(h)	0.14	0.26	-0.22	0.77	-1.43
(i)	0.71	0.64	0.19	1	1
(j)	0.39	*	*	0.70	-0.04
(k)	0.13	0.27	-0.44	0.46	-1.89
(l)	0.10	0.26	-0.41	0.54	-1.68
(m)	*	*	*	0.53	0.68
(n)	*	*	*	0.52	-0.26
(o)	0.14	0.19	-0.17	0.68	-1.30
(p)	0.21	0.25	0.00	0.80	0.45
(q)	0.64	0.64	0.12	0.88	0.55

* No literature value available.

Appendix B

Figure B-1a: $\Delta\delta H_e$ measured in $CDCl_3$ solutions versus $\sigma = \sigma_I + \alpha\sigma^o_R$ (Taft's system for $\alpha = 0.5, 1.0, 1.5, 2.0, 2.5, 3.0, 3.5$ and 4.0).

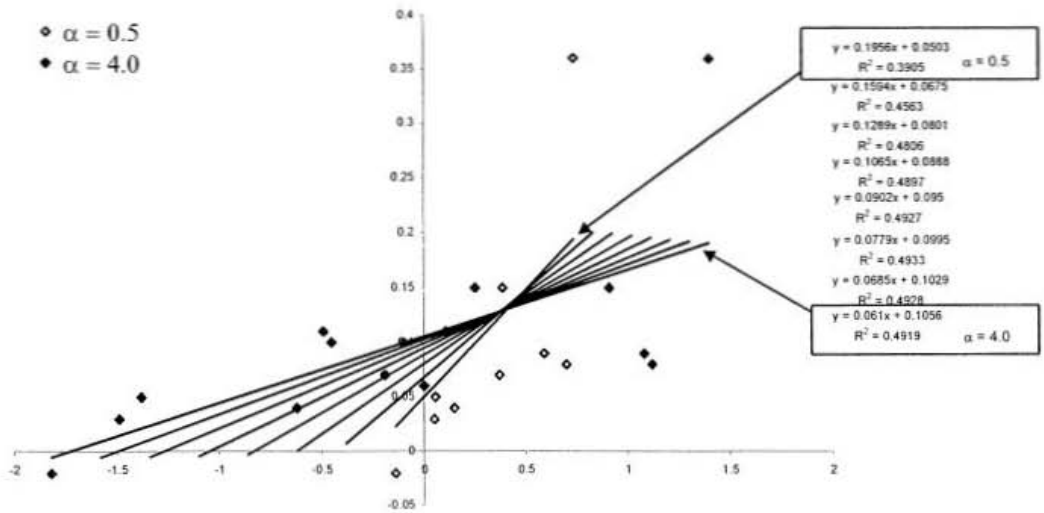

Figure B-1b: $\Delta\delta H_i$ measured in C_6D_6 solutions versus $\sigma = \sigma_I + \alpha\sigma^o_R$ (Taft's system for $\alpha = 0.5, 1.0, 1.5, 2.0, 2.5, 3.0, 3.5$ and 4.0).

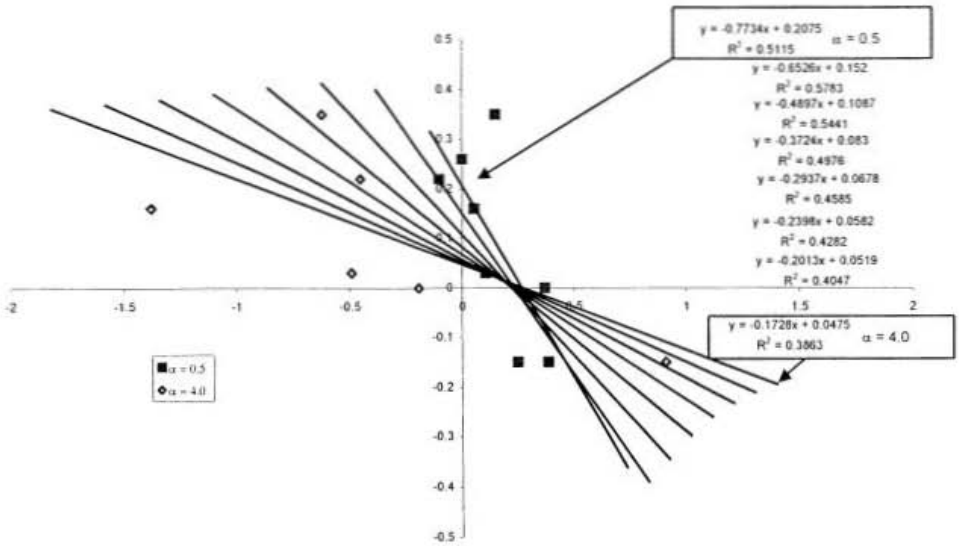

Figure B-1c: $\Delta\delta H_e$ measured in C_6D_6 solutions versus $\sigma = \sigma_I + \alpha\sigma^o_R$ (Taft's system for α = 0.5, 1.0, 1.5, 2.0, 2.5, 3.0, 3.5 and 4.0).

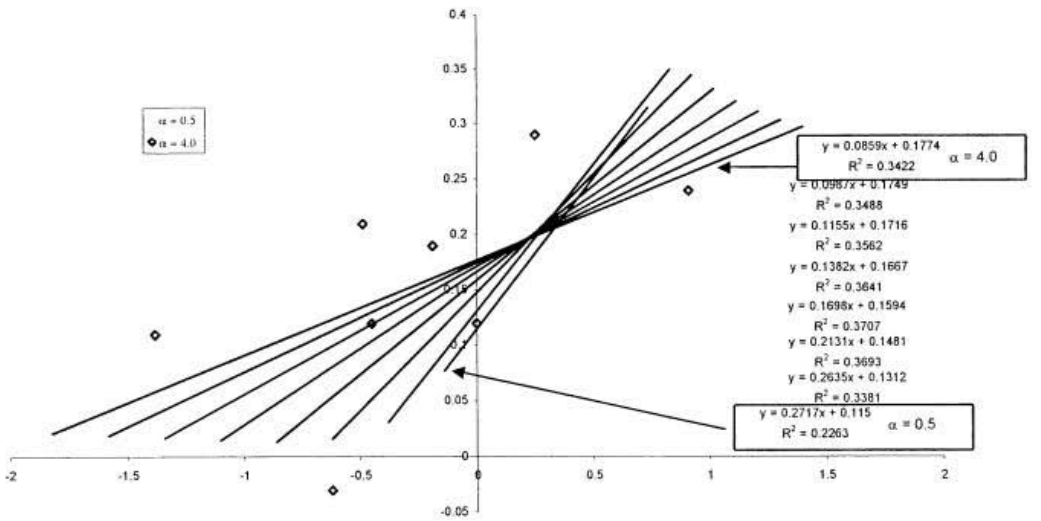

Figure B-1d: $\Delta\delta H_i$ measured in DMSO-d_6 solutions versus $\sigma = \sigma_I + \alpha\sigma^o_R$ (Taft's system for α = 0.5, 1.0, 1.5, 2.0, 2.5, 3.0, 3.5 and 4.0).

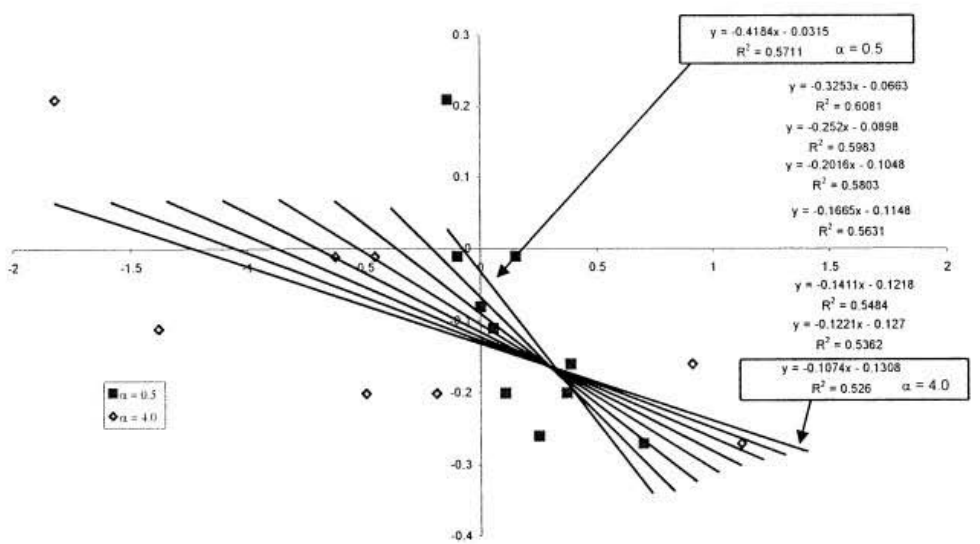

Figure B-1e: $\Delta\delta H_e$ measured in DMSO-d_6 solutions versus $\sigma = \sigma_I + \alpha\sigma^o_R$ (Taft's system for α = 0.5, 1.0, 1.5, 2.0, 2.5, 3.0, 3.5 and 4.0).

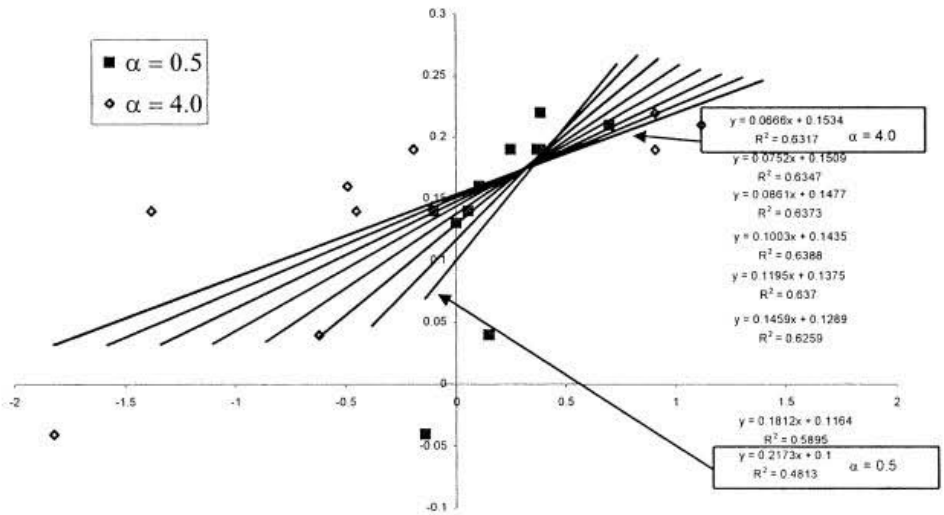

Figure B-2a: $\Delta\delta H_e$ measured in $CDCl_3$ solutions versus $\sigma = f\mathcal{F} + r\mathcal{R}$ (Swain and Lupton's system for f / r = 0.90/0.10, 0.85/0.15, 0.80/0.20, 0.75/0.25, 0.70/0.30, 0.65/0.35 and 0.60/0.40).

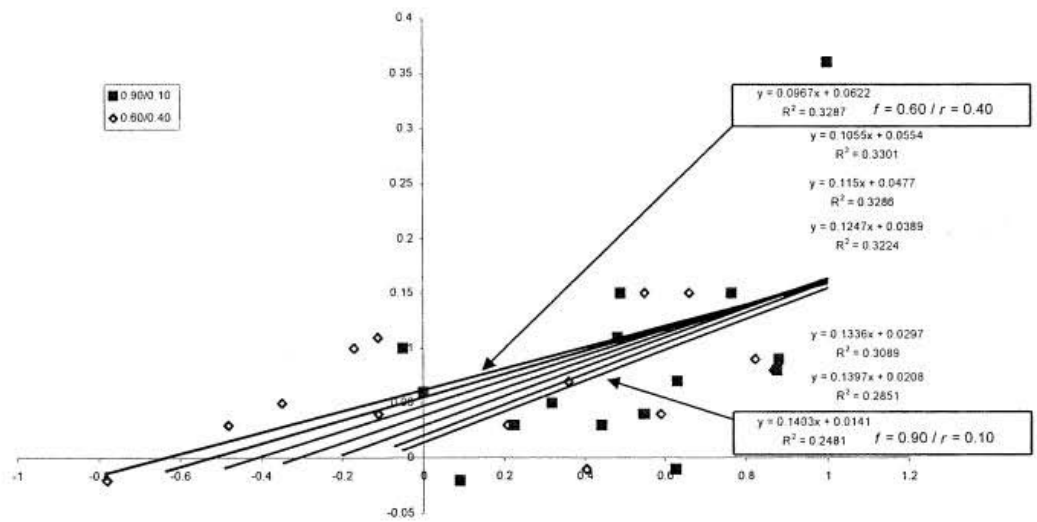

Figure B-2b: $\Delta\delta H_i$ measured in C_6D_6 solutions versus $\sigma = f\mathcal{F} + r\mathcal{R}$ (Swain and Lupton's system for f / r = 0.90/0.10, 0.85/0.15, 0.80/0.20, 0.75/0.25, 0.70/0.30, 0.65/0.35 and 0.60/0.40).

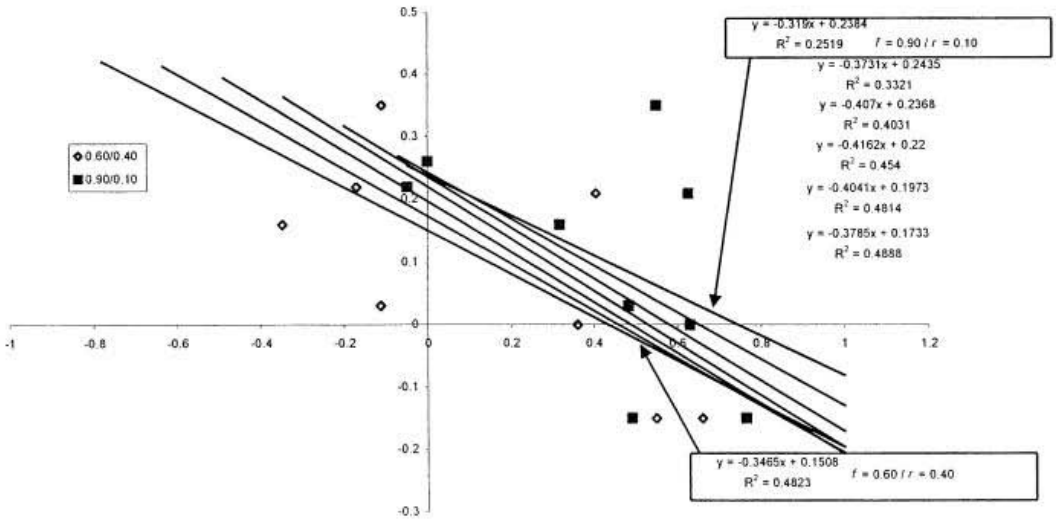

Figure B-2c: $\Delta\delta H_e$ measured in C_6D_6 solutions versus $\sigma = f\mathcal{F} + r\mathcal{R}$ (Swain and Lupton's system for f / r = 0.90/0.10, 0.85/0.15, 0.80/0.20, 0.75/0.25, 0.70/0.30, 0.65/0.35, 0.60/0.40, 0.55/0.45 and 0.50/0.50).

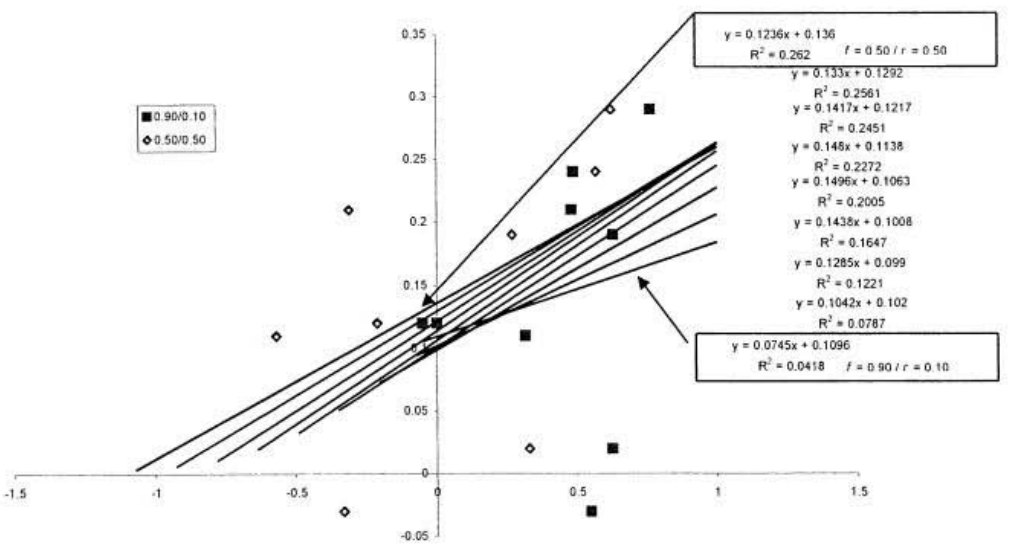

Figure B-2d: $\Delta\delta H_i$ measured in DMSO-d_6 solutions versus $\sigma = f\mathcal{F} + r\mathcal{R}$ (Swain and Lupton's system for f / r = 0.90/0.10, 0.85/0.15, 0.80/0.20, 0.75/0.25, 0.70/0.30, 0.65/0.35 and 0.60/0.40).

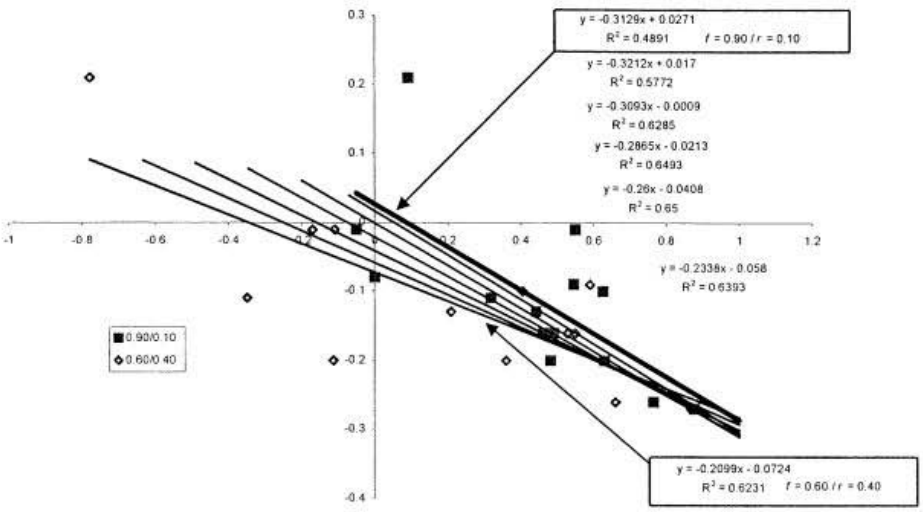

Figure B-2e: $\Delta\delta H_e$ measured in DMSO-d_6 solutions versus $\sigma = f\mathcal{F} + r\mathcal{R}$ (Swain and Lupton's system for f / r = 0.70/0.30, 0.65/0.35, 0.60/0.30, 0.55/0.45, 0.50/0.50, 0.45/0.55, 0.40/0.60, 0.35/0.65 and 0.30/0.70).

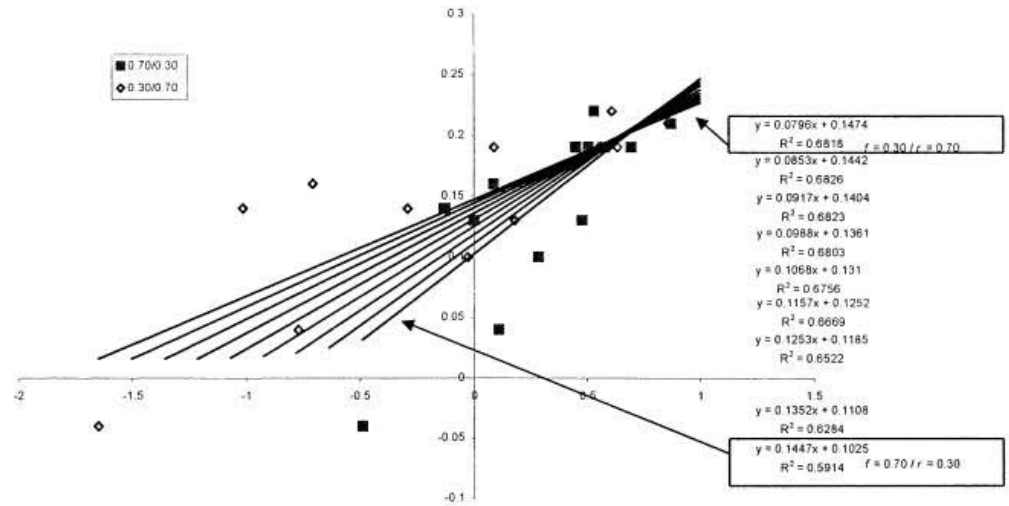

Appendix C

Table C-1: Published group electronegativity moments for substituents of 6.15-disubstituted *syn*-2.11-dithia[3.3]metacyclophanes and AM1 calculated dipole moments for 6.15-disubstituted *syn*-2.11-dithia[3.3]metacyclophanes.

Compound	Published group electronegativity value	Calculated group dipole moment *	
		c,c-4 (cyclophane)	*b,b*-4 (cyclophane)
(a)	3.208	7.294	3.617
(b)	2.176	1.471	2.581
(c)	**	3.901	0.092
(d)	2.832	3.73	0.847
(e)	**	***	***
(f)	2.472	0.953	3.046
(g)	2.992	1.084	4.592
(h)	**	***	***
(i)	3.421	***	***
(j)	3.510	0.151	4.953
(k)	3.494	2.242	1.630
(l)	3.543	1.221	2.687
(m)	**	0.369	3.750
(n)	2.616	2.583	1.255
(o)	2.592	1.380	2.508
(p)	2.841	4.342	1.068
(q)	2.998	9.452	6.763

* Dipole moments were calculated with the same conformation of the substituent for the *c,c* and *b,b* conformer. Conformations were chosen in such a way, that they aligned with the central axis of the molecule.

** No literature value available.

*** Calculations failed to coalesce to a reasonable conformation.

Figure C-1a: $\Delta\delta H_i$ and $\Delta\delta H_e$ measured in C_6D_6 solutions *versus* published group electronegativity moments for substituents R.

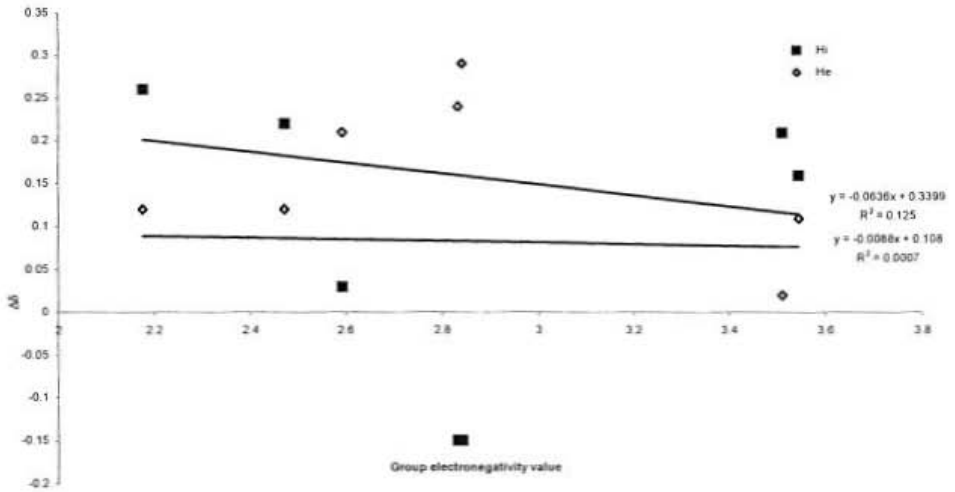

Figure C-1b: $\Delta\delta H_i$ and $\Delta\delta H_e$ measured in $CDCl_3$ solutions *versus* published group electronegativity moments for substituents R.

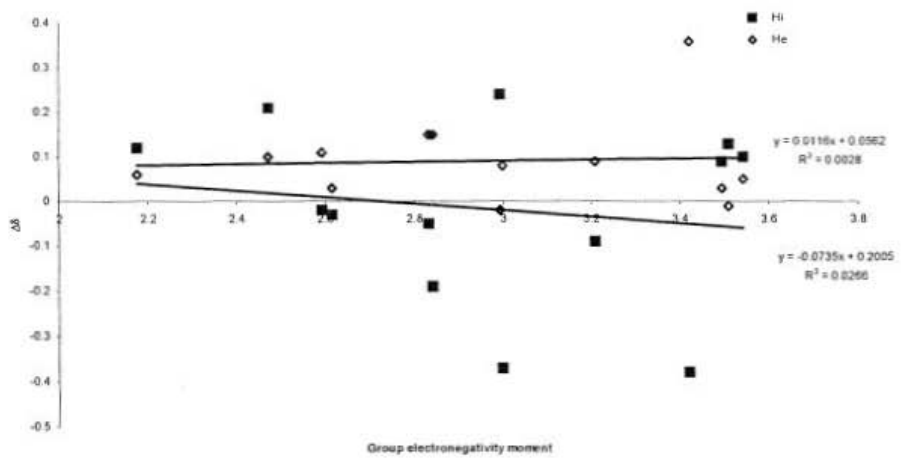

Figure C-1c: $\Delta\delta H_i$ and $\Delta\delta H_e$ measured in DMSO-d_6 solutions *versus* published group electronegativity moments for substituents R.

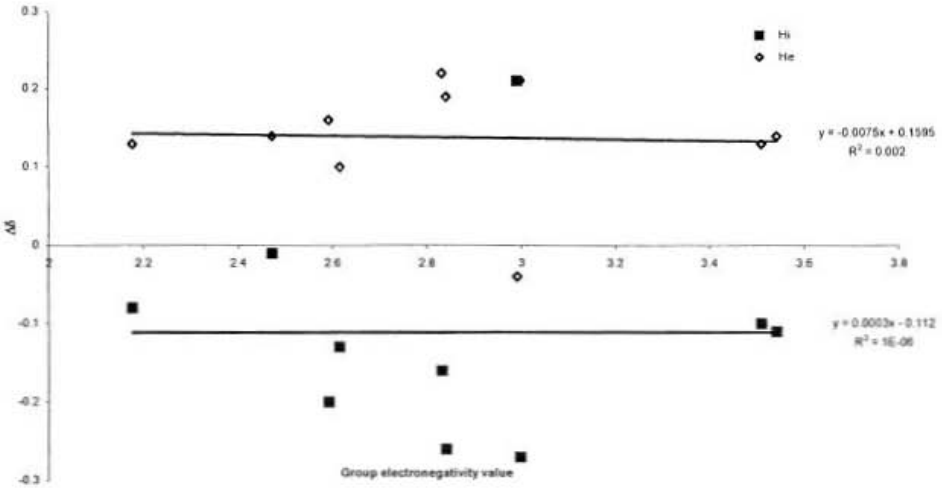

Figure C-2a: $\Delta\delta H_i$ and $\Delta\delta H_e$ measured in C_6D_6 solutions *versus* difference in calculated dipole moments between the *c,c* and *b,b*-conformers.

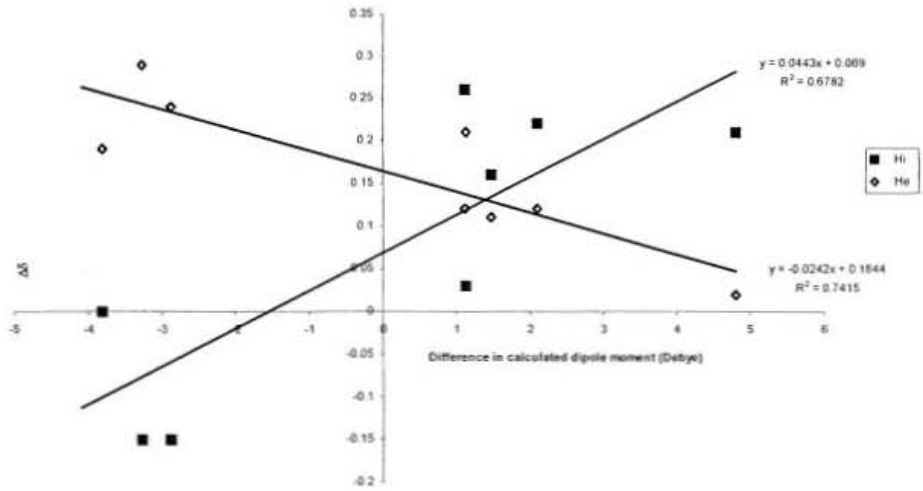

Figure C-2b: $\Delta\delta H_i$ and $\Delta\delta H_e$ measured in $CDCl_3$ solutions *versus* difference in calculated dipole moments between the *c,c* and *b,b*-conformers.

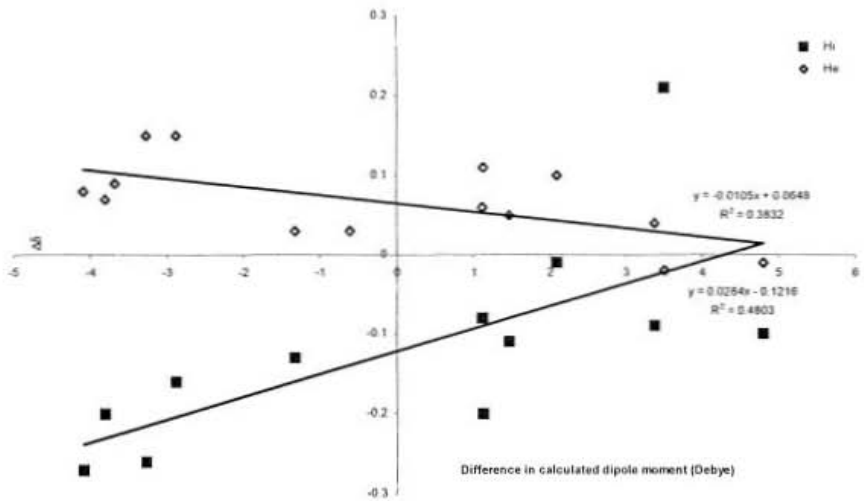

Figure C-2c: $\Delta\delta H_i$ and $\Delta\delta H_e$ measured in DMSO-d_6 solutions *versus* difference in calculated dipole moments between the *c,c* and *b,b*-conformers.

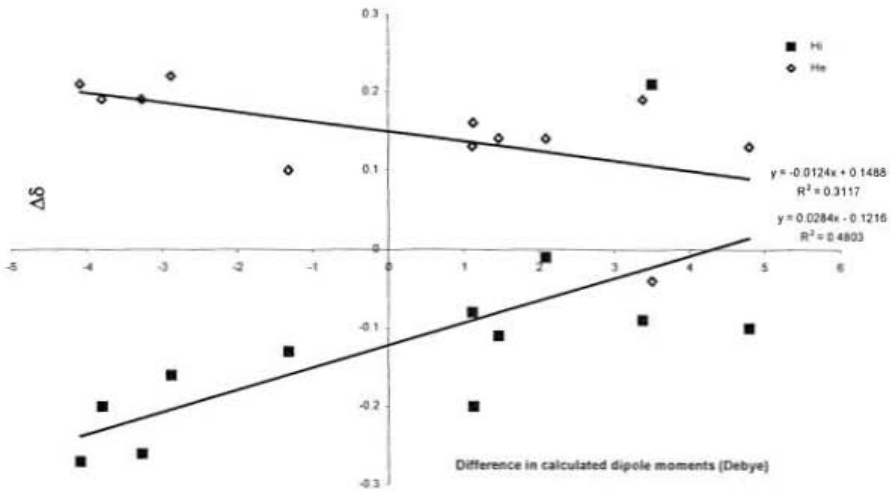

Appendix D

X-ray Structure Report

For
Dr. G. J. Bodwell

Prepared by
David O. Miller

December 3, 1999

Introduction

Collection, solution and refinement all proceeded normally. Hydrogens were introduced in calculated or difference map positions with isotropic thermal parameters set twenty percent greater than those of their bonding partners at the time of their inclusion. The carboxylic acid protons were found in the difference map.

Please acknowledge Dr. Bob McDonald, University of Alberta for data collection.

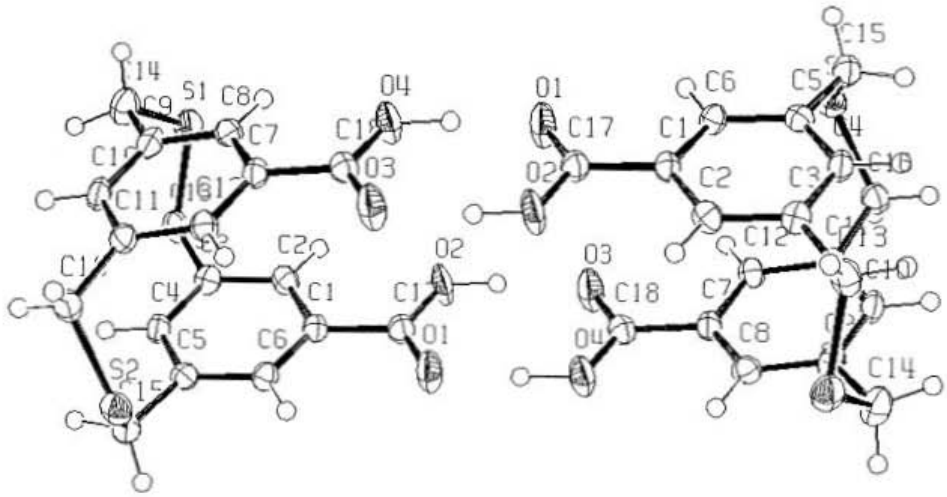
C14
S1
C8
O4
C9
C7
C1
C10
O3
C11
C2
O2
C1
C4
C1
C5
C6
O1
S2
O1
C17
C6
C5
C15
C1
C4
O2
C2
C3
C10
C12
C13
O3
C18
C7
C10
O4
C8
C14

Experimental

Data Collection

A colourless prism crystal of $C_{18}H_{16}O_4S_2$ having approximate dimensions of 0.20 x 0.05 x 0.02 mm was mounted on a glass fiber. All measurements were made on a Bruker P4/CCD system with graphite monochromated Mo-Kα radiation and a rotating anode generator.

Cell constants corresponded to a primitive monoclinic cell with dimensions:

a = 6.8646(4) Å
b = 14.891(1) Å β = 90.263(1)°
c = 15.923(1) Å
V = 1627.7(2) $Å^3$

For Z = 4 and F.W. = 360.44. the calculated density is 1.47 g/cm^3. The systematic absences of:

h0l: h+l ± 2n
0k0: k ± 2n

uniquely determine the space group to be:

$P2_1/n$ (#14)

The data were collected at a temperature of -80 ± 1°C.. The full hemisphere of data was collected with 30s.. 0.3 deg. frames to a maximum 2θ value of 52.8°.

Data Reduction

Of the 8164 reflections which were collected, 3486 were unique (R_{int} = 0.048). The linear absorption coefficient, μ, for Mo-Kα radiation is 3.5 cm^{-1}. The Siemens area detector absorption routine (SADABS) was used to correct the data with maximum and minimum effective transmissions of 0.971679 and 0.559440 respectively. The data were corrected for Lorentz and polarization effects.

Structure Solution and Refinement

The structure was solved by direct methods[1] and expanded using Fourier techniques[2]. The non-hydrogen atoms were refined anisotropically. Hydrogen atoms were included but not refined. The final cycle of full-matrix least-squares refinement[3] on F was based on 2232 observed reflections ($I > 2.00\sigma(I)$) and 217 variable parameters and converged (largest parameter shift was 0.00 times its esd) with unweighted and weighted agreement factors of:

$$R = \Sigma \, ||Fo| - |Fc|| \, / \, \Sigma \, |Fo| = 0.048$$

$$R_w = [\Sigma \, w \, (|Fo| - |Fc|)^2 \, / \, \Sigma \, w \, Fo^2]^{1/2} = 0.043$$

The standard deviation of an observation of unit weight[4] was 1.34. The weighting scheme was based on counting statistics Plots of $\Sigma \, w \, (|Fo| - |Fc|)^2$ versus |Fo|, reflection order in data collection, $\sin\theta/\lambda$ and various classes of indices showed no unusual trends. The maximum and minimum peaks on the final difference Fourier map corresponded to 0.34 and -0.33 $e^-/Å^3$, respectively.

Neutral atom scattering factors were taken from Cromer and Waber[5]. Anomalous dispersion effects were included in Fcalc[6]; the values for $\Delta f'$ and $\Delta f''$ were those of Creagh and McAuley[7]. The values for the mass attenuation coefficients are those of Creagh and Hubbell[8]. All calculations were performed using the teXsan[9] crystallographic software package of Molecular Structure Corporation.

References

(1) SHELX97: Sheldrick, G.M. (1997).

(1) SIR97: Altomare, A., Cascarano, M., Giacovazzo, C., Guagliardi, A. (1993). J. Appl. Cryst., 26, 343.

(2) DIRDIF94: Beurskens, P.T., Admiraal, G., Beurskens, G., Bosman, W.P., de Gelder, R., Israel, R. and Smits, J.M.M.(1994). The DIRDIF-94 program system, Technical Report of the Crystallography Laboratory, University of Nijmegen, The Netherlands.

(3) Least Squares function minimized:

$$\Sigma w(|F_o|-|F_c|)^2$$

(4) Standard deviation of an observation of unit weight:

$$[\Sigma w(|F_o|-|F_c|)^2/(N_o-N_v)]^{1/2}$$

where: N_o = number of observations
N_v = number of variables

(5) Cromer, D. T. & Waber, J. T.; "International Tables for X-ray Crystallography", Vol. IV, The Kynoch Press, Birmingham, England, Table 2.2 A (1974).

(6) Ibers, J. A. & Hamilton, W. C.; Acta Crystallogr., 17, 781 (1964).

(7) Creagh, D. C. & McAuley, W.J .; "International Tables for Crystallography", Vol C, (A.J.C. Wilson, ed.), Kluwer Academic Publishers, Boston, Table 4.2.6.8, pages 219-222 (1992).

(8) Creagh, D. C. & Hubbell, J.H..; "International Tables for Crystallography", Vol C, (A.J.C. Wilson, ed.), Kluwer Academic Publishers, Boston, Table 4.2.4.3, pages 200-206 (1992).

(9) teXsan for Windows: Crystal Structure Analysis Package, Molecular Structure Corporation (1997).

EXPERIMENTAL DETAILS

A. Crystal Data

Empirical Formula	$C_{18}H_{16}O_4S_2$
Formula Weight	360.44
Crystal Color, Habit	colourless, prism
Crystal Dimensions	0.20 X 0.05 X 0.02 mm
Crystal System	monoclinic
Lattice Type	Primitive
Lattice Parameters	a = 6.8646(4) Å b = 14.891(1) Å c = 15.923(1) Å β = 90.263(1) ° V = 1627.7(2) $Å^3$
Space Group	$P2_1/n$ (#14)
Z value	4
D_{calc}	1.471 g/cm^3
F_{000}	752.00
μ(MoKα)	3.46 cm^{-1}

B. Intensity Measurements

Diffractometer	Bruker P4/CCD
Radiation	MoKα (λ = 0.71073 Å) graphite monochromated
Temperature	-80 $\pm$ 1°C
Scan Rate	30s., 0.3 deg. frames
$2\theta_{max}$	52.8°
No. of Reflections Measured	Total: 8164
	Unique: 3486 (R_{int} = 0.048)
Corrections	Lorentz-polarization SADABS correction (trans. factors: 0.971679 – 0.559440)

C. Structure Solution and Refinement

Structure Solution	Direct Methods (SHELX97)
Refinement	Full-matrix least-squares on F
Function Minimized	Σ w (|Fo| - |Fc|)^2
Least Squares Weights	$1/\sigma^2(Fo) = 4Fo^2/\sigma^2(Fo^2$
Anomalous Dispersion	All non-hydrogen atoms
No. Observations (I>2.00σ(I))	2232
No. Variables	217
Reflection/Parameter Ratio	10.29
Residuals: R; Rw	0.048 : 0.043
Goodness of Fit Indicator	1.34
Max Shift/Error in Final Cycle	0.00
Maximum peak in Final Diff. Map	0.34 e^-/A^3
Minimum peak in Final Diff. Map	-0.33 e^-/A^3

Appendix E

X-ray Structure Report

For
Dr. G. J. Bodwell

Prepared by
David O. Miller

April 6, 2001

Introduction

Collection, solution and refinement all proceeded normally. Hydrogen atoms were introduced in calculated or difference map positions with isotropic thermal parameters set twenty percent greater than those of their bonding partners at the time of their inclusion. They were not refined.

The refinement values on this structure are not adequate for publication. There is also a shortage of data due to the presence of two molecules in the asymmetric unit. For this reason most of the atoms are not refined anisotropically.

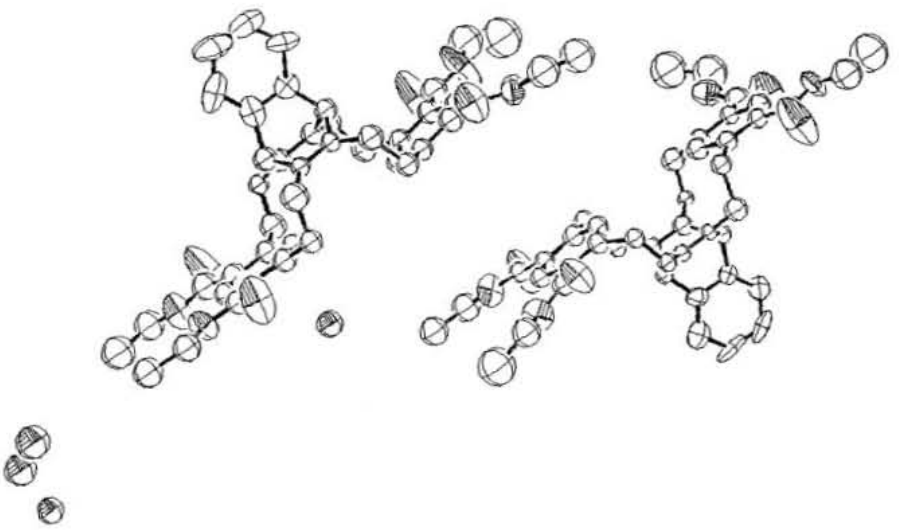

Experimental

Data Collection

A colourless prism crystal of $C_{44}H_{49.50}O_{9.75}$ having approximate dimensions of 0.40 x 0.40 x 0.40 mm was mounted on a glass fiber. All measurements were made on a Rigaku AFC6S diffractometer with graphite monochromated Mo-Kα radiation.

Cell constants and an orientation matrix for data collection, obtained from a least-squares refinement using the setting angles of 21 carefully centered reflections in the range $23.50 < 2\theta < 35.04^{o}$ corresponded to a primitive triclinic cell with dimensions

a = 16.021(2) Å $\quad \alpha = 100.47(2)^{o}$
b = 19.314(3) Å $\quad \beta = 112.29(1)^{o}$
c = 14.232(3) Å $\quad \gamma = 89.61(1)^{o}$
V = 3997(1) $Å^3$

For Z = 4 and F.W. = 734.37, the calculated density is 1.22 g/cm^3. Based on a statistical analysis of intensity distribution, and the successful solution and refinement of the structure, the space group was determined to be

P-1 (#2)

The data were collected at a temperature of 26 ± 1°C using the ω-2θ scan technique to a maximum 2θ value of 45.1°. Omega scans of several intense reflections, made prior to data collection, had an average width at half-height of 0.38° with a take-off angle of 6.0°. Scans of $(1.73 + 0.35 \tan\theta)^{o}$ were made at a speed of 4.0°/min (in ω). The weak reflections ($I < 10.0\sigma(I)$) were rescanned (maximum of 5 scans) and the counts were accumulated to ensure good counting statistics. Stationary background counts were recorded on each side of the reflection. The ratio of peak counting time to background counting time was 2:1. The diameter of the incident beam collimator was 1.0 mm, the crystal to detector distance was 400 mm, and the detector aperture was 6.0 x 3.0 mm (horizontal x vertical).

Data Reduction

Of the 10958 reflections which were collected, 10508 were unique (R_{int} = 0.046). The intensities of three representative reflections were measured after every 150 reflections. No decay correction was applied.

The linear absorption coefficient, μ, for Mo-Kα radiation is 0.9 cm^{-1}. An empirical absorption correction based on azimuthal scans of several reflections was applied which resulted in transmission factors ranging from 0.98 to 1.00. The data were corrected for Lorentz and polarization effects.

Structure Solution and Refinement

The structure was solved by direct methods[1] and expanded using Fourier techniques[2] Some non-hydrogen atoms were refined anisotropically, while the rest were refined isotropically Hydrogen atoms were included but not refined. The final cycle of full-matrix least-squares refinement[3] on F was based on 4835 observed reflections ($I > 2.00\sigma(I)$) and 573 variable parameters and converged (largest parameter shift was 0.00 times its esd) with unweighted and weighted agreement factors of:

$$R = \Sigma \; ||Fo| - |Fc|| \; / \; \Sigma \; |Fo| = 0.168$$

$$R_w = [\Sigma \; w \; (|Fo| - |Fc|)^2 \; / \; \Sigma \; w \; Fo^2]^{1/2} = 0.163$$

The standard deviation of an observation of unit weight[4] was 7.62. The weighting scheme was based on counting statistics and included a factor (p = 0.010) to downweight the intense reflections Plots of $\Sigma \; w \; (|Fo| - |Fc|)^2$ versus |Fo|, reflection order in data collection, $\sin\theta/\lambda$, and various classes of indices showed no unusual trends The maximum and minimum peaks on the final difference Fourier map corresponded to 1.02 and -0.55 e^-/A^3, respectively.

Neutral atom scattering factors were taken from Cromer and Waber[5] Anomalous dispersion effects were included in Fcalc[6]; the values for $\Delta f'$ and $\Delta f''$ were those of Creagh and McAuley[7] The values for the mass attenuation coefficients are those of Creagh and Hubbell[8] All calculations were performed using the teXsan[9] crystallographic software package of Molecular Structure Corporation

References

(1) SHELX97: Sheldrick, G.M. (1997).

(2) DIRDIF94: Beurskens, P.T., Admiraal, G., Beurskens, G., Bosman, W.P., de Gelder, R., Israel, R. and Smits, J.M.M.(1994). The DIRDIF-94 program system, Technical Report of the Crystallography Laboratory, University of Nijmegen, The Netherlands.

(3) Least Squares function minimized:

$\Sigma w(|F_o|-|F_c|)^2$ where

$w = 1/[\sigma^2(Fo)] = [\sigma^2_c(Fo) + p^2Fo^2/4]^{-1}$
$\sigma_c(Fo)$ = e.s.d. based on counting statistics
p = p-factor

(4) Standard deviation of an observation of unit weight:

$[\Sigma w(|F_o|-|F_c|)^2/(N_o-N_v)]^{1/2}$

where N_o = number of observations
N_v = number of variables

(5) Cromer, D. T & Waber, J. T., "International Tables for X-ray Crystallography", Vol. IV. The Kynoch Press, Birmingham, England, Table 2.2 A (1974).

(6) Ibers, J. A. & Hamilton, W. C., Acta Crystallogr., 17, 781 (1964).

(7) Creagh, D. C. & McAuley, W.J.; "International Tables for Crystallography", Vol C, (A.J.C. Wilson, ed.), Kluwer Academic Publishers, Boston, Table 4.2.6.8, pages 219-222 (1992).

(8) Creagh, D. C. & Hubbell, J.H..; "International Tables for Crystallography", Vol C, (A.J.C. Wilson, ed.), Kluwer Academic Publishers, Boston, Table 4.2.4.3, pages 200-206 (1992).

(9) teXsan for Windows version 1.06: Crystal Structure Analysis Package, Molecular Structure Corporation (1997-9).

EXPERIMENTAL DETAILS

A. Crystal Data

Empirical Formula	$C_{44}H_{49.50}O_{9.75}$
Formula Weight	734.37
Crystal Color, Habit	colourless, prism
Crystal Dimensions	0.40 X 0.40 X 0.40 mm
Crystal System	triclinic
Lattice Type	Primitive
No. of Reflections Used for Unit Cell Determination (2θ range)	21 (23.5 - 35.0°)
Omega Scan Peak Width at Half-height	0.38°
Lattice Parameters	a = 16.021(2) Å b = 19.314(3) Å c = 14.232(3) Å α = 100.47(2) ° β = 112.29(1) ° γ = 89.61(1) ° V = 3997(1) $Å^3$
Space Group	P-1 (#2)
Z value	4
D_{calc}	1.220 g/cm^3
F_{000}	1566.00
μ(MoKα)	0.85 cm^{-1}

B. Intensity Measurements

Diffractometer	Rigaku AFC6S
Radiation	MoKα (λ = 0.71069 Å) graphite monochromated
Take-off Angle	6.0°
Detector Aperture	6.0 mm horizontal 3.0 mm vertical
Crystal to Detector Distance	400 mm
Voltage, Current	50kV, 27.5mA
Temperature	26.0°C
Scan Type	ω-2θ
Scan Rate	4.0°/min (in ω) (up to 5 scans)
Scan Width	(1.73 + 0.35 tan θ)°
2θmax	45.1°
No. of Reflections Measured	Total: 10958 Unique: 10508 (R_{int} = 0.046)
Corrections	Lorentz-polarization Absorption (trans. factors: 0.9805 - 1.0000)

C. Structure Solution and Refinement

Structure Solution	Direct Methods (SHELX97)
Refinement	Full-matrix least-squares on F
Function Minimized	Σ w (|Fo| - |Fc|)^2
Least Squares Weights	$1/\sigma^2(Fo) = 4Fo^2/\sigma^2(Fo^2)$
p-factor	0 0100
Anomalous Dispersion	All non-hydrogen atoms
No. Observations (I>2 00σ(I))	4835
No. Variables	573
Reflection/Parameter Ratio	8 44
Residuals. R. Rw	0 168 0 163
Goodness of Fit Indicator	7 62
Max Shift/Error in Final Cycle	0 00
Maximum peak in Final Diff Map	1 02 e$^-$/A^3
Minimum peak in Final Diff Map	-0 55 e$^-$/A^3

Appendix F

X-ray Structure Report

For
Dr. G. J. Bodwell

Prepared by
David O. Miller

January 31, 2001

Introduction

Collection, solution and refinement all proceeded normally. Hydrogen atoms were introduced in calculated positions with isotropic thermal parameters set twenty percent greater than those of their bonding partners at the time of their inclusion. They were optimized by positional refinement but were fixed for the final round of least squares. This structure was refined on F-squared to maximize the data to parameter ratio.

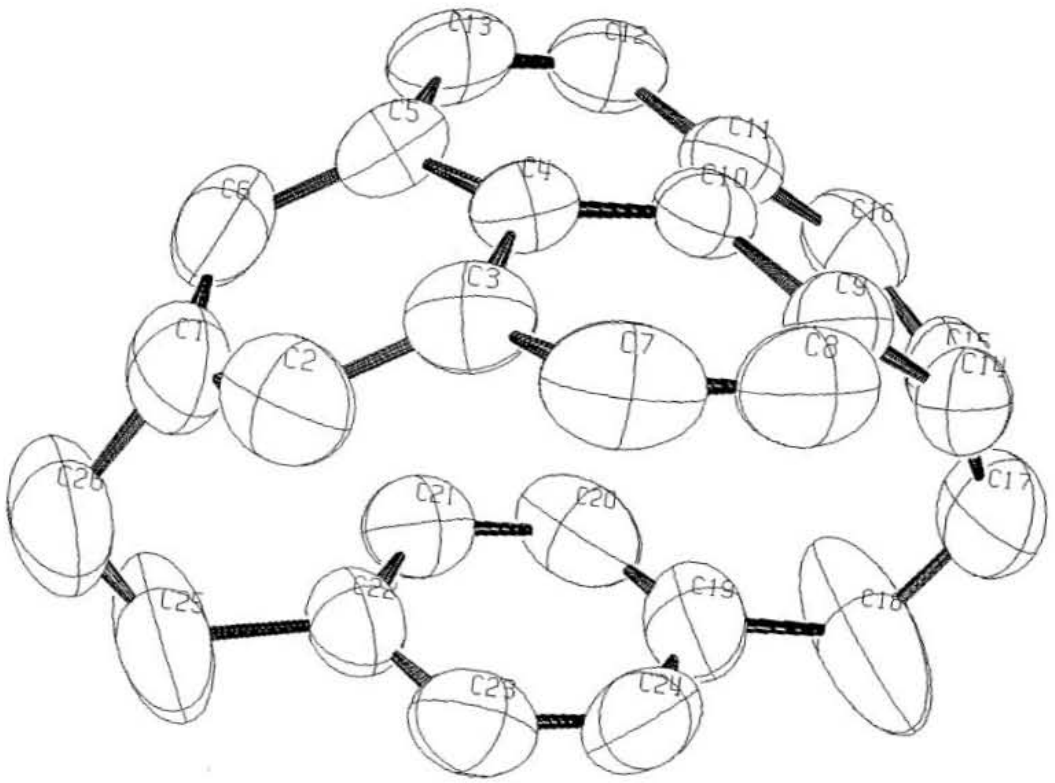
C13
C12
C5
C11
C4
C10
C6
C16
C3
C9
C7
C2
C8
C15
C14
C26
C21
C20
C17
C25
C22
C19
C18
C23
C24

Experimental

Data Collection

A colourless prism crystal of $C_{26}H_{20}$ having approximate dimensions of 0.30 x 0.15 x 0.40 mm was mounted on a glass fiber. All measurements were made on a Rigaku AFC6S diffractometer with graphite monochromated Cu-Kα radiation.

Cell constants and an orientation matrix for data collection, obtained from a least-squares refinement using the setting angles of 25 carefully centered reflections in the range $46.01 < 2\theta < 59.65^{o}$ corresponded to a primitive orthorhombic cell with dimensions.

a = 12.451(2) A
b = 15.773(3) A
c = 9.203(2) A
V = 1807.4(5) A^3

For Z = 4 and F.W. = 332.44, the calculated density is 1.22 g/cm^3. The systematic absences of

h00 h ± 2n
0k0 k ± 2n
00l l ± 2n

uniquely determine the space group to be

$P2_12_12_1$ (#19)

The data were collected at a temperature of 26 ± 1°C using the ω-2θ scan technique to a maximum 2θ value of 120.0°. Omega scans of several intense reflections, made prior to data collection, had an average width at half-height of 0.27° with a take-off angle of 6.0°. Scans of $(0.84 + 0.14 \tan\theta)^{o}$ were made at a speed of 4.0°/min (in ω). The weak reflections ($I < 10.0\sigma(I)$) were rescanned (maximum of 5 scans) and the counts were accumulated to ensure good counting statistics. Stationary background counts were recorded on each side of the reflection. The ratio of peak counting time to background counting time was 2:1. The diameter of the incident beam collimator was 1.0 mm, the crystal to detector distance was 400 mm, and the detector aperture was 4.5 x 3.0 mm (horizontal x vertical).

Data Reduction

A total of 1577 reflections were collected. The intensities of three representative reflections were measured after every 150 reflections. No decay correction was applied.

The linear absorption coefficient, μ, for Cu-Kα radiation is 5.2 cm^{-1}. An empirical absorption correction based on azimuthal scans of several reflections was applied which resulted in transmission factors ranging from 0.93 to 1.00. The data were corrected for Lorentz and polarization effects. A correction for secondary extinction was applied (coefficient = 1.79589e-005).

Structure Solution and Refinement

The structure was solved by direct methods[1] and expanded using Fourier techniques[2]. The non-hydrogen atoms were refined anisotropically. The final cycle of full-matrix least-squares refinement[3] on F^2 was based on 1556 observed reflections and 284 variable parameters and converged (largest parameter shift was 0.00 times its esd) with unweighted and weighted agreement factors of:

$$R1 = \Sigma \; ||Fo| - |Fc|| \; / \; \Sigma \; |Fo| = 0.059$$

$$wR2 = [\; \Sigma \; (\; w \; (Fo^2 - Fc^2)^2 \;) / \; \Sigma \; w(Fo^2)^2]^{1/2} = 0.085$$

The standard deviation of an observation of unit weight[4] was 1.84. The weighting scheme was based on counting statistics and included a factor ($p = 0.010$) to downweight the intense reflections. Plots of $\Sigma \; w \; (|Fo| - |Fc|)^2$ versus $|Fo|$, reflection order in data collection, $\sin \theta/\lambda$, and various classes of indices showed no unusual trends. The maximum and minimum peaks on the final difference Fourier map corresponded to 0.18 and -0.21 e^-/A^3, respectively.

Neutral atom scattering factors were taken from Cromer and Waber[5]. Anomalous dispersion effects were included in Fcalc[6]; the values for $\Delta f'$ and $\Delta f''$ were those of Creagh and McAuley[7]. The values for the mass attenuation coefficients are those of Creagh and Hubbell[8]. All calculations were performed using the teXsan[9] crystallographic software package of Molecular Structure Corporation.

References

(1) SIR92: Altomare, A., Cascarano, M., Giacovazzo, C., Guagliardi, A. (1994). J. Appl. Cryst., 26, 343.

(2) DIRDIF94: Beurskens, P.T., Admiraal, G., Beurskens, G., Bosman, W.P., de Gelder, R., Israel, R. and Smits, J.M.M.(1994). The DIRDIF-94 program system, Technical Report of the Crystallography Laboratory, University of Nijmegen, The Netherlands.

(3) Least Squares function minimized:

$\Sigma w(F_o^2-F_c^2)^2$ where

$w = 1/[\sigma^2(Fo)] = [\sigma^2_c(Fo) + p^2Fo^2/4]^{-1}$
$\sigma_c(Fo)$ = e.s.d. based on counting statistics
p = p-factor

(4) Standard deviation of an observation of unit weight:

$[\Sigma w(F_o^2-F_c^2)^2/(N_o-N_v)]^{1/2}$

where N_o = number of observations
N_v = number of variables

(5) Cromer, D. T. & Waber, J. T., "International Tables for X-ray Crystallography", Vol. IV. The Kynoch Press, Birmingham, England, Table 2.2.A (1974).

(6) Ibers, J. A. & Hamilton, W. C., Acta Crystallogr., 17, 781 (1964).

(7) Creagh, D. C. & McAuley, W.J., "International Tables for Crystallography", Vol C. (A.J.C. Wilson, ed.), Kluwer Academic Publishers, Boston, Table 4.2.6.8, pages 219-222 (1992).

(8) Creagh, D. C. & Hubbell, J.H.., "International Tables for Crystallography", Vol C. (A.J.C. Wilson, ed.), Kluwer Academic Publishers, Boston, Table 4.2.4.3, pages 200-206 (1992).

(9) teXsan for Windows version 1.06: Crystal Structure Analysis Package, Molecular Structure Corporation (1997-9).

EXPERIMENTAL DETAILS

A. Crystal Data

Empirical Formula	$C_{26}H_{20}$
Formula Weight	332.44
Crystal Color, Habit	colourless, prism
Crystal Dimensions	0.30 X 0.15 X 0.40 mm
Crystal System	orthorhombic
Lattice Type	Primitive
No. of Reflections Used for Unit Cell Determination (2θ range)	25 (46.0 - 59.7°)
Omega Scan Peak Width at Half-height	0.27°
Lattice Parameters	a = 12.451(2) A b = 15.773(3) A c = 9.203(2) A V = 1807.4(5) A^3
Space Group	$P2_12_12_1$ (#19)
Z value	4
D_{calc}	1.222 g/cm^3
F_{000}	704.00
μ(CuKα)	5.20 cm^{-1}

B. Intensity Measurements

Diffractometer	Rigaku AFC6S
Radiation	CuKα (λ = 1.54178 Å) graphite monochromated
Take-off Angle	6.0°
Detector Aperture	4.5 mm horizontal 3.0 mm vertical
Crystal to Detector Distance	400 mm
Voltage, Current	50kV, 27.5mA
Temperature	26.0°C
Scan Type	ω-2θ
Scan Rate	4.0°/min (in ω) (up to 5 scans)
Scan Width	(0.84 + 0.14 tan θ)°
$2\theta_{max}$	120.0°
No. of Reflections Measured	Total: 1577
Corrections	Lorentz-polarization Absorption (trans. factors: 0.9261 - 1.0000) Secondary Extinction (coefficient: 1.79589e-005)

C. Structure Solution and Refinement

Structure Solution	Direct Methods (SIR92)
Refinement	Full-matrix least-squares on F^2
Function Minimized	$\Sigma w (Fo^2 - Fc^2)^2$
Least Squares Weights	$1/\sigma^2(Fo) = 4Fo^2/\sigma^2(Fo^2)$
p-factor	0 0100
Anomalous Dispersion	All non-hydrogen atoms
No. Observations (I>0 00σ(I))	1556
No. Variables	284
Reflection/Parameter Ratio	5 48
Residuals: R1, wR2	0 059 ; 0.085
Goodness of Fit Indicator	1 84
Max Shift/Error in Final Cycle	0 00
Maximum peak in Final Diff. Map	0 18 e^-/A^3
Minimum peak in Final Diff. Map	-0.21 e^-/A^3

Appendix G

X-ray Structure Report

For
Dr G J. Bodwell

Prepared by
David O Miller

March 13, 2001

Introduction

Collection, solution and refinement all proceeded normally Hydrogen atoms were introduced with thermal parameters set twenty percent greater than those of their bonding partners at the time of their inclusion. They were optimized by positional refinement but were fixed for the final round of refinement due to the shortage of data Refinement was carried out on F-squared to maximize the data/variable ratio

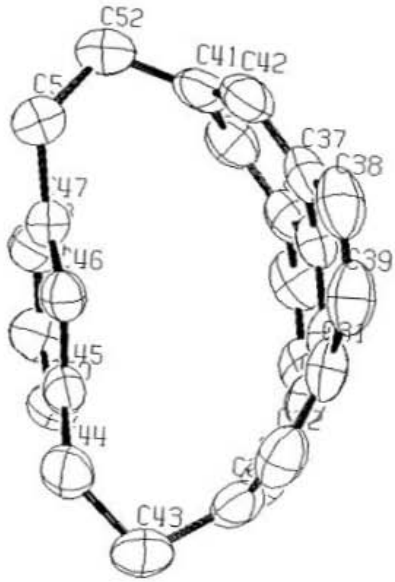
C52
C41
C42
C37
C38
C39
C46
C45
C44
C43

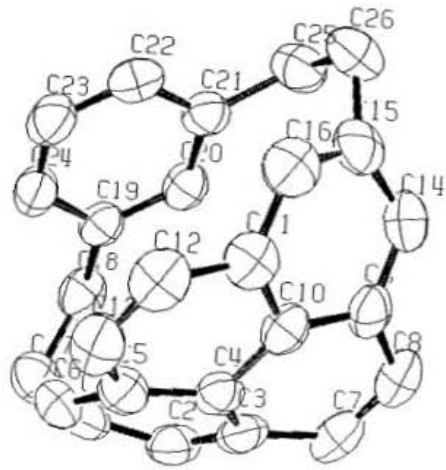
C22
C23
C21
C26
C16
C14
C19
C12
C10
C8
C4
C7

Experimental

Data Collection

A colourless prism crystal of $C_{26}H_{20}$ having approximate dimensions of 0.30 x 0.30 x 0.40 mm was mounted on a glass fiber. All measurements were made on a Rigaku AFC6S diffractometer with graphite monochromated Cu-Kα radiation.

Cell constants and an orientation matrix for data collection, obtained from a least-squares refinement using the setting angles of 24 carefully centered reflections in the range $58.55 < 2\theta < 59.77^{\circ}$ corresponded to a primitive monoclinic cell with dimensions:

a = 9.282(2) Å
b = 14.383(3) Å $\beta = 92.11(1)^{\circ}$
c = 13.412(2) Å
V = 1789.4(6) $Å^3$

For Z = 4 and F.W. = 332.44, the calculated density is 1.23 g/cm^3. Based on the systematic absences of:

0k0: k ± 2n

packing considerations, a statistical analysis of intensity distribution, and the successful solution and refinement of the structure, the space group was determined to be:

$P2_1$ (#4)

The data were collected at a temperature of 26 ± 1°C using the ω-2θ scan technique to a maximum 2θ value of 120.1°. Omega scans of several intense reflections, made prior to data collection, had an average width at half-height of 0.26° with a take-off angle of 6.0°. Scans of $(1.73 + 0.14 \tan\theta)^{\circ}$ were made at a speed of 4.0°/min (in ω). The weak reflections ($I < 10.0\sigma(I)$) were rescanned (maximum of 5 scans) and the counts were accumulated to ensure good counting statistics. Stationary background counts were recorded on each side of the reflection. The ratio of peak counting time to background counting time was 2:1. The diameter of the incident beam collimator was 1.0 mm, the crystal to detector distance was 400 mm, and the detector aperture was 4.5 x 3.0 mm (horizontal x vertical).

Data Reduction

Of the 2985 reflections which were collected, 2794 were unique (R_{int} = 0.014). The intensities of three representative reflections were measured after every 150 reflections. No decay correction was applied.

The linear absorption coefficient, μ, for Cu-Kα radiation is 5.3 cm^{-1}. An empirical absorption correction based on azimuthal scans of several reflections was applied which resulted in transmission factors ranging from 0.95 to 1.00. The data were corrected for Lorentz and polarization effects. A correction for secondary extinction was applied (coefficient = 3.81012e-005).

Structure Solution and Refinement

The structure was solved by direct methods[1] and expanded using Fourier techniques[2]. The non-hydrogen atoms were refined anisotropically. Hydrogen atoms were included but not refined. The final cycle of full-matrix least-squares refinement[3] on F^2 was based on 2786 observed reflections and 469 variable parameters and converged (largest parameter shift was 0.00 times its esd) with unweighted and weighted agreement factors of:

$$R1 = \Sigma \, ||Fo| - |Fc|| \, / \, \Sigma \, |Fo| = 0.036$$

$$wR2 = [\Sigma (w (Fo^2 - Fc^2)^2) / \Sigma \, w(Fo^2)^2]^{1/2} = 0.059$$

The standard deviation of an observation of unit weight[4] was 2.03. The weighting scheme was based on counting statistics and included a factor (p = 0.008) to downweight the intense reflections. Plots of $\Sigma \, w \, (|Fo| - |Fc|)^2$ versus |Fo|, reflection order in data collection, $\sin\theta/\lambda$, and various classes of indices showed no unusual trends. The maximum and minimum peaks on the final difference Fourier map corresponded to 0.10 and -0.11 e^-/A^3, respectively.

Neutral atom scattering factors were taken from Cromer and Waber[5]. Anomalous dispersion effects were included in Fcalc[6]; the values for $\Delta f'$ and $\Delta f''$ were those of Creagh and McAuley[7]. The values for the mass attenuation coefficients are those of Creagh and Hubbell[8]. All calculations were performed using the teXsan[9] crystallographic software package of Molecular Structure Corporation.

References

(1) SIR92: Altomare, A., Cascarano, M., Giacovazzo, C., Guagliardi, A. (1994) J. Appl. Cryst., 26, 343.

(2) DIRDIF94: Beurskens, P.T., Admiraal, G., Beurskens, G., Bosman, W.P., de Gelder, R., Israel, R. and Smits, J.M.M.(1994). The DIRDIF-94 program system, Technical Report of the Crystallography Laboratory, University of Nijmegen, The Netherlands.

(3) Least Squares function minimized:

$$\Sigma w(F_o^2-F_c^2)^2 \text{ where}$$

$w = 1/[\sigma^2(Fo)] = [\sigma^2_c(Fo) + p^2Fo^2/4]^{-1}$
$\sigma_c(Fo)$ = e.s.d. based on counting statistics
p = p-factor

(4) Standard deviation of an observation of unit weight:

$$[\Sigma w(F_o^2-F_c^2)^2/(N_o-N_v)]^{1/2}$$

where N_o = number of observations
N_v = number of variables

(5) Cromer, D. T. & Waber, J. T., "International Tables for X-ray Crystallography", Vol. IV, The Kynoch Press, Birmingham, England, Table 2.2 A (1974).

(6) Ibers, J. A. & Hamilton, W. C., Acta Crystallogr., 17, 781 (1964).

(7) Creagh, D. C. & McAuley, W.J., "International Tables for Crystallography", Vol C, (A.J.C. Wilson, ed.), Kluwer Academic Publishers, Boston, Table 4.2.6.8, pages 219-222 (1992).

(8) Creagh, D. C. & Hubbell, J.H., "International Tables for Crystallography", Vol C, (A.J.C. Wilson, ed.), Kluwer Academic Publishers, Boston, Table 4.2.4.3, pages 200-206 (1992).

(9) teXsan for Windows version 1.06: Crystal Structure Analysis Package, Molecular Structure Corporation (1997-9).

EXPERIMENTAL DETAILS

A. Crystal Data

Empirical Formula	$C_{26}H_{20}$
Formula Weight	332.44
Crystal Color, Habit	colourless, prism
Crystal Dimensions	0.30 X 0.30 X 0.40 mm
Crystal System	monoclinic
Lattice Type	Primitive
No. of Reflections Used for Unit Cell Determination (2θ range)	24 (58.5 - 59.8^{o})
Omega Scan Peak Width at Half-height	0.26^{o}
Lattice Parameters	a = 9.282(2) Å b = 14.383(3) Å c = 13.412(2) Å β = 92.11(1)^{o} V = 1789.4(6) Å^{3}
Space Group	$P2_1$ (#4)
Z value	4
D_{calc}	1.234 g/cm^{3}
F_{000}	704.00
μ(CuKα)	5.26 cm^{-1}

B. Intensity Measurements

Diffractometer	Rigaku AFC6S
Radiation	CuKα (λ = 1.54178 Å) graphite monochromated
Take-off Angle	6.0°
Detector Aperture	4 5 mm horizontal 3 0 mm vertical
Crystal to Detector Distance	400 mm
Voltage, Current	50kV, 27 5mA
Temperature	26.0°C
Scan Type	ω-2θ
Scan Rate	4 0°/min (in ω) (up to 5 scans)
Scan Width	(1 73 + 0 14 tan θ)°
$2\theta_{max}$	120 1°
No of Reflections Measured	Total 2985 Unique 2794 (R_{int} = 0 014)
Corrections	Lorentz-polarization Absorption (trans. factors: 0.9544 - 1 0000) Secondary Extinction (coefficient: 3.81012e-005)

C. Structure Solution and Refinement

Structure Solution	Direct Methods (SIR92)
Refinement	Full-matrix least-squares on F^2
Function Minimized	$\Sigma w (Fo^2 - Fc^2)^2$
Least Squares Weights	$1/\sigma^2(Fo) = 4Fo^2/\sigma^2(Fo^2)$
p-factor	0.0080
Anomalous Dispersion	All non-hydrogen atoms
No. Observations (I>-10.00σ(I))	2786
No. Variables	469
Reflection/Parameter Ratio	5.94
Residuals: R1; wR2	0.036 ; 0.059
Goodness of Fit Indicator	2.03
Max Shift/Error in Final Cycle	0.00
Maximum peak in Final Diff. Map	0.10 e^-/A^3
Minimum peak in Final Diff. Map	-0.11 e^-/A^3

Appendix H

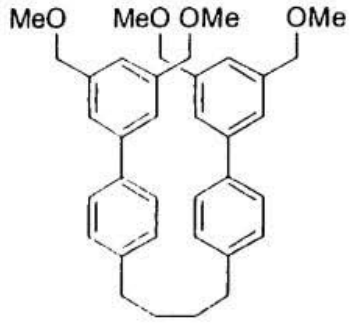

57

Chapter 3

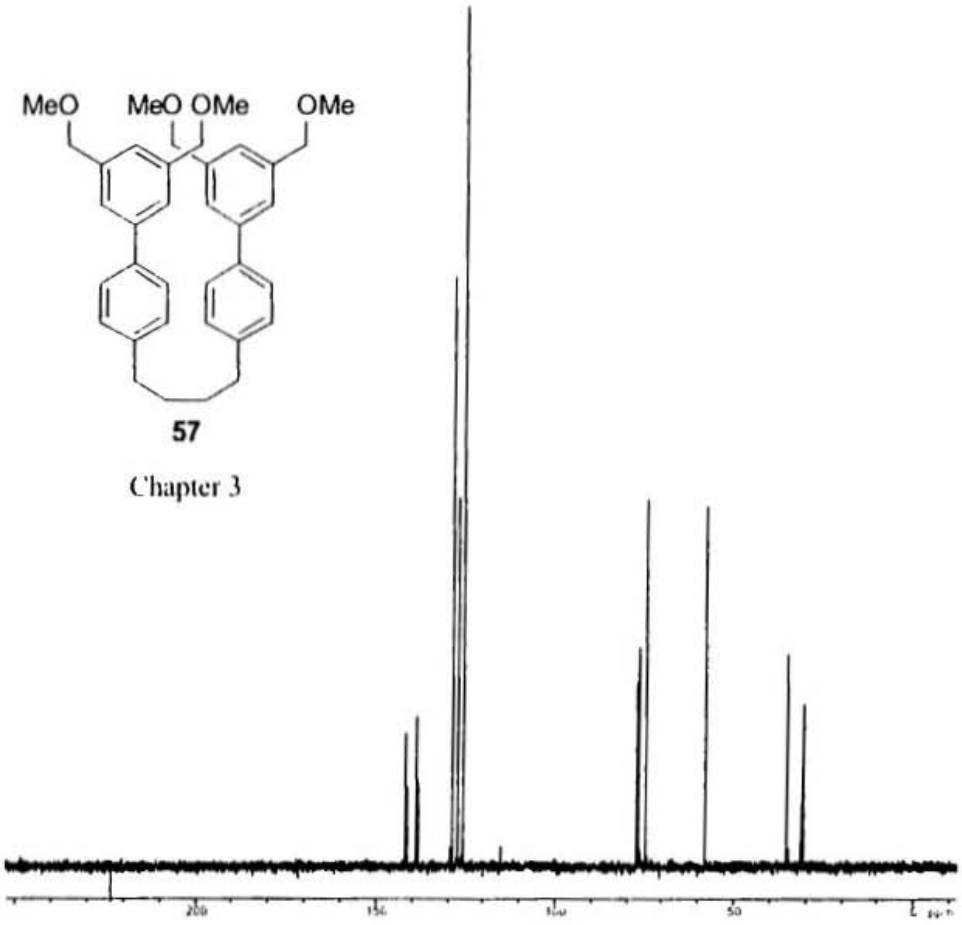

57

Chapter 3

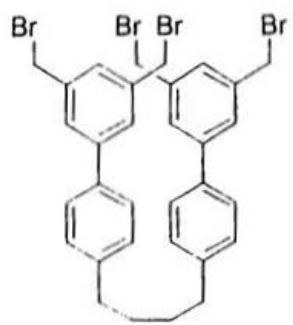

71

Chapter 3

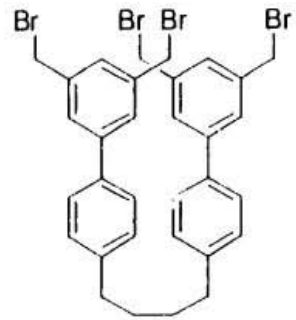

71

Chapter 3

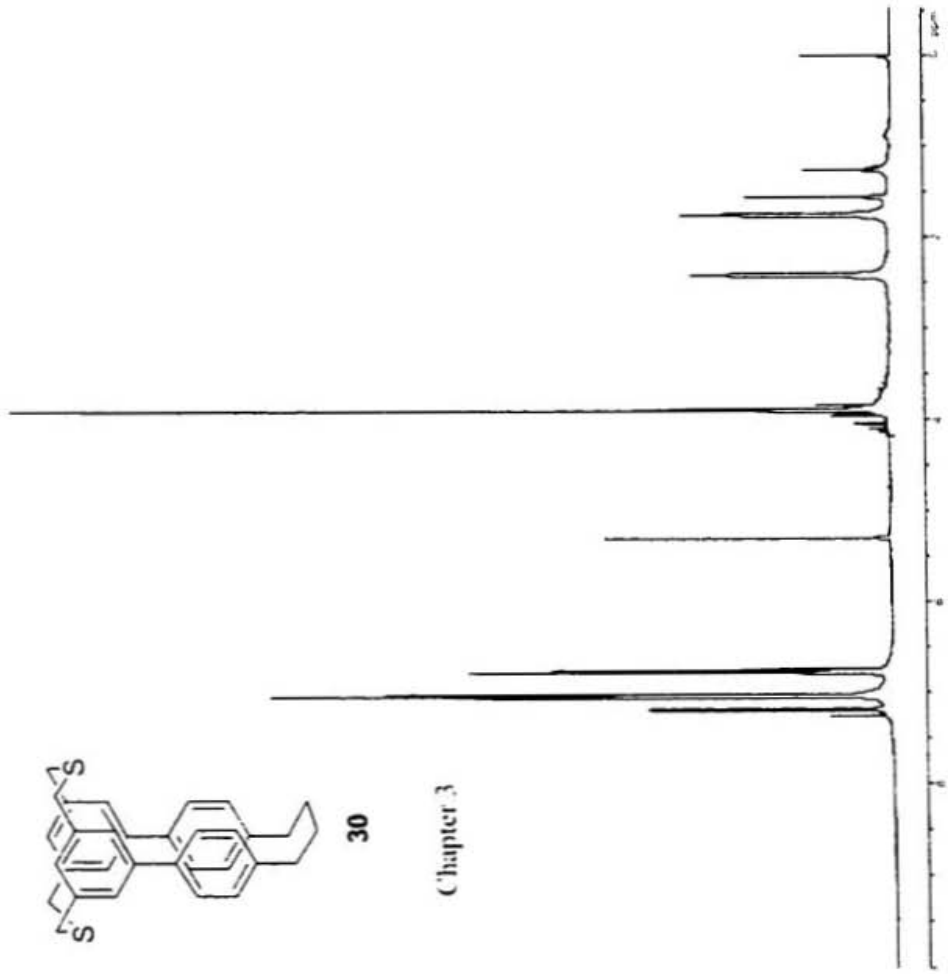

30

Chapter 3

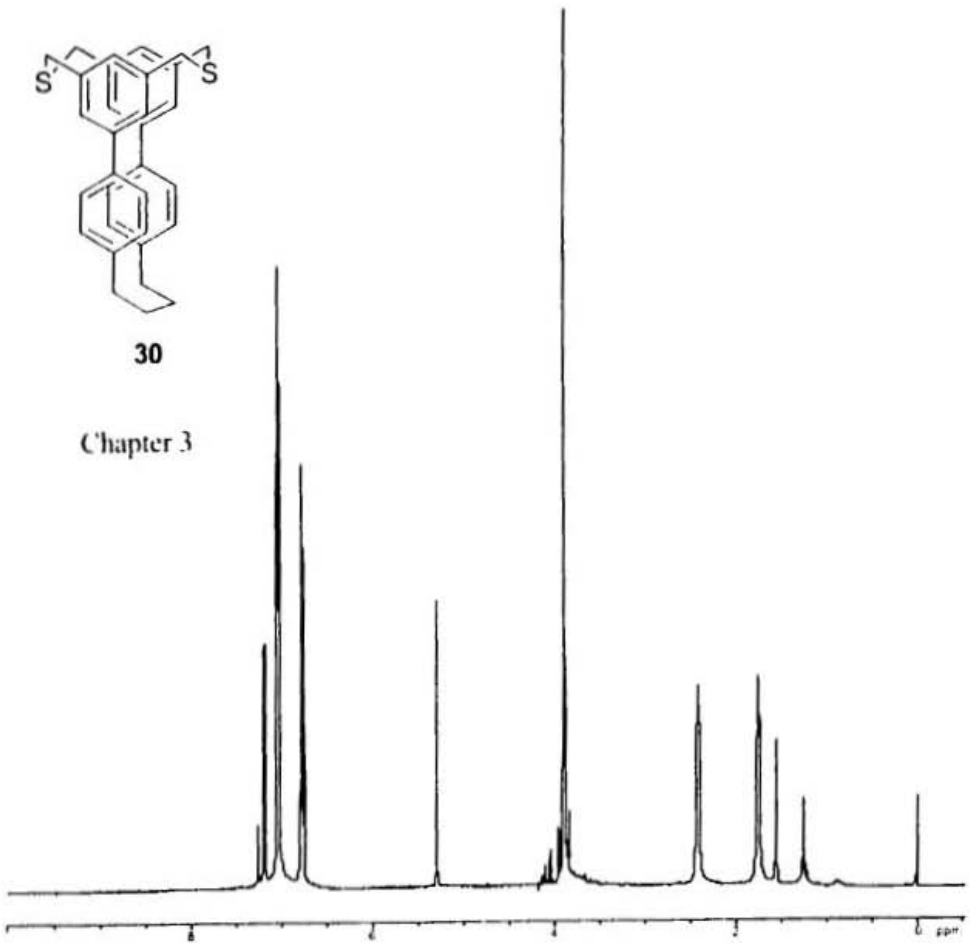

30

Chapter 3

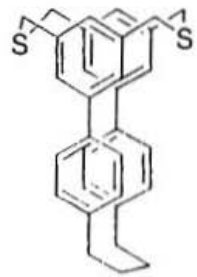

30

Chapter 3

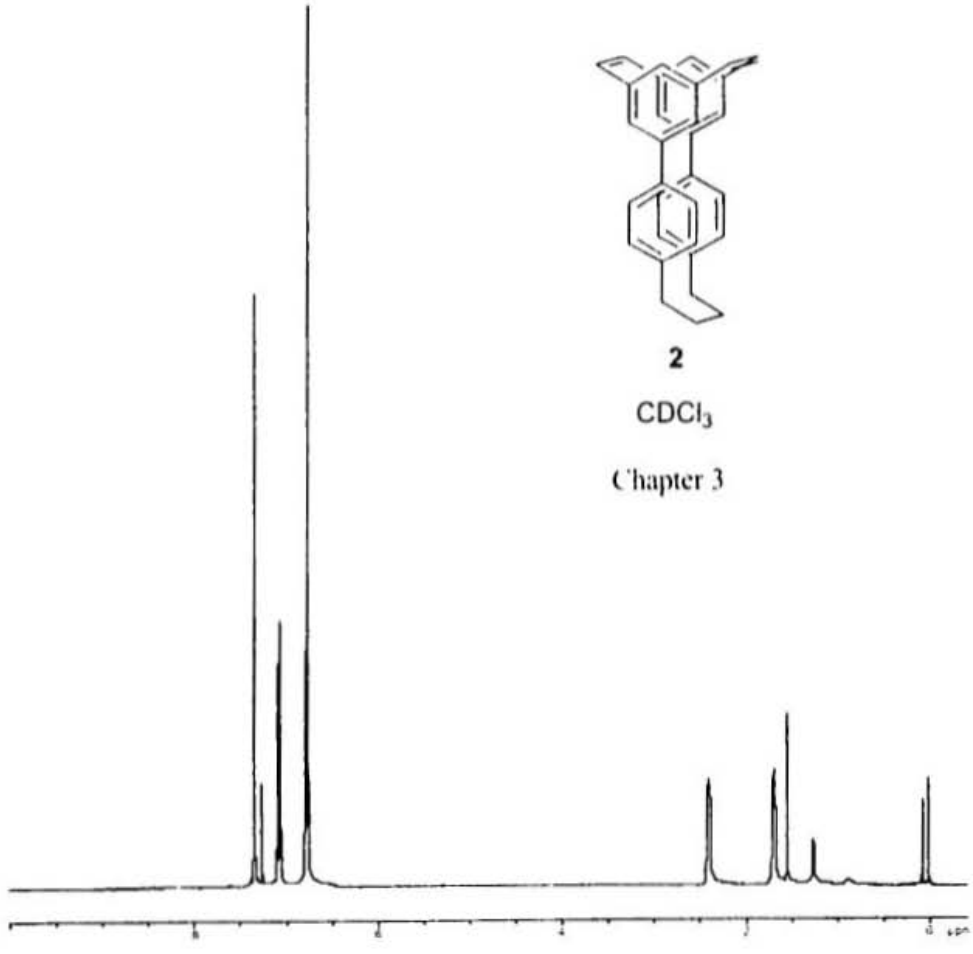

2

$CDCl_3$

Chapter 3

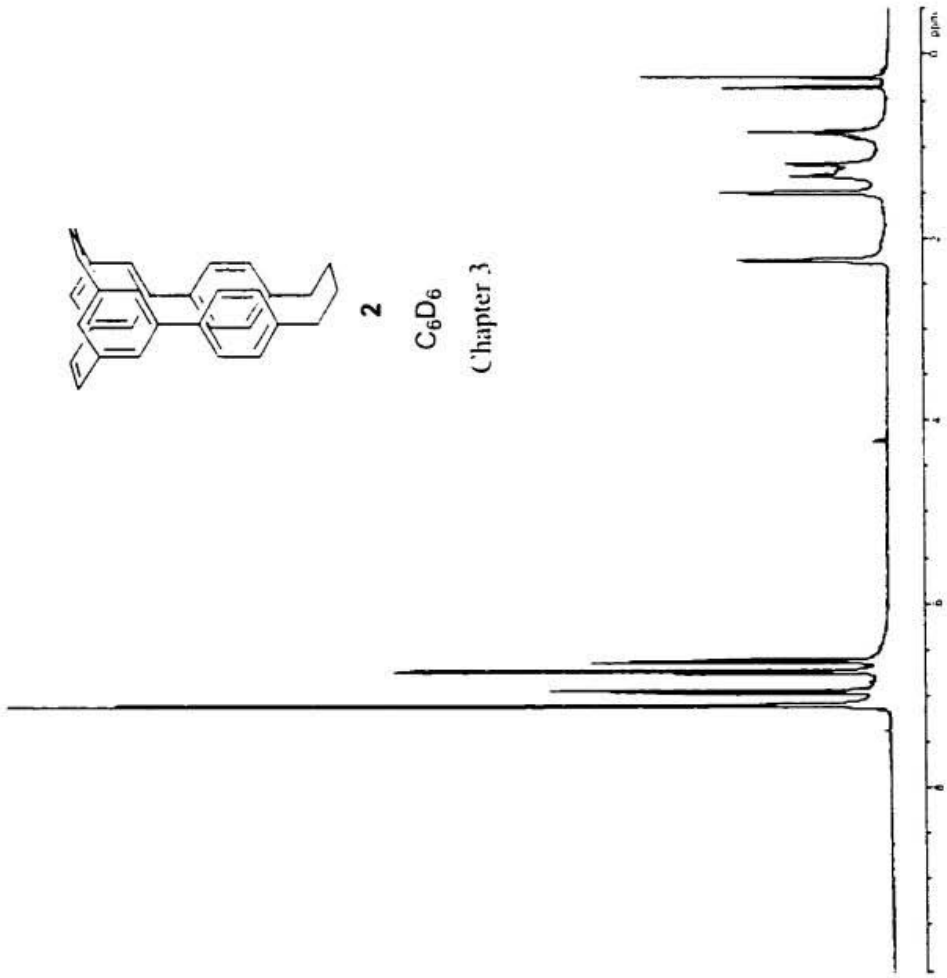

2

C_6D_6

Chapter 3

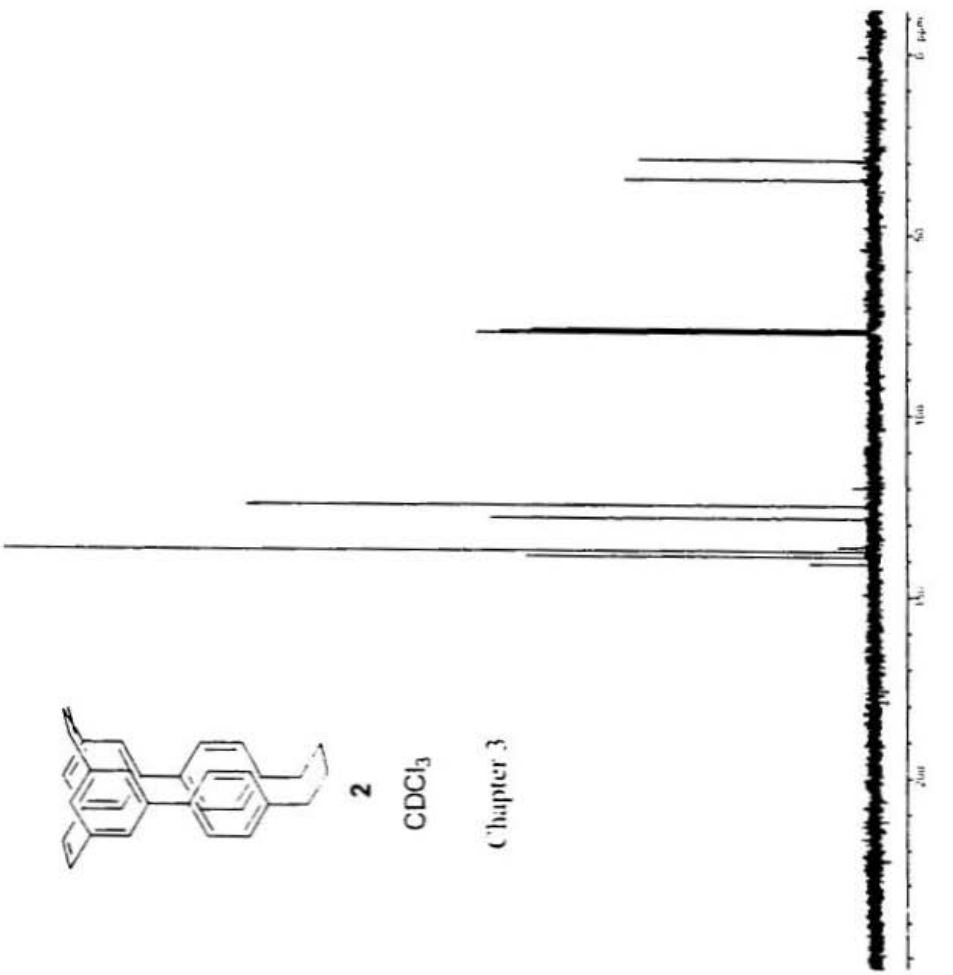

2

$CDCl_3$

Chapter 3

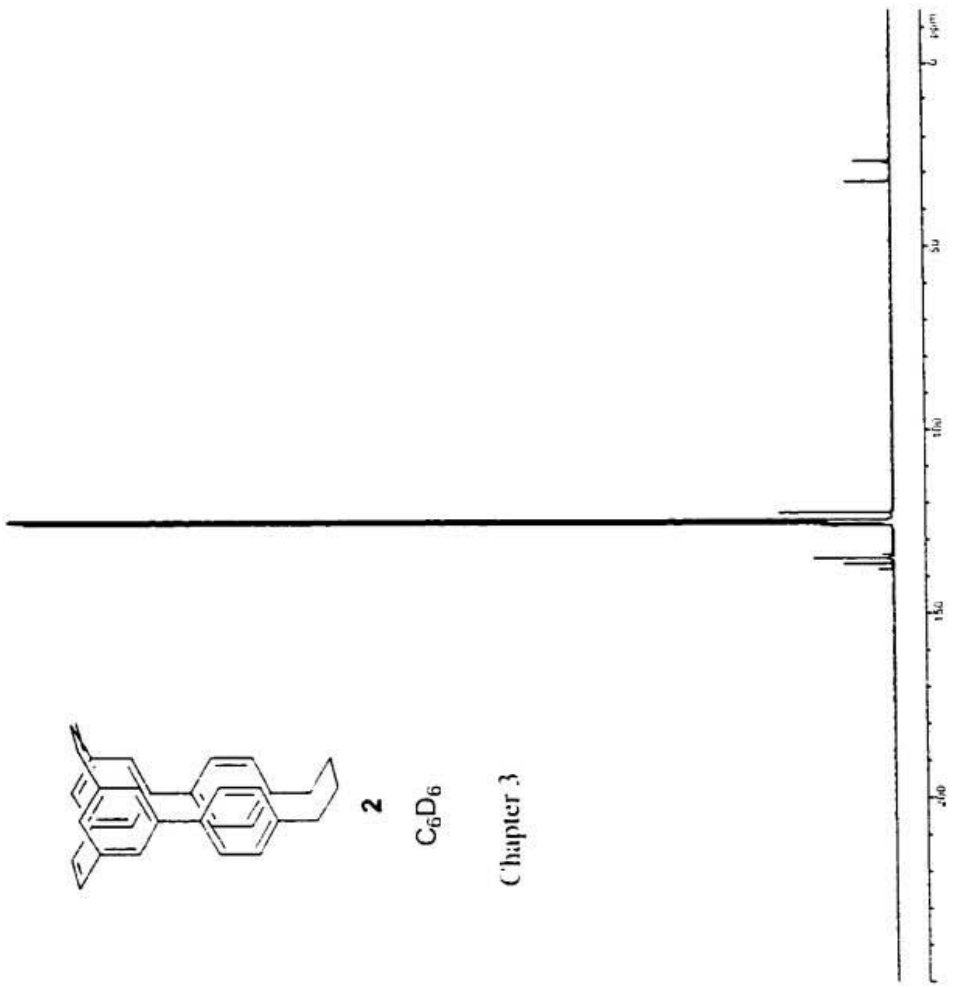

2

C_6D_6

Chapter 3

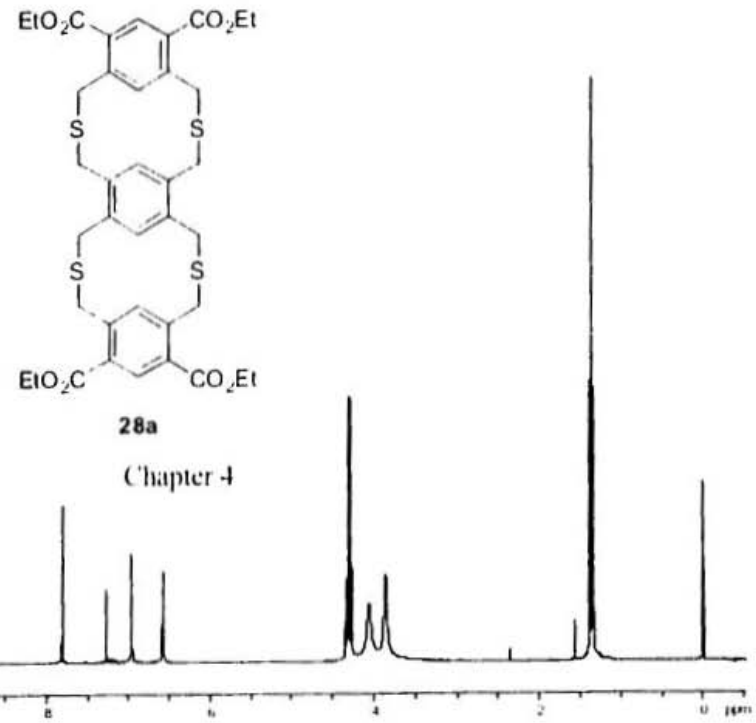

28a

Chapter 4

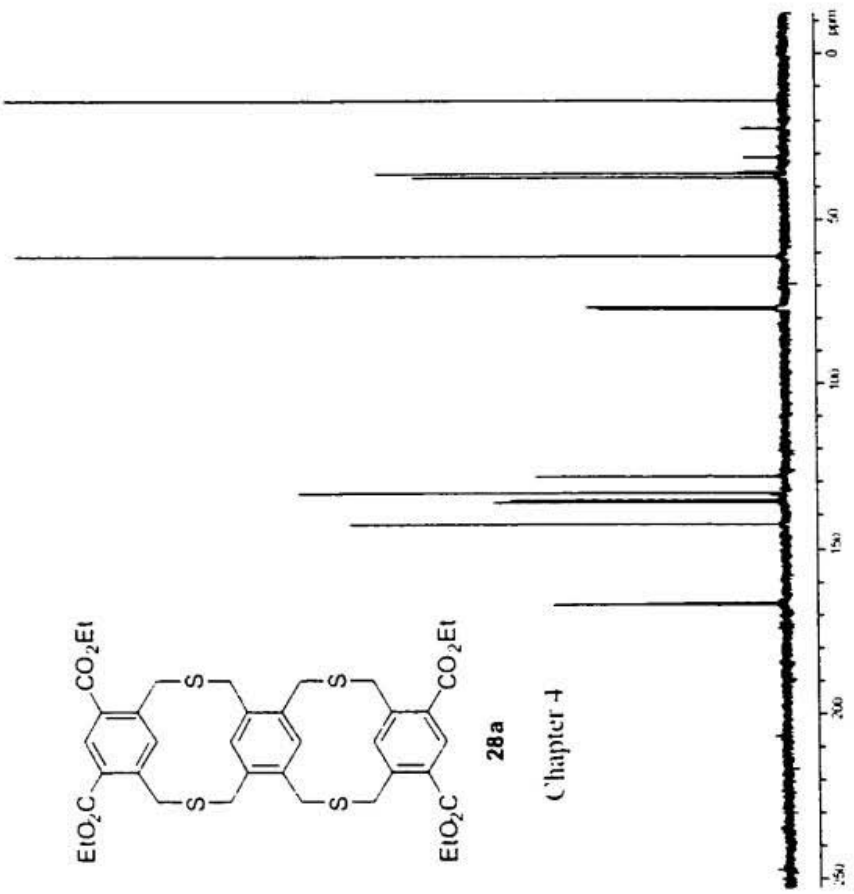
EtO2C
CO2Et
S
S
S
S
EtO2C
CO2Et
28a
Chapter 4
0 ppm

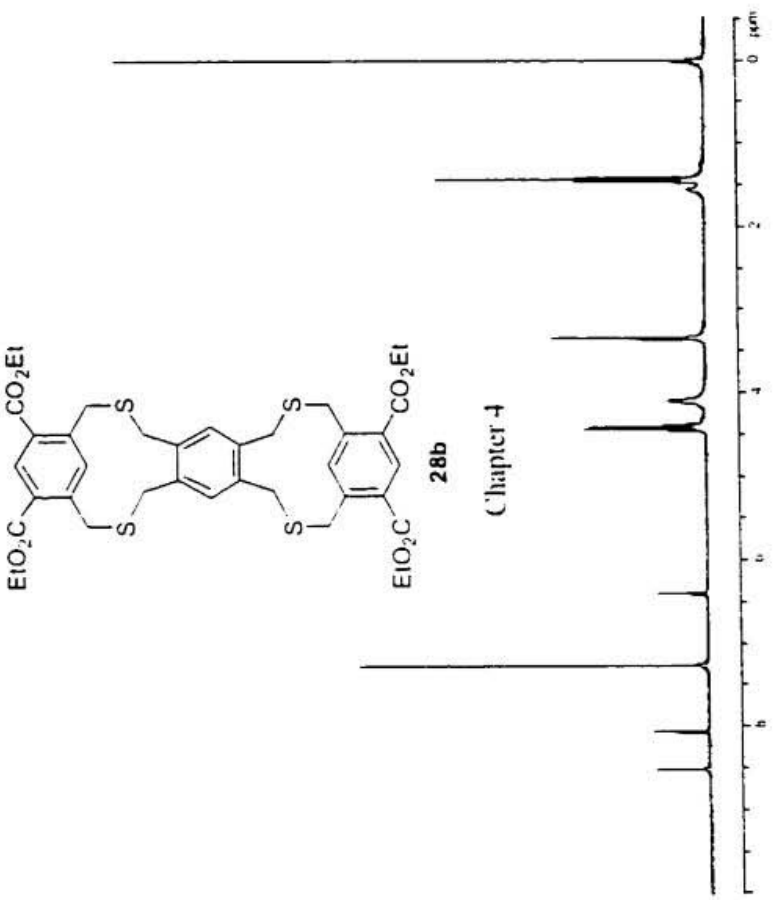
CO2Et
EtO2C
S
S
S
S
CO2Et
EtO2C
28b
Chapter 4

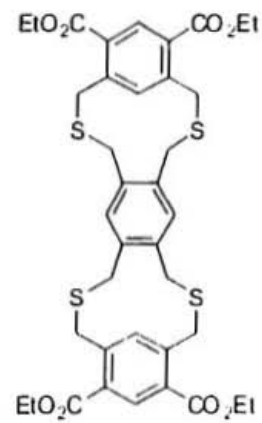

28b

Chapter 4

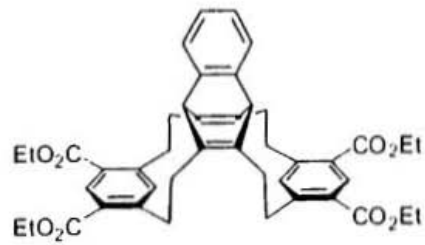

43

Chapter 4

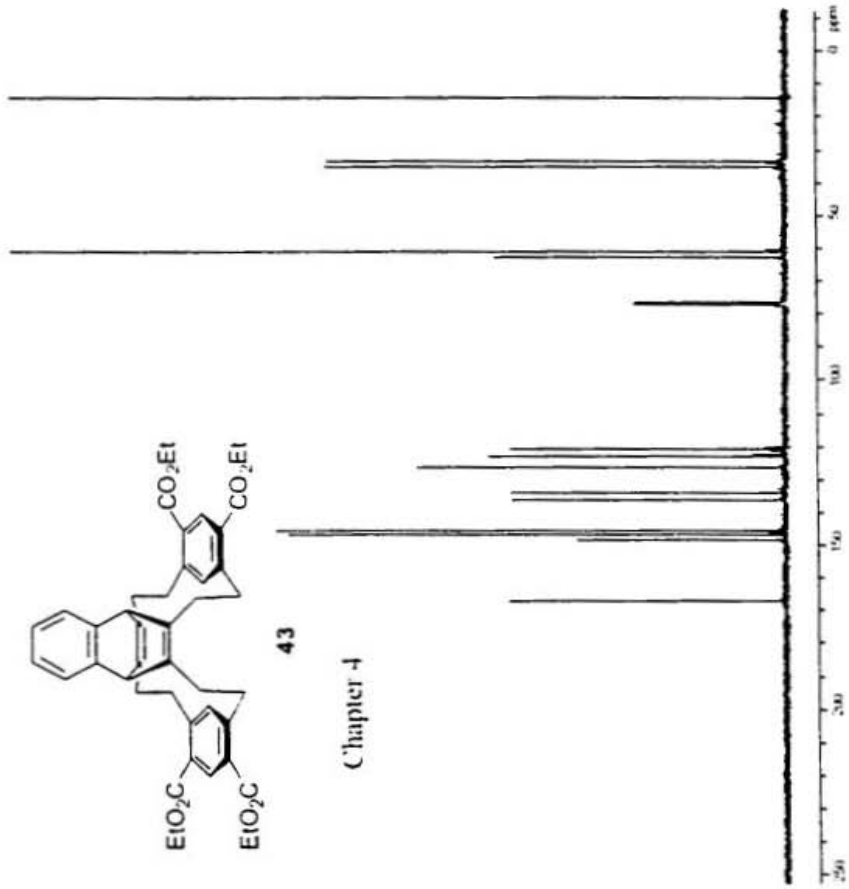

43

Chapter 4

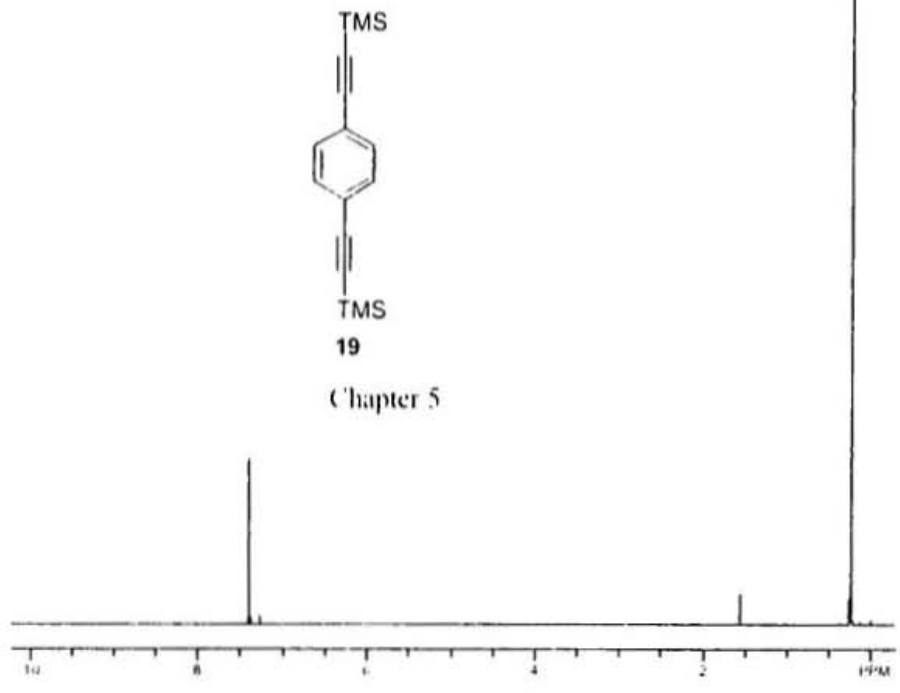

19

Chapter 5

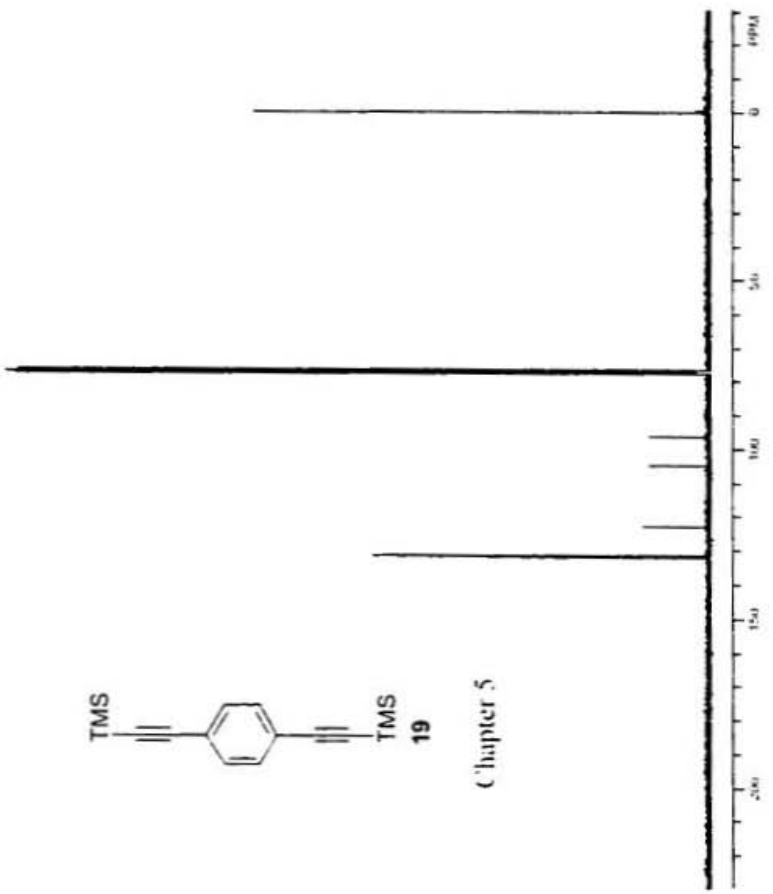

19

Chapter 5

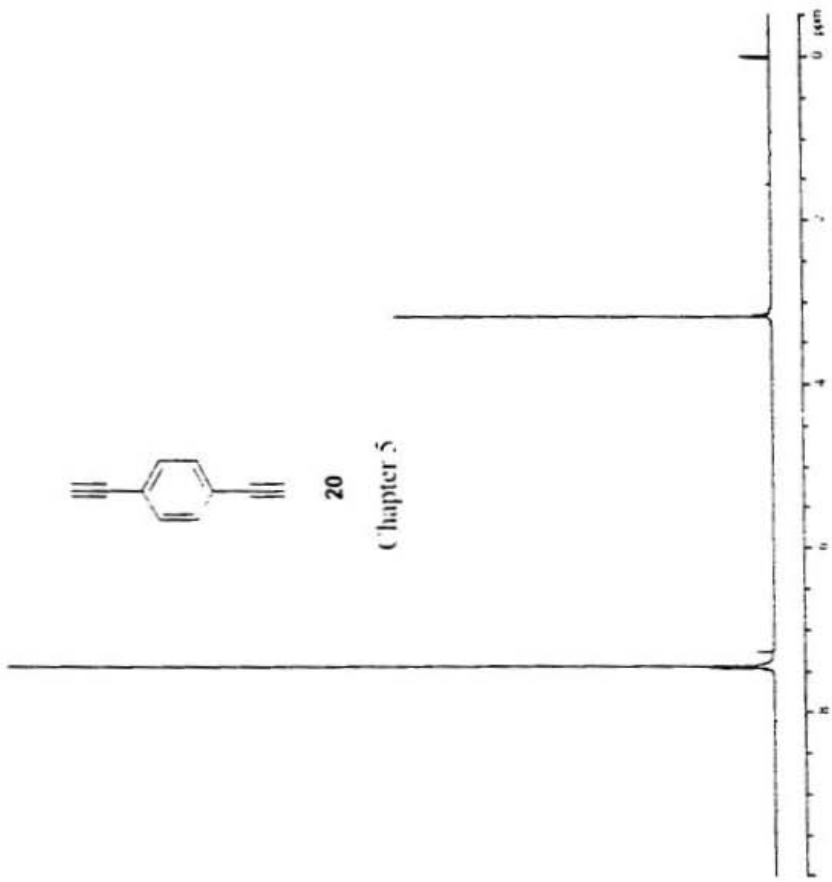

20

Chapter 5

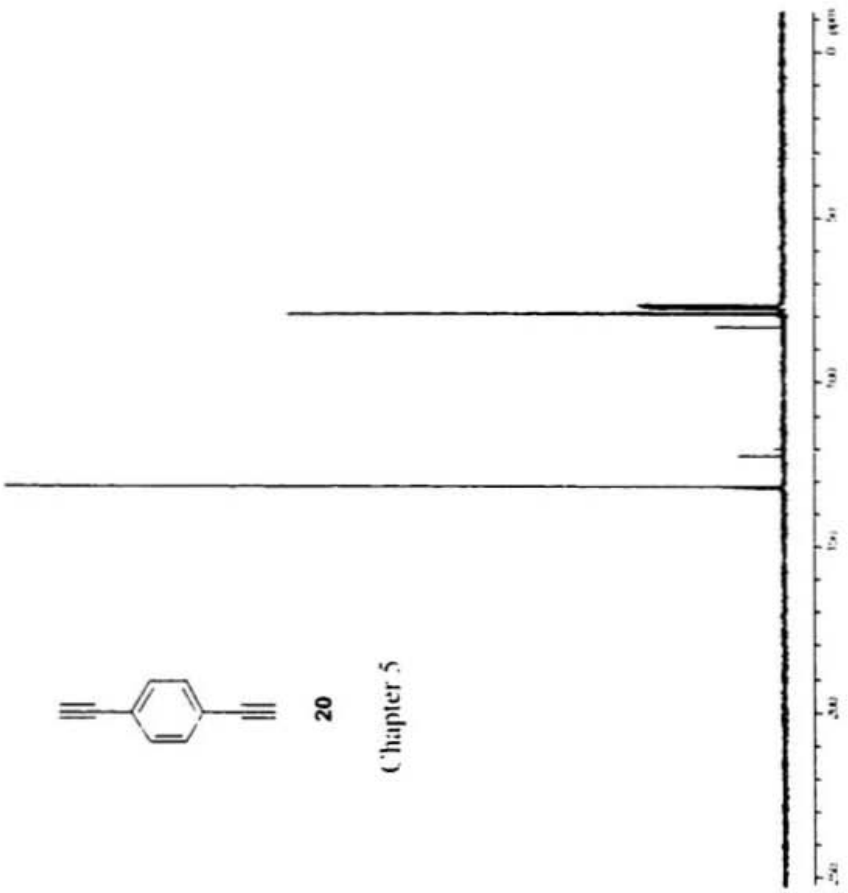

20

Chapter 5

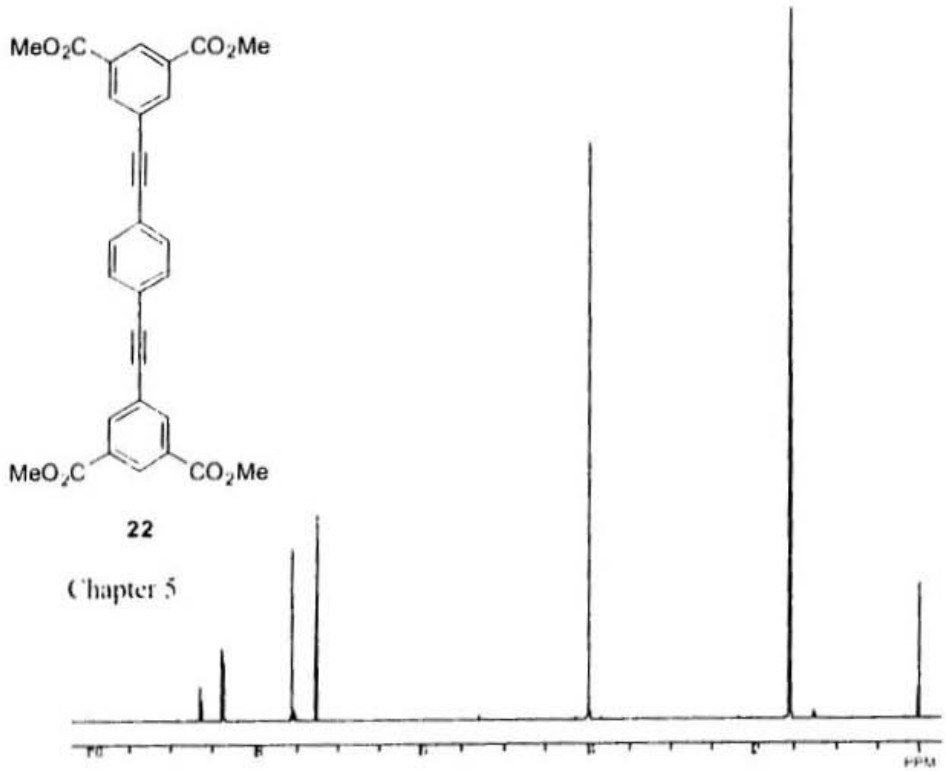
MeO2C
CO2Me
MeO2C
CO2Me
22
Chapter 5
PPM

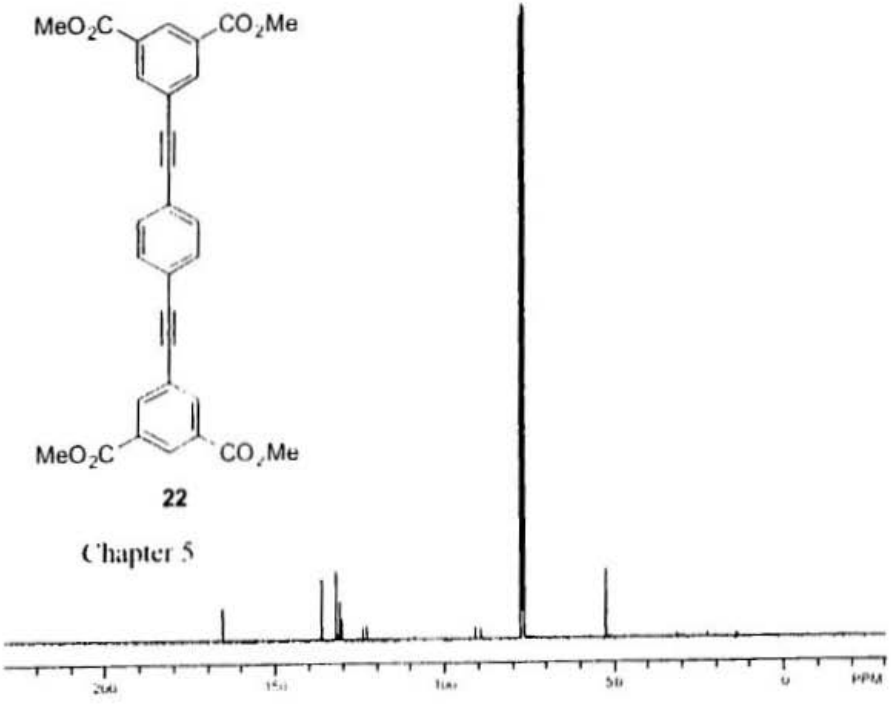
MeO2C
CO2Me
MeO2C
CO2Me
22
Chapter 5
PPM

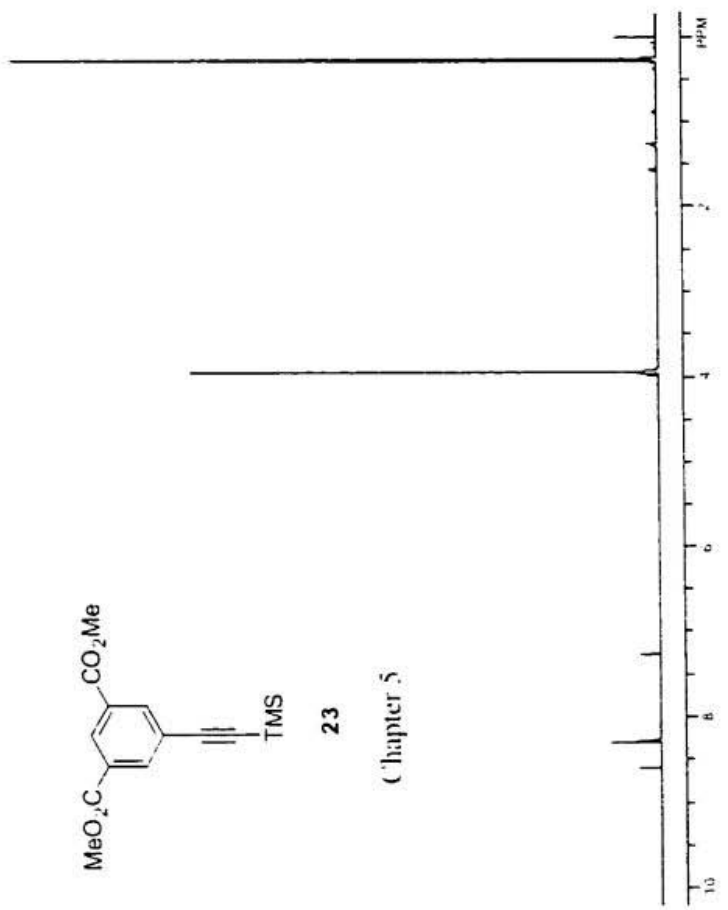
MeO2C
CO2Me
TMS
23
Chapter 5
PPM

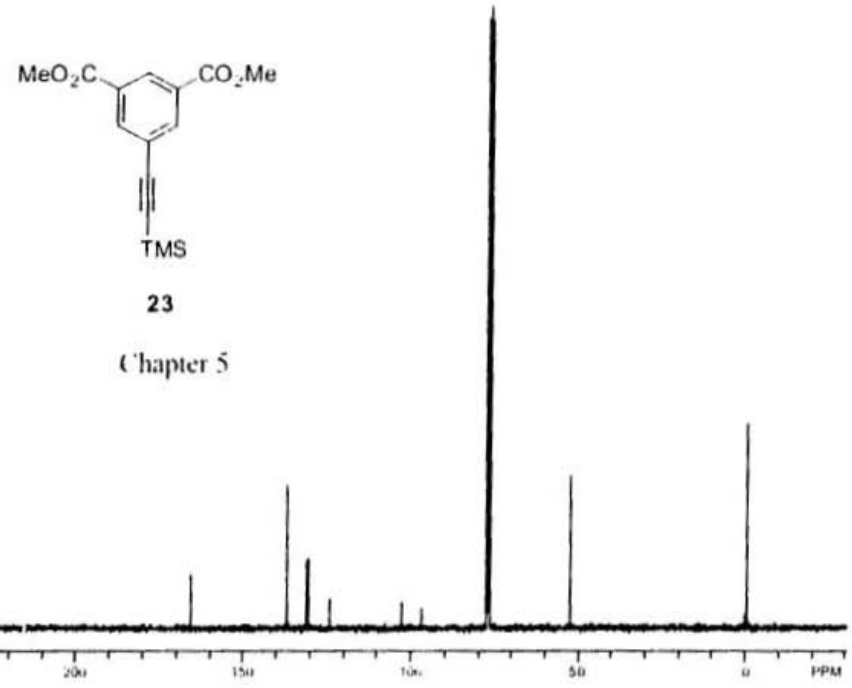

23

Chapter 5

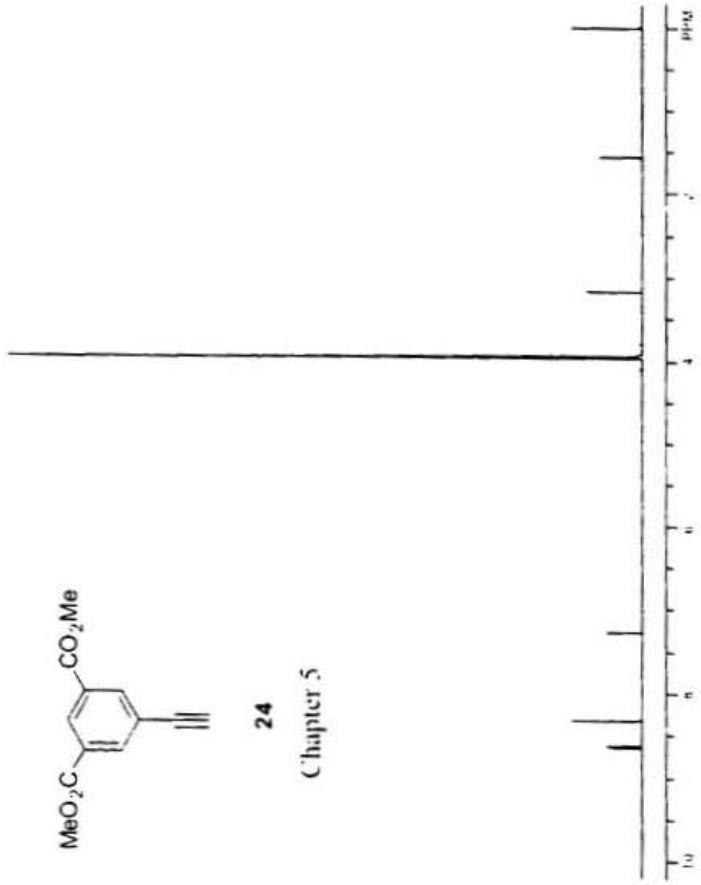

24

Chapter 5

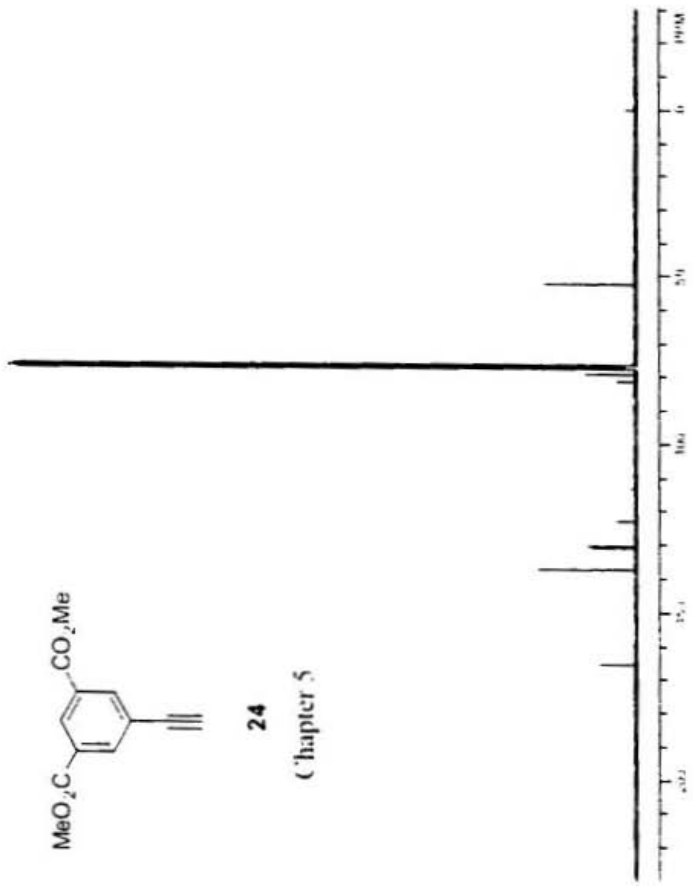

24

Chapter 5

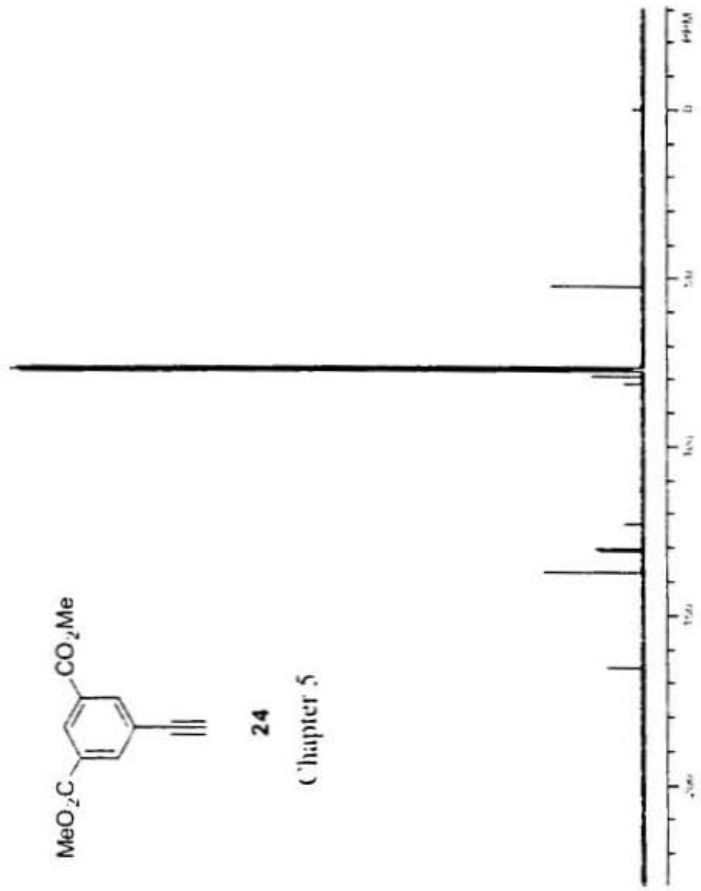

24

Chapter 5

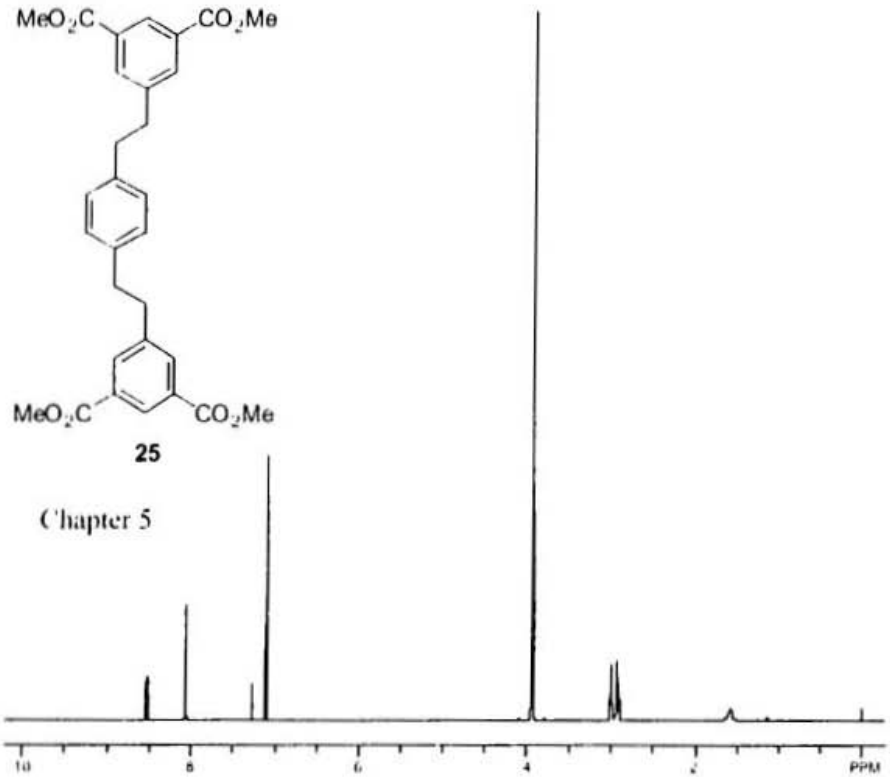

25

Chapter 5

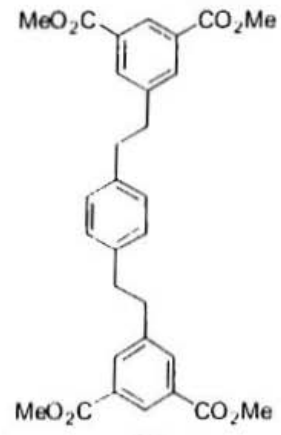

25

Chapter 5

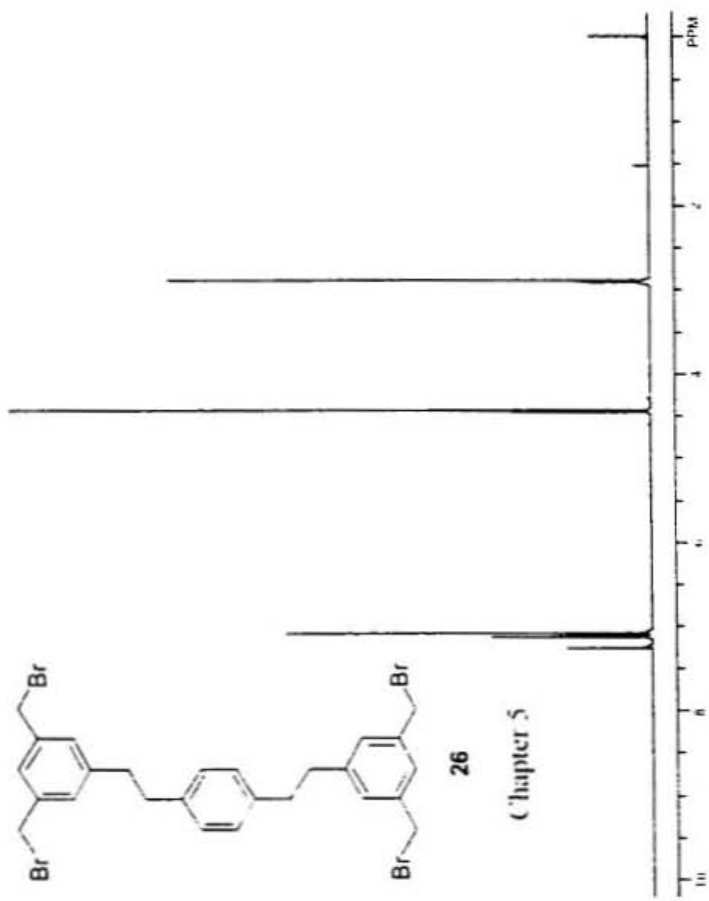
Br
Br
Br
Br
26
Chapter 5
PPM

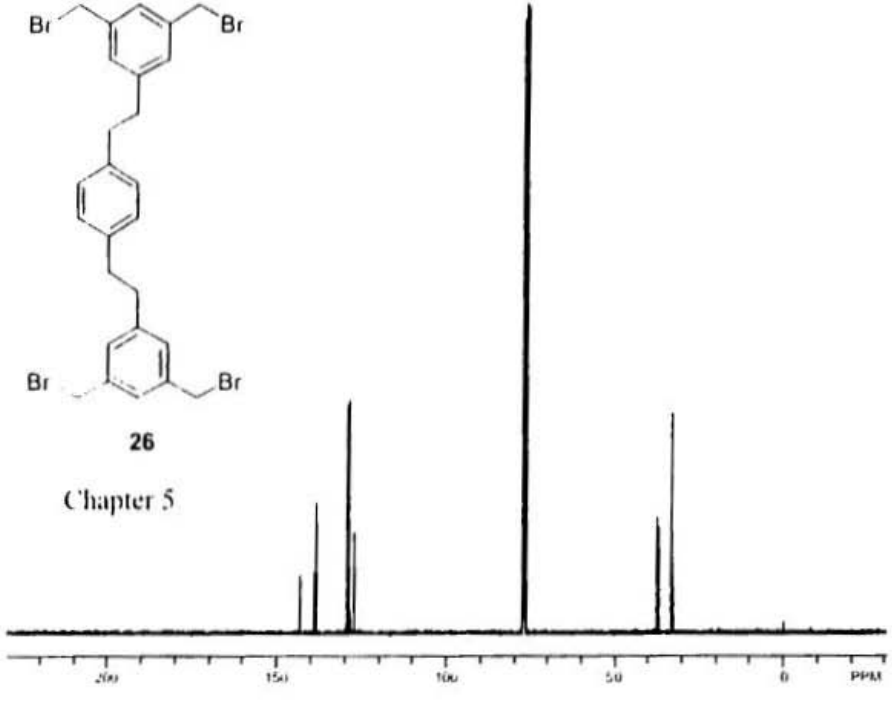
Br
Br
Br
Br
26
Chapter 5
PPM

27

Chapter 5

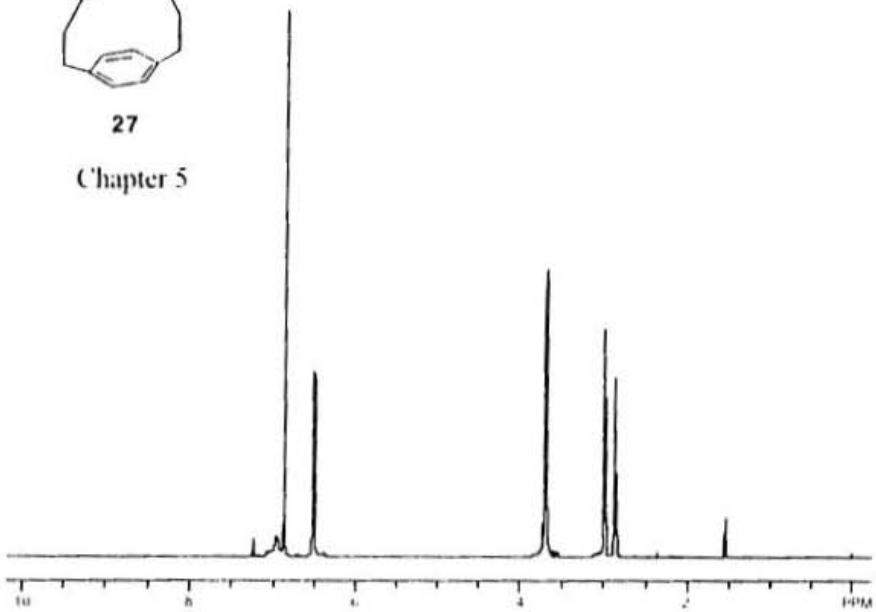

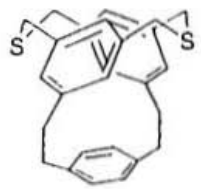

27

Chapter 5

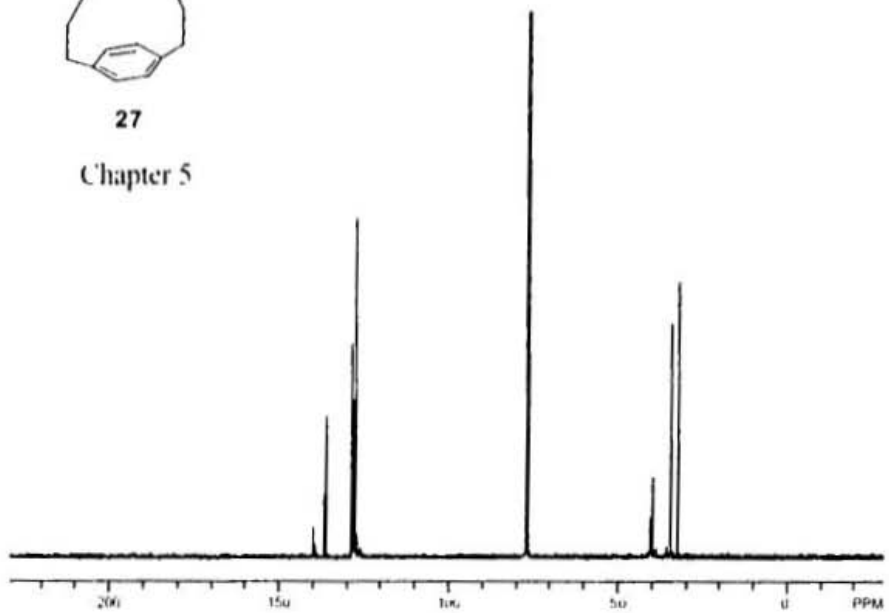

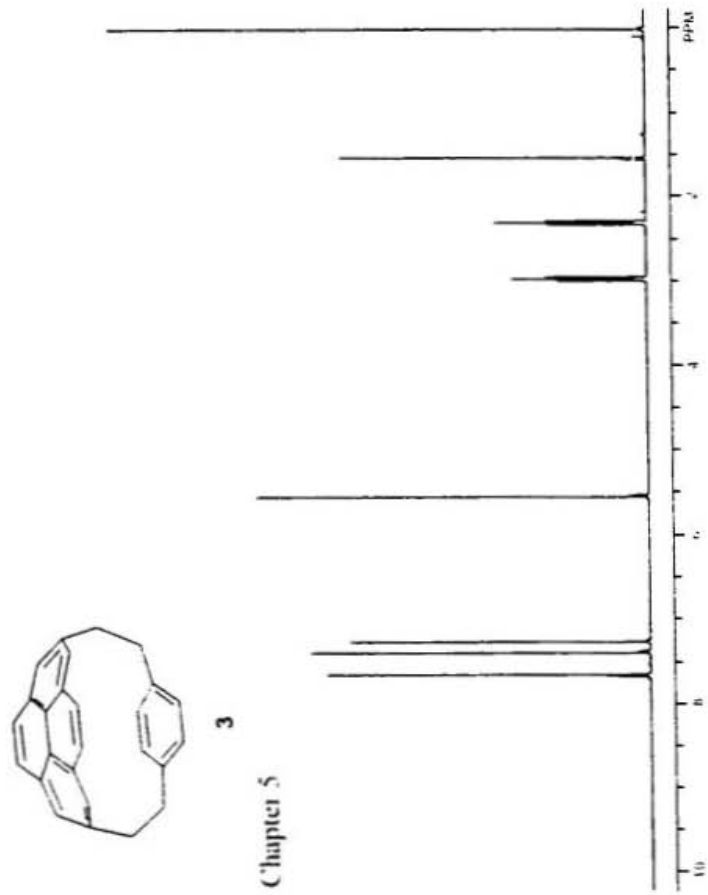

3

Chapter 5

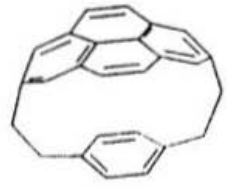

3

Chapter 5

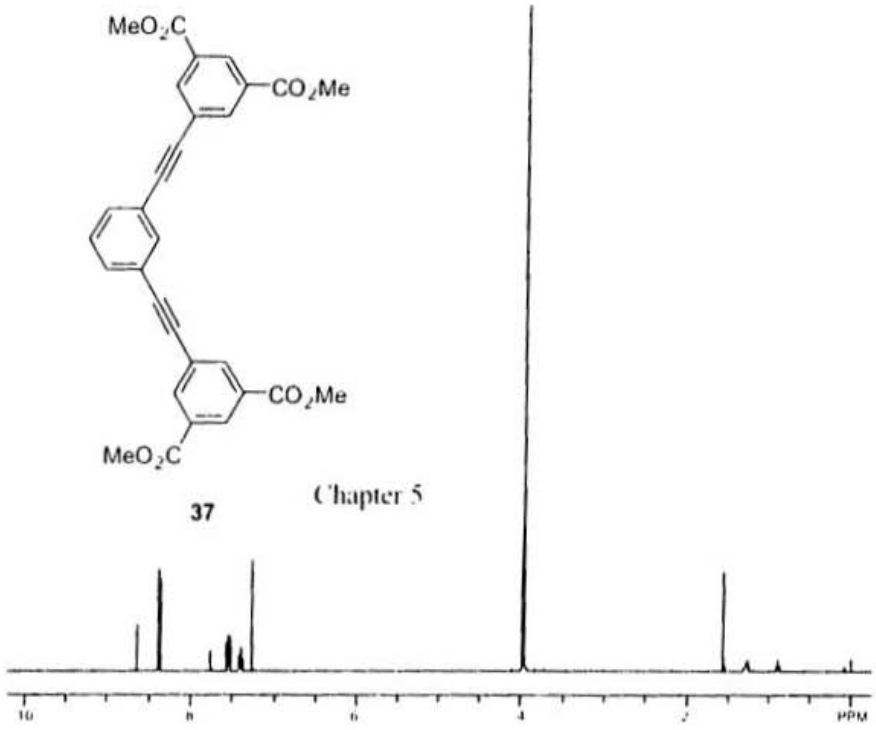

37

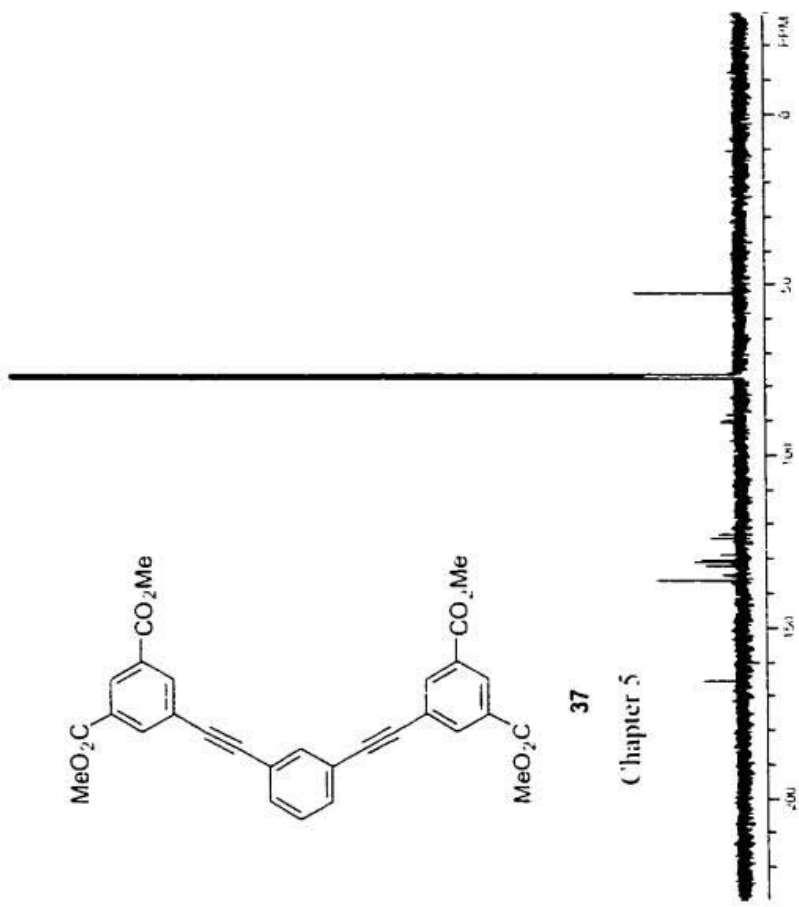

37

Chapter 5

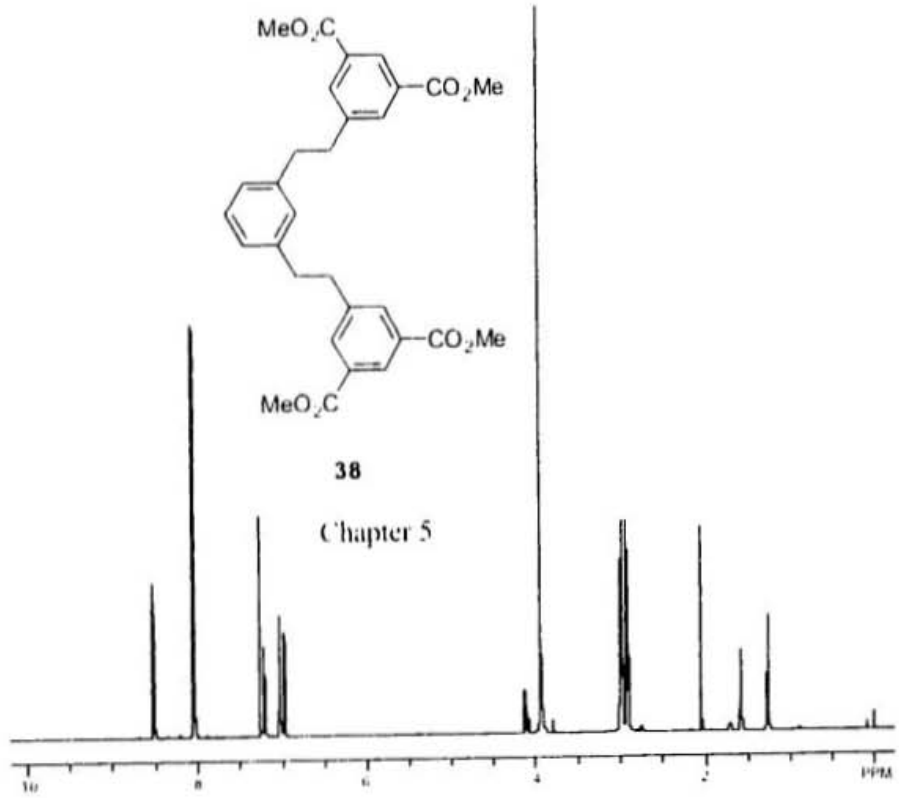

38

Chapter 5

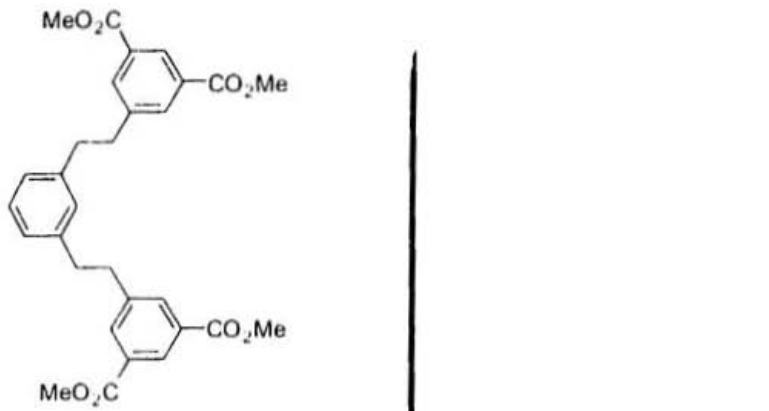

38

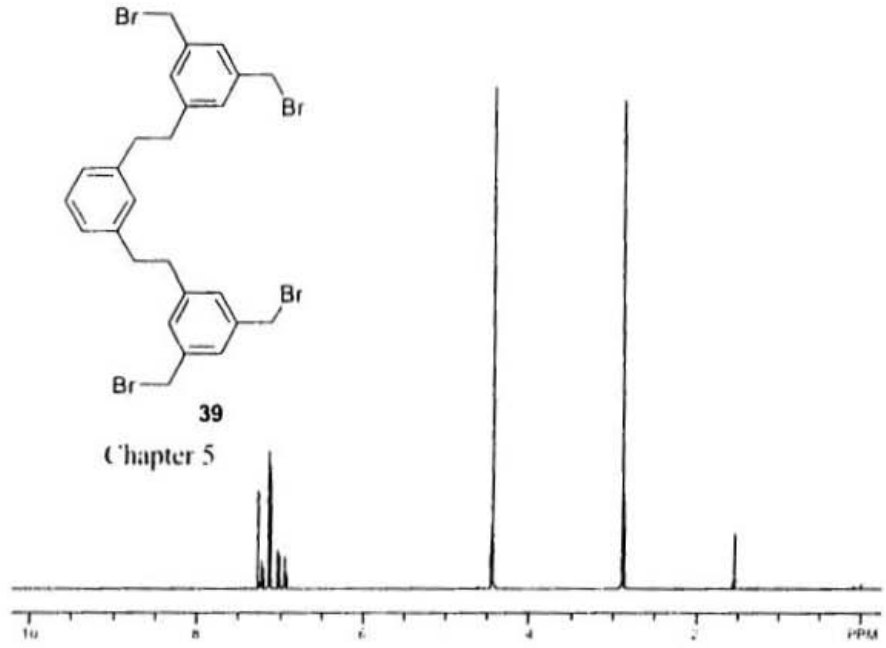
Br
Br
Br
Br
39
Chapter 5
PPM

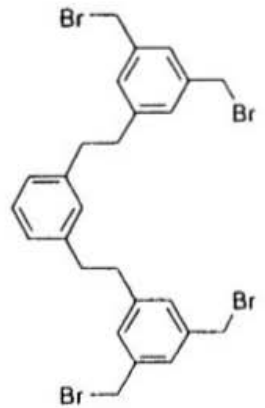

39

Chapter 5

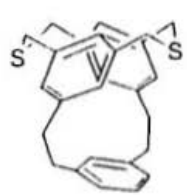

40

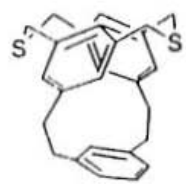

40

Chapter 5

42

Chapter 5

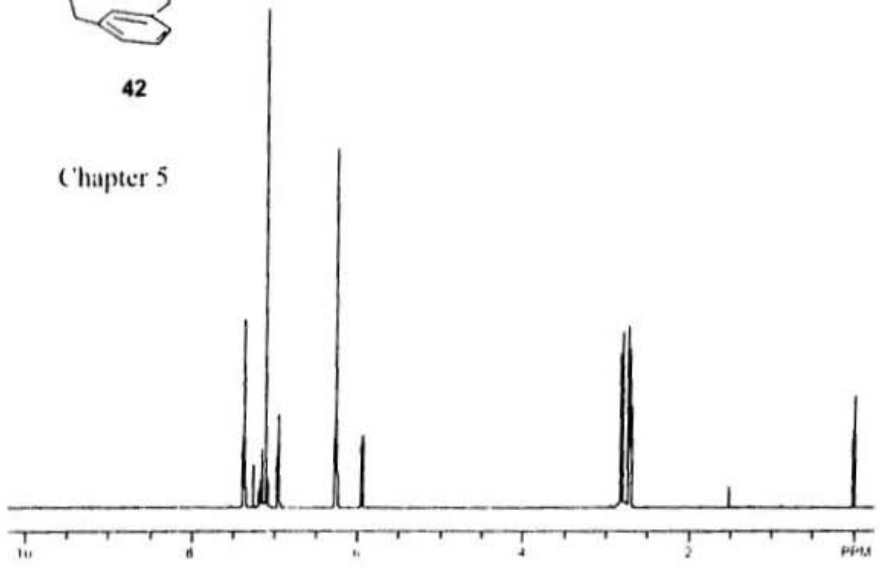

42

Chapter 5

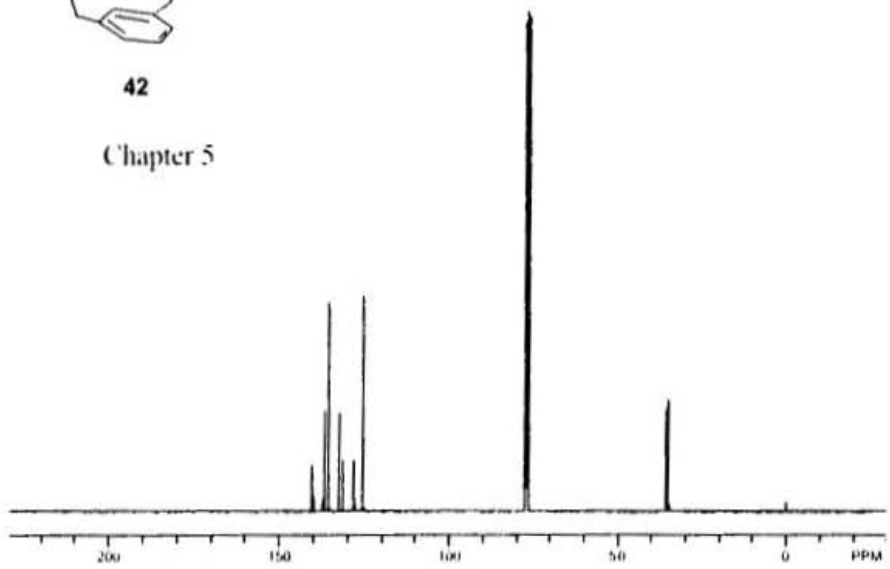

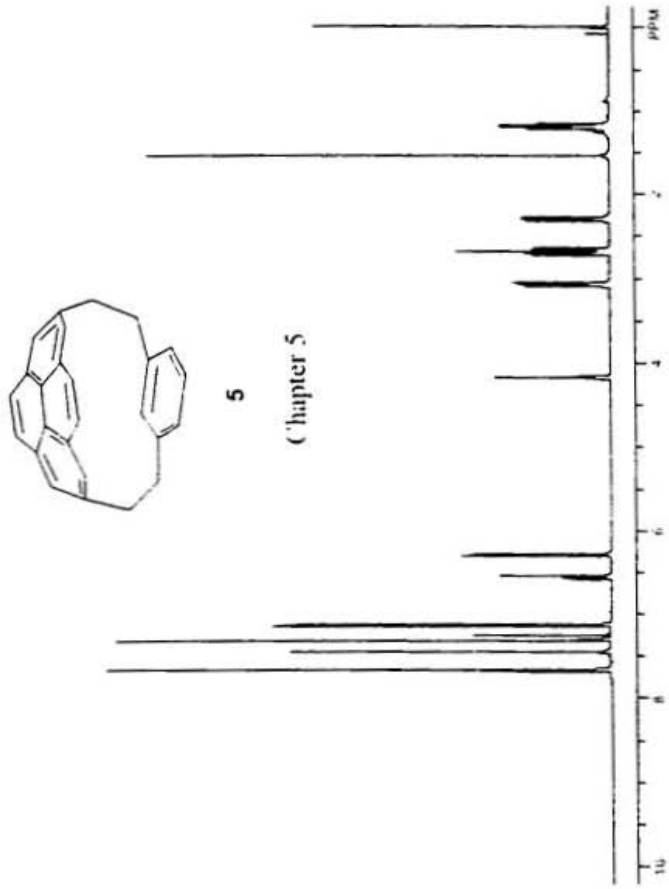
5
Chapter 5
ppm

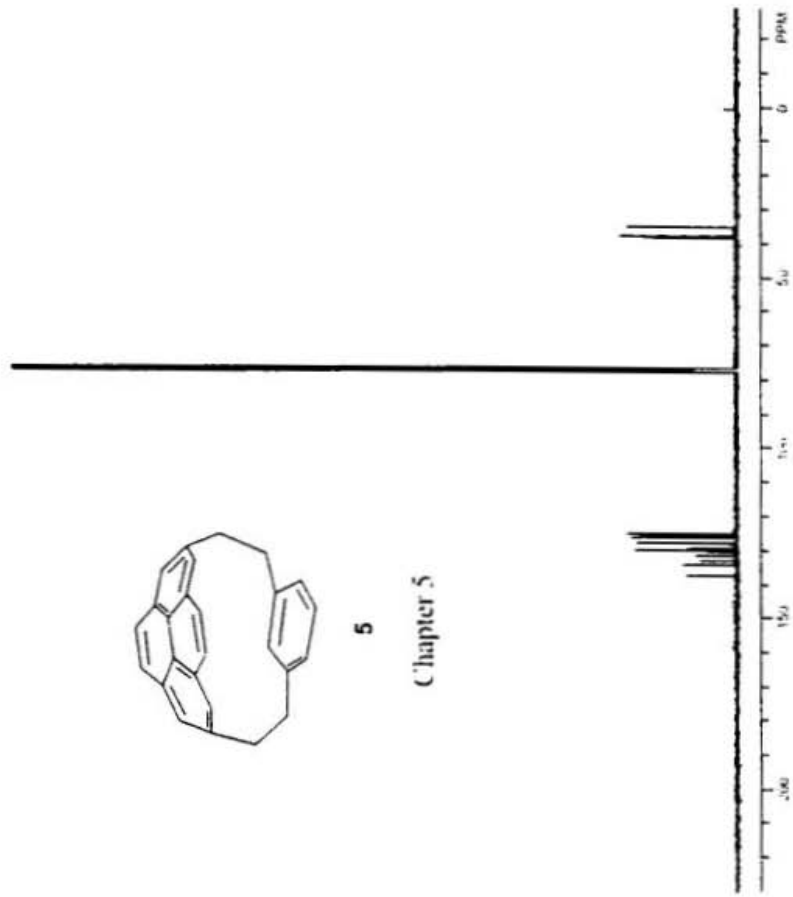

5

Chapter 5